SIM AUD 2012

Orlando FL USA

2012 Proceedings of the
Symposium on Simulation for Architecture and Urban Design

Edited by
Lira Nikolovska & Ramtin Attar

2012 Proceedings of the

Symposium on Simulation for Architecture and Urban Design

Edited By

Lira Nikolovska & Ramtin Attar

Cover by

Justin Matejka

Layout by

Ebenezer Hailemariam
Michael Glueck

Contents

Preface 1

Session 1: Materials 3

A New Material Practice - Integrating Design and Material Behavior 5
Martin Tamke, Elisa Lafuente Hernández, Anders Deleuran, Christoph Gengnagel, Mark Burry, Mette Ramsgard Thomsen
Centre for Information Technology and Architecture (CITA), The Royal Danish Academy of Fine Arts, Royal Melbourne Institute of Technology (RMIT), Universität der Künste Berlin (UdK)

Decision Support System Approach for Construction Materials Selection 13
Mansour N. Jadid, Mustafa K. Badrah
University of Dammam

Session 2: Early Stages of Design Process 21

Design Optioneering: Multi-disciplinary Design Optimization through Parameterization, Domain Integration and Automation of a Genetic Algorithm 23
David Jason Gerber, Shih-Hsin (Eve) Lin, Bei (Penny) Pan, Aslihan Senel Solmaz
University of Southern California (USC)

A Spatial Query & Analysis Tool for Architects 31
Ben Doherty, Dan Rumery, Ben Barnes, Bin Zhou
BVN Architecture, University of Sydney

Combining Sensitivity Analysis with Parametric Modeling to Inform Early Design 39
Julien Nembrini, Steffen Samberger, André Sternitzke,Guillaume Labelle
Universität der Künste Berlin (UdK), École polytechnique fédérale de Lausanne (EPFL)

Session 3: Design & Analysis 47

A Multi-Sensor Based Occupancy Estimation Model forSupporting Demand Driven HVAC Operations 49
Zheng Yang, Nan Li, Burcin Becerik-Gerber, Michael Orosz
University of Southern California (USC)

Preliminary Investigation of the Use of Sankey Diagrams to Enhance Building Performance Simulation-Supported Design 57
William (Liam) O'Brien
Carleton University

Automated Translation of Architectural Models for Energy Simulation 65
Kevin B. Pratt, Nathaniel L. Jones, Lars Schumann, David E. Bosworth, Andrew D. Heumann
Cornell University

Dynamic Annual Metrics for Contrast in Daylit Architecture 73
Siobhan Rockcastle, Marilyne Andersen
Massachusetts Institute of Technology (MIT), Northeastern University (NU), École polytechnique fédérale de Lausanne (EPFL)

Performance Driven Design and Simulation Interfaces: A Multi-Objective Parametric Optimization Process 81
Angelos Chronis, Martha Tsigkari, Evangelos Giouvanos, Francis Aish, Anis Abou Zaki
Foster + Partners

Climatic Based Consideration of Double Skin Façade System: Comparative Analysis of Energy Performance of a Double Skin Facade Building in Boston 89
Mona Azarbayjani, Jigisha Mehta
University of North Carolina (UNC)

A Visual-Performative Language of Façade Patterns for the Connected Sustainable Home 97
Sotirios D. Kotsopoulos, Federico Casalegno, Guglielmo Carra, Wesley Graybil, Bob Hsiung
Massachusetts Institute of Technology (MIT), Politecnico di Milano

Session 4: Urban Planning **109**

Urban Network Analysis: A New Toolbox for Measuring City Form in ArcGIS 111
Andres Sevtsuk, Michael Mekonnen
Singapore University of Technology and Design (SUTD), Massahusetts Institute of Technology (MIT)

The Parametric Exploration of Spatial Properties – Coupling Parametric Geometry Modeling and the Graph-Based Spatial Analysis of Urban Street Networks 123
Sven Schneider, Martin Bielik, Reinhard König
Bauhaus University

Session 5: Work in Progress **131**

Spatial Simulation Model of Urban Retail System 133
Sanna Iltanen
Tampere University of Technology (TUT)

Automatic Building Design with Genetic Algorithms and Artificial Neural Networks 137
Negin Behboudi, Fouad Butt, Abdolreza Abhari
Ryerson University

Visualization Framework of Thermal Comfort for Architects 141
Pascal Goffin, Arno Schlueter
Swiss Federal Institute of Technology Zurich (ETH Zürich)

Experimental Validation of Simulation Software for Daylight Evaluation in Street Canyons 145
Manolis Patriarche, Dominique Dumortier
KiloWattsol, Université de Lyon

A Morpho-Energetic Tool to Model Energy and Density Reasoned City Areas: Methodology (Part I) 149
Laetitia Arantes, Olivier Baverel, Daniel Quenard, Nicolas Dubus
Ecole Nationale Supérieure d'Architecture de Grenoble, Centre Scientifique et Technique du Bâtiment (CSTB), École des Ponts Paris-Tech

Presenting Author Biographies 153

Organizers 157

Technical Paper Reviewers 158

Sponsors 159

Cover Image Credits 160

Author Index 161

Preface

This year marks the third year of the Symposium on Simulation for Architecture and Urban Design (SimAUD). Both technical and work-in-progress papers presented at SimAUD continue to explore new frontiers and to engage diverse communities of researchers, academics, designers and practitioners. Together, they contribute to the advancement of research and knowledge that are instrumental to the future of how buildings and cities are conceived, designed, built and inhabited.

From over 50 initial submissions, we accepted 15 papers and 4 work-in-progress papers. These selections are the result of a very rigorous, thoughtful and thorough reviews that were provided by our distinguished reviewers and committee members. Several broad themes emerged during the selection process: Materials, Early Stages of Design Process, Design & Analysis and Urban Planning. The papers and work-in-progress papers will be presented at SimAUD 2012 in Orlando, Florida.

We would like to thank Azam Khan for establishing SimAUD and for his continued insights and guidance, Michael Glueck, Ebenezer Hailemariam and Michael Lee for their work on the website and the proceedings, and Rhys Goldstein and Simon Berslav for their help in developing the Easy DEVS workshop. Our gratitude is also extended to Nancy Clark Brown from Autodesk Education who generously funded SimAUD' s first Student Travel Scholarship. Finally, we would like to thank Gord Kurtenbach, Jason Winstanley, Phil Bernstein, and Jeff Kowalski of Autodesk for their support and encouragement.

SimAUD would not have been possible without the generous involvement of our Committee members and 36 reviewers, the SimAUD advisory board, and most important, the authors themselves. We sincerely thank them for their hard work, support, inspiration and endless patience in making sure that the SimAUD community continues to grow and provide authors with the opportunity to share and publish high quality research.

Lira Nikolovska, Autodesk
SimAUD 2012 Chair

Ramtin Attar, Autodesk Research
SimAUD 2012 Co-Chair

All accepted papers will be published in the ACM Digital Library at the SpringSim Archive.
Sponsored by The Society for Modeling and Simulation International.

Session 1: Materials

A New Material Practice - Integrating Design and Material Behavior 5
Martin Tamke, Elisa Lafuente Hernández, Anders Deleuran, Christoph Gengnagel, Mark Burry, Mette Ramsgard Thomsen
Centre for Information Technology and Architecture (CITA), The Royal Danish Academy of Fine Arts, Royal Melbourne Institute of Technology (RMIT), Universität der Künste Berlin (UdK)

Decision Support System Approach for Construction Materials Selection 13
Mansour N. Jadid, Mustafa K. Badrah
University of Dammam

A New Material Practice - Integrating Design and Material Behavior

Martin Tamke[1], Elisa Lafuente Hernández[3], Anders Deleuran[1], Christoph Gengnagel[3], Mark Burry[2], Mette Ramsgard Thomsen[1]

[1] Centre for Information Technology and Architecture (CITA)
The Royal Danish Academy of Fine Arts, Schools of Architecture, Design and Conservation (KADK)
Copenhagen/Denmark
Martin.tamke@kadk.dk
Mette.Thomsen@kadk.dk

[2]Spatial Information Architecture Laboratory (SIAL)
RMIT University
Melbourne/ Australia
MBurry@rmit.edu.au

[3]Institute of Architecture and Urban Planning (IAS)
UdK Berlin
gengnagel@udk-berlin.de
lafuente@udk-berlin.de

Keywords: Material Behavior, Complex Modeling, Feedback, integrated FEA Simulation, Active Bending, 1:1 Demonstrator, Aggregate Structures

Abstract

Advances in computational techniques allow for the integration of simulation in the initial design phase of architecture. This approach extends the range of the architectural intent to performative aspects of the overall structure and its elements. However, this also changes the process of design from the primacy of geometrical concerns to the negotiation between encoded parameters. Material behavior was the focus of the research project that led to the Dermoid 1:1 demonstrator build in Copenhagen. Dermoid was a 1:1 prototype, plywood structure that explored how the induced flex of plywood meets structural loads. The integration of simulation tools into the digital design and fabrication process allows producing bespoke members. Contrary to the ease of the concept its realization needed in depth collaboration between engineers, architects and the use of a wide range of customized computational tools. The project challenge today's protocols in design and production and emphasizes the importance of feedback channels in more holistic design and building practice.

1. INTRODUCTION TO THE PROJECT

Today, architects and engineers engage a chain of digital design and fabrication techniques in order to generate, simulate and fabricate building structures that are bespoke to local climatic, programmatic and geometric needs. Although, the performative approach (Schwitter 2005) of using parametric tools is aware of its environment, it is not sensitive towards inherent material behavior as it only understands matter purely from a geometrical perspective.

Working with wood we aimed to understand how the simulation of material behaviour, its bend and flex, can be incorporated as active parameters in the design process and become part of a structural principle. Traditional building structures facilitate load bearing through a correlation of compressive and tensile forces passing loads linearly through the building envelope. However, materials hold internal forces that can be incorporated into structural systems – as in the Shukhov Towers (Picon 1997) – thereby reducing material use and leading to a more intelligent and potentially sustainable building practice.

Figure 1. The 2nd Dermoid Demonstrator during the Copenhagen Design Week.

The subsequent question of how material properties can be introduced into contemporary design practice was the focus of the 2010-2011 Velux Guest Professorship of Prof. Mark Burry at the Centre for IT and Architecture (CITA) in Copenhagen. The collaboration culminated in two

demonstrator objects exhibited in March and September 2011 (Fig1).

2. NEW DESIGN PRACTICES LINKING MODELLING AND SIMULATION

Dermoid is a probe that queries the tools needed to engage and develop a new shared practice. The key research inquiry is a speculation on the new kinds of design practices required to link architectural design practice and the field of material performance simulation, which is traditionally part of engineering practices. The linking interface should be lightweight and work in near to real-time, to enable creative and efficient incorporation of material simulation in the decisive early design phase. As a practice–led research project, (Ramsgard Thomsen Tamke 2009) Dermoid takes on the role of a demonstrator. Through material enquiry the project's leading research questions can be addressed, examined and at least partially resolved.

3. INTRODUCING THE DERMOID STRUCTURE

The development of the structural system looked at integrating bending behavior into short elements that form large structures with a focus in reciprocal truss systems that offer structural capacity due to networked behavior (Popovich 2008). The introduction of curved beams, generative design techniques and digital fabrication (Scheurer 2008) opened the restricted spatial vocabulary of these structures. The fast assembly of this non-standard element system (Cache & Speaks 1995) was supported by traditional wood joinery, using namely wedges and notches.

The final Dermoid structure consists of a bifurcated lattice shell composed of curved plywood T-profiles. The profiles are connecte½d to each other through pinned tenon joints. The T-profiles used exclusively planar elements, the initially straight flanges were elastically bent and afterwards mortised into the planar-curved webs (*Fig. 2*).

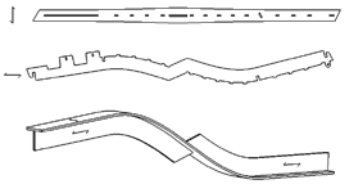

Figure 2. Orientation of plywood in web and flange. Initial planar geometry (u) / schematic perspective (d).

The beams were connected by a glueless 'zipper' based purely on friction between web and flange.The top chord of the web sprouted teeth along its length, and the flange (4mm ply) was cut with receiving holes. The dimensional relationship between the holes width, material thickness and laser-cutter offset resulted in a high friction junction.

Two T-Profiles were connected into V-shaped elements. Three of these were joined reciprocally with their wide ends into a trident with a dehisced center. Six of these pods formed the basis of a honeycomb structure. As the pods flat ends joined each other, a characteristic undulating section emerged (Fig 3). The diverging high parts of the offset pattern provided the structural strength.

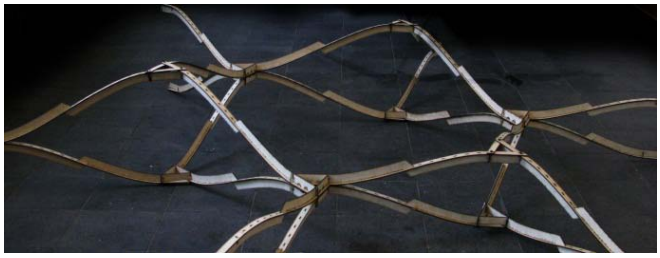

Figure 3. The hex shaped undulating structure.

4. INTEGRATING DESIGN AND SIMULATION

The development took place in a series of physical models on the scale of the overall interconnected structure and the linked development of the fabrication driven parametric model. Tests conducted with finite element simulation that incorporated details such as the plywood layering showed the overall structural behaviour. However, this analytical approach was labour and time intensive and required a static set of boundary conditions. This is yet hardly given in design, which is usually characterised by a constantly changing framework (Rittel 1973), as the performance of the Dermoid, which is depended on the interlink of material, element and structure. Hence geometry generation and simulation required new approaches.

1.1. Challenges on the level of modeling

The traditional development of a structure uses a sequential process from an abstract representation of the overall structure to detailed description. Initial tests in modeling Dermoid followed this course using a chain of parametric tools. This did not succeed because the decisive parameters in the Dermoid structure are highly interdependent. A radical different modeling approach was required in which an initial structure is formed by the

interplay of forces, material and boundary conditions (Tamke 2011).

We learned to differentiate between parameters that are directly dependent on others and those that are mutually interdependent. We could hence split the modeling into an initial iterative process and a later parametric environment.

Based on the experiences from former projects (Deleuran 2011) we looked at the physics solver incorporated in the nucleus engine of Maya™ and established a time-based process. Based on the abstraction of the hex system a particle/spring based system used the underlying polygon mesh as an input. A geometric understanding of the constraints and their interdependency and relation to the overall system was established:

Design:	• Definition of space and function through fixed heights and boundary lines • Readability, density and appearance
Structure:	• Nodal and angle requirements of the reciprocal system (i.e. preferably equal angles in nodes) • Minimum length of beams to allow for node connections • Definition of cell sizes • Even distribution of cells • Even curvature across topology
Material:	• Control of angle and distance in support • Maximum and minimum curvature of the wood
Production and Assembly:	• Maximum length of beams to stay within plate sizes • Staging and accessibility during construction

Table 1. Geometrical constraints and boundaries.

Though these parameters stem from different scalar levels, we could model their mutual dependency in a digital environment solving several layers of constraints in parallel.

Experiments with the underlying hexagon grid furthered an understanding of the generative nature of the structure. However, the mapping of components into the UV space of a NURBS surface and the discretization of surfaces (Pottmann 2007) is limited when dealing with more complex topologies.
The base topology is therefore built from interconnected hexagonal polygons. Here the single cell can be easily manipulated and the overall topology can branch, rejoin and develop spaces between multiple connected layers. The paradigm of the single wrapped surface is overcome (Fig4).

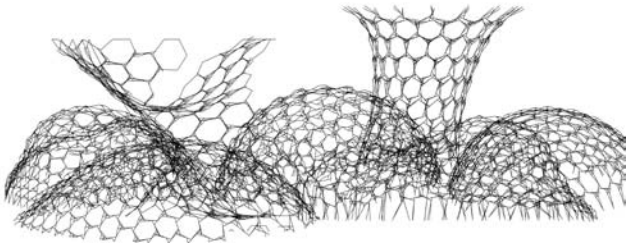

Figure 4. Manifold topologies of the Dermoid structure.

The stacked polygons (Fig.5) were linked and subsequently constrained to boundary conditions, such as the support points, heights and openings. Each line is furthermore informed by its inner limits (Tab.1).

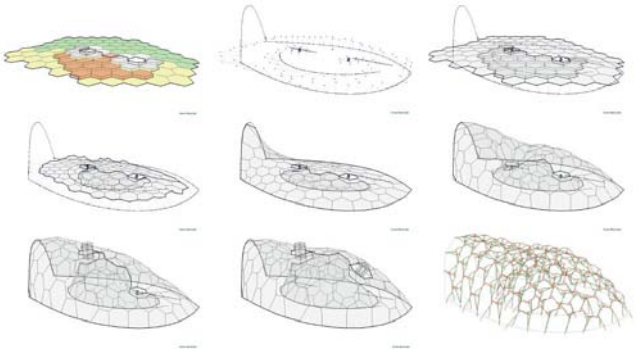

Figure 5. Development of the structure using a time-based process.

The introduction of an inner overpressure in the elements resulted in ark and dome–like conditions. Though not optimal for a structure with both compressive and tensile forces, the generated shapes provided a good point of departure. The combination of surface relaxation, internal pressure and perimeter constraints initiated a generative process that is open to direct design engagement through changes in the boundary conditions and the rapid change of topology.

Changes of the boundary conditions were especially important as we found that the change of inner parameters (i.e. amount of cell sizes) helped little in addressing the design goals. It was the ability to change the polygon topology rapidly while maintaining the structural and materials boundaries that allowed us to iterate different spatial configurations. This process relied on the mature and intuitive polygon modelling environment of Maya, where the following generation of shape employed the generative approach of the physics engine.

Although the physics engine is not directly based on real world physics results could be validated in our physical models and provide a basis for feedback loops. The custom geometric mesh description was interfaced with the parametric component distribution in Grasshopper. Here we evaluated whether a generated node system was viable for making. Here the mesh was first refined and the three-dimensional axis curves of the T-profiles were generated.

1.2. Challenges on the level of simulation

The complexity of the FE-simulation resides in the innovative assembling process of the structure, taking into account the partially-bent members with composite sections and reversible joints, as well as the irregularity of its geometry.

A further level of complexity was introduced by the activation of the orthogonal-anisotropic properties of the plywood. The flanges were oriented transversally, grain direction of the outer veneer perpendicular to profile's neutral axis with lower Young's modulus, to facilitate their bending. In the webs the grain was oriented longitudinally, orientation with a higher Young's modulus, to provide the beams with more rigidity. Due to the bending of the flanges, residual stresses appear on the profiles and on the overall structure.

The aim of the structural simulation was to understand the load-bearing behaviour early and quickly during the short three week long design process. A similar project by the ICD and ITKE in Stuttgart employed active bending in its structures, used FE methods to simulate the elastic bending and subsequent coupling of single strips to form the shape (Menges 2011). Since the Dermoid consisted of a network of bended strips and the aim was to receive instant feedback from simulation, another way to integrate the effect of bending material was required.

A simplified and flexible model was defined that allows modifications and posterior changes in the structure. In order to check the structural impact of the simplifications, physical and computational local models have been calibrated.

Simulation by means of FE-Modelling

The load-bearing behaviour of the structure was analysed with a three-dimensional, geometric non-linear finite element model using the FEA software Sofistik (*Fig. 6*). Spread sheets provided the FEA key coordinates of each of the axis curves and linked boundary and material information. These coordinates were used to regenerate the structure in Sofistik.

The plywood profiles were defined as beam elements. In order to avoid complex coupling elements, the mortise joints between webs and flanges were not modelled. Different material properties were assigned to the web and flange according to the plywood orientation. The variation of the cross-section in the profiles was reduced to the interpolation of four section values. A total of 19 different cross-sections were used for the whole structure.

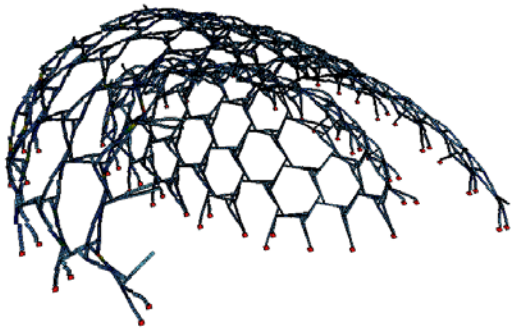

Figure 6. Global FE-Model.

The pinned tenon connections between the profiles were simplified and defined as clamped joints. The earth-stakes used to anchor the structure to the ground (*Fig. 7*) were modelled as pin supports, due to their low sectional stiffness, which gave conservative results when calculating the maximum deformations. In reality, slight moments will be resisted by the supports.

Figure 7. Earth-stakes anchor the structure.

Due to the minor effect of the flange's bending on the structure's stiffness, their shaping has not been simulated on the global model. The post-bending residual stresses have been separately calculated according to the profile's imposed curvature and afterwards added to the stresses resulting from the FE-simulation. The minimum radius of curvature in the profiles is 82,5mm, which corresponds to approximately 85% of the plywood's bending strength in

transversal direction. Nevertheless, membrane forces are predominant in shell-like structures and axial strength in transversal direction is approximately two times higher than bending strength.

1.3. Calibration of simulation through physical tests

We assumed that the simplification of the connections between web and flange and between profiles would lead to an increment of the structure's stiffness in the FE-Model. Therefore, physical tests were undertaken to determine the variation of stiffness between the real and the simulated structures induced by the simplifications in the modelled elements (connections, sections) and approximations in the material definitions. Through comparison of the deformations of both structures, a reduction stiffness factor (rsf) was calculated and later applied on the global model when predicting the deviations of the overall structure, using a multiscalar modelling approach.

The pod tested has ca. 1m-long profiles and varying T-sections (39- 42mm web, 33-46mm flange. Beam width 1510 height 340mm). The beam is restrained and supported at the extremity of two arms and moveable in horizontal direction at the extremity of the third.

By testing two load cases, the profiles are subjected to different forces and subsequently different inaccuracies can be activated. In the first case, an in-plane loading characteristic of shell structures is represented: a horizontal load of 3,17 kN, incremented in 0,22 kN-steps. The second case corresponds to an out-of-plane loading: a vertical load of 22,6 kN, incremented in a 0,22 kN-steps.

The load-bearing behaviour (twisting of the beam, direction of displacements) was analogue in both load cases (*Fig. 8*). However, depending on the loading, different reduction factors were obtained, requesting differentiated simplifications and material stiffnesses for axial or bending loading.

By applying a horizontal load, the beams are homogeneously subjected to axial forces and bending around the Y-axis, as well as locally subjected to bending around the Z-axis. (rsf 0,85). In the vertical load scenario, the difference between the real and the simulated models were higher. Normal forces are concentrated on the upper beams and bending around the Y-axis is predominant (rsf 0,40). In the global structural analysis, the stiffness's reduction factor was used according the applied load cases.

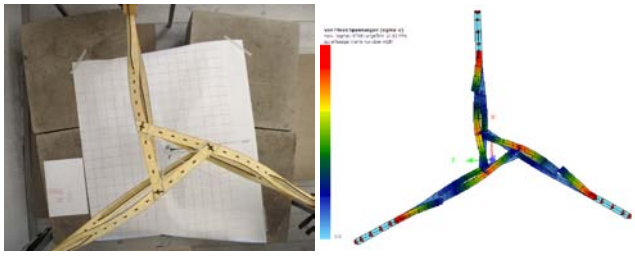

Figure 8. Deformed structure under vertical loading, physical (l.) and FE models (r.).

1.4. Calculation of the global structure and iterative optimization

In the first instance, the FE-calculation of the global structure helped to identify weak points on topological level by applying self-weight. These points could be observed on the outer arch-like areas. Changing the orientation of the beams, the polarity of the lattice and increasing the curvature of the arch in the longitudinal direction reduced deviations on the arch-like side up to 78 percent. (*Fig. 9*)

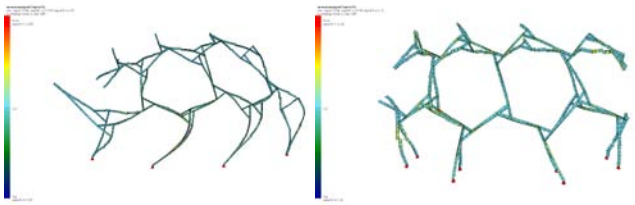

Figure 9: Deformations under self-weight (exaggerated by a factor of 10) before and after structural optimization

1.5. Fabrication

The generation of the structure's fabrication data was derived from the parametric environments axis curves. The curves were then projected into 2D and further refined with offset and detail information.

The incorporation of production and material parameters was easy in comparison to the overall complexity of the model caused by the inherent reciprocal logic and the border conditions as free edges and support zones. Several layers of filter and sorting algorithms identified extreme beams and conditions and informed them with special solutions.

The parametric environment provided a detailed control on every aspect of the beams. It included all fixed

parameters as tolerances, material and section sizing and could calculate local adaptions. The internal numbering of the beams is refined on several positions of the parametric model in order to establish a three layered code reflecting the position of the beam in a pod and the overall structure. The position number was engraved on each beam and gave efficient guidance for inexperienced personnel to set up a structure with more than 1290 individual elements within four days (Fig 10).

Figure 10. Dermoid with a span of 12m and 4m height.

5. THE MISSING LINK – INTEGRATING FEEDBACK INTO GENERATIVE SYSTEMS

As digital fabrication allowed us to fabricate individual elements at the same cost as standard ones each element could bear a bespoke structural capacity defined by cross-section and material.

Although, the connection of FE and Parametric software can be achieved on technical level, (Tessmann 2008) the conceptual question of how and where the feedback is integrated into the model remains. The Dermoid structure offers at least four levels of engagement:

- Material – shift of material with i.e. increased stiffness
- Element – change of cross section and joint details
- Structure – height of pods, size and orientation of nodes
- Topology - size of elements, overall shape, height, span and curvature

Each of these levels has an embedded range of potentials: i.e. the change of a beam's cross section enhances its load bearing capacity has yet almost no impact on the structures shape. However, the change of the structures shape might annul or reverse the need for a bigger cross section at all. It is the interconnectivity of the levels and the emerging effects that prohibits a simple link between the analysis and the model. Where the work with a specific element, material or technology usually generates an intuition about a system's behavior that allows identifying decisive parameters; it is the exploration of the unknown space of the newly created that is challenging in design (Rittel 1973). In highly interconnected systems, a logical link between input and output parameters cannot be observed (Frazer 1995). Several approaches to working with inter-scalar feedback have been proposed. The typical methods of using time based approaches to explore a multidimensional solution space are: multi-scalar material modeling (Weinstock 2006), evolutionary algorithms (Elliott 2011) and self-organization (Tamke 2010).

The practice–based approach within the Dermoid project allows for an alternative avenue employing a staged process of speculative probes, prototypes and demonstrators (Ramsgard Thomsen, Tamke 2009). Physical tests and simulations of different scaled models, full scale prototypes and finally the two demonstrators established an intuition about the general behavior of the system and the relation between the digital and physical model. This intuition allowed estimating the potentials and costs regarding time, labor and economy linked to the different feedback levels.

6. CREATING THE LOOP

We concluded that a direct link from FEA to single beams was pointless. The aim was rather to inform the global model through trends.

The appropriate means were colour graded stress diagrams, animated gifs of the structure's loading as well as colour-coded elements in the design model to denote stress values. This generated a precise understanding of the internal stresses and interplay of forces and establised measures to iterate the structure. To influence the structure on a more general level we chose an indirect approach and linked a property of an object, i.e. cross section, to its spatial relation to a control element (Fig. 10). The attractor curves for each parameter addressed a range of upper and lower bounds. Additional filter algorithms guaranteed a consistent behavior that followed the established parametrical relations.

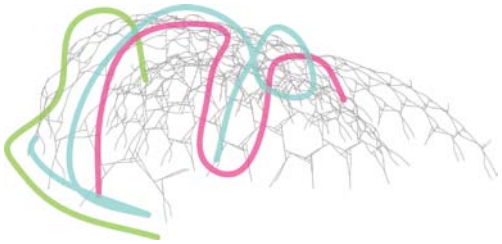

Figure 11. Attractor curves (height-cyan, pink-cross-section, green-triangle size) provide graded global control.

7. DEFINING MATERIAL - INTEGRATION ENABLES A BESPOKE PRACTICE

The attractor curves informed the structure at the beam level about material thickness (4 - 6.5mm Plywood), and cross section (30mm - 120mm height). On structural level depth and node width were varied. Due to the nature of the parametric model a linear response to the input could yet not be achieved. As i.e. material boundaries are encoded all further external influence cannot take place in absolute values but only relative within the given local limits. This limits the global effect of local adjustments.

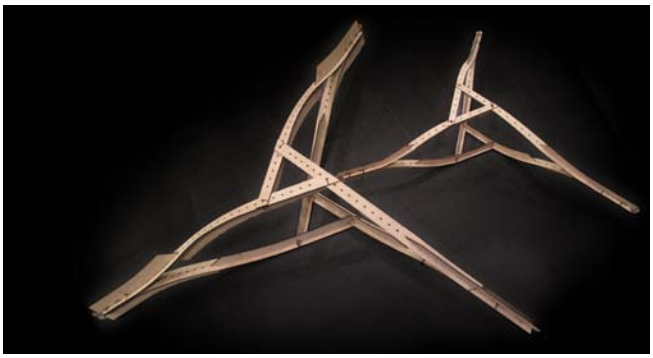

Figure 12. Largest and smallest element in the Dermoid.

1.6. Discussion of the effectiveness of measures taken

The exchange of information between the design and structural models was fast and systematically. Employing a hybrid modelling method, (Moshfegh 2004) additional physical tests provided essential information about the stiffness of the beam members, later implemented in FE.

Nevertheless it was hard to find appropriate answers to the FE Analysis in the generative design environment. Modifications with a bigger structural effect were more complex and took more time. Changes on topological level had the biggest impact on deformation and stresses but were too labour-intensive. A decision was therefore taken to concentrate on incremental changes as changing the widest span from an arc to a more shell like condition. The project offered only little time for posterior iterative optimization. The executed iterations reduced the maximum stresses already by 44%, without increasing the weight of the structure. The comparison of a laser scan of the installation and the calculated deformed geometry revealed their qualitative correlation.

Interfacing FEA and the design model gave an understanding of the flow within the structure. This interconnectivity was as well observable in the demonstrator. In both the partially change to stiffer material did not eliminate stresses but rather shifted the tension zone into the interface between the thinner and thicker beams - a slight kink in the structures curvature became visible in both cases.

The attractor based control mechanism provided an interface that addressed the structural capacity of the single element as well as general considerations as the structures internal trends, readability and appearance. The systems near real-time feedback enabled the designer to build up an intuitive understanding of the systems behavior and the interplay within the parameter space.

The approach chosen proved to be robust and docile towards the topological changes. These were finally the key to the implementation of feedback from FEA.

8. MEANS OF INTEGRATING MATERIAL AND DESIGN PRACTICE

The integration of material behavior into design demands a holistic understanding where scales are both conceptually and logically linked. As our toolset is driven by a downstream digital chain, the establishment of digital loops is challenging. Yet fast feedback loops are the prerequisite for any improvement of design solutions.

Integrating material behavior can not be achieved in a simple technological manner. We observe that the impact of high level changes - as variation in topology - is far higher than element based adjustments. The potential to execute these changes comes along with a commitment to a far higher complexity on tool, communication and process management level. We need tools and methods to handle complexity, interpret feedback and position acquired knowledge. The Dermoid project shows that an indirect link of levels - as the attractor fields - has the potential to negotiate numeric parameters with abstract constraints from design, program and economy.

Finding the right representation for material behavior is an intellectually challenging endeavor. An appropriate representation can be a set of straightforward geometric rules. As computation of a structure is only happening in the physical world, simulation and modeling remains abstract. It

is up to the designer to define the adequate means of representation on every level. Physical tests provide an effective means to conclude from material and element level to the behavior of a general structure. Simulation is not a generic tool but an environment that needs calibration to real-world behavior through measurements specific to the area of application. The calibration can take place on the level of material or through tests on larger entities, as the pods in Dermoid. Simulation shifts from being an analytical to a design tool. Sound design decisions can be furthers through a global structural analysis in the early stages of the design. Structural analysis has consequence on two levels:

- In the design phase, it helps to identify weak points in the topology with a strong impact on the deformations and stresses of the structure.
- In a more advanced stage, the information provided by the FE-Analysis enables an increase in structural performance by local optimization.

Through the knowledge of an element's performance, a material practice is introduced that works with graded properties. Here the behavior of material is as much a part of design as its specification. Where we are looking in Dermoid at the information of an element, parallel investigations allow the speculation about the role of the making of material (Nicholas 2011).

The introduction of material properties is points towards a paradigm shift in architectural design and its representation.

Acknowledgements

Dermoid is supported by the VELUX Visiting Professor Programme 2009-2010 of the Villum Foundation, the School of Architecture in Copenhagen and the Copenhagen Design Week 2011.
Photos: Anders Ingvartsen.
Project participants:
SIAL: Mark Burry, Jane Burry, Alexander Pena, Daniel Davis, Michael Wilson
CITA: Martin Tamke, Mette Ramsgaard Thomsen, Phil Ayres, Anders Holden Deleuran, Stig Anton Nielsen, Aaron Fidjeland, Morten Winther, Tore Banke and students from the departments 2 and 10 (Copenhagen).
UDK: Elisa Lafuente Hernández, Christoph Gengnagel

References

Cache, B., & Speaks, M. (1995). Earth moves: the furnishing of territories. Cambridge, Mass.: MIT Press.

Elliott, J. A. (2011) “Novel Approaches to Multiscale Modelling in Materials Science” Invited review article in International Materials Reviews, Maney Publishing and ASM International

Frazer, J. H., (1995), An Evolutionary Architecture, Architectural Association, London

Menges, A., Schleicher S., Fleisshcmann M. (2011), Research Pavillion ICD/ITKE in Glynn E., Sheil B. (ed) Sheil, Bob. Fabricate: making digital architecture. Toronto: Riverside Architectural Press, 2011.

Moshfegh R., Ottosson P. (2004) Hybrid prototyping. International Journal of Manufacturing Technology and Management Vol.6, No.6 pp. 523 - 533

Nicholas, P. 2011, Embedding Designed Deformation: Towaqrds the Computational Design of Graded Material Components, in proceedings of Ambience 2011 conference, University of Borås, Sweden, pp. 145-151

Picon, Antoine (dir.), "L'art de l'ingenieur : constructeur, entrepreneur, inventeur", Éditions du Centre Georges Pompidou, Paris, 1997.

Popovich Larsen, O. (2008). Reciprocal Frame Architecture. London: Architectural Press.

Pottmann H, Liu Y (2007) Discrete surfaces in isotropic geometry. Mathematics of surfaces, in Lecture notes in computer Science Vol. 4647:341-363.

Ramsgard Thomsen, M., Tamke, M., (2009), ”Narratives of Making: thinking practice led research in architecture” in Communicating by Design, International Conference on Research and Practice in Architecture and Design, Bruxelles.

Rittel, H., & Melvin W., (1973), "Dilemmas in a General Theory of Planning," in, Policy Sciences, Vol.4, Elsevier Scientific Publishing Company, Amsterdam, pp. 155-169.

Scheurer, F., (2008), Architectural CAD/CAM - Pushing the Boundaries of CNC-Fabrication in Building,in Kolarevic B., Klinger K. (Ed.): Manufacturing Material Effects - Rethinking Design and Making in Architecture, pp. 211-222, Routledge, New York.

Schwitter, C., (2005). Engineering Complexity: Performance-based Design in use, in “Performative Architecture – Beyond Instrumentality” Kolarevic, B., Malkawi, A., M. (eds), Spon Press, 2005.

Tamke, M., Riiber, J. & Jungjohann H. (2010) Generated Lamella in Proceedings of the 30th Annual Conference of the Association for Computer Aided Design in Architecture, ACADIA.

Tamke, M., Burry, M., Ayres, P., Burry, J., Ramsgard Thomsen, M. (2011), Design Environments for material Performance, in Computational Design Modelling, proceedings of the Design Modelling Symposium Berlin 2011, Springer, Vienna, pp.309-318

Tessmann, O. 2008. Collaborative design procedures for architects and engineers. Norderstedt: Books on Demand.

Weinstock, M., (2006), Self-Organisation and Material Constructions, Architectural Design, 76, 2, pp. 34-4

Decision Support System Approach for Construction Materials Selection

Mansour N. Jadid[1], Mustafa K. Badrah[2]

[1]University of Dammam
P. O. Box 30973,
Alkobar, Saudi Arabia, 31952
mnjadid@yahoo.com

[2]University of Dammam
P. O. Box 1982,
Dammam, Saudi Arabia, 31441
badrahmk@gmail.com

Keywords: Decision Support System, Construction, Consultants, Classification, Items, Supplier, Owners, Materials, Selection, Contractors.

Abstract

The objective of this paper is to implement a decision support system for materials selection for projects under design or construction by consultants and owners. The paper focuses on issues of materials approval, selection criteria and materials information management. The proposed system includes database and decision support components. The database can enhance the functionality of the selection process as it provides a source of information to feed into the decision support component. The decision support component relies on the quantitative methods of value engineering. Construction involves processes that deal with materials in all stages of a project. Decision making in project meetings requires the application of knowledge from many disciplines, by all parties in the project teams to select materials and avoid delays for the project under construction. Acquiring and recording information (in a database) regarding material quality, durability, specifications, and maintenance requirements is a vital part of good project management practice. It is anticipated that using such a system for materials selection will provide an improved tool that systematically enhances the selection process and enables upgrading the system during project life cycle.

1. INTRODUCTION

The construction industry is expanding at an exponential rate, which causes huge demands for materials. The selection of materials significantly impacts the sustainability of a project and can markedly reduce the impact of the project on the environment. High quality materials are generally recommended, but cheap materials are desirable to reduce project costs, taking into consideration the fact that high initial cost is often offset by reduced maintenance requirements. In general, materials have a major impact on the environment, especially on air quality, which can affect the occupants of the building. Therefore, it is highly recommended to select environmentally friendly materials and to provide proper ventilation, and to choose materials that are suitable for day-to-day operation and make future maintenance easier.

A qualitative and quantitative analysis for evaluating and selecting model for floor materials was carried out by (Mahmoud, et al. 1994). Decision support systems have been applied in a wide variety of contexts. One approach have used a simple form to provide help in managing water uses, identifying water quality problems, evaluating the performance of pollution control programs, and presenting technical information to public, specialist, and non specialist decision makers (El-Gafy, et al. 2005). Another study involved implementing a decision support system, for a large apartment building project, in which the clients can make cost based decisions which meet the requirements, while the builders can control both resource planning and interior design construction costs Lee et al. 2008).

There are certain criteria that the designer must take into consideration for materials selection during the early design stage, but which will have an impact on the whole project. These criteria include, but are not limited to:

- Durable, with low maintenance requirements;
- Made of natural and renewable resources;

- Affordable and available from local manufacturers;
- Do not affect indoor air quality and are environmentally friendly;
- Do not contain toxic compounds

Generally, construction involves processes that deal with all types of materials at different stages of construction. Materials procurement and approval activities accompany a project from A to Z. Contractors usually try to satisfy the contract specifications while keeping the cost of materials affordable. On the other hand, consultants and owners want to obtain higher quality materials. Acquiring and recording information on material and system quality, durability, specifications, and maintenance requirements is vital for obtaining high quality materials. This paper focuses on issues of materials approval, and selection and materials information management. It proposes a structure for a materials database that can be used by consultants (designers / supervisors) and owners as a source of information to feed into a decision support system for materials selection. The decision support system itself relies on the quantitative methods of value engineering.

2. CONSTRUCTION MATERIALS

2.1. Relationship with the Project Planning

Project construction involves execution activities that can be classified according to the Master format of Construction Standards Institute (CSI), shown in Table 1, (Masterformat 1998) or another standard format. To execute these activities, the construction firm needs specific resources including material, equipment, labor, engineering and technical support. In construction projects, materials account for more than 40% of the project cost, as noted by (Chitkara 2002). Materials procurement and selection are closely linked with project planning, and should be considered during project planning and scheduling. To be an effective tool for planning and scheduling, the project schedule should include materials approval and supply activities as main separated groups correlated with other project activities. This ensures that materials will be provided on time to the site before the execution of related activities. On the other hand, many material items may not be available in stock and may need time to be fabricated. Other materials may need to be imported and may therefore need an extra time allowance for shipping and customs clearance. Therefore, integrating materials approval and supply into the project schedule is important to facilitate materials and construction management.

Division 1. General Reuirements
1-2- Shop drawing submittals
1-3- Material submittals
1-3-1 Earthwork (e.g. backfilling material)
1-3-2 Structural works (e.g. steel bars)
1-3-3 Architectural works (e.g. paints)
1-3-4 Mechanical works (e.g. elevators)
1-3-5 Electrical works (e.g. switches)
Division 2. Site Work
Division 3. Concrete
Division 4. Masonry
Division 5. Metals
Division 6. Carpentry
Division 7. Thermal & Moisture Protection
Division 8. Doors, Windows and Glazing
Division 9. Finishes
Division 10. Specialties
Division 11. Equipment
Division 12. Furnishings
Division 13. Special Construction
Division 14. Convey Systems
Division 15. Mechanical
Division 16. Electrical

Table 1: Master format classification of CSI.

2.2. ABC Classification

The most used method for classifying construction materials is to group them into high- value, medium-value, and low-value materials as recommended by (Chitkara 2002) is shown in Table 2. This classification is performed using **ABC** analysis as follows.

- **Group A**: high-value items, which are 10% of the total number of items and account for 70% of the inventory cost.
- **Group B**: medium-value items, which are 20% of the total number of items and account for 20% of the inventory cost.
- **Group C**: low-value items, which are 70% of the total number of items and account for 10% of the inventory cost.

Examples of **A** items	Elevator	AC System	PVC Pipes
Examples of **B** items	Ceramic tiles	Emulusion paint	Doors/windows profiles
Examples of **C** items	PVC conduits and accessories	Telephone sockets	Wood screws

Table 2: ABC materials classification.

The **ABC** classification system is based on the principle of "control selection" which implies that it is not necessary to give the same degree of attention to procurement, storage, issue, and control of all types of materials. This principle is summarized in Table 3.

Policy consideration	A items	B items	C items	Project participant
Degree of control required	Strict	Moderate	Loose	Contractor
Authority of ordering	Senior level	Middle level	Junior level	Contractor
Suppliers to contacted	Maximum	3-5 reliable	2-3 reliable	Contractor
Estimation accuracy	Accurate quantities	Approximate quantities	Rough quantities	Contractor
Selection method	Decision support / Systematic	Systematic	Systematic	Consultant /Owner

Table 3: Control selection levels.

2.3. Materials Approval Procedure

The contractor usually communicates with suppliers to procure materials according to drawings, specifications and other tender documents. The contractor then submits to the consultant/owner committee one or more samples/catalogues for materials approval. The consultant/owner reviews the submittals and either accepts them, recommends resubmittal with notes, or rejects them. The following points should be considered during the materials approval process:

- It may be to the owner's benefit to obtain the same trade mark of mechanical and electrical equipment for all projects under consideration. This will facilitate maintenance and reduce maintenance cost.
- Components which involve natural raw minerals (granite, ceramics) should be approved with the provision that the supplier can supply the whole quantity with the same color and specifications.
- The consultant/owner committee may approve materials for which scaled samples are submitted. In these cases, it is advisable for the contractor to prepare a real sample on site (e.g., a full-scale door or window). A mock-up model may also be recommended for several items (floor, false ceiling, wall paints, etc.).

3. MATERIALS SELECTION CRITERIA

Criteria for materials selection may differ from one project to another and from one company to another. Authors suggest the following criteria for materials selection:

1) **Durability**: to make sure that a system/sub-system will not deteriorate during the life span of the project.

2) **Maintainability**: to ensure that the system/sub-system can be maintained during service and that agents who will provide spare parts and labor exist.

3) **Sustainability**: to ensure that the system/subsystem is composed of elements or materials that can be reused at the end of the life span of the structure. For example, a warehouse structure erected using steel girder frames (bolt-connected) can be reused in another project.

4) **Aesthetics**: This is very important in selecting internal and external finishing materials.

5) **Adaptability**: In the service stage, of many facilities like hospitals and educational institutions, there is a need for redistribution of space as these facilities develop and the services provided evolve. Therefore, the designer should take this possibility into consideration and select suitable systems or sub systems to provide the required flexibility. For example, it is easier to relocate metal partitions than block partitions.

6) **Lack of Toxicity**: Manufacturers use certain composites in their products some of which may be harmful to human beings or to the environment (e.g., asbestos).

7) **Cost Efficiency**: Projects can be very costly or less costly. The important thing is that the cost incurred will result in the anticipated value.

The decision support system may be used for materials selection and approval in various phases of a project: in the design stage, where designers and owners decide on the specification and quality of the project systems and elements, and also during construction stage, for example, in the case of multiple submittals by contractors for a specific material item.

4. PROPOSED DECISION SUPPORT SYSTEM FOR MATERIALS SELECTION

The proposed decision support system for materials selection uses weighted criteria. The major source of input data for this system is a central database developed from previous and current projects, as shown in Figure 1. This database could be used by many large organizations that own and develop facilities, such as directorates of health, education, etc. A large mass of information exists about materials and systems, but if this information is not recorded, it cannot be used to formulate knowledge. This database is assumed to be managed centrally at the senior level of corporate administration (design team, project management). Information on various materials (descriptions, procurement and supplier data, etc.) is supplied by construction managers. Information regarding evaluations of used materials (durability, maintainability, etc.) can be obtained from the corporate facilities management department.

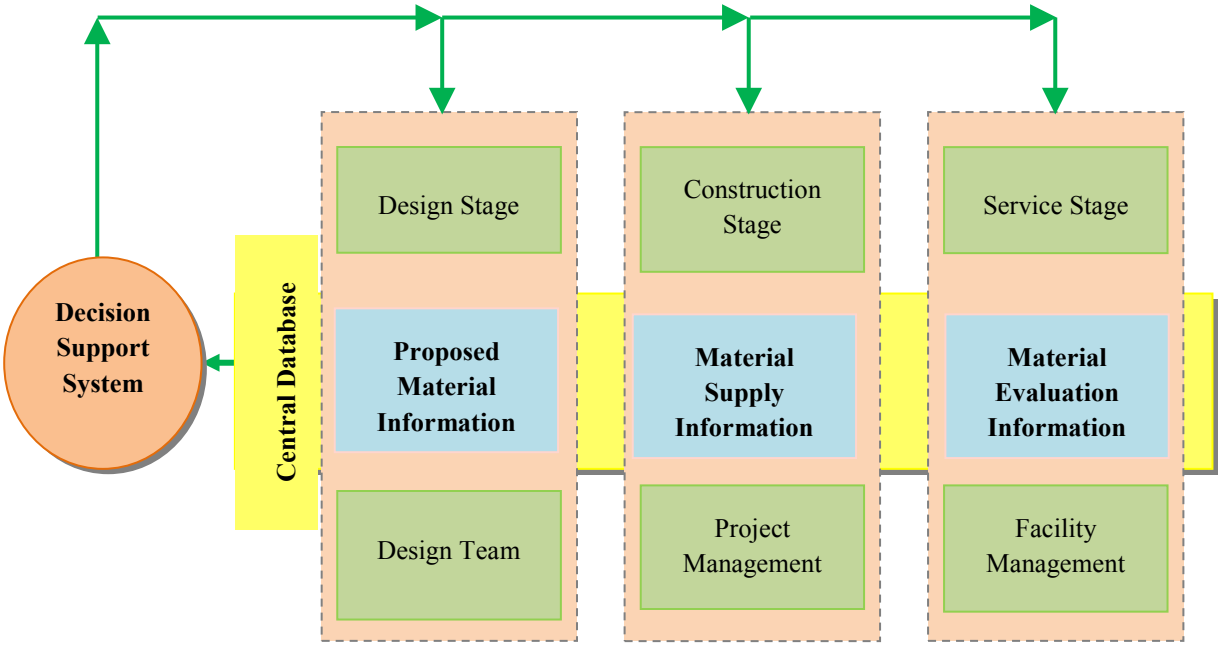

Figure 1: Flow chart of decision support system.

5. PROPOSED DATABASE STRUCTURE

The database consists of material, project, supplier and evaluation tables as shown in Table 4. Figure 2 shows a sample of data entry for the material table (15 records). It is anticipated that the database for a large firm (e.g. health directorate having series of hospitals across the country or recently founded educational facility) may include few thousands of records for materials/systems related to different construction item divisions. It should be noted that the evaluation table may contains a large number of criteria but only some of them are applicable to a specific material. This is organized by using datasheet forms. The user of the decision support system can make a query to find information in the database that assists him in filling the evaluation matrix for a specific selection. The database can be further developed by including pictures of different views of the material/system. This database can be used by:

- Owners and Design Consultants: to help them selecting and preparing specification for materials and systems based on accumulated firm experience.
- Supervising Consultants: to help them in material submittal review and approval.
- Contractors: to have records of previously used materials and use them for more accurate project estimation and price analysis.

Table name	Table fields					
Material	Material description	Specs reference	Discipline: D1-D16	ABC code	Building code	Supplier code
Project	Building code	Building type	Designer	Consultant	Contractor	Project start date
	Project finish date	Project cost	Project area			
Supplier	Supplier code	Manufacturing company	Country of origin	Local agent	Material code	
Evaluation	Building code	Supplier code	Durability	Maintainability	Aesthetics	Energy saving
	Cost efficiency	Manufacturing company	Country of origin	Sustainability	Environmentally friendly	Adaptability

Table 4: Proposed database tables.

Material

Material Co	Material De	Specs Refer	Descipline	ABC Code	Building Co	Supplier Co
M001	Vinyle tiles	9650	D09	B	4A	S001
M002	Ceiling Metal T	9545	D09	A	4A	S002
M003	Ceramic Tiles	9310	D09	B	4A	S003
M004	Lighting units	16500	D16	B	4A	S004
M005	Air handling ur	15720	D15	A	4A	S005
M006	Hollow doors &	8100	D08	A	6B	S006
M007	Door hardwaer	8100	D08	A	6B	S007
M008	Granite tiles (c	9634	D09	B	6B	S008
M009	Passenger elev	14212	D14	A	6B	S009
M010	Fire alarm syst	13850	D13	A	6B	S010
M011	Air handling ur	15720	D15	A	6B	S005
M012	Metal partitior	9250	D09	A	9B	S011
M013	Ceiling Metal T	9545	D09	A	9B	S012
M014	Laboratory furi		D12	A	6E	S013
M015	Passenger elev	14212	D14	A	4A	S014

Figure 2. Flow Sample data entry form for material table (15 records).

6. APPLICATION

A qualitative method of value engineering for evaluating alternatives to be used in the manufacturing industry has been proposed by (Miles 1989). The method includes comparing several options against weighted criteria and multiplying the satisfaction factor of each criterion/option with the criterion weight and summing the results to obtain a total score for each option. The option with the highest score is the optimum. The same procedure was applied for material selection in the proposed decision support system. As an example, it is assumed that a contractor has submitted two alternatives for some major system (e.g. elevators) in a construction project, as shown in Table 5. These are referred to as Supplier I and Supplier II. The two submittals are compared against six criteria shown in column 1. Each criterion has assigned a satisfaction factor coded (YES/NO or A-D). The satisfaction factors are then converted to numerical score from 2 to 9. The weighted factors are calculated and by summing the results, Supplier I scored 303 and supplier II 268. So supplier I submittal is the optimal choice.

It should be noted that the satisfaction factors can be estimated from reviewing and evaluating submittals and also from using past information retrieved from the central database. In the elevator example problem, the first three criteria: "approved in previous projects", "durability evaluation" and "maintenance-wise evaluation" are retrieved from a relational database implemented using Microsoft Access.

Satisfaction factors are calculated using indicator sheets that include attributes facilitating evaluation of alternatives according to the considered criteria. An extracted attribute sheet and related partial satisfaction factors regarding maintainability in elevator selection problems is shown in Table 6. The weight factors are based on the selection committee experience and preferness. The relational database was implemented using Microsoft AccessTM.

7. CONCLUSION

One of the most important decisions to be made during construction is the selection of materials to be used. This paper has presented a simple materials selection procedure based on a decision support system. A number of criteria have been proposed for materials selection including durability, maintainability, sustainability, aesthetics, adaptability, lack of toxicity and cost efficiency. These can help decision making by considering larger number of material options and comparing them to offer various degrees of efficiency and effectiveness.

	Satisfaction Factor (Score Y/N, A-D)		Satisfaction Factor (Score out of 10)			Evaluation Result	
Criterion	Supplier I	Supplier II	Supplier I	Supplier II	Weight	Supplier I	Supplier II
Approved in previous projects	YES	NO	9	5	2	18	10
Durability evaluation	A	B	9	7	6	54	42
Maintenance evaluation	B	A	7	9	6	42	54
Aesthetics	C	D	5	2	9	45	18
Cost efficiency	A	A	9	9	8	72	72
Manufacture company	A	A	9	9	8	72	72
						303	268

Table 5: Evaluation matrix result of two suppliers I and II.

Much information on materials and systems is acquired during the life span of a project (design, construction, and services). This information, if not recorded, cannot be used to formulate knowledge. Acquiring and recording information (in a database) regarding material and system quality, durability, specifications, and maintenance requirements is vital for obtaining high quality materials.

The decision support component itself relies on the quantitative methods of value engineering. It is anticipated that using such a decision support system for materials selection will provide an improved tool that systematically enhances the selection process.

Indictor attribute	Partial satisfaction factor(Score 1-10)
Mechanical problems	6
Electrical problems	6
Vibration problems	7
Cabinet problems	8
Reported accidents (elevator is totally out of service)	7
Reported accidents (elevator is partially out of service)	7
Availability of spare parts	8
Satisfaction factor = ∑Partial satisfaction factors / Number of partial satisfaction factors	49/7=7

Table 6: An attribute sheet sample for evaluating the maintainability criterion in the elevator example (Supplier I) based on performance of similar equipment in past projects.

8. FUTURE WORK

Using Web based approach for the database incorporated in the proposed decision support system for material selection will provides possibility of feeding information of project participants on different locations. The interface for the Web based approach is currently being designed and will be implemented in the near future. Efforts are already underway to integrate a wider range of materials into the database. The target is to concentrate primarily on automating materials selection using the Web based approach. This is a topic for future research which will attempt to develop a full scale automated system. This system will include procedures adopted to simplify the traditional approaches to selection and management of the wide variety of materials encountered in the construction industry. The interface with the Web based system will integrate materials selection with a decision support system which will provide engineers with sufficient information to make decisions without delaying their work and a means of communicating more effectively among the parties involved. This paper has proposed a structure of a decision support system for materials selection that can be used by consultants (designers / supervisors). This system composes of database used a source of information to feed into decision support component.

References

Mahmoud, M., Al-Hammad, A., Assaf, S., and Aref, M. 1994, An Evaluation and Selecting Model for Floor Finishing Materials, Cost Engineering Journal, 36(9): 21-24.

El-Gafy, I., Farid, M. N., El-Bahrawy, A., Khalifa, A., El-Basiony, E. and Abdelmotaleb, M. 2005. Decision-support System for Evaluating Groundwater Quality, Emirates Journal for Engineering Research, 10(1): 69-78.

Lee, H.-K., Lee, Y.-S., and Kim, J.-J. 2008, A Cost-Based Interior Design Decision-support System for Large-Scale Housing Projects. ITcon 13:20-38.

Masterformat 1998, Master list of the titles and numbers of the construction industry. The Construction Specification Institute (CSI).

Chitkara, K.-K. 2002. Construction project management: planning, scheduling and controlling. Tata McGraw-Hill.

Miles, L.-D. 1989. Techniques of value analysis and engineering. Text available at *URL*: http://wendt.Library.wisc.edu/miles/index.html

Session 2: Early Stages of Design Process

Design Optioneering: Multi-disciplinary Design Optimization through Parameterization, Domain Integration and Automation of a Genetic Algorithm 23
David Jason Gerber, Shih-Hsin (Eve) Lin, Bei (Penny) Pan, Aslihan Senel Solmaz
University of Southern California (USC)

A Spatial Query & Analysis Tool for Architects 31
Ben Doherty, Dan Rumery, Ben Barnes, Bin Zhou
BVN Architecture, University of Sydney

Combining Sensitivity Analysis with Parametric Modeling to Inform Early Design 39
Julien Nembrini, Steffen Samberger, André Sternitzke,Guillaume Labelle
Universität der Künste Berlin (UdK), École polytechnique fédérale de Lausanne (EPFL)

Design Optioneering: Multi-disciplinary Design Optimization through Parameterization, Domain Integration and Automation of a Genetic Algorithm

David Jason Gerber[1], Shih-Hsin (Eve) Lin[1], Bei (Penny) Pan[2], Aslihan Senel Solmaz[1]

[1]University of Southern California
School of Architecture,
Watt Hall 204, Los Angeles,
CA90089
dgerber@usc.edu, shihhsil@usc.edu, as_593@usc.edu

[2]University of Southern California
Computer Science Department,
RTH 323, Los Angeles,
CA90089
beipan@usc.edu

Keywords: parametric design, generative design, performance based design, genetic algorithm, multi-disciplinary design optimization

Abstract

The overall performance of buildings is heavily impacted by design decisions made during the early stages of the design process. Design professionals are most often unable to explore design alternatives and their impact on energy profiles adequately during this phase. Combining parametric modeling with multi-disciplinary design optimization has been previously identified as a potential solution. By utilizing parametric design and multi-disciplinary design optimization to influence design at the schematic level in the interest of exploring more energy efficient design configurations, the H.D.S. Beagle 1.0 tool was developed. The tool enables the generation of design alternatives according to user defined parameter ranges; automatically gathers the energy analysis result of each design alternative; automatically calculates three objective functions; and uses Genetic Algorithm to intelligently search, rank, select, and breed the solution space for decision making. Current case studies demonstrate our tool's ability to reduce design cycle latency and improve quality. However, the future work is needed to further investigate how to acclimate this process to accommodate early design stages and processes.

1. INTRODUCTION

Current parametric design tools offer more rapid design iterations through quick visualization and modification of geometry (Burry and Murray 1997; Aish and Woodbury 2005; Gerber 2009). Slow paced manual adjustment to design geometry is being replaced by parametric design methodologies. More prevalently designers now can generate and evaluate many design alternatives to aid in the multi domain development processes: designer, consultants and client. However, simply providing multiple geometric design options is not a solution for practice, as a design team needs to consider performance criteria of the design as well. Simulation tools assist the design team in evaluating design performance and here with a focus on energy use intensity (EUI), design compliance, and finance. However, simulating many design alternatives and running their analysis can be a very time consuming endeavor and therefore designers are forced to select a reduced set of possible and potentially better designs to explore. Moreover, there are multiple performance priorities to be satisfied in order to reach what can be considered the final optimal design solution; including finding optimality in structural design, EUI, construction and operation cost, programming for examples. In pursuit of improving upon early stage design decision making and the domain integrations necessary researchers have used several optimization methods including Genetic Algorithms (GA) and other Meta-heuristic techniques to rapidly generate and evaluate multiple design solutions and find the optimum results (Shea et al. 2006; Keough and Benjamin 2010; Turrin et al. 2011). This body of research describes and our research extends these new design exploration / multi-disciplinary design optimization process tools where parametric design, GA, financial models and energy simulation tools are combined to accelerate the design cycle and systematically explore –generate and evaluate- design options faster than current conventional design processes would allow.

By utilizing a methodology that is composed of parametric modeling, platform integration and genetic algorithm based optimization, this research enables: rapid design exploration, increased correlation between disparate

domains, rapid visualization of the cause and effect of these correlated decisions, quantified understanding of the multi-objective trade offs, and reduced design decision latency given transparency and automation of the generation and evaluation of the design solution spaces.

This body of research is unique in that it enables designers to more efficiently and with more certainty explore more complex and tightly coupled design solution spaces. In conjunction this area of research provides for flexible and extensible platforms for designers to better integrate parametric thinking with Genetic Algorithms for optimizing through simulation design, EUI, and financials and other expert domains. In addition, the workflow allows for designers themselves to explore the process of these simulations and subsequent optimization without relegating this work exclusively and in isolation to consulting engineers. In other words the research brings the often-disparate domains, their models, their individual modes of representation and constraint spaces into a more tightly coupled process. The potential of the research is to bring improved design decision certainty and efficiency through *designing-in* performance via automated simulation earlier in the design process where greater impact on a designs' energy use intensity will have greater impact while maintaining the coupling of other competing project objectives.

2. OVERVIEW OF CURRENT DESIGN TECHNOLOGY AND PERFORMANCE BASED DESIGN

2.1. Advantages of Parametric Design Process

Contemporary CAD tools permit parametric representation of objects and rapid alteration of design dimensions and structure. Parametric modeling can decrease the time and effort needed to change or modify the design at hand, and can also yield improved form finding (Aish and Woodbury 2005). It facilitates the rapid change of geometric and non-geometric variables according to particular design logic (Shah and Mäntylä 1995; Shea et al. 2005). It also aids in the set up of structural alternatives in an efficient manner that allows design teams to communicate results affected by altering parameter values and the subsequent impact on the potential design solution (Rolvink et al. 2010). Performance based design can also benefit from integration with parametric design methods. Exploring parametric alternatives while assessing structural impact in real time is an example of such integration (Shea et al. 2005). Increased integration of design alternative generation combined with performance evaluation may be accomplished by designing parametrically (Malkawi 2005; Gerber and Flager 2011).

2.2. Current State of Multi-disciplinary Design Optimization

Multi-disciplinary optimization (MDO) (or Multi-objective optimization) referes to optimization methods to solve design problems which having several objectives functions and incorporates a number of disciplines (Coello Coello et al. 2007). As defined by Prof. Carlo Poloni, MDO is "the art of finding the best compromise" (Poloni C. 1997). Although the notion of integrating parametric design tools with simulation tools is a recent trend (Oxman 2008), building energy simulation tools have been extensively used by professionals to optimize energy use, and factors in occupant comfort for over 50 years (Crawley et al. 2008). However one drawback, is the fact that these tools are often limited to designs developed to a certain level of completeness and require specialized familiarity with simulation tools in or order to yield relevant results (Aish and Marsh 2011). Building performance optimization is always a multidisciplinary problem requiring expert analysis from multiple fields (Flager et al. 2009). Insufficient data exchange and interfacing between digital tools used by professionals from different domains is considered a significant obstacle for multi-disciplinary design optimization (Holzer et al. 2007b). A lack of real-time analysis linking architectural geometry and engineering parameters is another deficiency in current AEC multidisciplinary design (Sanguinetti et al. 2010).

There have been numerous solutions that proposed parametric modeling for multi-disciplinary (multi-objective) design optimization (Shea et al. 2005; Holzer et al. 2007a) due to the potential for generating integrated design alternatives more rapidly. Holzer refers to these processes as *Design Optioneering*. One example of such an integrated design toolbox consisting of parametric modeling software, structural performance simulation software and multi-disciplinary design optimization software was developed to provide feedback between performance results and geometry, and one that enabled a more automated multi-domain workflow for searching for an optimum solution space (Keough and Benjamin 2010). Genetic Algorithms (GA) also have drawn the attention of design computing

researchers interested in optimizing multiple performance criteria (Frazer 1995; Miles et al. 2001; Wang et al. 2005).

In an attempt to pursue alternative methods of solution generation, Genetic Algorithms have been explored. The Genetic Algorithm (GA) was first introduced by John Holland in 1970s and is a heuristic search method inspired by natural evolution processes (Holland 1975). The GA is used for optimization purposes and includes terms and processes such as genes, generations, chromosomes, mutations, cross-over, offspring, and inheritance. The application of GAs in multi-disciplinary design optimization are generally suitable for managing large number of variables and provide lists of optimum solutions – a Pareto front - rather than a single solution (Haupt and Haupt 2004).

With regards to design, GAs have been used for pursuing the optimizing of multiple performance criteria. For example, a multi-criteria Genetic Algorithm method was applied to optimize the trade-off relationship between building energy costs and the occupant thermal comfort (Wright et al. 2002). GA-based optimization has also been used to both shape a building's envelope according to simulated energy performance (Tuhus-Dubrow and Krarti 2010) and to size and place glazing elements with regards to expected thermal and lighting performance (Caldas and Norford 2002) thus guiding both the shape and façade of the resulting design. GAs have also been demonstrated as useful for geometrical form optimization (Narahara and Terzidis 2006) and for taking into account construction costs (Rüdenauer and Dohmen 2007; Znouda et al. 2007) and real-estate value (Alfaris and Merello 2008). Another precedent employed GA to optimize structural geometry and was able to identify the optimum solution out of approximately 30,000 possible designs (Flager et al. 2009). Furthermore, recent works have combined parameterization and GA in pursuit of performance optimization (Yi and Malkawi 2009).

Critical to the research is the fact that design is often understood as not having a singular optimum but rather optimality is found through understanding of tradeoffs (Aish and Marsh 2011). Design problems generally are considered as 'ill defined' (Simon 1973) and by virtue are very time consuming given the computing time necessary for detailed search and optimization of very large solution spaces (Goldberg 1989; Turrin et al. 2011). Therefore, GAs are considered a more efficient means for handling complex design problems where a Pareto front of candidates can be evolved and trade-offs can design explored.

3. 'H.D.S. BEAGLE 1.0' PROTOTYPE TOOL

The purpose of H.D.S. Beagle 1.0 is to provide multi-disciplinary design teams with a large number of systematically explored design options that are more rapidly generated than current conventional methods. The tool and method are predicated on automated generation and evaluation of highly coupled design solution spaces. To accomplish this H.D.S. Beagle 1.0 integrates the domains, tasks and tools for conceptual design and conceptual energy analysis with development economics in an automation and optimization routine.

3.1. H.D.S. Beagle 1.0 System Architecture

The H.D.S. Beagle 1.0 development consists of three primary activities: problem formulation, process integration, and design optimization. For the purpose of this research the platforms selected were Autodesk® Revit™ and Autodesk® Green Building Studio™ web-based energy analysis service with a Microsoft® Excel™ based financial model coded into an automation and optimization routine. The overall system architecture is illustrated in **Figure 1**.

3.2. H.D.S. Beagle 1.0: Problem Formulation

The problem formulation is understood as a need to visualize and optimize the trade-offs between the three correlated design domains: design program, energy use intensity, and a financial pro-forma. Design parameters are treated as design problem specific parameters to be specified by the designer such as form driving parameters, site constraints parameters, and level setting parameters. Energy setting parameters are determined according to specific variables for schematic energy analysis. Financial pro-forma parameters are based on a simplified financial calculation model in order to determine net present value of the design in question. Once the design problem has been formalized, the next step is to utilize these parameters to generate possible design alternatives for finding optimality across multiple axes of the objective functions.

3.3. H.D.S. Beagle 1.0: Process Integration

Autodesk® Revit™ is the platform enabling designers to define their geometry through parameter ranges and directed acyclic graph relationships. For our research this is the geometric constraint and solution space definition platform. Autodesk® Revit™ provides the capability to generate

energy models from a conceptual mass family and pass parameters necessary for energy analysis to Autodesk® Green Building Studio™ (Smith et al. 2011). As a result, this platform also serves as an insertion point for the energy settings necessary for a schematic energy analysis calculated through Autodesk® Green Building Studio™. The process utilizes the Energy Setting dialog box within Autodesk® Revit™ which intentionally employs a simplified energy assessment designed to be more accessible at the early stages of the design phase.

Autodesk® Green Building Studio™ is a web-based energy analysis service that serves as the energy simulation engine for H.D.S. Beagle 1.0. Our tool also uses Microsoft® Excel™ to provide, not only a means of containing the financial parameters and formula, but also a platform in which designers can set up design parameter ranges, constraints, space programing requirement and the design score calculation formula. There are currently seven worksheets in the Excel template provided with H.D.S. Beagle 1.0. The function of each template is listed in . Microsoft® Excel™ was selected as the second platform in which designers are able to inform and operate the H.D.S. Beagle 1.0. This was done for two primary reasons 1) extensive familiarity of Microsoft® Excel™ within the professional field of architecture and 2) the clarity provided in organizing data needed by H.D.S. Beagle 1.0 for both parameter boundaries and design score calculations. As design problems are unique combinations of parameters and constraints, the research team found that the most straightforward method was to generate an Excel template from which H.D.S. Beagle 1.0 could extract the user-defined parameter ranges, level settings, and formulae for calculation. The template has been designed to provide flexibility and extensibility to accommodate the broadest range of early stage design decision making problems.

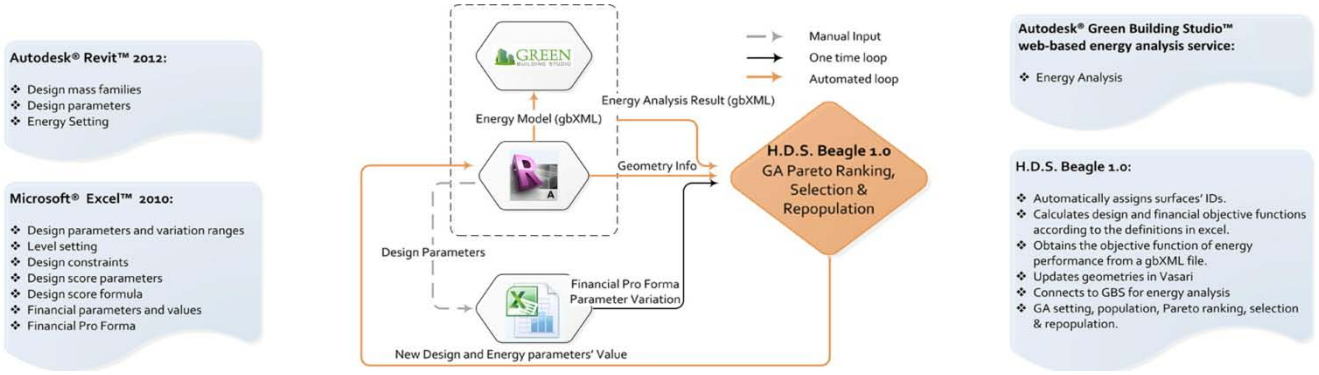

Figure 1. H.D.S. Beagle 1.0 system architecture.

Worksheet Name	Description
GeometryParam	This worksheet defines the parameter names and ranges of the modifiable parameters that relate directly to architectural geometry.
LevelSetting	This worksheet defines the level settings of each mass geometry.
ProjectConstraints	This worksheet defines the project constraints, such as FAR, height, setback, etc. The application will check the model according to the information provided in this worksheet.
DesignScoreParam	This worksheet defines the parameter information that will be used in the DesignFormula worksheet.
DesignFormula	This worksheet defines the calculation method of the design compliance score. Currently, the project uses the difference between the designed space area and the required space area to rank the design.
FinancialParam	This worksheet defines the parameter information that will be used in the FinancialProForma worksheet.
FinancialProForma	This worksheet defines the calculation method of the financial performance. Currently, the project uses Net Present Value (NPV) as the basis of the financial score.

Table 1: H.D.S. Beagle 1.0 Excel template worksheet functions.

In order to integrate the three domains -design, energy, and finance- through the Autodesk® Revit™, Autodesk® Green Building Studio™ and Microsoft® Excel™ platforms, H.D.S. Beagle 1.0 was developed in C# as a plugin for Autodesk® Revit™. Our technology is able to automatically assign unique identification for all surfaces, calculate design and financial objective functions according to definitions provided by Excel, send gbXML and retrieve energy simulation results from a gbXML file, and automatically update geometry definitions in Autodesk® Revit™ according to the populated parametric values. In addition, H.D.S. Beagle 1.0 enables user-defined Genetic Algorithm settings including: population initialization method, crossover ratio, mutation rate, tournament selection size, and maximum iteration number.

3.4. H.D.S. Beagle 1.0: Design Optimization

In order to formalize design parameters to be adopted for our GA, encoding was necessary to convert design intent into a language recognizable by the GA. In H.D.S. Beagle 1.0, genes are equal to modifiable parameters, and chromosomes correspond to individuals that are composed of these genes. The GA then optimizes an initialized set of individuals (population) using three main steps: 1) evaluation, 2) selection, and 3) population. These solutions are then evaluated based on a series of "fitness criteria." The "fitness criteria" are defined in H.D.S. Beagle 1.0 by the objective functions of the design solution. The closer to fulfilling all "fitness criteria" the more "fit" a design solution is considered. The more "fit" a solution is, the higher the probability that the solution will be selected to "survive" in the next generation, using a tournament selection (Goldberg 1990). The next population serves to propagate the next generation from these "survivors" through a recombination of genes and mutation. Through this recombination and mutation the population is able to generate more diversified offspring. This three-step process is then repeated, with each cycle representing one step of the evolution, i.e., a new generation. The process is cyclical and continuous until the algorithm converges or other stopping criteria are reached.

Currently, the population method, crossover ratio, mutation rate, selection size, and maximum iteration number are set by the user manually in our tool in order to accommodate for user preference and due to varying complexity and scale of design problems.

The "fitness criteria" of the offspring is determined by H.D.S. Beagle 1.0 based on compliance with defined objectives from the three integrated design domains: design compliance, energy performance, and financial performance. The categories are then used to rank design solutions and identify design solutions with the potential for optimization or trade-off analysis in all three categories. The definition of the objective functions used in determining ranking within these three categories was deliberately bracketed within H.D.S. Beagle 1.0 in order to evaluate the effectiveness of this evaluation methodology. For example, the aesthetic of design is subjective in nature and therefore does not possess the ability to be ranked quantitatively in an accurate and effective fashion. In response, H.D.S. Beagle 1.0's determination of 'Design Compliance' was constrained to the use of meeting specified design program requirements. In order to determine energy performance, the Energy Use Intensity (EUI) provided by Autodesk® Green Building Studio™ was chosen as the objective function representative of the energy performance category. The objective is to identify and explore the potential design solution with the lowest calculated EUI. The financial performance's primary goal was to reflect the expected initial cost of different geometry configurations, potential returns, and maintenance costs. To provide this information the program extracts relevant information from proposed geometry and translates it into an expected financial cost generated by provided material costs. For the purpose of the initial experiments a simplified version of the net present value formula was utilized to provide broad estimates regarding the cost of construction, operation costs, and expected revenue values. However, when more detailed information is integrated by an owner's market data for example a more accurate estimate of costs and revenues can be generated.

Objective Functions of H.D.S. Beagle 1.0:

Dobj = Max. DRCP
Fobj = Max. NPV
Eobj = Min. EUI
Where
Dobj = Design Objective Function
Fobj = Financial Objective Function
Eobj = Energy Objective Function
DRCP =Design Requirement Compliance Percentage
NPV = Net Present Value
EUI = Energy Use Intensity

In the current version of the H.D.S. Beagle 1.0, there are two mechanisms that will stop the GA; the first is defined by the user as the maximum iteration number when initializing the GA; and the second is defined when the GA reaches the convergent criteria. The convergence criteria is defined when there are three generations that have the same optimal result i.e. there no longer is a quantifiable improvement or difference. At this point the GA will determine the design has reached the optimal solution.

4. CASE STUDIES & ANALYSIS RESULTS

In order to objectively evaluate the performance of H.D.S. Beagle 1.0, testing was implemented utilizing both hypothetical design scenarios and on going real world case studies. Presented here are three design scenarios, all hypothetical, that were tested, ranked and visualized.

For the initial hypothetical scenario, a site on Sunset Boulevard, in West Hollywood was used as the project site.

This selection was made based on the availability of site related information and potential design projects associated with this site. Three scenario examples are used to demonstrate H.D.S. Beagle 1.0's current capabilities and limitations all on the same site. The matrix of geometric complexity, modifiable parameter numbers, running time, and the results and performance are summarized in **Table 2**.

Example 1 as illustrated in **Table 2**, utilized a simple orthogonal box. The purpose of Example 1 was to test and benchmark performance capabilities of H.D.S. Beagle 1.0 and to verify that utilized algorithms had been properly calibrated. With this simple geometry H.D.S. Beagle 1.0 generated 741 offspring according to the user defined GA settings with an average 1.5 minutes per result speed. 18 generations were populated with a measurable increase in performance in all three categories over subsequent generations, thereby verifying the functionality of the optimization algorithms used.

Example 2 explored an extreme geometric case in order to test the limitations of H.D.S. Beagle 1.0. In fact when calculating the energy simulation of this example the maximum number of surfaces capable of being processed by the energy simulation engine was reached. Therefore, while H.D.S. Beagle 1.0 was able to generate new iterations of the design, Autodesk® Green Building Studio™ was unable to provide the energy analysis of resulting designs. H.D.S. Beagle 1.0 is currently limited by surface counts used by the energy simulation engine Autodesk® Green Building Studio™. As a result of this condition a second version of Example 2 was used that involved a design problem with less geometric complexity. Version 2 of Example 2 was able to complete a successful run time of up to 1.5 hours per offspring.

Example 3 provides a more moderately complex geometric design scenario. This was done to demonstrate the feasibility of using H.D.S. Beagle 1.0 in a typical real world scenario such as designing a commercial office building or mixed-use building. In the case of Example 3 an office program was utilized in order to drive the design. For the third experiment 10 generations were populated at 3.5 minutes per offspring. Within 10 generations there was a measurable improvement over previous generations, resulting in design alternatives with the trending potential for optimization in future generations. It should be noted that for the third test case, 10 was set as the maximum generation number for yielding results, therefore convergence of optimization for all three categories was not achieved.

5. CONCLUSION AND FUTURE OUTLOOK

While H.D.S. Beagle 1.0 is still under development this research has successfully demonstrated improvement in ameliorating the design cycle latency between the design, financing, and energy analysis domains. It does so by automating and integrating through parameterization and algorithmic optimization the platforms of the design, energy simulation and financial models. Also, H.D.S. Beagle 1.0 presents a measurable improvement over conventional design and design analysis methods through the application of a genetic algorithm for defining of Pareto optimality. It provides an example of an improved solution space generation and evaluation methodology an example of improved *design optioneering* in early stage design decision-making.

The purpose of this tool is to provide easily accessible performance analysis in a tightly coupled feedback loop with geometric and financial consideration in order to influence early design decision making to be more EUI conscious. While there are questions of process map simplification given the complexity of translating and parameterizing design problems in order to run H.D.S. Beagle 1.0 that potentially require an investment of additional time by designers at the beginning of the process, improving upon this is a key target for the continuation of the research. In so doing the research seeks to further develop, test, and validate a *design optioneering* method to allow for more efficient use by students and practitioners to capture the design intent by integrating parametric modeling with expert analysis domains, which can then generate a large number of alternatives from which to choose optimality more easily. Finally, the potential of our *design optioneering* research to reduce latency, advance domain integration, and enable the quantifiable evaluation of more design alternatives in practice will be furthered through experimenting with high performance computing.

Acknowledgements

We would like to acknowledge and thank Autodesk's IDEA studio, Kimberly Whinna, all the Autodesk personnel who contributed to our progress and in particular Matt Jezyk and John Kennedy for all their help and support.

	Example 1			Example 2			Example 3		
Site Constraints	Lot Area = 21,600 sqft Max. Floor Area Ratio = 6.5 Height Constraint = 180 ft								
Program Requriement	Office Area = 55,000 sqft Hotel Area = 50,000 sqft Retail Area = 40,000 sqft Parking Area = 22,680 sqft			Office Area = 64,000 sqft Parking Area = 22,680 sqft			Office Area Requirement = 140,400 sqft		
Geometry complexity	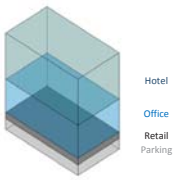 Analyzed Surface Number: 142			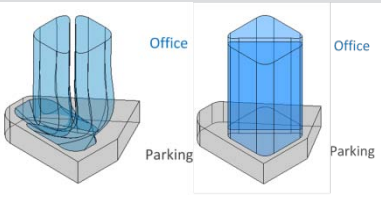 Version 1 Version 2 Analyzed Surface Number: V1. 9547 & V2. 2660			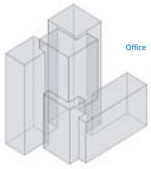 Analyzed Surface Number = 335		
Modifiable parameters	**Name**	**Type /Unit**	**Range**	**Name**	**Type /Unit**	**Range**	**Name**	**Type /Unit**	**Range**
Design parameter	Level#Hotel	Integer	[1,7]	Curvature	Number	[0.1,0.4]	Height_1	Length/ft	[20,180]
	Level#Office	Integer	[1,5]	DifferenceOfWidth	Length/ft	[-10,10]	Height_2	Length/ft	[20,180]
	Level#Parking	Integer	[1,3]	CanyonWidth	Length/ft	[10,30]	Height_3	Length/ft	[20,180]
	Level#Retail	Integer	[1,2]	Level#Office	Integer	[5,18]	Height_4	Length/ft	[20,180]
	LevelHeightHotel	Length/ft	[8,12]	Setback	Length/ft	[5,20]	LevelHeightOffice	Length/ft	[10,15]
	LevelHeightOffice	Length/ft	[8,12]				Level#Office	Integer	[10,15]
	LevelHeightParking	Length/ft	[8,10]						
	LevelHeightRetail	Length/ft	[10,15]						
	Setback	Length/ft	[15,30]						
Global Energy Setting	Percentage Glazing	Number	[0.4, 0.8]	NA	NA	NA	NA	NA	NA
	Shade Depth	Length/ft	[0,2]						
	Percentage Skylight	Number	[0,0.5]						
Run time	1.5 minutes/offsrping			1.5 hours/offspring			3.5 minutes/offspring		
Maximum Generation	18			10			10		
Results	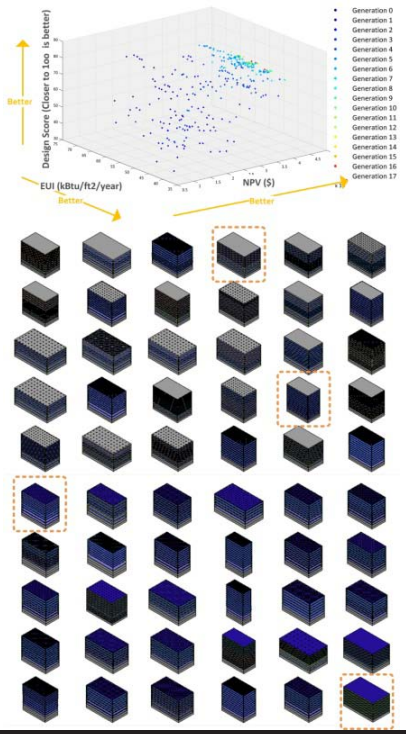			Version 1 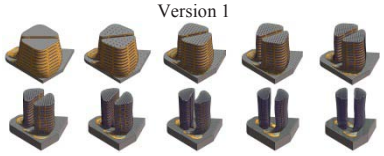 Version 2 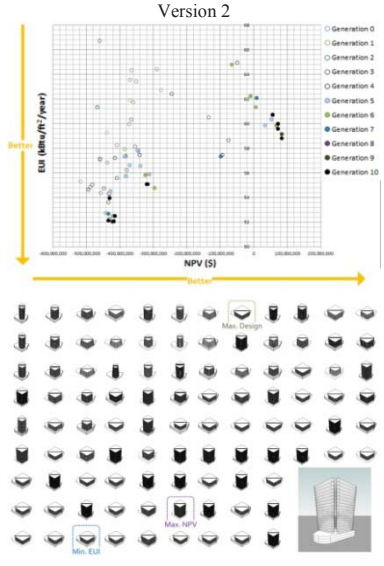			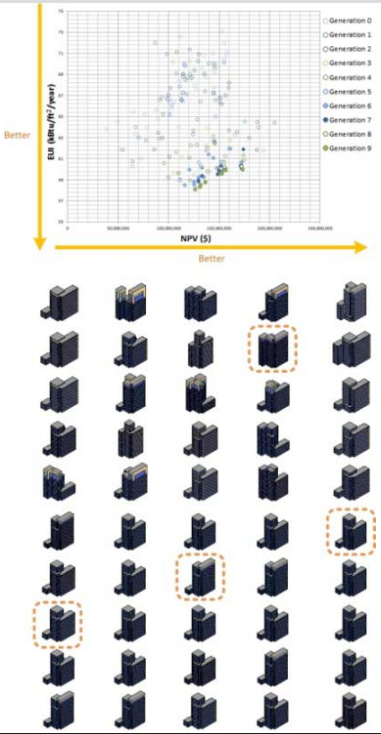		

Table 2: Case Studies Summaries.

References

AISH, R. and MARSH, A. 2011. An Integrated Approach to Algorithmic Design and Environmental Analysis SimAUD 2011, Boston MA, USA.

AISH, R. and WOODBURY, R. 2005. Multi-level Interaction in Parametric Design. Smart Graphics. A. Butz, B. Fisher, A. Krüger and P. Olivier, Springer Berlin / Heidelberg. 3638**:** 924-924.

ALFARIS, A. and MERELLO, R. 2008. The Generative Multi-Performance Design System. Silicon + Skin: Biological Processes and Computation [28th ACADIA], Minneapolis.

BURRY, M. and MURRAY, Z. 1997 of Conference. Architectural Design Based on Parametric Variation and Associative Geometry. 15th eCAADe Conference, Vienna (Austria)

CALDAS, L. G. and NORFORD, L. K. 2002. "A design optimization tool based on a genetic algorithm." Automation in Construction 11(2): 173-184.

COELLO COELLO, C. A., LAMONT, G. B., VAN VELDHUISEN, D. A. 2007. Evolutionary Algorithms for Solving Multi-objective Problems, Genetic and Evolutionary Computation Series, 2nd ed., New York, Spring.

CRAWLEY, D. B., HAND, J. W., KUMMERT, M. and GRIFFITH, B. T. 2008. "Contrasting the capabilities of building energy performance simulation programs." Building and Environment 43(4): 661-673.

EIJADI, D., VAIDYA, P. and BAKER, C. 2011 of Conference. Building Energy Efficiency from the First Decisions. Energy efficiency first: The foundation of a low-carbon society [eceee 2011 Summer Study], Belambra Presqu'île de Giens, France.

FLAGER, F., WELLE, B., BANSAL, P., SOREMEKUN, G. and HAYMAKER, J. 2009. "Multidisciplinary Process Integration and Design Optimization of a Classroom Building." Information Technology in Construction 14(38): 595-612.

FRAZER, J. 1995. An evolutionary architecture. London, Architectural Association.

GERBER, D. and FLAGER, F. 2011. "Teaching Design Optioneering: A Method for Multidisciplinary Design Optimization." ASCE Conf. Proc. 416(41182): 109.

GERBER, D. J. 2009. The Parametric Affect: Computation, Innovation and Models for Design Exploration in Contemporary Architectural Practice. Cambridge, MA, Harvard Design School.

GOLDBERG, D. E. 1989. Genetic algorithms in search, optimization, and machine learning. Reading, Mass., Addison-Wesley Pub. Co.

GOLDBERG, D. E. 1990. "A note on Boltzmann tournament selection for genetic algorithms and population-oriented simulated annealing." Complex Systems 4: 445-460.

HAUPT, R. L. and HAUPT, S. E. 2004. Practical genetic algorithms. Hoboken, N.J., John Wiley.

HOLLAND, J. H. 1975. Adaptation in natural and artificial systems : an introductory analysis with applications to biology, control, and artificial intelligence. Ann Arbor, University of Michigan Press.

HOLZER, D., HOUGH, R. and BURRY, M. 2007a. "Parametric Design and Structural Optimisation for Early Design Exploration." International Journal of Architectural Computing 5(4): 625-643.

HOLZER, D., TENGONO, Y. and DOWNING, S. 2007b. Developing a Framework for Linking Design Intelligence from Multiple Professions in the AEC Industry. CAADFutures 2007. A. Dong, A. V. Moere and J. S. Gero, Springer Netherlands**:** 303-316.

KEOUGH, I. and BENJAMIN, D. 2010. Multi-Objective Optimization In Architectural Design. SimAUD 2010, Orlando FL, USA.

MALKAWI, A. 2005. Performance simulation: research and tools. Performative architecture : beyond instrumentality. B. Kolarevic and A. Malkawi. New York, Spon Press**:** 85-96.

MILES, J. C., SISK, G. M. and MOORE, C. J. 2001. "The conceptual design of commercial buildings using a genetic algorithm." Computers and Structures 79(17): 1583-1592.

NARAHARA, T. and TERZIDIS, K. 2006 Multiple-constraint Genetic Algorithm in Housing Design, Synthetic Landscapes 25th ACADIA.

OXMAN, R. 2008. "Performance-based Design: Current Practices and Research Issues." International Journal of Architectural Computing 6(1): 1-17.

POLONI, C. 1997. "GA coupled with Computationally Expensive Simulations: Tool to Improve Efficiency." Genetic Algorithms and Evolution Strategies in Engineering and Computer Science.

ROLVINK, A., VAN DE STRAAT, R. and COENDERS, J. 2010. "Parametric Structural Design and beyond." International Journal of Architectural Computing 8(3): 319-336.

RÜDENAUER, K. and DOHMEN, P. 2007 of Conference. Heuristic Methods in Architectural Design Optimization: Monte Rosa Shelter: Digital Optimization and Construction System Design. 25th eCAADe Conference, Frankfurt am Main.

SANGUINETTI, P., BERNAL, M., EL-KHALDI, M. and ERWIN, M. 2010. Real-Time Design Feedback: Coupling Performance-Knowledge with Design. SimAUD 2010, Orlando FL, USA.

SHAH, J. J. and MÄNTYLÄ, M. 1995. Parametric and Feature-Based CAD/CAM: Concepts, Techniques, and Applications, John Wiley and Sons.

SHEA, K., AISH, R. and GOURTOVAIA, M. 2005. "Towards integrated performance-driven generative design tools." Automation in Construction 14(2): 253-264.

SHEA, K., SEDGWICK, A. and ANTONUNTTO, G. 2006. Multicriteria Optimization of Paneled Building Envelopes Using Ant Colony Optimization. Intelligent Computing in Engineering and Architecture. I. Smith, Springer Berlin / Heidelberg. 4200**:** 627-636.

SIMON, H. A. 1973. "The structure of ill structured problems." Artificial Intelligence 4(3-4): 181-201.

SMITH, L., BERNHARDT, K. and JEZYK, M. 2011. Automated Energy Model Creation for Conceptual Design. SimAUD 2011, Boston MA, USA.

TUHUS-DUBROW, D. and KRARTI, M. 2010. "Genetic-algorithm based approach to optimize building envelope design for residential buildings." Building and Environment 45(7): 1574-1581.

TURRIN, M., VON BUELOW, P. and STOUFFS, R. 2011. "Design explorations of performance driven geometry in architectural design using parametric modeling and genetic algorithms." Advanced Engineering Informatics 25(4): 656-675.

WANG, W., ZMEUREANU, R. and RIVARD, H. 2005. "Applying multi-objective genetic algorithms in green building design optimization." Building and Environment 40(11): 1512-1525.

WRIGHT, J. A., LOOSEMORE, H. A. and FARMANI, R. 2002. "Optimization of building thermal design and control by multi-criterion genetic algorithm." Energy and Buildings 34(9): 959-972.

YI, Y. K. and MALKAWI, A. M. 2009. "Optimizing building form for energy performance based on hierarchical geometry relation." Automation in Construction 18(6): 825-833.

ZNOUDA, E., GHRAB-MORCOS, N. and HADJ-ALOUANE, A. 2007. "Optimization of Mediterranean building design using genetic algorithms." Energy and Buildings 39(2): 148-153.

A Spatial Query & Analysis Tool for Architects

Ben Doherty[1], Dan Rumery[1,2], Ben Barnes[1], Bin Zhou[2]

[1]BVN Architecture
255 Pitt St,
Sydney, NSW, Australia, 2000
Ben_Doherty@bvn.com.au

[2] School of Information Technologies, J12
University of Sydney
Sydney, NSW, Australia, 2006
drum1335@uni.sydney.edu.au

Keywords: Navigation, Graph, Revit, Python, Distance.

Abstract

There exists a lack of 'off the shelf' and user-friendly computational tools that allow architects and other design consultants to quickly analyse and simulate circulation patterns of buildings. Other developments of such tools have so far failed to penetrate the mainstream market for architectural design software. The research presented in this paper focuses on the development of a graph-based building navigation and distance measurement tool; the Spatial Analysis and Query Tool (SQ&AT), that plugs into the most common design documentation software (Autodesk Revit) with the ability for extension into other tools.

The resulting software allows users to test point-to-point shortest distances, produces several grid based metrics and allows scenarios to be built. These results may expose areas where the designer's intuition and bias has led them to make inaccurate assumptions about quantitative design aspects.

1. INTRODUCTION

Navigation through spaces is a long-standing problem for researchers in robotics and psychology but relatively little empirical work seems to have been done in architecture. Rather than needing to discover the spatial relationships of a building design in the way that a robot or a mouse would, one advantage that building designers have is *access* to all the information about the way that spaces are interconnected. However, the *implications* of the way that those spaces are interconnected are less obvious. The *intention* of the designer will often cloud their rational assessment of the proposal. Humans seem to prefer routes that don't have abrupt changes in direction or sections that backtrack, as if when a person plans a route they have some mental inertia. Computational tools have none of this mental baggage, and will provide routes according to a specification, even if the resulting route looks very strange to its human operator.

The Spatial Analysis and Query Tool (SQ&AT) is a tool that allows designers to test their proposals for distance related queries. It has an interactive user interface and a Python API which enables it to run simple point-to-point shortest route queries as well as more complicated grid-based metrics and scenarios. This paper introduces this tool and gives examples of its use.

2. BACKGROUND

Computational building navigation has been discussed by Steadman (1983) mainly from a topological point of view; where he explores the theoretical challenges to setting up a graph based circulation network. More recently the Design Computing group at Georgia Tech has developed the GT metric graph (Lee et al., 2008, 2009, 2010) as a plugin for the Solibri™ model checker. Their model allows an exported model to be queried for shortest path distances. Internally it uses an approach similar to our own. At a larger scale Aedas Research have been working with urban navigation (Coates & Derix 2008, Aedas R&D 2011) using a similar graph based approach which is queried using a Java applet. Their work is focused on aiding designers and clients in the early stages of a project.

The authors can only speculate on why there has not been wide-spread penetration by building navigation and distance measurement tools. This may be because the current architectural workflow relies heavily on experience and heuristics with accurate checking happening only at the end. This may explain the far greater proportion of the literature devoted to agent based navigation and crowd simulation compared to literature available about spatial queries in architecture.

Computational building navigation can be considered as a series of steps: Parsing the input for salient features (finding walls and doors etc. and discarding information not related to navigation), converting that to a symbolic form, creating a computer navigable model (e.g. a nav-mesh or a vis-graph), and search this model for shortest paths. There may also be another step after these of building sequences of searches that relate to more complicated concepts like regulations.

3. PROJECT OBJECTIVES

This project started in late 2010 as a summer scholarship project in conjunction with [A] University computer science department and is still ongoing at the time of publishing. The scholarship offers students a chance to work on a real project in an industry setting.

Upon the completion of the prototype that was developed during the scholarship it was decided to develop a more robust tool that lead on from the work already completed. The project became a collaboration between academics and practicing architects. Once a study of the existing developments in this area had been completed the authors consulted practitioners actively involved in building design at [B]; using semi-structured interviews to find out their requirements from a tool related to navigation.

The objectives that drove the design and development of SQ&AT were firstly the ability for users to perform queries without interrupting architectural workflow, as identified by the interviews. Secondly, the process of conducting queries must be straightforward and intuitive, as feedback indicated that a requirement for significant additional learning would be enough of a barrier to prevent use of the tool altogether. Existing spatial query tools for architects are limited in their current capacities; so thirdly, in response to this problem, SQ&AT has a high level of extensibility by end users. This goal posed challenges in the addition of a software specific API.

4. SOFTWARE DEVELOPMENT

SQ&AT is a standalone package, but most users will experience it as a Revit plug-in as the generation of the data it consumes is currently done by Revit although it could be implemented elsewhere. Working off a Revit base is motivated by two reasons. The first is mainly pragmatic– our practice uses Revit as our main CAD application, which means that there is a lot of Revit geometry ready for people to use. The second is driven by the desire to have a streamlined workflow, particularly early on. Anything that impedes iterative design process is likely to cause sufficient cognitive stress that teams will simply not use the tool, which defeats its purpose for existence.

4.1. Standards modification

In order to support a workflow that incorporates SQ&AT some additions to the [B] family library were made. Some of these have been automated through batching, and are invisible to regular users while others are new additions to the types of objects that people use in Revit and have required extra training for architectural staff.

Navigable boundaries: The default SQ&AT obstacle boundary finding algorithm wraps a convex hull around a flattening of the 3d representation's vertices onto a 2d plane. For a lot of objects such as a washing machine or a photocopier this is ideal because they have convex boundaries and impede travel. For objects like a rug or a beach umbrella, which have a very different navigable boundary, it is not useful. Until a robust, automatic method of finding these boundaries is implemented, users can modify the generated boundary themselves to provide a polygon that overrides the calculated hull boundary while calculating the vis-graph.

Point markers: Room names are addressable directly in SQ&AT, but specific locations are identified by an XYZ triple. This would be virtually unusable in practice without the UI, so significant locations are marked with a point marker– a custom family that contains a unique name and a point object. This allows queries to be substantially closer to natural language than if they were based on a tuple.

Outside zone: If some sections of a building are only accessible from outside then, unless there is an ‘outside’ room that goes at least to the site boundary, these will show up as disjoint graphs from an adjacency point of view. Therefore they will appear to not be accessible to the other sections of the building. This seems trivial, but often there are spaces like pump rooms and other maintenance facilities that are only accessed from the outside zone.

New parameters: There are a number of objects that have a relevance to navigation. This relevance is captured as shared parameters on the Revit family. Doors in particular have a significant impact on where a certain route can go.

Door valency: certain doors can allow travel in one direction but not the other, for example fire escape doors, turnstiles and entry & exit doors in shops. The navigation graph is implemented to create a directed edge going in each direction. To model door valency in the graph, an infinite cost is placed on the edge that crosses the door in the refused direction.

Security levels: by virtue of their door hardware (locks etc.) not all doors are navigable by all people at all times. The exact specification of security clearance is hard to define cleanly. It is not a neatly nested structure and at its most complex each person could have different access to each room. This is currently implemented in a naïve way until a formal description of security clearance is implemented.

Clear width: Wall insetting is used to limit the space available to paths through spaces. However after insetting doors exist outside these spaces; rendering them inaccessible so they are treated as a special case. A pair of reference planes reports the clear width of the opening of the door. This usually works well, but can fail in some circumstances e.g. if the door swing is interrupted or if the leaf has extra width built onto it. This will be solved with the introduction of the navigable boundary calculator mentioned above.

4.2. Algorithms

In order to support queries related to pathfinding and path distance SQ&AT generates a graph representation of the network of shortest paths in a building, essentially identical to the Universal Circulation Network described by Lee et. al. Door entry points (or other points-of-interest) are represented by vertices in the graph. Each door-to-door shortest path within a navigable space (one or more rooms spatially open to one another) is represented by an edge whose value is the length of the shortest path between the door entry points corresponding to its endpoints. This graph is a Navigation Graph (Nav-graph for short) of sorts, and can be searched efficiently for any shortest path between points of interest in the building.

To get the Nav-graph representation, the SQ&AT core generate visgraphs for each navigable space, on a polygon representing the space's boundary (Minkowski-sum-insetted to simulate path wall-clearance). Door points are included in the visgraph as extra vertices on the offsetted boundary. For each visgraph it finds all shortest paths among door points and points of interest, producing an edge in the Nav graph for each path found. Additional edges are made to connect the door points on either side of each door (these edges essentially represent a path through the centre of the doorway). Each non-door edge is made to reference the shortest path it represents, so that it can construct a visual path representation given a path found in the Nav-graph.

Shortest paths are found using a standard graph search, namely Dijsktra's algorithm.

In the case where an arbitrary point-to-point path search is required, the core first computes, in the appropriate visgraph, a path from the start point to each door point within its navigable space; likewise for the endpoint. These paths are dynamically added to the Nav-graph as additional path edges; with the start and endpoint added as additional vertices. The Nav-graph can now be searched efficiently for a shortest path between these endpoints, and a visual path representation derived from the resulting edges.

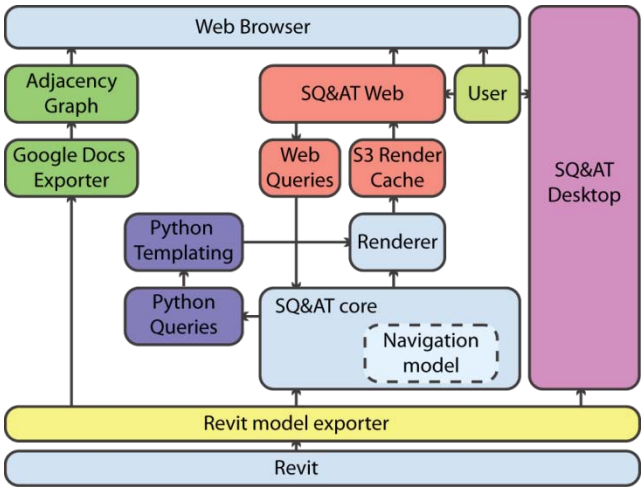

Figure 1. Software architecture.

4.3. Main challenges

Inexact arithmetic and robust geometry computation: Algorithm decisions made on the basis of inexact calculations involving geometric objects can produce invalid or unexpected results (e.g. bad data; a crash due to invalid/inconsistent state) rather than acceptable approximated output depending on the nature of the algorithms used.

Interpreting and manipulating model geometry extracted from the Revit API in a robust way requires, in certain

instances, the use of exact computational methods in order to ensure our tools produce sane results. For example, determining whether or not to add a visibility line edge between two vertices on a room boundary in the vis-graph, when such a line crosses through a near-parallel wall segment, requires careful calculation of a line segment intersection predicate: because these line segments are near-parallel there can be significant variability in the finite-precision calculation of the intersection predicate, leading to both false positives (vislines excluded from the graph when they should be included) and negatives (vislines included in the graph when they shouldn't be). Instead of coding such calculations themselves (a somewhat daunting task when efficiency is also required) the authors implemented a significant portion of the geometry algorithms using the exact geometric predicates and primitives of the C++-based CGAL library.

Separation lines and room merging problems: Revit bounds the conceptual object of a room using bounding elements like walls and columns. Room boundaries also include bounding separation lines, which divide spatially contiguous volumes into rooms. Treating rooms that are spatially open to one another as a single navigable space requires bringing together the corresponding room boundaries to form a boundary of the navigable space; essentially ignoring room separation lines. To achieve this, we join together the room boundary polygons that meet at room separation lines. However, due to the inexact representation of the separation-line boundary segments (extracted through the API), this has proven to be error prone in some cases; leading to room boundaries that remain disjoint despite being spatially open to one another via a separation line.

4.4. Query primitives

These queries can be manipulated by the API to create much more complicated and valuable queries.

Point to single point: This is the most obvious type of query. It simply gives the least cost route through the navigation graph. As our costs are metric distance this returns the shortest route, and its associated information (distance etc.).

Point to many points: SQ&AT can process sets of several start and end points at once. There are a number of ways that the starts can be mapped to the ends, the most straightforward being by corresponding indices, i.e. when the first placed start point goes to the first placed end point and so on. There is also an all-to-all (Cartesian product) option that provides a complete set of paths. The final option finds the shortest path between a set of start points and a set of end points.

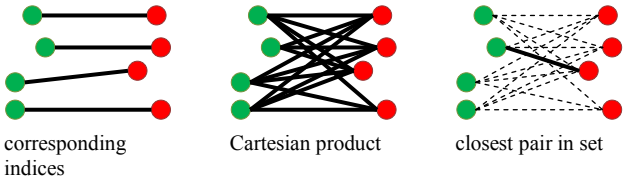

Figure 2. Options for matching starts to ends.

4.5. Desktop interface

This version is available to all Revit users across our studios. This allows designers to get quick feedback at any time.

Users are able to export a SQ&AT file and open it in one step, or open a previously exported file. The export of files, rather than opening SQ&AT directly, produces datasets for the web version and the python version to work with.

4.6. Python API

By exposing the control of SQ&AT through a Python API it allows the tool to become extensible by end users. It is impossible to cater for all users' requirements; this way users can write their own searches for paths that meet certain requirements or test complex situations. The API also interfaces with the Jinja2 Python templating library (Mitsuhiko. n.d.) to enable the generation of reports.

5. APPLICATIONS

5.1. Point-to-point shortest route queries

This type of query is the most straightforward, and the user is offered the choice of start-end combinations as shown in figure 3. Figures 5 through 8 illustrate the point-to-point route querying method and the options of adding rooms/points to visit (figure 6) and rooms to avoid (figure 8).

The user starts with a settings dialogue that allows them to modify the boundary-offset and simplification-tolerance. The offset allows the user to simulate different sized obstacles moving through the space, i.e. a bariatric bed or a person, in much the same way as Lee et al. (2008) do.

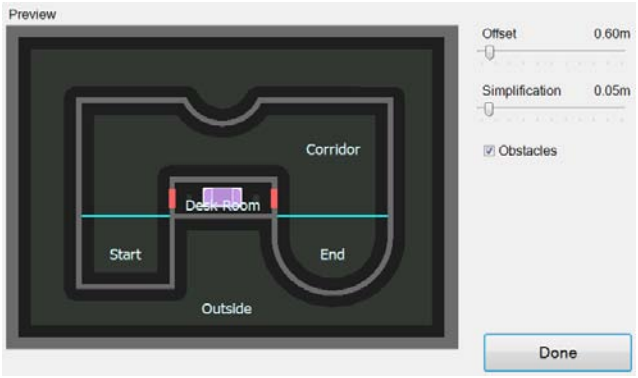

Figure 3. Offset and simplification settings. Once these settings are acceptable the user is then able to start exploring path options.

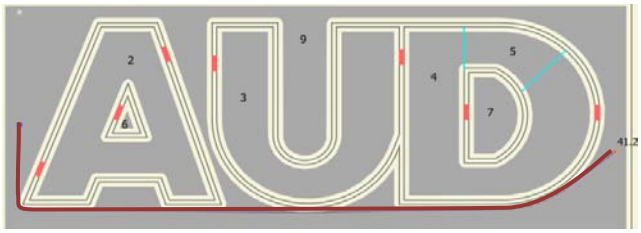

Figure 4. The shortest path from the start point (left) to the end point (right) goes around the interior spaces all together.

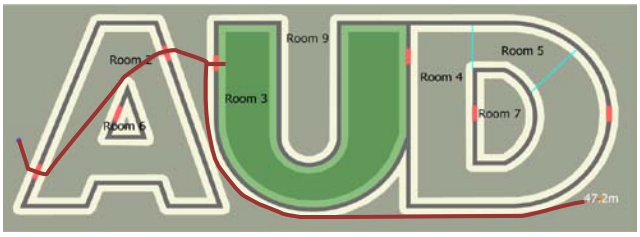

Figure 5. When the requirement to visit somewhere in room 3 is added the path traverses room 2, enters room 3 and then continues the rest of the journey outside as there is no specified waypoint within room 3 and entering it through either of the doors satisfies the requirement.

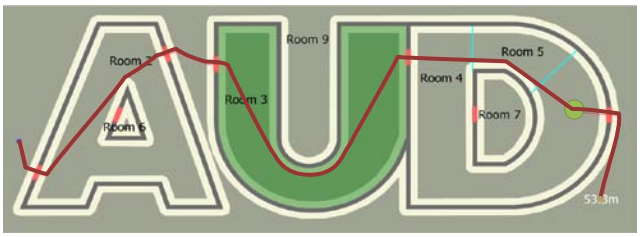

Figure 6. Once a 'through' point is specified near the door in room 4 (the green circle) the path travels all the way through the spaces.

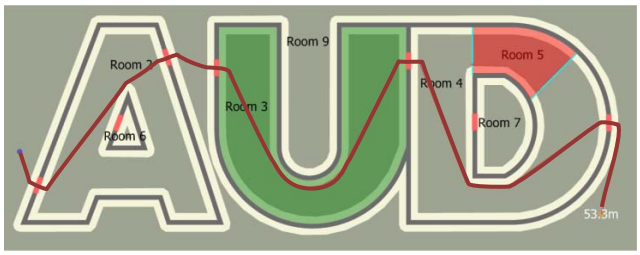

Figure 7. If room 5 is specified as a space that must be avoided the path travels the other way around room 7 to get to the endpoint. It should be noted that only *spaces* make sense as 'avoid'.

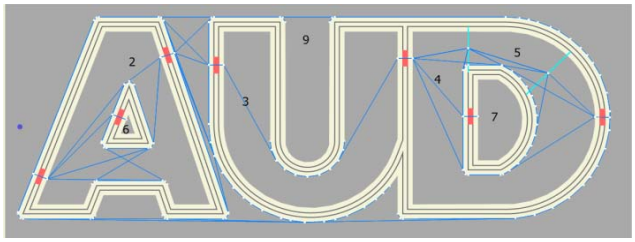

Figure 8. The underlying graph can be viewed to check it for consistency. Edges that end in a concave corner are ignored as they cannot be the shortest path to anywhere.

The paths that the user produces are saved as a series of Python code snippets that can be re-run on another version of the file to allow easy comparisons between versions.

Figure 5, where the path enters room 3, and then immediately leaves in order to satisfy the requirement of visiting that room but still achieve the shortest path, is a good example of the kind of unintuitive result that the authors had hoped to uncover.

5.2. Grid based metrics

There are currently two grid based metrics available. They both lay a grid of sample points over the navigable space. One computes the distance from a set of points that the user has placed to all other points in the model (as shown in figure 9). In the default settings the tool scales the gradient to be fully blue for the longest path, but the user can adjust a slider to change the minimum and maximum extents of the gradient. This can be best seen if the maximum is adjusted; the gradient spreads from the sample points, and arcs emerge as if the frontier was the limit of where a piece of string of that length could go.

This is particularly useful for regulations that state that something must be within a certain distance of a class of other things. For example, if an office chair must be within a certain minimum distance of a printer then a sample point could be placed at the printer, and the maximum extent set; any chair that is still in a red area doesn't comply with the regulation.

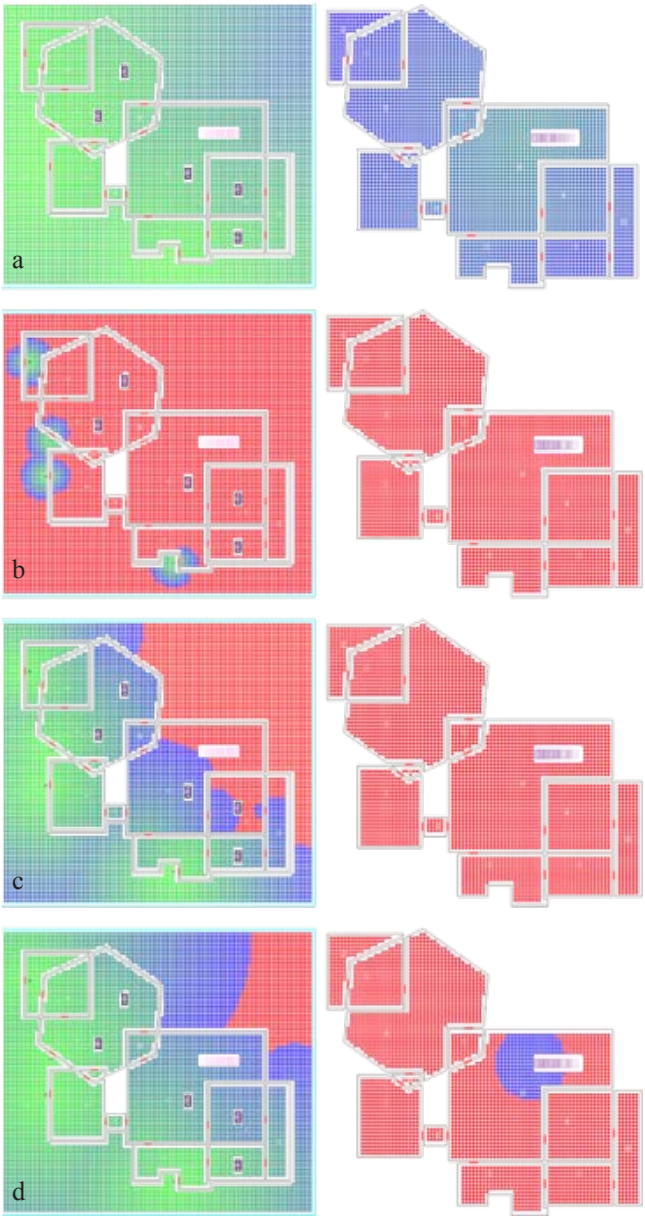

Figure 9. The four doors to this building are tagged as the sample points. a) The gradient is scaled from green: closest to these points, to blue: furthest. b) The maximum allowable distance is set to a much lower value. c) The maximum allowable distance is increased; this shows how the blue frontier bleeds around corners and through doors. d) The maximum distance has started to include a small area of the upper floor.

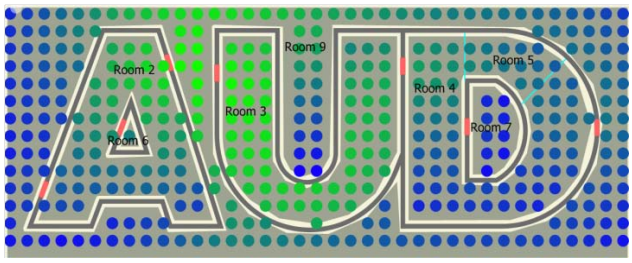

Figure 10. Mean Euclidean path lengths or centrality.

The other is an 'all to all' measure (figure 10) that is similar to spatial integration (Turner, Doxa, O'Sullivan & Penn, 2001), but is geometric rather than topological. It is called centrality in network analysis (e.g. Kang et. al (2011)). This indicates to designers the spaces that are most accessible from all over the building. It might be a good place to put a cafe, or the inverse might indicate some sort of 'loneliness factor'.

5.3. Scenarios

To illustrate how SQ&AT can be extended with our Python scripting interface we go beyond the conventional scenario-testing exercise performed where a single (or small number of) scenario(s) is envisioned and that path is then manually mapped out and measured.

The distance traveled by nurses in hospitals is a constant concern for designers and stakeholders in health care projects. For example, a nurse may visit the patient in bed 1, visit the 'clean and dirty utility' (CDU) then visit patients in bed 1 and bed 4 before heading back to the nurses' station to write up.

In this example the environment is a 30 bed ward with 5 nurses, each one tending to 6 patients. They are not realistic ward layouts, but abstractions designed to provide a clear set of results. Scenarios are built up via a series of calls to a route building function. The routes that each nurse follows are tested against both layouts. Again this is not strictly indicative of the real world, but is an abstraction that prevents randomness from driving one nurse's total path length up uncharacteristically.

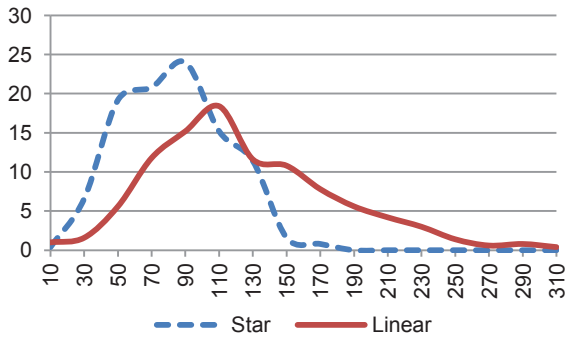

Figure 11. Comparison of nurse journey distance distributions.

In these graphs the horizontal axis is the length of each path and the vertical is the number of times a path of that length occurs i.e. the path length distribution.

Unsurprisingly the star layout has a much tighter distribution of nurse travel distances (figure 11), and these are also further to the left meaning that a greater proportion of those nurses' day can be spent tending patients rather than walking.

These results could conceivably be calculated directly but this methodology allows for a more exploratory way of working, and allows less technical people the opportunity to develop scenarios simply by describing the possible decisions that might be made in a health care environment. It is also considerably faster than a comparable agent simulation, and can run with far less information provided at the outset.

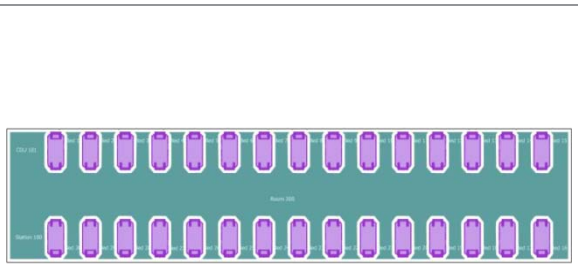

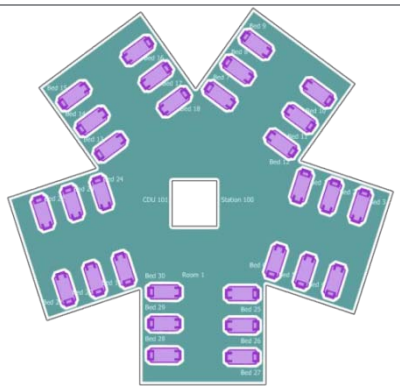

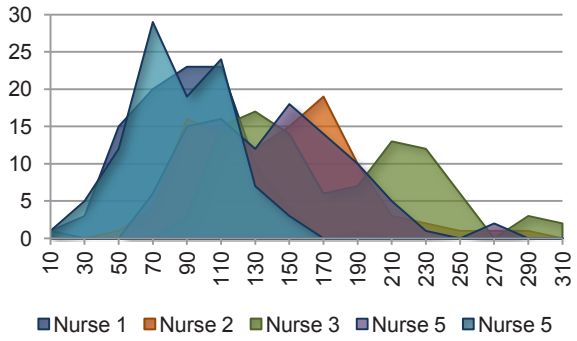

	Nurse					Total	
	1	2	3	4	5	Max	Avg
Min	10	10	10	10	10		
Max	183	277	380	266	149	360	251
Ave	79	131	164	129	76	164	116
Stdev	30	46	60	45	29	60	42

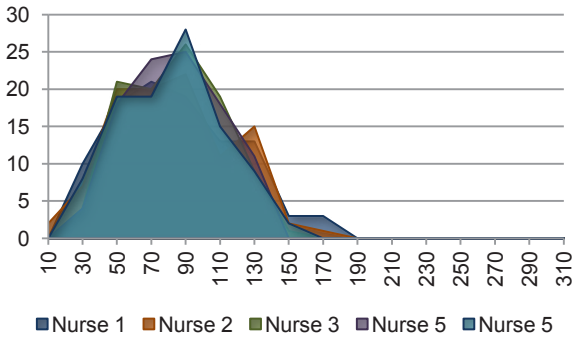

	Nurse					Total	
	1	2	3	4	5	Max	Avg
Min	10	9	16	16	16		
Max	162	151	133	124	136	162	141
Ave	73	72	73	73	71	73	73
Stdev	35	33	28	26	29	35	30

Figure 12. A templated output driven by the API.

6. DISCUSSION

SQ&AT is still very much in its infancy. It is being continuously developed, with updates being included in the fortnightly [B] tools releases and there is constant refactoring work to make components available to other projects. The underlying engine allows for many more query types to be developed; there are many distance-related building codes that could be encoded (taking inspiration from *Depthmap* (Turner 2001) and *Syntax2D* (Turner et al. 2008) for example), and many of the traditional Space Syntax analysis methods can be easily added e.g. axial lines and isovists with very little extra code.

This research could be extended by parallelizing queries that involve significant compute times to allow simulations that involve large datasets and developing an alternative underlying data structure that uses a navigation mesh rather than a visibility graph, which trades accuracy for performance.

The frustrations posed by geometry calculation and the shortcomings of the current Revit API were a significant hurdle, but now that they have been overcome to some extent the ability to quickly and robustly measure distance from with their design environment has been enthusiastically welcomed by staff at [B], particularly the sample point queries (figure 10).

The most important future developments are human issues. As a part of the release schedule the authors continue to conduct user testing to improve usability and also to discover how differing user groups really use the tool and how they would like it to be extended.

References

AEDAS R&D. (2011). Accessibility and Movement. aedasresearch.com. Retrieved from http://goo.gl/oV1H1

COATES, P., & DERIX, C. (2008). Design support systems for sustainable development in the Thames Gateway area of London: "Smart Solutions for Spatial Planning "(SSSP). eCAADe

COMPUTATIONAL GEOMETRY ALGORITHMS LIBRARY. (N.D.). CGAL. Retrieved from http://www.cgal.org

EASTMAN, C. M., LEE, J.-MIN, JEONG, Y.-SUK, & LEE, J.-KOOK. (2009). Automatic rule-based checking of building designs. Automation in Construction, 18(8), 1011-1033.

HELBING, D., MOLNÁR, P., FARKAS, I. J., & BOLAY, K. (2001). Self-organizing pedestrian movement. Environment and Planning B: Planning and Design, 28(3), 361-383. doi:10.1068/b2697

HÖLSCHER, C., BRÖSAMLE, M., & VRACHLIOTIS, G. (2011). Challenges in multilevel wayfinding: a case study with the space syntax technique. Environment and Planning B: Planning and Design, 1-20.

KANG, U., PAPADIMITRIOU, S., SUN, J., & TONG, H. (2011). Centralities in Large Networks Alg orithms and Observations. SIAM International Conference on Data Mining.

LEE, J.-K., EASTMAN, C. M., LEE, J.-MIN, JEONG, Y.-SUK, & KANNALA, M. (2008). Accessable Distance Measurement Using The GT Metric Graph. Environments, (May), 142-149.

LEE, J.-KOOK, EASTMAN, C. M., LEE, J.-MIN, KANNALA, M., & JEONG, Y.-SUK. (2010). Computing walking distances within buildings using the universal circulation network. Environment and Planning B: Planning and Design, 37(4), 628-645.

MITSUHIKO. (N.D.). Jinja2 (The Python Template Engine).

PENN, A., & TURNER, A. (2002). Space syntax based agent simulation. Pedestrian and Evacuation dynamics, 99–114.

STEADMAN, P. (1983). Architectural morphology: an introduction to the geometry of building plans.

TURNER, A. (2001). Depthmap: a program to perform visibility graph analysis. Proceedings 3rd International Symposium on Space Syntax

TURNER, A., DOXA, M., O'SULLIVAN, D., & PENN, A. (2001). From isovists to visibility graphs: a methodology for the analysis of architectural space. Environment and Planning B: Planning and Design, 28(1), 103-121

TURNER, J., WINEMAN, J., PSARRA, S., JUNG, S. K., & SENSKE, N. (2008). Syntax2D. Regents of the University of Michigan.

WEBER, J., & QVIST, I. (2011). Farseer Physics Engine. Farseer. Retrieved from http://farseerphysics.codeplex.com

Combining Sensitivity Analysis with Parametric Modeling to Inform Early Design

Julien Nembrini[1], Steffen Samberger[1], André Sternitzke[1] and Guillaume Labelle[2]

[1]Structural design and Technology
Universität der Künste
Berlin, Germany, D-10623
nembrini@udk-berlin.de

[2]Media & Design Lab
EPFL Station 14
Lausanne, Switzerland, CH-1015

Keywords: Early design, parametric modeling, scripting, thermal analysis, BPS, sensitivity analysis.

Abstract

By combining parametric scripting with building performance simulations, this work presents how sensitivity analysis can help in the early stages of the design process.

By providing quantitative analysis of parameters that influence chosen performance metrics, we can increases the capacity of designers to arbitrate between conflicting performance and design goals. Using a scripted environment linked with EnergyPlus and by using the Morris screening method, we present our approach through a case study. Experiments show the influence of model simplifications and the number of trajectories on accuracy. Qualitative results enable the singling out of specific parameter effects on performance, thereby representing effective design assistance.

1. INTRODUCTION

Early on in the architectural design process, variants are typically explored in parallel until only one dominates and takes precedence. During this time, design elements such as context, overall form and typology are only partly defined and evolve and solidify as the design process unfolds. Unfortunately in practice, indoor climate rarely plays a preponderant role in driving design, despite the dramatic impact on performance that decisions taken at that time have (Hönger et al. 2009). As a result, indoor comfort is often only subsequently addressed, resulting in an overly strong dependence on building technology to guarantee comfort and performance needs.

Finer design details such as window openings or shading elements are typically left to later design stages. However, such details have great impact and interact strongly with form and context (Hensen 2004). The aim for a better performing built form thus requires consideration of the entire building system and need to include all relevant elements at all levels of detail.

To this end, use of computer models for early design performance assessment by designers has demonstrated that higher levels of sustainability can be achieved (Bambardekar and Poerschke 2009). However, such non-expert usage of building simulation tools is controversial, with arguments for and against the development of simplified tools and simplified interfaces to expert-level tools.

In parallel, in the architectural design practice and in research, we have observed a growing use of *scripting* and the use of *parametric design*.

We define *scripting* as using computer (visual) code instructions to define architectural form. *Parametric design* enables the maintaining of dynamic links between parameters and their use. Individually, these concepts can be used in form definition to achieve real-time continuous modifications. By coupling parametric scripting to Building Performance Simulation (BPS), we enable non-experts in generating design details and running fully-featured BPS tests in the early design stages. By using parametric modifications, we enable the exploration and comparison of alternative designs in achieving performance goals.

The present study shows how a parametric model in conjunction with a simulation engine naturally lends itself to sensitivity analysis (SA). It allows the identification of key parameters that influence building performance and aims at "assisting design" instead of automating it (Struck et al. 2009).

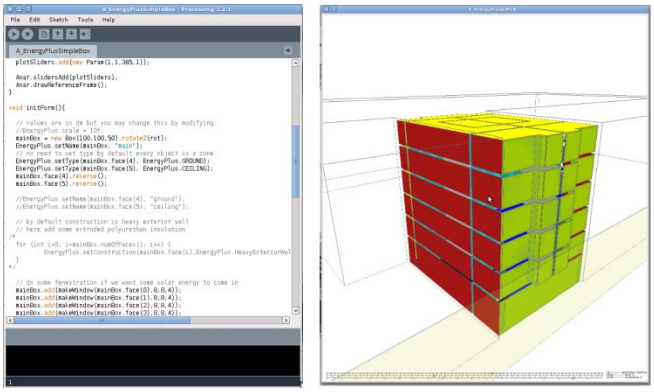

Figure 1. The ANAR+ framework decouples model describing code (left) from the 3D representation (right).

2. APPROACH

We propose a specific approach to generating a model description by exclusively using code instructions. Starting with hand sketches, designers write shape-describing code and compile it to represent the model (Fig. 1). This results in decoupling *form definition* from *form representation* and forces designers to "think before modeling". Decoupling forces designers to apply changes to the code rather than directly on the representation and engages them in a *reflexive process* in the sense of (Schoen 1983).

Specifying material properties and input detail by means of instructions allows for the involvement of fully-featured, validated BPS from the beginning. Although limited in absolute terms by users' lack of expertise, early testing provides insights into building performance. Furthermore, given a parametric model, Sensitivity Analysis can be used to automatically quantify the parameter influences on specific performance metrics. Incoherent results are seen and understood early, and invalid designs rejected. When parameter influences on building performance are observed and studied, designers embark upon *reflection-in-action* and focus attention on specific areas of the design space.

As a case study, a housing building in an urban infill context is considered. By using an alternative functional layout and its interplay with environmental conditions (Fig. 4), the performance of numerous variants spanning the whole parameter space are explored. Specific parameter influences are studied as well as the consequences of model simplification with respect to computing time and sensitivity measures.

3. RELATED WORK

Given interface and tool democratization, there are numerous examples of performance-based design. However, many such examples tend to mirror tool availability and capabilities whose relevance to the design question are crucial to producing meaningful results (Kolarevic and Malkawi 2006). The difficulty in assessing the quality of results by designers, who are non-experts in simulation, raises a conceptual question on the overall scheme (Ibarra and Reinhart 2009), especially since the final building performance is tributary to choices made at early design stages.

There have been several proposals to overcome the problem, which can be grouped into two categories *simplified tools* and *simplified and reduced interfaces* to expert-level tools (Hensen 2004). Of these two categories, *simplified tools* tend to be more popular (Itard 2005; Urban and Glicksman 2007). However, *simplified* tools over-simplify geometry and can use models considered too unreliable by building systems engineers (Toth et al. 2011).

In contrast, when expert-level tools are given *simplified and reduced interfaces*, usage is restricted to implemented functionality, hindering customization (such as DesignBuilder) or mainly translating geometric information (such as OpenStudio). What this second category lacks is the possibility of tuning accuracy sufficiently to address demanding design questions, such as the potential for natural ventilation (Toth et al. 2011).

The goal of sensitivity analysis (SA) is to assess the influence of uncertainties in input data on a given model output. SA techniques can be categorized into two different sets: global sensitivity methods and local SA. Global sensitivity methods aim at capturing the influence of a given set of input parameters over the whole parameter space. Local SA consists of altering one parameter value at a time to compute the sensitivity around a given point of interest (Saltelli et al. 2008).

The hybrid elementary effect method screens parameter space along multiple trajectories with single parameter changes per step (Morris 1991). The method is quite effective with computationally intensive models prohibiting large numbers of simulation runs.

There are numerous examples of SA applications to BPS (McDonald and Strachan 2001). The majority are interested in assessing model sensitivity stemming from parameter

uncertainties such as material properties, climatic parameters, usage schedules, etc. In standard practice, model geometry is fixed and the uncertainty in predicting the model behaviour is studied. Instead, our research focuses on the high variability of design parameters at early design stages. Using the same technique in a different context and on a different set of parameters provides completely different information: the focus, initially on quantifying simulation accuracy, is shifted towards indicating performance influencing parameters to the designer.

A noticeable exception is the work of Struck, in which the *design option space* is thoroughly studied in different design settings: design studio, built references, and interviews with practitioners (Struck et al. 2009). Potential advantages of the use of SA for design support are outlined and we further argue that the paradigm of parametric design actually makes such advantages straightforwardly available.

4. METHODS

By using validated, expert-level simulation tools, our method restricts the space of possible building designs only by their extended capabilities. The problem is transformed into exposing these capabilities to the user appropriately. To accomplish this, we must first enable fast simulation and fast analysis setup. We then need to allow for different levels of user involvement and interaction and to allow the corresponding learning curves to take place. Finally, we need to allow access to extended - unexpected - capabilities. These three characteristics are believed to be crucial for usage in early design: when unexpected design proposals typically emerge and need to be rapidly compared to standard solutions.

4.1. Scripting framework

To achieve the desired characteristics, our method makes use of the prototype framework part of *ANAR+*, an open source parametric scripting tool used in architectural design studios (Labelle et al. 2009). Implemented as a library extension to the popular coding framework *Processing.org*, the framework primarily concentrates on geometry definition through written code instructions. The graphical user interface allows continuous alteration of parameters through *sliders*, whereas topological transformations must happen through code modifications. This geometric framework is extended by defining sets of higher-level functions (e.g. an *API*) that provide interfaces to expert-level BPS software, such as EnergyPlus.

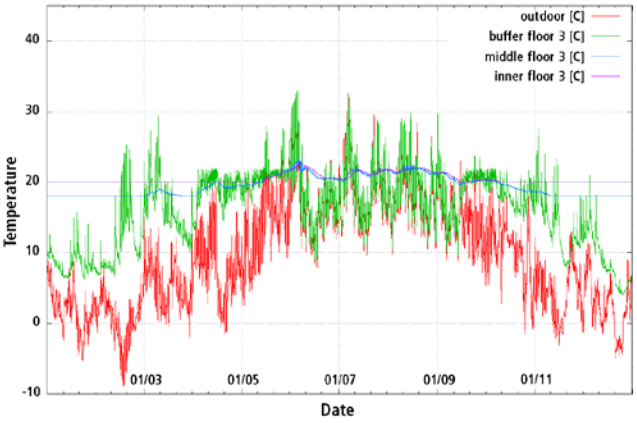

Figure 2. Typical case study showing yearly temperature time series for different thermal zones.

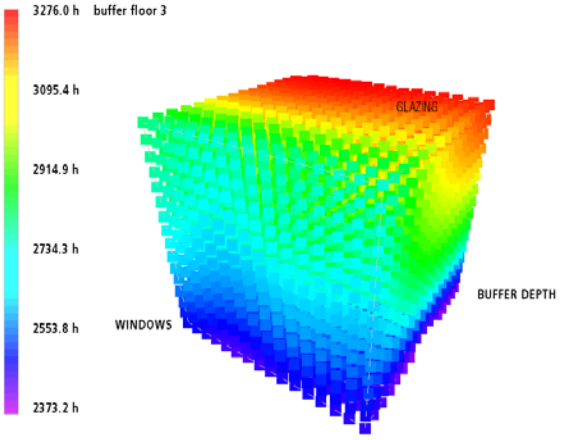

Figure 3. 4D performance visualization of contribution to comfort hours (glazing, buffer depth, inside windows).

By parametrically modifying geometry using the framework, the corresponding thermal gains, solar gains and airflow analysis can be analyzed from the BPS runs, providing the opportunity to explore the influence of parameters on different design alternatives. This is achieved through automatic generation of simulation input from the geometric description, annotated with physical information in a fashion similar to Lagios (Lagios et al. 2010) and Toth (Toth et al. 2011). The interface can be extended to access the full capability of the underlying BPS, addressing needs from non-experts up to advanced users. To speed up simulation, the model can be simplified by excluding thermal zones from the computation (Nembrini et al 2011a, 2011b).

Providing the means to simulate building thermal behavior by itself is not sufficient and doesn't improve the understanding of interactions in a large set of parameters. Exploring variations by hand and making design decisions based on the results can quickly become a tremendous task: simulations typically output yearly temperature time series which are difficult to analyze and compare (Fig 2). Our goal is to assist design, rather than automate it. To accomplish this, we need to translate performance results into a form accessible to the designer and we accomplish this through the use of sensitivity analysis and visualization (Fig. 3).

4.2. Morris Method

Our study uses the elementary effect method (Morris 1991). The method consists of defining trajectories within parameter space from which every position differs from the preceding position by a change in a single parameter by a fixed value Δ. Here, Δ is defined by setting p steps over each parameter range. The elementary effect EE_i of the parameter i for trajectory j is defined as

$$EE_i^j = \frac{Y\left(X_1^j,..,X_i^j,..,X_n^j\right) \pm Y\left(X_1^j,..,X_i+\Delta,..,X_n^j\right)}{\Delta}$$

Y is the model output whose sign depends on whether Δ is increased or decreased between both $X^j = (X_1^j,...,X_i^j,...,X_n^j)$ positions. For T trajectories, the following statistics are proposed by Morris

$$\mu_i = \frac{1}{T}\sum EE_i^j \qquad \sigma_i^2 = \frac{1}{T-1}\sum\left(EE_i^j - \mu\right)^2$$

Here, μ measures the mean parameter influence on the output. The standard deviation σ^2 measures the global parameter effects, either coming from non-linearities and/or from interactions with other parameters. In (Campolongo et al. 2007) an additional statistic μ^* is proposed.

$$\mu_i^* = \frac{1}{T}\sum\left|EE_i^j\right|$$

μ^* is shown to represent a good approximation of the *total sensitivity effect* : a measure of the overall effect of a parameter on sthe output, including effects of interactions with other parameters. The Morris Method is reported to behave well with a number of steps $p=4$ and trajectories of $T=10$, meaning $10(N+1)$ simulation runs are required for analyzing N parameters (Saltelli et al. 2008). The method has the added advantage of computing a global sensitivity measure without a preferred parameter space position. Requiring the specification of a preferred space position can be detrimental to the exploration of design space. A global sensitivity measure also allows for fast screening when the model is computationally expensive.

5. CASE STUDY

To demonstrate the potential of our approach, we consider a case study consisting of an urban infill house in Berlin, Germany. This is a typical context within an existing 19th century continuous square block complete with backyards. Facades typically include oriels (Fig. 4). Although a common situation in the city, the context is abstract and does not correspond to a specific site.

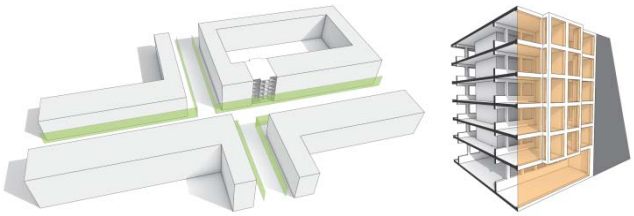

Figure 4. Urban infill housing case study with typical Berlin urban context (left) and facade buffer glazing (right).

5.1. Alternative typology

For demonstration purposes, an alternative typology to uniformly heated space is proposed. Taking inspiration from the work of Lacaton & Vassal (Ruby 2009), we differentiate the outside edge of the building as un-heated, allowing it to act as thermal insulation and usable space. The remaining inner space is heated to standard comfort levels, insulated and double-glazed. The facade is extensively glazed to allow rapid heating through solar radiation in the winter and can be fully opened to avoid overheating in the summer. The space acts as a buffer, protecting from outside weather fluctuations,

After an initial, in-depth hand sketch study, a specific typology was chosen to be parametrically scripted to express constraints, such as global orientation or facade window-to-wall ratios. Additional code generates the detail and material definitions required for EnergyPlus.

Differing thermal conditions in the typology are described in the simulation model by dividing floors into the *thermal zones* labeled: *buffer space*, *middle* and *core*. Although regarded as a typically difficult task for architects, it is argued here, that linking such a task with simulation,

directly sets typology design in relation to usage and performance.

By using automatic model translation into Energy Plus, advanced design techniques, such as the use of natural ventilation, can be explored simply by using the *airflow networks* feature. This makes these design features available to non-experts, while the coding interface allows further, fine-grained control of the simulation model. In order to model inner zone heating, an idealized HVAC plant model is used and is always able to meet heating or cooling demands.

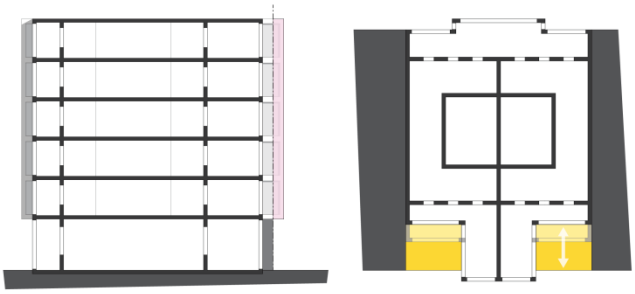

Figure 5. Case study plan and section, displaying the oriel depth parameter (left) and façade set-off (right).

The final building in the case study is composed of 6 floors. Each floor, except the ground floor, have 3 buffer spaces: two on the street side and one in the backyard. The two middle zones are heated to 19 degrees while the two inner core zones are heated to 24 degrees (see Fig. 5). This results in a total of 38 zones. In previous work, we have shown that airflow modeling is crucial to effectively cool using natural ventilation, especially when considering the potentially large solar gains in buffer spaces and the environment in Berlin (Nembrini et al. 2011a, 2011b). Our previous work also presents how the framework allows for the exploration of how variations of the outside window to wall ratio influence performance and the comparison between reference and alternative typology cases.

5.2. Parameters

At early design stages, parametric models typically have a great number of driving parameters. Even with instant performance assessment, exploring this richly multidimensional parameter space is impossible by hand, even for only moderately complex cases. Morris screening provides us with an established method to quantify a given parameter's influence. Table 1 shows the parameters chosen for our case study.

Name	Description	Min	Max	Unit
Buffer depth	Depth of street facade buffer spaces	1	6	m
Windows	Window-to-wall ratio of inner windows	20	50	%
Glazing	Window-to-wall ratio of facade glazing	50	100	%
Set-off	Set-off of the facade from the surrounding street facades	0	4	m
Oriel depth	Facade oriel depth	0.1	1.15	m

Table 1: Case study parameters chosen for experiments.

5.3. Performance metrics

Like a garden, the actual usability of the buffer space depends on outside weather, which naturally leads clients to ask questions such as: When is the buffer space actually usable? Does the buffer space actually help in saving energy?

To answer these questions and to help quantify the influence of our design parameters, we use two performance metrics: *Comfort frequency* and *Energy consumption*. *Comfort frequency* is defined as amount of hours in a yearly simulation in which buffer space is within comfort bounds (17° to 27° C). *Energy consumption* is computed in Kwh/m^2 and changes with heated floor area.

Note that the framework only needs to run the computationally intensive simulations once for a given set of parameters. Performance metrics are then extracted from existing result data and can be repeated. Trial and error on the metrics become part of the reflexive design process and combining them provides deeper insights into the different performance dimensions of a real-world building.

5.4. Experimental setup

In order to understand the impact of model simplification on computed results, case study results for simulating 6 floors (38 thermal zones) are compared to the results from simulating only 3 floors (21 zones, floors 2, 3 and 4) and a single floor (7 zones, floor 3). The cases take advantage of the vertical repetition in the typology. Changes are made transparent to the user who only specifies which zones are included in the model. The necessary inclusion of

adiabatic walls is performed automatically, with the rest of the model remaining unchanged. This improves computation time: the full model takes on average 92 minutes on a 2.53 GHz CoreDuo computer to complete, while the 3 and single floor cases take 25 and 13 minutes respectively, as measured in CPU time. Given that a linear increase in simulation runs is needed for SA, such simplifications allow larger sets of parameters to be screened. For example, a complete model screening for 37 parameters and 10 trajectories requires 24.28 days to complete on a similar machine.

Moreover, as suggested in Garcia Sanchez (Garcia Sanchez et al. 2011), the influence of the number of trajectories on the quality of results is studied by monitoring the evolution of respective parameter sensitivities when taking more trajectories into account. This study uses the single floor simplified model.

5.5. Results

By presenting sensitivity measures using our two metrics, we will first discuss the potential of SA to provide sufficient information to discriminate whether design parameters are influential or not to the given metric. The implication of model simplification on our results is studied, and finally, the number of trajectories needed to reach average equilibrium are studied. For the sake of brevity, only results for measures μ^* and μ are shown.

When considering comfort frequency (Fig. 6), it is clear that SA results enable us to determine that inside window-to-wall ratio or oriel depth have little influence on performance. Considering energy consumption reveals instead that window to wall ratio is indeed an important factor to take into consideration (Fig. 7). Comparing μ^* and μ allows us to understand whether the influence is actually positive (increasing the performance metric) or negative. For instance, increasing outside glazing actually diminishes energy consumption while increasing comfort frequency in the buffer space. Closely studying differences between whole and simplified models show the occurrence of inaccuracies. However, these do not lead to qualitative differences, except on the inside window-to-wall ratio influence over energy consumption. In this case, simplified models globally underestimate energy consumption (Fig. 8).

Looking at the evolution of μ^* with an increasing number of trajectories (Fig. 9) reveals that 10 trajectories are not enough to see mean values stabilize for the comfort frequency, while energy consumption means settle earlier, at least qualitatively. These results suggest using simplified models to define a minimal number of trajectories to take into account and then run the analysis with the most complex model possible, depending on available computing power.

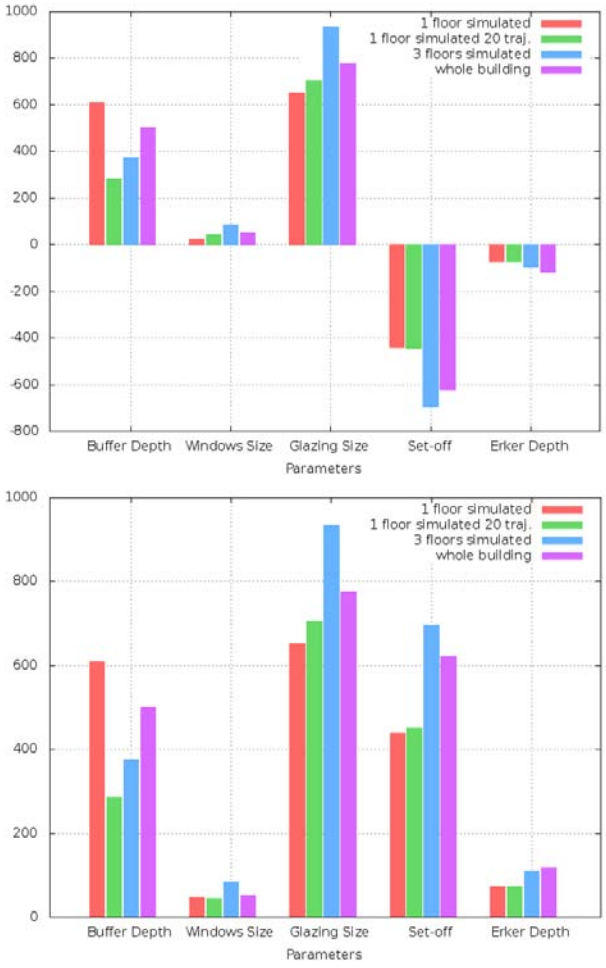

Figure 6. Sensitivity analysis of comfort frequency in hours, (up) μ*, (down) μ.

Note that the sensitivity measure corresponds to a global effect *over the whole range* of a given parameter as defined in the parametric model. Given that changes to ranges influence sensitivity output, the designer has to provide meaningful bounds. Changing the range definition however requires model re-computation since the method is sensitive to the parameter step Δ.

Albeit dependent on the specific case study, these results show how, by generating and analyzing large amounts of data, SA provides an understanding of the respective

influence of several parameters on a given metric. Comparing such influences with multiple metrics focus the architect's attention on dimensions having significant impact on the physical behaviour of the design. Our approach "assists design" by allowing the informed arbitration of conflicting goals.

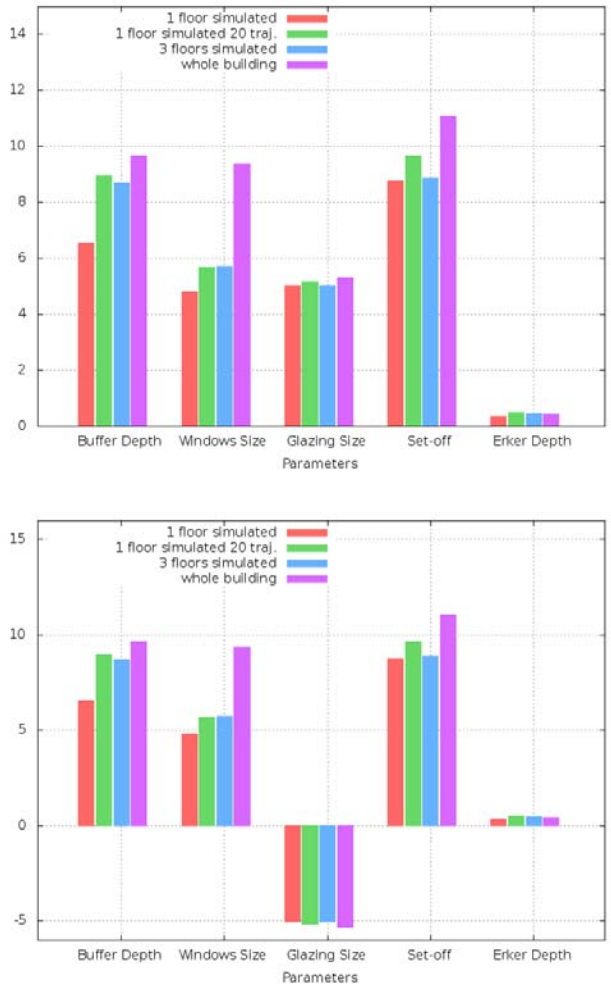

Figure 7. Sensitivity analysis of energy consumption in kwh/m^2, (up) μ^*, (down) μ.

Secondly, SA helps in choosing a level of simplification by monitoring how good the results are. The use of scripting for creating simulation input can easily generate overly complex models, whose increased CPU consumption does not provide any additional useful information. The possibility of balancing qualitative and quantitative feedback suits early design needs for fast feedback and rapid iteration.

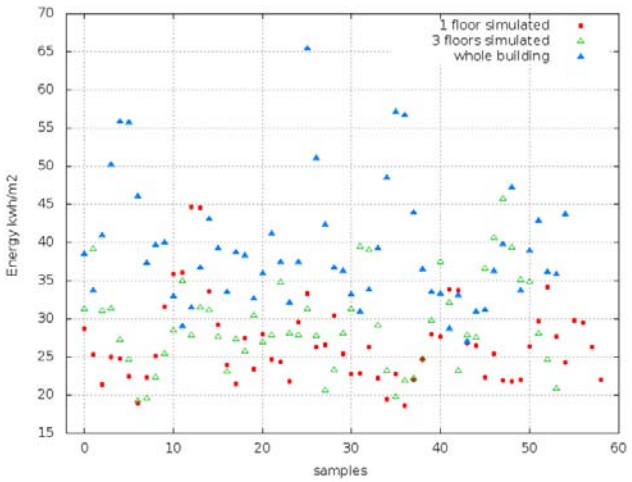

Figure 8. Sample distribution in energy consumption metric over the 60 sensitivity analysis runs according to model simplification

6. CONCLUSION

A common trait in early design stages is to leave options open as long as they are not proven wrong. This often results in developing parallel design variants until only one takes precedence. Another common trait is to open up the range of possibilities being considered, including more experimental choices in order to push the project forward: designers are taught to "think out of the box". The ability to approximate thermal behaviour at early stages as well as to systematically explore design parameter space has been demonstrated and brings valuable insight to the design process.

The advantages of using a parametric scripting interface both to describe form and run performance analysis have been presented. By evaluating the influence of design parameters for an urban infill context and studying the influence of model simplification on result interpretation, the potential for sensitivity analysis in parametric performance-based design has been demonstrated.

Still in development, this research aims to enhance performance capabilities through additional tool modularity in order to more effectively support the design process. Such aptitude for modularity makes the parametric scripting

approach a good candidate to empower designers to intertwine architectonic value with sustainability by conducting meaningful performance analysis.

Acknowledgements

The authors would like to thank the anonymous reviewers for their insightful comments and Alexander Tessier for his help in making the text understandable. Julien Nembrini and Guillaume Labelle are supported by the Swiss National Science Foundation grant numbers PA00P1_129120 and K-12K1-118078 respectively.

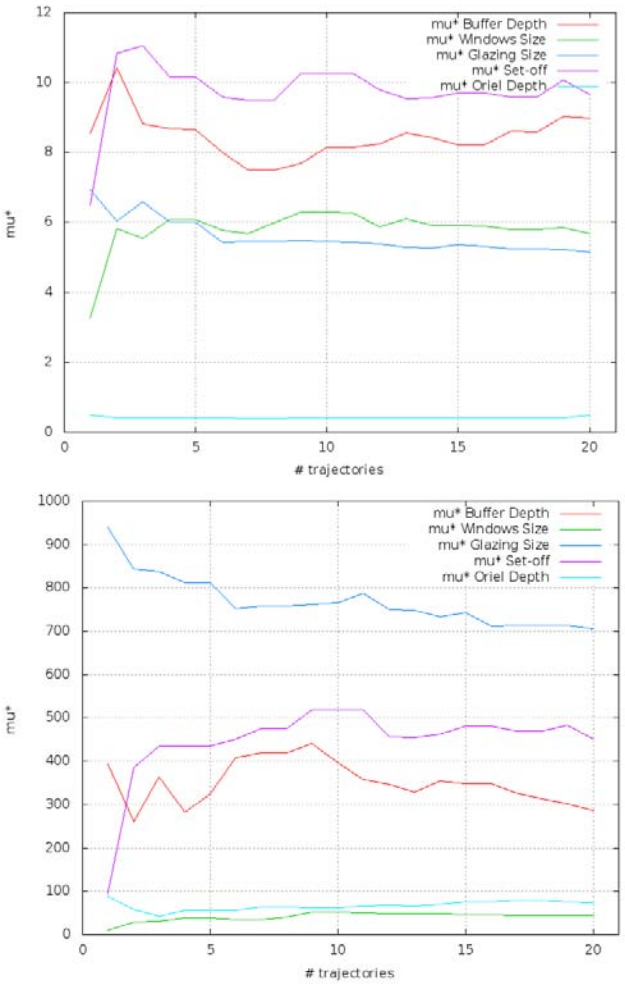

Figure 9. Evolution of μ^* when increasing trajectory number, (up) comfort frequency, (down) energy (single floor model)

References

Bambardekar, S. and Poerschke, U. (2009). The architect as performer of energy simulation in the early design stage. In Building Simulation 2009, 11th International IBPSA Conference, pages 1306–1313, Glasgow, Scotland.

Campolongo, F., Cariboni, J., and Saltelli, A. (2007). An effective screening design for sensitivity analysis of large models. Environmental Modelling and Software, 22:1509–1518.

Garcia Sanchez, D., Lacarriere, B., Bourges, B., and Musy, M. (2011). The application of sensitivity analysis in building energy simulation. In CISBAT 2011, Lausanne.

Hensen, J. L. M. (2004). Towards more effective use of building performance simulation in design. In Developments in Design & Decision Support Systems.

Hönger, C., Brunner, R., Menti, U.-P., and Wieser, C. (2009). Climate as a Design Factor, volume 1 of Laboratorium. Quart Verlag, Luzern, CH.

Ibarra, D. I. and Reinhart, C. F. (2009). Daylight factor simulations how close do simulation beginners really get? In Building Simulation 2009, 11th International IBPSA Conference, Glasgow, Scotland.

Itard, L. (2005). Implementation of exergy calculations in an existing software tool for energy-flow calculations in the early design stage. In Building Simulation 2005, Ninth International IBPSA Conference, pages 459–466.

Kolarevic, B. and Malkawi, A. M., editors (2006). Performative Architecture: Beyond Instrumentality. Spon Press.

LaBelle, G., Nembrini, J., and Huang, J. (2009). Programming framework for architectural design [anar+]. In CAAD Futures'09, Montreal,Canada.

Lagios, K., Niemasz, J., and Reinhart, C. F. (2010). Animated building performance simulation (abps) – linking Rhinoceros/grasshopper with radiance/daysim. In SimBuild 2010, New York, USA.

Macdonald, I. and Strachan, P. (2001). Practical application of uncertainty analysis. Energy and Buildings, 33:219–227.

Morris, M. (1991). Factorial sampling plans for preliminary computational experiments. Technometrics, 33(2):161–174.

Nembrini, J., Labelle, G., and Nytsch-Geusen, C. (2011a). Parametric scripting for early design building simulation. In CISBAT 2011, EPFL, Switzerland.

Nembrini, J., Samberger, S., Sternitzke, A., and LaBelle, G. (2011b). The potential of scripting interfaces for form and performance systemic co-design. In Proceedings of Design Modelling Symposium, Berlin. Springer.

Ruby, A. (2009). Lacaton & Vassal. Editions HYX, France.

Saltelli, A., Ratto, M., Andres, T., Campolongo, F., Cariboni, J., Gatelli, D., Saisana, M., and Tarantola, S. (2008). Global Sensitivity Analysis, the Primer. Wiley.

Schoen, D. (1983). The Reflexive Practitioner: How Professionals Think in Action. Basic Books.

Session 3: Design & Analysis

A Multi-Sensor Based Occupancy Estimation Model forSupporting Demand Driven HVAC Operations 49
Zheng Yang, Nan Li, Burcin Becerik-Gerber, Michael Orosz
University of Southern California (USC)

Preliminary Investigation of the Use of Sankey Diagrams to Enhance Building Performance Simulation-Supported Design 57
William (Liam) O'Brien
Carleton University

Automated Translation of Architectural Models for Energy Simulation 65
Kevin B. Pratt, Nathaniel L. Jones, Lars Schumann, David E. Bosworth, Andrew D. Heumann
Cornell University

Dynamic Annual Metrics for Contrast in Daylit Architecture 73
Siobhan Rockcastle, Marilyne Andersen
Massachusetts Institute of Technology (MIT), Northeastern University (NU), École polytechnique fédérale de Lausanne (EPFL)

Performance Driven Design and Simulation Interfaces: A Multi-Objective Parametric Optimization Process 81
Angelos Chronis, Martha Tsigkari, Evangelos Giouvanos, Francis Aish, Anis Abou Zaki
Foster + Partners

Climatic Based Consideration of Double Skin Façade System: Comparative Analysis of Energy Performance of a Double Skin Facade Building in Boston 89
Mona Azarbayjani, Jigisha Mehta
University of North Carolina (UNC)

A Visual-Performative Language of Façade Patterns for the Connected Sustainable Home 97
Sotirios D. Kotsopoulos, Federico Casalegno, Guglielmo Carra, Wesley Graybil, Bob Hsiung
Massachusetts Institute of Technology (MIT), Politecnico di Milano

A Multi-Sensor Based Occupancy Estimation Model for Supporting Demand Driven HVAC Operations

Zheng Yang[1], Nan Li[2], Burcin Becerik-Gerber[3], Michael Orosz[4]

[1]Unizversity of Southern California 3620 S Vermont Ave Los Angeles, CA, U.S.A 90089 zhengyan@usc.edu

[2]University of Southern California 3620 S Vermont Ave Los Angeles, CA, U.S.A.90089 nanl@usc.edu

[3]University of Southern California 3620 S Vermont Ave Los Angeles, CA, U.S.A. 90089 becerik@usc.edu

[4]University of Southern California 4676 Admiralty Way #1001 Marina del Rey, CA, U.S.A. 90292 mdorosz@isi.edu

Keywords: Building energy consumption; HVAC; Demand driven; Occupancy estimation; Non-intrusive sensor

Abstract

Heating, ventilation, and air conditioning (HVAC) is a major energy consumer in buildings, and. implementing demand driven HVAC operations is a way to reduce HVAC related energy consumption. This relies on the availability of occupancy information, which determines peak/off-hour modes that impact cooling/heating loads of HVAC systems. This research proposes an occupancy estimation model that is built on a combination of non-intrusive sensors that can detect indoor temperature, humidity, CO_2 concentration, light, sound and motion. Sensor data is processed in real time using a radial basis function (RBF) neural network to estimate the number of occupants. Field tests carried out in two shared lab spaces for 20 consecutive days report an overall detection rate of 87.62% for self-estimation and 64.83% for cross-estimation. The results indicate the ability of the proposed system to monitor the occupancy information of multi-occupancy spaces in real time, supporting demand driven HVAC operations.

1. INTRODUCTION

Due to the rising energy demand and diminishing energy resources, sustainability and energy conservation is becoming an increasingly important topic. In the U.S., buildings account for 40% of total energy consumption, 48% of which is consumed by heating, ventilation, and air conditioning (HVAC) systems (DOE 2011). Given the fact that in the U.S., new construction represents only less than three percent of the existing building stock in any given year (Shelley and Roessner 2004) and that buildings are generally in operation for 30 to 50 years, there is great potential of energy savings through improving the operations of HVAC systems in existing buildings. This has attracted considerable attention in the academia and given rise to active research on this topic. The Building Level Energy Management System (BLEMS) project is such a research effort. The objective of this DOE sponsored project is to study the behavior of buildings and that of building occupants, and to proactively and reactively optimize the building energy consumption while responding to comfort preferences of the occupants. The study reported in this paper was completed within the scope of the BLEMS project as a reactive energy-saving measure, which has a focus on estimating the occupancy to support the implementation of demand driven HVAC operations.

In traditional HVAC operations, the ventilation and conditioning demand is assumed to be at the peak based on maximum occupancy during operational hours, and the temperature and humidity are used as the sole inputs in adjusting the operations, which often results in waste of HVAC related energy consumption (Agarwal et al. 2010). Even with improved HVAC systems that run at different capacities at different times of the day, e.g. minimum capacity at off hours, energy can still be wasted e.g. by over cooling unoccupied spaces. The idea of demand driven HVAC operations is therefore proposed and researched in the academia as a way to address such waste of energy. Demand driven HVAC operations replace the assumption that the ventilation and conditioning demand is at the peak with the actual demand based on real-time sensing of the environment. Previous research has proven that the application of demand driven HVAC operations

could save up to 56% of HVAC related energy consumption (Sun et al. 2011). The actual ventilation and conditioning demands depend on various factors that should be input into HVAC systems for energy-efficient operations, among which fine-grained occupancy information is a key input (Agarwal et al. 2010). Occupancy information enables timely reaction to changing ventilation and conditioning demands, and minimizes energy consumption without compromising the occupant comfort.

Due to the importance of the occupancy information, a number of occupancy detection systems have been proposed in previous research, which reported consequent HVAC energy savings between 10% and 56% based on simulations (Erickson et al. 2009; Erickson and Cerpa 2010; Sun et al. 2011; Tachwali et al. 2007; Warren and Harper 1991). However, these occupancy detection systems have certain limitations with respect to their accuracy, cost, intrusiveness, and privacy, and therefore bear potentials for improvement. This paper proposes an occupancy estimation model that has the following features: (1) affordable. This study uses a number of off-the-shelf low-cost sensors; (2) high-resolution. The proposed model can count the number of occupants at the room level with a sample rate of one reading per minute; (3) accurate,. The proposed model can achieve an accuracy of around 85%; and (4) non-intrusive. The system causes little intrusion to either the buildings or the occupants.

2. PREVIOUS STUDIES

Potential benefits of energy savings by implementing demand driven HVAC operations have motivated research efforts in providing effective occupancy detection solutions. CO_2 sensors have been widely used for this purpose (Leephakpreeda et al. 2001; Nielsen and Drivsholm 2010; Sun et al. 2011), as a larger occupancy in a space usually results in higher CO_2 concentrations. However, it usually takes some time for the CO_2 concentration to build up, and the CO_2 concentration is affected by not only occupancy but also other factors such as passive ventilation (e.g. through open windows). Such limitations indicate that the CO_2 sensor based systems are unable to provide accurate and real-time occupancy information by themselves. Researchers have also proposed various video based systems (Benezeth et al. 2011; Erickson et al. 2009; Wang et al. 2010), which detect the occupancy in a monitored space by using image-processing techniques. These video based systems generally suffer from the requirement for line of sight in the monitored spaces, which compromises the applicability of these systems especially in heavily-partitioned spaces. Moreover, the use of video cameras usually requires large image storage space, and can cause privacy concerns among users.

To overcome these limitations, researchers have proposed to use a combination of various ambient sensors. Agarwal et al. (2010) used a magnetic reed switch door sensor and a passive infrared (PIR) sensor for occupancy detection, which could report the actual occupancy most of the time. Their occupancy detection algorithm was only applicable for single-occupancy offices, and was built on an assumption that occupants always keep their doors open when they are in the offices or being somewhere nearby. Meyn et al. (2009) used measurements from cameras, PIRs, and CO_2 sensors, as well as historical data of building utilization, to estimate the building occupancy level. The estimation was done by solving a receding-horizon convex optimization problem. The reported accuracy was 89%. The system was not able to estimate the number of occupants at the room level, and the error tended to accrue over time. Henze et al. (2006) proposed an occupancy detection system that comprised of three PIRs and one telephone sensor for each room and relied on the belief networks algorithm. The system could detect if any occupant was present with an accuracy of 76%, but was not able to count the number of occupants. Dong et al. (2010) proposed a system that estimated the occupancy of a space by sensing the CO_2 concentration, acoustics, and motion in the space. Field tests were carried out in two rooms, with three algorithms including supporting vector machine, artificial neural network, and hidden Markov model. All algorithms yielded an accuracy of around 75%. The authors indicated that the reported accuracy can be further improved. Hailemariam et al. (2011) built an occupancy detection system that used light sensors, motion sensors, CO_2 sensors, and sound sensors. Decision trees algorithm was used to estimate the occupancy of cubicles in an office. An accuracy of 98.4% was achieved using the motion sensor alone, and a decline in the accuracy was reported when other sensors were integrated. The system was not configured to count the number of occupants. Melfi et al.

(2011) proposed a novel occupancy detection system that used existing IT infrastructure. Occupants' MAC and IP addresses, and mouse and keyboard activities are monitored for occupancy detection. Accuracies reported in field tests done in two buildings were around 80% at the building level and 40% at the floor level. The system was not able to detect the occupants that do not use a computer. Hutchins et al. (2007) proposed an approach that could recover missing or corrupted sensor data in occupancy estimation. The proposed approach consisted of an inhomogeneous Poison process and a hidden Markov process. The system was not validated with field tests, and was only applicable at the building level.

3. METHODOLOGY

Radial basis function (RBF) neural network is a multidimensional spatial interpolation approach in a neural network, which is based on the local response feature of biological neurons. RBF neural network has a simple and direct training process, as well as rapid learning convergence rates. It has an efficient uniform approximation property for arbitrary, non-linear functions that make the RBF neural network desirable for the application in this study.

The study is conducted for fitting the estimated occupancy and the ground truth. The data is dispersed, and groups of such data $(x_{ij}, y_i)(i = 1,2,...m; j = 1,2,...n)$ are obtained from the BLEMS sensors. Then a suitable and appropriate analytic expression $y = f(x_j, c)(j = 1,2,..n)$ is used to reflect the relationship between $x_j(j = 1,2,..n)$ and y , which is used to "optimally" approximate the sensor data or fit the ground truth data. The most common way to solve the analytic expression is utilizing parameter selection. For this study, the relationship between the sensor data and occupancy is considered as non-linear, which makes it applicable and necessary to apply the RBF neural network to solve the relationship expression $y = f(x_j, c)(j = 1,2,..n)$ .between sensor data and occupancy ground truth,

RBF neural network is a type of feedforward neural network. The network structure is similar to the multilayer feedforward network, consisting of three layers: the input layer composed of source sensor nodes, the hidden layer with local responding function, and the output layer for response to input. The RBF neural network uses the radial basis function as the basis for hidden units to establish the hidden layers, which are used to convert low-dimensional inputs to high-dimensional inputs. In this way, a linear inseparable problem in low-dimensional space can be made separable in high-dimensional space.

The neuron model of RBF neural network is shown in Figure 1. In this model, the node activation function applies radial basis function, which is always defined as function of Euclidean distance from one arbitrary point to another. Here *x* is the input vector, with the *w as the weight vector; while y is the output vector.*

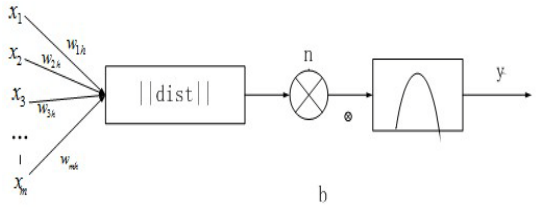

Figure 1. Neuron model of the RBF neural network.

It can be seen in figure 1 that the activation function of the RBF neural network considers the distances $\|dist\|$ between the input vector and the weight vector as independent variables. The general expression of the RBF neural network is:

$$R(\|\, dist\,\|) = e^{-\|dist\|^2}$$

In figure 1, b is a threshold used for adjusting the sensitivity of neurons. As the distances between the weight vector and the input vector reduce, the output of the network will increase. When the weight vector and the input vector converge, the output will equal to 1. Therefore, applying the radial basis neuron and the linear neuron can establish a generalized regression neural network for function approximation.

As aforementioned, the general structure of the RBF neural network contains an input layer, a hidden layer, and an output layer, as shown in Figure 2. The input layer is responsible for transmitting signals. The hidden layer and the output layer have different roles in network, so their learning strategies differ from each other. The

hidden layer adjusts the parameters of the activation function at a relatively low speed for non-linear optimization, while the output layer adjusts the linear weights at a high learning speed for linear optimization.

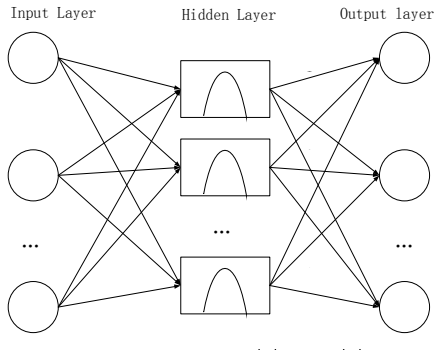

Figure 2. General structure of a RBF neural network.

The RBF neural network has three types of parameters to solve: the basis function centers, the variances, and the weights between the hidden layer and the output layer. The basis function centers are always calculated based by the K-means clustering approach: first of all, *h* training samples are randomly selected as the clustering centers $c_i \left(i = 1,2,3...,h\right)$. Then group these samples according to the nearest neighbor rule, applying the Euclidean distance between x_p and c_i to assign x_p to different groups $\vartheta_p \left(p = 1,2,...,P\right)$. The last step is to readjust the clustering centers, by calculating the mean of training samples in each clustering group ϑ_p. If the new clustering center c_i stays constant, it can be considered as the final basis function center. The second type of parameter is the Variances. As the Gaussian function is utilized as the basis function of the RBF neural network, variances can be generated by the following equation: $\sigma_i = \frac{c_{\max}}{\sqrt{2h}}, i = 1,2,...,h$, in which $c_{\max}$ is the maximum distance between the clustering centers. The third type of parameter is the Weights between the hidden layer and the output layer, reachable by the least square method: $w = \exp(\frac{h}{c^2_{\max}} \| x_p - c_i \|^2)$

where $i = 1,2,...h; p = 1,2,3,...P$

In this study, Matlab was utilized to realize the RBF neural network. Three steps were followed The first step was to design an approximate radial basis function network, this is a trial process of adding the number of neurons in a hidden layer until the output error satisfies the preset value; The next step is to develop an exact radial basis function network based on the input vectors and expansion velocity, compared to the first step, this step requires a quick and error free generation of radial basis function; and the last step is to calculate the returned matrix from the input matrix handled by the radial basis function, compare it with ground truth and finally acquire the error rate.

4. TEST SETUP

BLEMS sensor nodes are built and used in the tests (Figure 3). Each sensor node consists of an Arduino Black Widow stand-alone single-board microcontroller computer with integrated support for 802.11 WiFi. Mounted close to the door at a height of about 1.5 m, each sensor node includes the following sensors: a light sensor, a sound sensor, a motion sensor, a CO_2 sensor, a temperature sensor, a relative humidity sensor, and a PIR sensor that detects objects as they pass through the door. A script is written and uploaded to the sensor node using Arduino to configure the microcontroller to process the raw data. The processed data reported by the sensor node include 11 variables, which can be categorized into three types: instant variables that show the instant output of a sensor at the time the data is queried, including *lighting, sound, motion, CO_2 concentration*, *temperature, relative humidity,* and *reflector* (infrared); count variables that sum the number of times a sensor's output changes in the last minute, including *motion count* and *reflector count*; average variables that show the average value of a sensor's output over a certain period of time, including *sound average* (5 seconds) and *long sound average* (5 minutes). The data is automatically queried every one minute, time stamped, and stored in an SQL database.

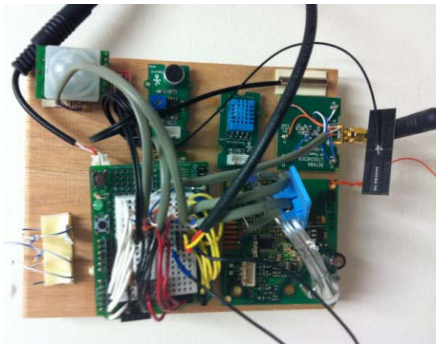

Figure 3. BLEMS sensor node.

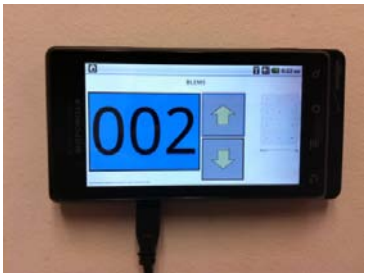

Figure 4. Mobile device used to collect occupancy ground truth.

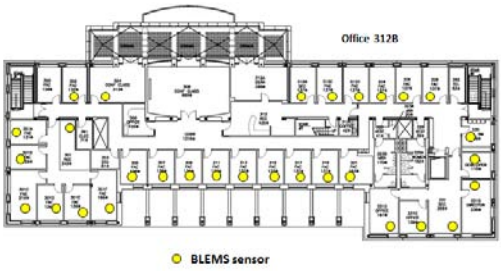

Figure 5. BLEMS test bed layout.

The BLEMS project uses a three-story educational building at the University of Southern California as the test bed. A total of 50 BLEMS sensors are planned to be deployed in the building. Figure 5 shows the deployment on the third floor. In order to train the occupancy estimation model to be used in the test bed building, this study installed two sensor nodes in two multi-occupancy labs and collected sensor data and occupancy data for a period of 20 days. Lab 1 has an area of about 40 m^2, and is shared by 5 PhD students. The lab hosts meetings at times, which can involve up to 10 attendees. Lab 2 has a similar size and is shared by up to 8 PhD students. A touch-screen mobile device is mounted close to the door in both labs to collect the ground truth of the occupancy (Figure 4). During the test period, all occupants are told to log in or out when they enter or leave the lab using the mobile device. The ground truth data is then sent to and stored in the same database where the sensor data resides. In lab 2, a camera is also installed to validate the collected ground truth by manual random spot-checking.

The sensor data was collected for 20 consecutive days, starting from 00:00 AM, Sep. 12th to 00:00 AM, Oct. 1st. At a one-minute sampling rate, after excluding all corrupted data points due to wireless connection breaks, a total of 25,898 data points were collected in both labs. The data is divided into four groups (G1, G2, G3, G4) as shown in Table 1.

Four tests are carried out using different groups of sensor data (Table 2). In order to implement self-estimation, in tests 1 and 2, the model is trained, validated and tested using sensor data from the same lab. In order to implement cross-estimation, in tests 3 and 4, the model is trained and validated using sensor data from one lab, and tested using the sensor data from the other lab.

Period of time	Lab 1	Lab 2
Sep 12th – Sep 21st	12916 (G1)	12934 (G3)
Sep 22nd – Oct 1st	12982 (G2)	12964 (G4)

Table 1: Group of sensor data.

	Training + Validation	Testing
Test 1	G1	G2
Test 2	G3	G4
Test 3	G1,G2	G3,G4
Test 4	G3,G4	G1,G2

Table 2: Test design.

5. TEST RESULTS

Two parameters are defined to evaluate the results. The first one is the root mean square error (RMSE) of the results, which measures the deviation of the estimated occupancy from the actual occupancy. The second parameter is the error rate, which shows the accuracy of all validated data. The concept of tolerance is also introduced. Tolerance measures the tolerated error between the estimated and the actual occupancy. Tolerance is necessary in that for the purpose of driving HVAC systems, a small error can be acceptable, and the

HVAC systems do not need to be adjusted every time the occupancy slightly changes. Due to the initialization random feature, for each step, five experiments were carried out and the best one was chosen for analysis. The following results are all based on tolerance =1.

5.1. Self-estimation

Test 1 adopted all the data from lab 1 for training, validation, and testing. The test yielded an RMSE of 1.202 and error rate of 11.26%, or an accuracy of 88.74%. Test 2 used the data from lab 2 and resulted in an accuracy of 86.50%, with an RMSE of 1.499. To better compare the estimated output and the ground truth to visualize the differences between them, both the estimated occupancy (rounded) data and the ground truth occupancy data are depicted in Figure 6 (test 1) and Figure 7 (test 2). The test results also show that the events when the space switched from occupied to unoccupied or vice versa could be detected by the model 82.35% of the time and 70.13% of the time for test 1 and test 2, respectively.

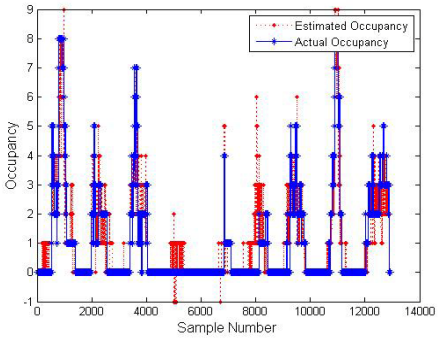

Figure 6. Estimation result for test 1.

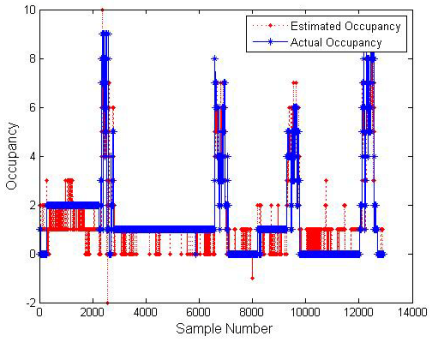

Figure 7. Estimation result for test 2.

5.2. Cross Estimation

Tests 3 and 4 are cross estimation results, where data from one lab is applied for training and validation, and data from the other lab is used for testing. Test 3 utilized the model, which was trained using the data from lab 1 to estimate the occupancy in lab 2. The RMSE was 2.310 and the error rate was 33.57%, or an accuracy of 66.43%. Test 4 utilized the model which was trained using the data from lab 2 to estimate the occupancy in lab 1. The error rate was 36.77%, and the RMSE was 2.743. To better compare the estimated output and the ground truth data to visualize the differences between them, both estimated occupancy (rounded) data and ground truth occupancy data are shown on Figure 8 (test 3) and Figure 9 (test 4). The test results also show that the events when the space switched from occupied to unoccupied or vice versa could be detected by the model 71.21% of the time and 77.04% of the time for test 3 and test 4, respectively.

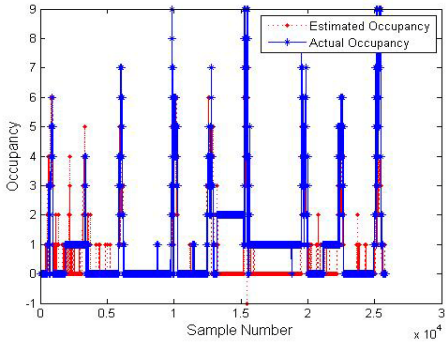

Figure 8. Estimation result for test 3.

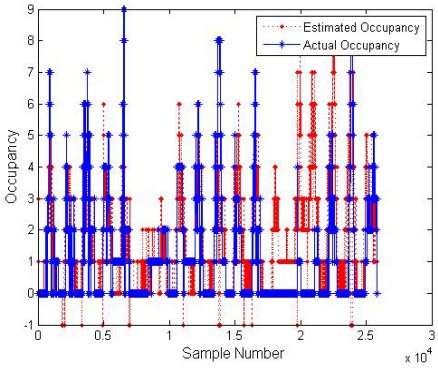

Figure 9. Estimation result for test 4.

6. DISCUSSION AND CONCLUSIONS

The self-estimation test results show that the proposed model can yield accurate estimates of the number of occupants (tolerance=1) 88.74% and 86.50% of the time for lab 1 and lab 2, respectively. The tolerance is necessary because the estimated occupancy is given by the model in a decimal format, which needs to be rounded to compare with the ground truth. The rounding process causes additional errors and need to be offset by the tolerance. In addition, when used for demand driven HVAC operations, a certain level of error is fairly acceptable, as the HVAC systems do not need to be so sensitive that they respond to any slight changes in occupancy. Instead, adding or subtracting one occupant in a room shouldn't cause significant changes in HVAC operations, unless the room switches form unoccupied to occupied or vice versa.

The cross-estimation tests yield an accuracy of 66.43% when the model is trained and validated in lab 1 and tested in lab 2, or 63.23% the other way round. Compared with the self-estimation results, a decline in the accuracies indicates that possibility of having a universal occupancy estimation model, which is trained in one space and used in other spaces, is limited by certain constraints. One such constraint is the differences in environmental settings. For example, there is no window hence no natural lighting in lab 1, and the artificial lighting is always off whenever the lab is unoccupied. Therefore, that lighting sensor reading is zero always indicates the lab is unoccupied. However, the door in lab 2 is always open, and the lighting sensor reading is always positive even late at night, due to the lighting in the corridor. Another constraint lies in the fact that the temperature sensors, humidity sensors and CO_2 sensors used in this study are not calibrated. Therefore, a consistent CO_2 sensor reading of 0.20 may be associated with 3 occupants in lab 1 but 6 occupants in lab 2. For the building level estimation, the authors plan to classify test bed spaces based on their characteristics and implement a cross-estimation model for each category of space. Lastly, the chosen test bed differs from regular office spaces in terms of the behaviors of occupants (PhD students vs. office workers). Therefore the model obtained from this study needs to be calibrated or re-measured before it is applied to office spaces, though the approach used in this study will remain valid.

The proposed system is low-cost and high-resolution. The sensor node prototype cost about $230 USD, and will be even lower if mass-produced. As respect to resolution, the proposed system can provide the occupancy information at the room level, and indicate the exact number of occupants, which can all be done instantly upon users' request.

Acknowledgements

Authors would like to acknowledge the support of the Department of Energy through the grant # DE-EE0004019. Any opinions and findings presented in this paper are those of the authors and do not necessarily reflect the views of the Department of Energy.

References

Agarwal, Y., Balaji, B., Gupta, R., Lyles, J., Wei, M., Weng, T. (2010). "Occupancy-driven energy management for smart building automation." Proc., 2nd ACM Workshop on Embedded Sensing Systems for Energy-Efficiency in Buildings, BuildSys'10, November 2, 2010 - November 2, Association for Computing Machinery, 1-6.

Alpaydın, E. (2010). Introduction to Machine Learning 2nd edition Ed., MIT Press, Cambridge, Mass.

Benezeth, Y., Laurent, H., Emile, B., Rosenberger, C. (2011). "Towards a Sensor for Detecting Human Presence and Characterizing Activity." Energy Build., 43(2-3), 305-314.

Buhmann, Martin D. (2003), Radial Basis Functions: Theory and Implementations, Cambridge University Press, ISBN 978-0-521-63338-3.

DOE. (2011). "Building energy data book." <http://buildingsdatabook.eren.doe.gov/> (Nov. 10, 2011).

Dong, B., Andrews, B., Khee, P. L., Hoynck, M., Zhang, R., Yun-Shang Chiou, Benitez, D. (2010). "An Information Technology Enabled Sustainability Test-Bed (ITEST) for Occupancy Detection through an Environmental Sensing Network." Energy Build., 42(7), 1038-46.

Erickson, V. L., and Cerpa, A. E. (2010). "Occupancy based demand response HVAC control strategy." Proc., 2nd ACM Workshop on Embedded Sensing Systems for Energy-Efficiency in Buildings, BuildSys'10, November 2, 2010 - November 2, Association for Computing Machinery, 7-12.

Erickson, V. L., Lin, Y., Kamthe, A., Brahme, R., Surana, A., Cerpa, A. E., Sohn, M. D., Narayanan, S. (2009). "Energy efficient building environment control strategies using real-time occupancy measurements." Proc., 1st ACM Workshop on Embedded Sensing Systems for Energy-Efficiency in Buildings, BUILDSYS 2009, in Conjunction with ACM SenSys 2009, November 3, 2009 - November 3, Association for Computing Machinery, 19-24.

Hailemariam, E., Goldstein, R., Attar, R., Khan, A. (2011). "Real-time occupancy detection using decision trees with multiple sensor types." in Proceedings of the Symposium on Simulation for Architecture and Urban Design 2011, April 4-7, 2011, Boston, MA.

Hardy, R.L. (1971) "Multiquadric equations of topography and other irregular surfaces." Journal of Geophysical Research, 76(8):1905–1915.

Henze, G. P., Dodier, R. H., Tiller, D. K., Guo, X. (2006). "Building Occupancy Detection through Sensor Belief Networks." Energy Build., 38(9), 1033-43.

Hutchins, J., Ihler, A., Smyth, P. (2007). "Modeling count data from multiple sensors: A building occupancy model." Proc., 2007 2nd IEEE International Workshop on Computational Advances in Multi-Sensor Adaptive Processing, IEEE, 241-4.

Leephakpreeda, T., Thitipatanapong, R., Grittiyachot, T., Yungchareon, V. (2001). "Occupancy-Based Control of Indoor Air Ventilation: A Theoretical and Experimental Study." Science Asia, 27(4), 279-84.

Melfi, R., Rosenblum, B., Nordman, B., Christensen, K. (2011). "Measuring building occupancy using existing network infrastructure." Proc., 2011 International Green Computing Conference, IGCC 2011, July 25, 2011 - July 28, IEEE Computer Society.

Meyn, S., Surana, A., Lin, Y., Oggianu, S. M., Narayanan, S., Frewen, T. A. (2009). "A sensor-utility-network method for estimation of occupancy in buildings." Proc., 48th IEEE Conference on Decision and Control Held Jointly with 2009 28th Chinese Control Conference, CDC/CCC 2009, December 15, 2009 - December 18, Institute of Electrical and Electronics Engineers Inc, 1494-1500.

Nielsen, T. R., and Drivsholm, C. (2010). "Energy Efficient Demand Controlled Ventilation in Single Family Houses." Energy Build., 42(11), 1995-8.

Shelley, I., and Roessner, H. (2004). "RFID tagging." <http://www.global-id-magazine.com/0904/140904.pdf> (Dec. 10, 2009).

Sun, Z., Wang, S., Ma, Z. (2011). "In-Situ Implementation and Validation of a CO2-Based Adaptive Demand-Controlled Ventilation Strategy in a Multi-Zone Office Building." Build. Environ., 46(1), 124-133.

Tachwali, Y., Refai, H., Fagan, J. E. (2007). "Minimizing HVAC energy consumption using a wireless sensor network." Proc., 33rd Annual Conference of the IEEE Industrial Electronics, IEEE, , 439-44.

Wang, H., Jia, Q., Song, C., Yuan, R., Guan, X. (2010). "Estimation of occupancy level in indoor environment based on heterogeneous information fusion." Proc., 2010 49th IEEE Conference on Decision and Control, CDC 2010, December 15, 2010 - December 17, Institute of Electrical and Electronics Engineers Inc, 5086-5091.

Warren, B. F., and Harper, N. C. (1991). "Demand Controlled Ventilation by Room CO2 Concentration. A Comparison of Simulated Energy Savings in an Auditorium Space." Energy Build., 17(2), 87-96.

Preliminary Investigation of the Use of Sankey Diagrams to Enhance Building Performance Simulation-Supported Design

William (Liam) O'Brien[1]

[1]Department of Civil and Environmental Engineering, Carleton University
1125 Colonel By Drive, Ottawa, Canada, K1S 5B6
Liam_OBrien@carleton.ca

Keywords: Building performance simulation, high-performance building design, user interface, design tools, Sankey diagrams

Abstract

Building performance simulation (BPS) is a powerful tool for assessing the performance of unbuilt buildings to improve their design. However, numerous obstacles resulting from limited resources of designers and poor presentation of results reduce the applicability of BPS to design practice. This paper introduces the concept of using Sankey diagrams to represent building energy performance data obtained from BPS tools. While being simple upon first examination Sankey diagrams are complex and reveal many questions that BPS tool users should be considering, including: appropriate spatial and temporal boundaries and model resolution; and it answers questions about how a particular design aspect or technology integrates into the whole building. The paper is a first investigation into the suitability of the application of Sankey diagrams as a tool to communicate BPS data to building designers.

1. INTRODUCTION

Building performance simulation (BPS) tools provide a means to accurately predict a building's performance (e.g., energy use, renewable energy generation, thermal and visual comfort, etc.) long before its construction commences. For the past 40 to 50 years, BPS tools have become more capable (e.g., accuracy and number of building technologies) and more efficient to use (e.g., better user interfaces and software interoperability). However, encouraging the use of BPS tools in early stage building design remains a challenge. This is partly because many BPS tools require detailed design specifications (which take significant time to collect and input) to be operated and because the form of output is not geared at informing designers how to improve upon a design.

One of the most valuable features that design tool developers can provide building designers with is a "big picture" education about how a proposed building performs. One of the most significant barriers to simulation use is communication of results, rather than being purely technical in nature. There is tremendous value in answering the *why*, *when*, and *how* questions and not merely presenting the aggregated predicted building performance data (e.g., total annual energy consumption). This allows "what if" questions to be answered without necessarily performing incremental (one-change-at-a-time) simulations.

Sankey diagrams, which are typically used to represent material or energy flows, have existed for over a 100 years (Schmidt 2008). However, there are very few instances of their application to building energy performance and particularly with the intent of supporting the design process. Those that exist, tend to be simplified and aggregated, and therefore, fall short of educating designers about the operating energy of buildings. Only one building design tool was found that includes Sankey diagrams: CASAnova (IDEAS, 2002). However, its Sankey diagrams are relatively simple and somewhat difficult to follow.

Sankey diagrams have a major advantage over simpler representations of energy use distributions: they show the interrelationships between subsystems. For instance, improving lighting efficiency not only reduces electricity use for lighting, but it also affects the heating and cooling energy of buildings because of the radiant heat gains from lighting. Other advantages to using Sankey diagrams for building design, particularly in the context of modern performance standards, is that they identify and quantify several important metrics such as solar fraction (the fraction of total building energy use that is supplied with solar energy) and the net energy level (difference between energy use and on-site renewable energy generation).

The objective of this paper is to preliminarily address major issues involved in creating Sankey diagrams to represent building energy flows, including: establishing a definition for usefulness of internal and solar heat gains, representing energy conversation processes, representing feedback processes, addressing temporal and energy storage issues, and choosing the appropriate level of model resolution. The theoretical background is supported by an example Sankey diagram for a high-performance solar house. This example demonstrates that creating a Sankey diagram from BPS data is surprisingly difficult and that, without some form of automation of the process, would be impractical to apply in practice at the present.

2. METHODOLOGY

The ultimate objective of this paper is to establish a methodology for converting a BPS model to a Sankey diagram to represent its energy flows. The first step in the process, other than creating a BPS model of a specific building, is to list all sources of heat gains, heat losses, and heat transfer or energy conversion processes and mechanisms. Examples of these that pertain to the example of a passive solar house discussed throughout this paper are shown in Table 1.

<table>
<tr><td>Heat gains
People
Lights
Equipment and appliances
Solar gains</td><td>Heat losses/sinks
Conduction through the foundation or basement</td><td rowspan="2">Heat/energy transfer and conversion processes
HVAC equipment
Equipment that converts purchased energy into heat gains
Conduction, convection, radiation through or between building surfaces and/or openings</td></tr>
<tr><td colspan="2">Heat gains or losses
Conductive gains through the envelope
Short-wave radiation exchange between indoors and outdoors
Ventilation and infiltration heat transfer</td></tr>
</table>

Table 1: Summary of typical heat gains, losses, and energy/heat conversion processes.

Next, the BPS tool must be set up to report timestep variables with as much resolution as desired (as explained in Section 2.5). The simulation should be run one or more times (as explained in Section 2.6). A conservation of energy equation must be formulated that contains all building heat sources, sinks, and heat transfer/energy conversion processes, with the following equation as a starting point.

$$\text{Energy in} + \text{Released stored energy} =$$

$$\text{Energy out} + \text{Stored Energy}$$

An important, and nontrivial, step is to confirm that the BPS results adhere to this balance. Here, the spatial boundaries must be clearly defined, as explained in Section 2.2. For the building envelope, the boundary should probably be within the insulation layer, depending on the construction details. Ideally, it should contain all insulated thermal mass, such that passive storage is included in the analysis, as described in Section 2.4. The boundary for windows is less critical because their magnitude of heat transfer is relatively high compared to their thermal storage capacity. The envelope boundaries should form a bound volume, within which convective heat gains and losses, and all radiant heating and cooling systems exist.

Supposing the conservation of energy is confirmed, the Sankey diagram may be constructed, such as the one in Figure 6. While several commercial software programs exist for creating generic Sankey diagrams, the example was created using MS Visio, for its flexibility. Because Sankey diagrams represent magnitudes of flows by the width of arrows (energy in this case), the conservation can be visually confirmed. The following sections examine various important aspects and complications of creating a Sankey diagram to represent energy flows in buildings.

2.1. Energy Conversion Issues

The relative value of different forms of energy has not been significantly addressed in literature discussing Sankey diagrams. Fundamentally, Sankey diagrams represent a conservation of the quantity being represented (mass, power, energy). In graphical terms, that means that the sum of the widths of all input arrows equals the sum of the widths of output arrows at every process. A number of building processes involve conversion of energy from one form of to another. For instance, ground source heat pumps, which typically deliver (or remove) about 3 to 4 Watts of thermal energy for every Watt of electrical energy input. Note that in the example provided, the energy balance is for thermal energy and that electrical energy input is ultimately converted into thermal energy. It is important to show the sources of energy even if they are not purchased, to

maintain the conservation of energy. In Figure 6, the main source of energy for the heat pump is thermal energy stored in the ground.

An interesting energy conversion issue relates to solar energy, daylighting, and solar heat gains. A Joule of transmitted solar energy may displace a Joule of light energy (e.g., less required electrical lighting) while also reducing heating energy. However, this Joule must not be double-counted; instead, it passes through the system linearly, as shown in Figure 1.

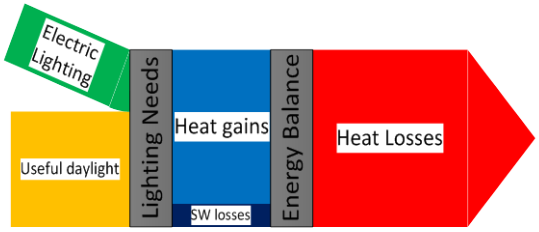

Figure 1. A simple Sankey diagram showing that solar gains used to displace electric lighting eventually turns into heat gains which leaves through a number of mechanisms, including back out glazing in the form of shortwave radiation ("SW losses") .

2.2. Spatial Boundaries

As buildings increase their resourcefulness by obtaining energy from their local surroundings, the question of where to draw the energy boundary becomes more interesting. In the past, the boundary could have been simply drawn at the energy meter (electricity or gas meter) and included the building envelope. However, some newer buildings obtain energy from, or store energy in, the ground (e.g., ground source heat pumps and bore-hole thermal storage). They may also collect solar or wind energy. If these solar collectors are building integrated, the boundary is relatively straightforward. But if the collectors are off-site, care must be taken to ensure that the building gets credit for the energy, and conversely that these energy sources are not double-counted. For example, there are many building-mounted solar collector installations which are operated by a third party. For net-zero energy buildings, for which a thorough examination of definitions (and spatial boundaries) was explored by Torcellini, Pless et al (2006) and Marszal, Heiselberg, et al (2011), a Sankey diagram would clearly indicate that the net purchased energy over a year is zero. One of the visions for the current work is that a Sankey diagram representing individual buildings in a community could be integrated with major energy sources (e.g., electric power plants). This may uncover potential energy conservation measures, such as mutualistic opportunities like using waste or excess thermal energy from one building to supply another.

2.3. Feedback loops

There are several instances of building energy processes where energy is recovered and fed back into buildings. For example, heat recover ventilators (HRVs) use heat exchangers and a fan to recover the sensible energy in exhaust air to pre-heat (or pre-cool) incoming supply air.

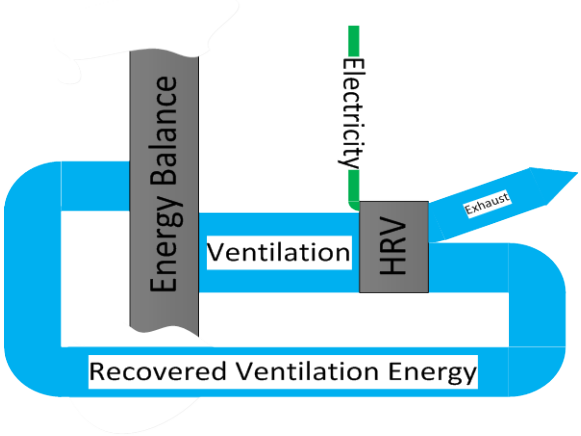

Figure 2. A heat recovery ventilator (HRV) represented as a feedback loop in a Sankey diagram.

There is value in representing this process with a Sankey diagram, as it illustrates the relative energy quantities and may identify instances when heat recovery consumes more energy than it uses (i.e., mild climates when the value of fan electricity use exceeds that of the recovered thermal energy).

2.4. Temporal Boundaries

Traditionally, BPS results have been reported as aggregated values on a monthly or annual level (though for detailed simulation engines, this can be reduced to the timestep-level: seconds or minutes). In understanding the energy flows of a building it is often useful to use a relatively short time period so that designers can focus on one set of weather phenomena at a time. A week was chosen for most examples in this paper for this reason and others that follow. However, there is value in using Sankey diagrams to represent an entire year because this is a single climatic cycle; and ultimately, a high-performance building is one that is robust to all expected weather conditions that it may encounter.

All existing examples of building energy Sankey diagrams that were found in the literature are created with the notion that there is no storage term in the conservation of energy. However, all buildings have some storage (e.g., hot water storage tank), even if it is passive (e.g., a masonry wall). Furthermore, renewable energy systems such as solar thermal systems or electric cars that are connected to photovoltaic systems, include storage. Several buildings or communities have been built to have long-term storage, with thermal storage that takes as long as five years to fully charge or discharge (e.g., Drake Landing Solar Community (Sibbitt et al. 2007)).

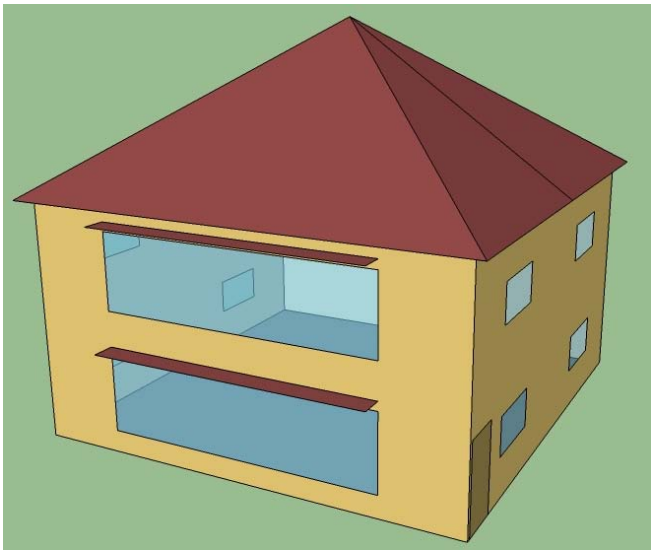

Figure 3. An image of the house that is used for most examples of Sankey diagrams throughout this paper.

Sankey diagrams must either be created to represent buildings for long enough periods that the energy storage (or depletion of storage) is insignificant relative to the energy flow quantities or storage must explicitly be shown. For example, consider the house represented by Figure 3. Note that all remaining results in this paper are based on this house in the Toronto climate. A summation of the energy inputs and outputs during the course of a week in the winter reveals that the house passively stored (i.e., within its inherent structural thermal mass and air contained within it) about 35 kWh (as shown at the bottom of Figure 6). This represents a mere 1°C increase in the interior surface temperature and no increase in the indoor air temperature. This example illustrates the importance of representing a sufficiently long period with a Sankey diagram. Otherwise, the solar gains could be under-credited in usefulness because their benefit extends into the period following that of interest and will not all be realized. It follows that Sankey diagrams can also use storage as an energy source (i.e., entering from the left), just as it is shown as a sink in Figure 6.

2.5. Model Resolution

A question that every building energy modeller should be constantly asking themselves is: how detailed should the model be? There is often an inverse relationship between detail and accuracy; but one with diminishing returns (O'Brien et al. 2011). For instance, a model that integrates two systems that barely interact is cumbersome, yet offers little benefit or insight. Therefore, building modellers must determine the required level of accuracy in the context that achieving greater levels of accuracy may be time-consuming (and costly).

In representing building energy flows with a Sankey diagram, the objective is to inform the designer of strengths and weaknesses of the energy systems components and their integration. Therefore, in general, processes over which the designer has the greatest amount of control should be represented in the most detail. For example, a simple off-the-shelf component (e.g., a furnace) need not be represented in vast amount of detail because the main concern of the designer is overall system performance (e.g., efficiency of primary to secondary energy conversion). In contrast, the designer may have much more control over a wall construction, in which case, showing such details as thermal bridging through framing elements could be useful.

The convenient feature of Sankey diagrams is that they permit the level of model resolution may vary from subsystem to subsystem within a single diagram. For example, one could imagine a user interface in which users could zoom into a particular part of the diagram to investigate it more deeply. One major limitation is that the Sankey diagram cannot be represented in more detail than the underlying BPS model. And, in fact, the tool must also report state variables to sufficient detail. For this reason, detailed BPS engines such as EnergyPlus, ESP-r, TRNSYS, and DOE-2 are favourable over simpler tools.

A major, though understandable, limitation of most BPS tools is that certain quantities are internally aggregated and reported as such. As a result, the ultimate objective of this work to track every Joule of energy from the point it enters

to the point in leaves the building is challenging. For instance, Figure 6 shows all of the heat sources entering the house and sinks to the environment. But it does not specify whether any given Joule entering via the glazing ultimately leaves through the glazing or via some other route. EnergyPlus, which was used for all simulation here, performs an energy balance about the air node, where it is effectively mixed and aggregated. There is a minor exception to this limitation: short-wave radiation can be tracked from source (e.g., light bulb or solar gains) to the point where (and if) it exits a non-opaque surface (e.g., a window).

2.6. Useful, Adverse and Neutral Heat Gains

Buildings encounter many sources of heat gains, including solar gains, electrical equipment and lighting, and metabolic heat of occupants. While usually not being an efficient or intentional source of heating, waste heat from these sources does contribute to heating and can offset purchased heating energy; however, it can also contribute to cooling loads. Under certain conditions, usually in the shoulder seasons, it is possible for these internal gains to not affect heating or cooling loads, if the indoor air temperature remains between the heating and cooling setpoint or if the heat gains the affect the magnitude heat losses (e.g., an elevated indoor air temperature results in greater heat loss from ventilation and infiltration).

Generally speaking, it can be assumed that all energy input into electrical devices (e.g., lights, appliances, equipment) in a building is eventually converted to heat gains in that building. However, several notable exceptions occur, including:

- Short-wave radiation (including the visible range) emitted from lights and displays (e.g., computer monitors) that is transmitted through glazing.
- Appliances that directly exhaust warm and/or moist air to the outdoors (e.g., stovetops and clothes dryers).
- Domestic hot water (DHW) heaters and appliances that heat and then drain water (e.g., dishwashers). It is standard practice to assume that all DHW heating energy is lost through drains without incurring heat gains indoors (Barnaby et al. 2005).

A beneficial calculation before creating a Sankey diagram is to quantify all heat gains in terms of useful, adverse, and neutral. The approach used here is to sequentially perform simulations with and without each type of heat gain. The gains that decrease the purchased heating energy are considered *useful*, the gains that increase the purchased cooling energy are considered *adverse*, and the gains that do not affect heating or cooling are considered *neutral*. The equations used to determine the useful, adverse and neutral heat gains from people are shown below. The same approach is used for all other forms of internal heat gains and solar gains.

$$G_{people,useful} = E_{heating}|_{no\ people} - E_{heating}|_{people}$$

$$G_{people,adverse} = E_{cooling}|_{people} - E_{cooling}|_{no\ people}$$

$$G_{people,neutral} = G_{people,total} - G_{people,useful} - G_{people,adverse}$$

This procedure adheres to the procedure proposed by Balcomb (1992) to quantify the useful solar gains. Specifically, his approach involves performing two simulations: one with the solar gains and one without. This was implemented by creating a modified weather data file with zero solar radiation. It is important to note that it would be inappropriate to limit the analysis to steady-state (e.g., determining the usefulness of solar gains on whether mechanical heating is required at that instant) because solar gains may not be useful at one moment, but may contribute to reducing purchased heating in the future.

There could be many instances where different sources of heat gains "compete" for usefulness. To overcome this, gains are prioritized in order from those that are a given to those that the building designer has control over: people, equipment, lighting, and solar gains. That is, the designer cannot control occupancy as much (assuming that the building is to perform a certain function) as lighting and solar gains. This order is selected considering one of the objectives of this work: to inform designers of building energy performance.

Using the aforementioned procedure, Sankey diagrams were created for the example house for a week in January and a week in July, as shown in Figures 4 and 5, respectively. In the winter week (Figure 4), the majority of the heat gains are useful; owing to the fact that Toronto's

winter climate is cold and thus, heating is on throughout most of the day to compensate for heat losses. Regardless, about 15% of the solar gains do not reduce the heating energy and are deemed "neutral". This 15% is either a result of elevated air and surface temperatures that actually increase heat losses relative to a case without solar gains or that some of the solar radiation is reflected back out the glazing. The heat losses that are not fed by naturally-occurring heat gains must be supplemented with purchased heating (i.e., the heat intentionally delivered by the HVAC system). Note that this analysis is premised on the fact that thermal comfort is considered equivalent for any conditions between the 21 and 25°C setpoints.

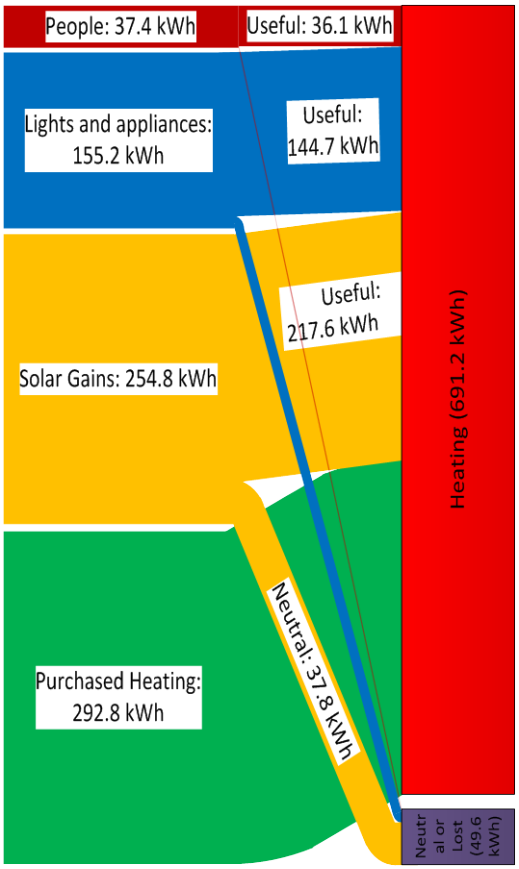

Figure 4. Useful, neutral, and adverse heat gains a mid-winter week.

The summer week (Figure 5) demonstrates that, in fact, without any heat gains, a modest level of heating is required. Furthermore, even with the heat gains from people, lighting, and appliances, the necessary purchased heating is not eliminated. However, the addition of solar gains changes the balance to having a cooling load; and thus, there is a need for some mechanical cooling (50.4 kWh) to maintain comfort throughout the period. The large amount of neutral heat gains indicate that the majority of heat gains are lost before they cause the indoor air temperature to exceed the cooling setpoint.

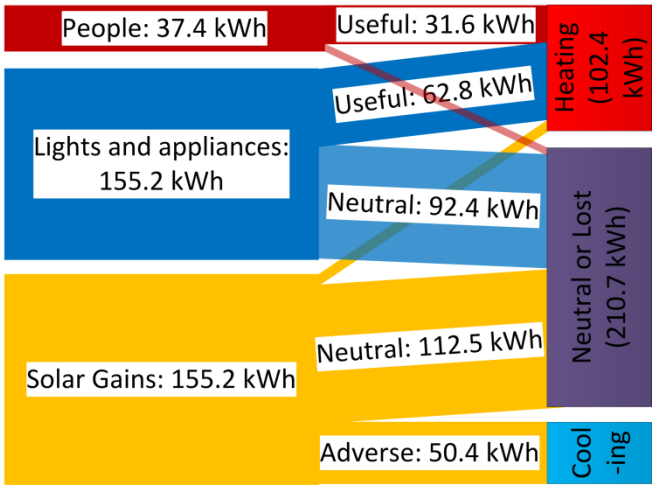

Figure 5. Useful, neutral, and adverse heat gains a mid-summer week.

An important metric for solar buildings (those that meet a significant portion of their energy needs with solar energy) is "solar fraction". Solar fraction is normally defined as the fraction of energy needs that are met by useful on-site collected solar energy. In general, solar fraction is calculated by:

$$f = \frac{useful\ solar\ energy\ collected}{total\ energy\ needs\ of\ the\ sytem\ without\ solar}$$

Where "useful solar energy collected" is the magnitude of the collected solar energy that *actually* reduces purchased energy – not the total amount collected. Solar fraction is frequently quoted for solar thermal systems, but rarely for passive solar performance. Using the Sankey diagram methodology, the passive solar fraction can be efficiently extracted because the diagrams explicitly show useful solar gains. For example, in Figure 4, the total heating energy without the solar gains is found to be 510.4 kWh (the sum of useful solar gains and purchased heating). A second simulation with the solar gains included shows that the heating energy is reduced to 292.8 kWh. Given that the solar gains displace 217.6 kWh of the heating energy, the solar fraction is 43% [217.6/(217.6+292.8)]. This definition of solar fraction for cooling is not applicable because the solar gains clearly have a net adverse effect.

3. APPLICATION OF SANKEY DIAGRAMS TO BUILDING DESIGN

The ultimate objective of this work is to apply Sankey diagrams to inform building designers of the impact of different design decisions. Several methods in which they could be applied to early stage design are:

- Identify the major energy sources and sinks and prioritize those as potential opportunities to reduce purchased energy use;
- Quantify the electrical and thermal interactions between a particular subsystem (e.g., HRV, PV array, window) and the rest of the building.
- Visually compare the energy performance of two different building designs.

4. CONCLUSION AND FUTURE WORK

This paper proposed the outline for a methodology for creating Sankey diagrams to represent energy flows in buildings, with the eventual intent that the methodology be integrated into a software tool. Though Sankey diagrams are a relatively simple means to visualize complex energy flows, the underlying creation process, when performed manually, can be quite complex and requires a high level of understanding of building physics and simulation methodologies. For instance, the first attempt at creating the Sankey diagram in Figure 6 took about four days of research and analysis, despite the fact that the model uses a single zone and ideal HVAC equipment and controls. Much of this was devoted to identifying exactly which variables (e.g., conduction through walls at the inside surface) should be reported and ensuring that the energy into the house equaled the energy out plus stored energy. The greatest challenge was in quantifying total solar heat gains (i.e., transmitted solar energy that eventually flows into the zone via convection and long-wave radiation) and not just transmitted (short-wave) solar radiation. Future steps for this research initiative include:

- Automating the process using a software toolkit that automatically creates a Sankey diagram from a BPS input file;
- Applying the methodology to a more complex, multi-zone building;
- A zoomable Sankey diagram in which designers can view a large range of detail levels from whole-building performance to component level (e.g., individual windows) to a high level of detail (e.g., heat transfer through window frames, spacers, glazing, etc.);
- Standardized representations for certain building energy processes (e.g., heat pumps and HRVs);
- Inclusion and representation of intermediate steps of energy flows within a building (e.g., long-wave radiation between interior surfaces and short-term passive storage is massive floors) rather than merely the entry and exit points, as shown in the example in Figure 6;
- Different methods for configuring Sankey diagrams, such as superimposing the flows with a graphical schematic of buildings; and,
- A software-based user interface that allows a designer to inspect instantaneous heat transfer and power use in a building at any given time; and in video form over a finite period.

References

Balcomb, J. D. (1992). Passive solar buildings. Cambridge, MA, The MIT Press.

Barnaby, C. S., C. Spitler, et al. (2005). "The Residential Heat Balance Method for Heating and Cooling Load Calculations." ASHRAE Transactions 111(1).

Interactive Database for Energy-efficient Architecture. (2002). "CASAnova." Retrieved January 3, 2012, from http://nesa1.uni-siegen.de/wwwextern/idea/main.htm.

Marszal, A. J., P. Heiselberg, et al. (2011). "Zero Energy Building – A review of definitions and calculation methodologies." Energy and Buildings 43(4): 971-979.

O'Brien, W., A. Athienitis, et al. (2011). "Parametric Analysis to support the integrated design and performance modeling of net-zero energy houses." ASHRAE Transactions 117, Part 1: 1-13.

Schmidt, M. (2008). "The Sankey diagram in energy and material flow management." Journal of Industrial Ecology 12(1): 82-94.

Sibbitt, B., T. Onno, et al. (2007). The Drake Landing solar community project: early results. 2nd SBRN and SESCI 32nd Joint Conference, Calgary, AB.

Torcellini, P., S. Pless, et al. (2006). "Zero Energy Buildings: A Critical Look at the Definition." ACEEE Summer Study, Pacific Grove, California.

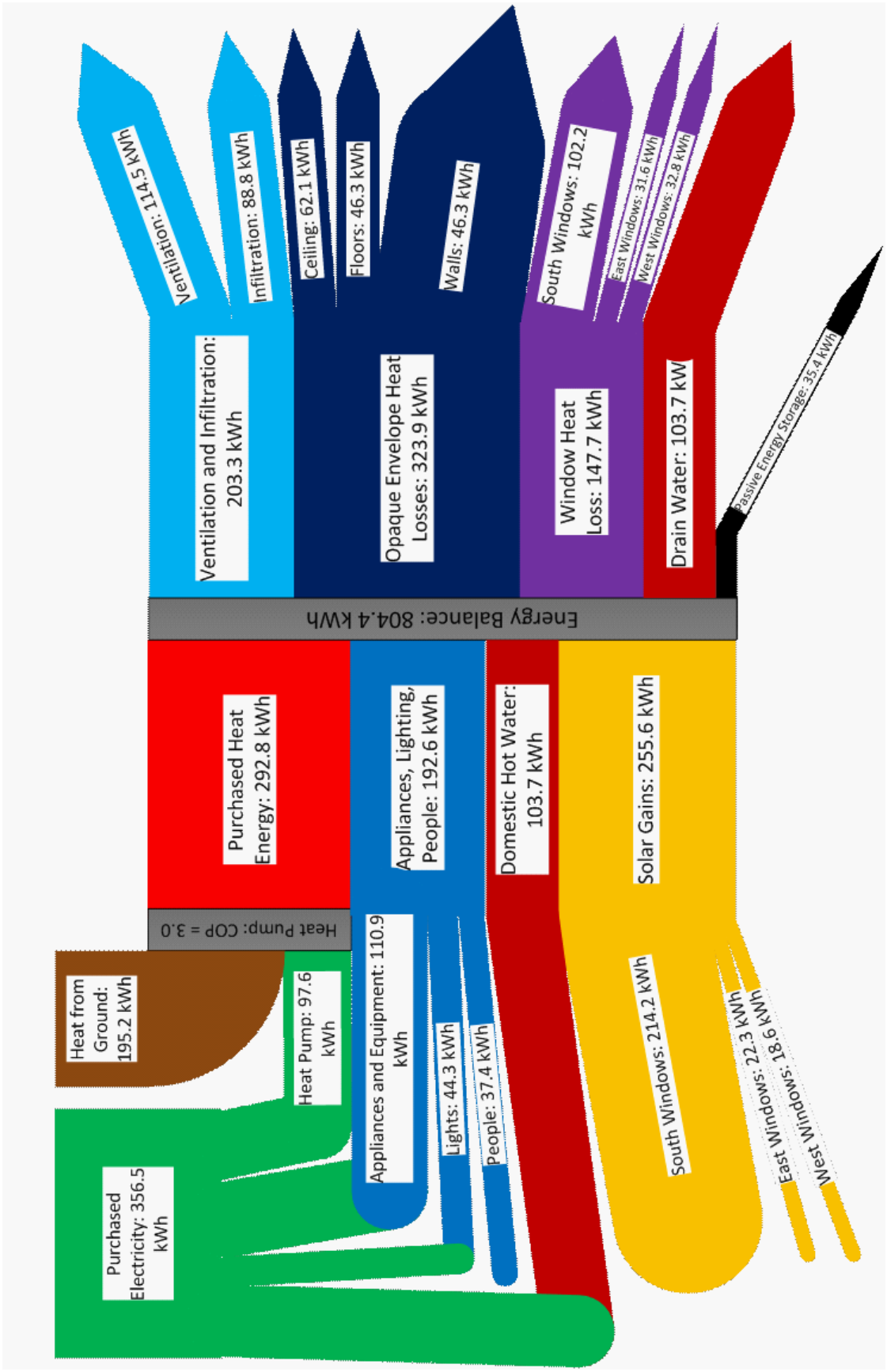

Figure 6. Sankey diagram representing the energy balance for a house for a mid-winter week.

Automated Translation of Architectural Models for Energy Simulation

Kevin B. Pratt[1], Nathaniel L. Jones[2], Lars Schumann[2], David E. Bosworth[2], Andrew D. Heumann[1]

[1]Cornell University
Department of Architecture
139 East Sibley Hall
Ithaca, NY, USA, 14853
kp238@cornell.edu

[2]Cornell University
Program of Computer Graphics
580 Rhodes Hall
Ithaca, NY, USA, 14853
nlj5@cornell.edu

Keywords: design process, early design stage, building performance simulation, whole building energy analysis.

Abstract

In the early stages of building design, architects rapidly produce, explore, analyze, and eliminate design options. Ideally, energy analysis should accompany and inform each design option, but in reality, the creation of building models for thermal simulation is too slow to keep up with the pace of design exploration. This paper describes a framework for rapid energy analysis of architectural early design models. The framework consists of a flexible modeling protocol to be followed by the user, a standard communication protocol that may be implemented in virtually any architectural modeling software as a script or plug-in, and a translation protocol for automated production of energy models to be run in a stand-alone program simultaneously with the modeling environment. A prototype implementation of these protocols has successfully performed EnergyPlus analysis of early design stage architectural models created in SketchUp, Grasshopper for Rhinoceros, and 3ds Max. This allows timely feedback on building energy consumption to be displayed side-by-side with an actively changing architectural model.

1. INTRODUCTION

The ability of architects to reduce projected building energy consumption through changes to building form, massing, and orientation is greatest during conceptual and schematic design. However, despite repeated calls from the building simulation community, energy analysis of early design models remains rare (Smith et al. 2011). There is little or no compatibility between most computer-aided design (CAD) tools used for formal exploration and the building energy simulation (BES) software used for evaluation. In CAD applications able to initiate simulations, such as Revit (Autodesk 2011a; Smith et al. 2011) or SketchUp (Google 2011) using the OpenStudio plug-in (NREL 2011), the energy modeling processes differ so much from normal use of the software that a different knowledge base and skill set are required of the user. More commonly, exchange file formats such as IFC (Bazjanac and Crawley 1997), gbXML (Green Building Studio 2010), or IDF (Crawley et al. 2001) are used to facilitate data transfer between applications, often dividing the work of design and analysis between two different people or even two different offices. Attempts to automate the creation of these exchange files tend to assume that the necessary data is already present in a building information model (BIM) (Bazjanac 2009). However, BIMs are often incomplete and rarely available early in the design process. In order to integrate energy simulation into the toolkit of the architect so that it can affect early design decisions, BES tools must interact naturally with the tools of architectural design.

File formats such as IFC and IDF implicitly define standards for the types of data that must be gathered in order to run energy simulations. The CAD tool (or a person acting as an intermediary) must be capable of generating a complete input file of the correct type for the given BES software. Unfortunately, the authors are not aware of any formally agreed upon standard that describes how to generate a thermal model from an architectural geometric model, a process which necessarily involves augmenting the model with information from other sources. If the response is that this translation requires a certain know-how on the user's part, then designers who lack special training or in-house consulting services will be unable to take advantage of performative feedback during early design exploration.

This paper describes a minimal set of protocols that provide rules and steps necessary for the creation of a thermal building model from a digital geometric model. The protocols concern three actors: first, a human architect or designer who interacts with a CAD tool; second, a program that filters and communicates the geometric data from the CAD model; third, a program that translates the received information into a thermal model using heuristic methods (Figure 1). The latter two actors could be components of a single software package or communicate with each other via an exchange file format. In practice, they are best separated so that the task of communication rests with the CAD tool and translation with the BES software.

The authors tested these protocols in Sustain, a prototype framework for energy modeling and research. The implementation consists of a CAD plug-in and a stand-alone translation program that communicate via a transmission control protocol (TCP) socket connection. This is preferred for a variety of reasons. First, sharing information over the socket is faster and more versatile than reading and writing any existing file format. The translation tool receives input directly and may send its output to the appropriate file format for any BES tool, depending on the user's choice. Second, since the translation tool runs in the background simultaneously with the CAD software, the architect is able to view simulation feedback while the building model is still open and editable. Third, the CAD plug-in is written with relatively few lines of code and can easily be duplicated for virtually any CAD software package. Finally, TCP makes communication in the reverse direction possible, which could in the future enable automated design optimization.

These protocols are intended to minimize the restrictions placed on the architect when modeling. This not only reduces the need for training, but also increases the variety and complexity of architectural form that can be made amenable to BES analysis. More importantly, by reducing the additional effort required to create a thermal building model beyond what is required by the architectural model, BES results can be generated faster, earlier, and more frequently in the design process, enabling more intelligent choices of building form, massing, and materials.

2. MODELING PROTOCOL

While the authors' intent is to impose as few restrictions on the architect as possible, it is clear that not everything that can be produced with CAD software can be understood as a building model capable of producing meaningful BES analysis. Hence, it is necessary to develop minimum requirements for what may be given to the CAD plug-in as input. The protocol described here gives minimal rules that guarantee correct interpretation of the model by the translation tool.

2.1. Modeling Environments

Architects choose to use various CAD software packages based on familiarity, ease of use, cost, and convention. Depending on the design stage, building type, and desired form, the choice of CAD software will vary. A protocol that is uniform across all CAD packages will help architects to develop familiarity with BES feedback and will not restrict formal design choices because of limitation to a single CAD toolset.

Three CAD programs have been used with the current protocol implementation. SketchUp is commonly used as an early design tool thanks to its intuitive user interface and simple toolset (Figure 2). While it stores only planar surfaces, its object-oriented geometric hierarchy and its rendering engine allow the user to interact with geometric

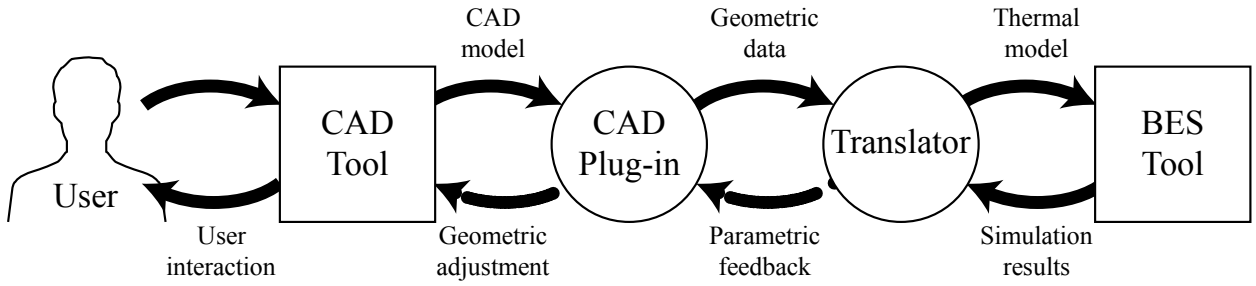

Figure 1. The three actors involved in building design and analysis are a human user of CAD software, a CAD plug-in that communicates relevant information from the user's input, and a translation tool that converts and augments the input to prepare it for BES analysis. Reverse communication (dotted line) may eventually support parametric design optimization.

components that appear more complex. Rhinoceros (McNeel 2010) is a non-uniform rational B-spline (NURBS) modeler capable of representing planar and free-form surfaces. It also supports decomposition of curved surfaces into triangulated or quadrilateral meshes. As with SketchUp, geometry in Rhinoceros is static. However, the Grasshopper plug-in (McNeel 2011) can create parametric geometry in Rhinoceros manipulated by sliders and other user controls (Figure 3). Static geometry may include site context, topography, and aspects of the building that are not open to design variation, while parametrically controlled geometry is especially useful where the architect wishes to fine-tune parts of the model through performance simulation. Autodesk 3ds Max (Autodesk 2011b) is a modeling and animation tool with a large toolset for both planar and NURBS geometry (Figure 4). Its primary use in the architectural profession is for presentation rendering.

Other CAD programs may also be used in conjunction with this protocol, but all need to meet three minimal requirements. First, all must provide an application programming interface (API) or a scripting language to allow the creation of a plug-in. Second, all must support the creation of surface geometry that can be described with vertices defined by spatial coordinates. Finally, each surface must have two assignable properties stored as metadata; by convention, these are called material and layer. For this last requirement, a work-around had to be introduced for Grasshopper, which does not access the layer or render material properties from Rhinoceros. Instead, these fields are provided using a custom component that accepts geometry along with text string data.

2.2. Modeling Requirements

The requirements placed on the architect fall into the categories of surface rules and space rules. Surface rules apply to the model entities that represent walls, floors, roofs, windows, and doors. Space rules apply to groups of surfaces that together form the envelope of an enclosed volume, which can be understood as a thermal zone by BES software. To some extent, these requirements will depend on the methods implemented in the other protocols. For instance, if the translation protocol is able to detect and cap incomplete polyhedra, then the user requirement that all conditioned spaces must be fully enclosed may be relaxed or omitted. The requirements on the modeler, along with steps that may be implemented in software to alleviate these restrictions, are listed in Table 1.

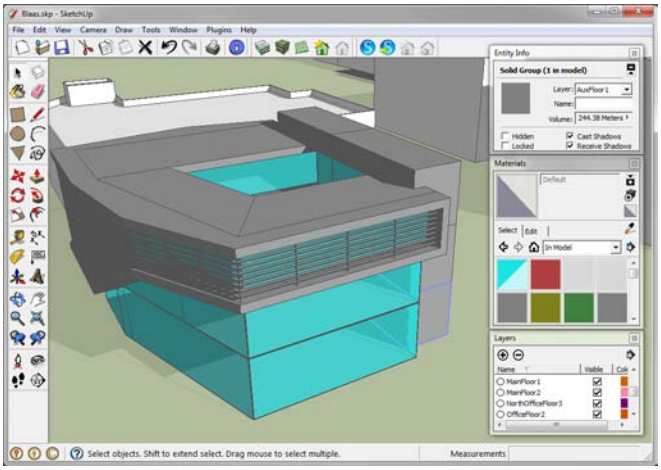

Figure 2. The SketchUp plug-in creates toolbars to allow user interaction with the translation tool.

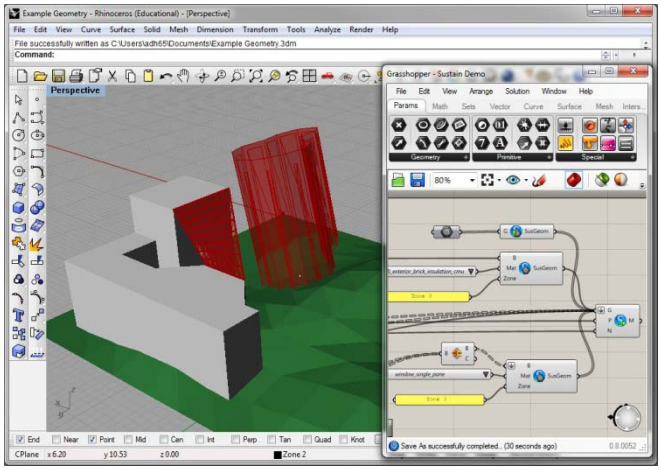

Figure 3. Custom components within the Grasshopper interface send static and parametric geometry from Rhinoceros to the translation tool.

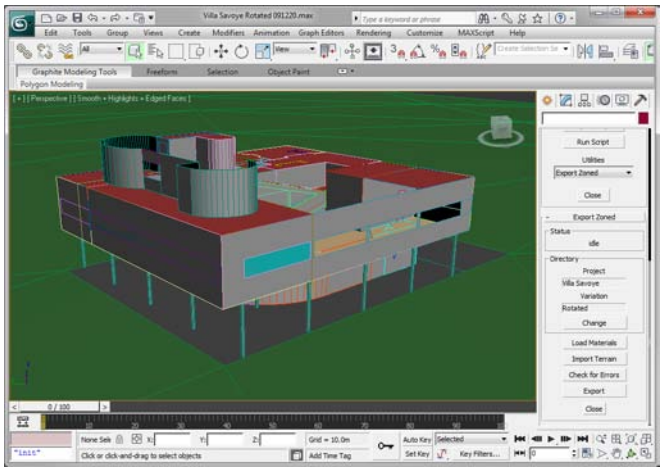

Figure 4. The plug-in script for 3ds Max creates user interface elements in the side bar.

	Rule	Omit if…
Surface Rules	Surfaces must be modeled as planar polygons.	…the plug-in can decompose a curved or NURBS surface into a polygon mesh.
	Surfaces must be assigned a material corresponding to one of the construction types available to the BES tool. Two surfaces that form opposite sides of the same wall must be assigned the same material.	…the translation tool can resolve material discrepancies and guess the material based on neighboring surfaces.
	Windows and doors must be rectangular or triangular surfaces fully contained within a parent wall surface.	…the translation tool can subdivide polygons with more than four vertices and determine a parent based on edge relationships.
	Surfaces cannot contain holes.	…the translation tool can divide complex polygons into simple ones or add void child surfaces.
Space Rules	Interior spaces must be water tight. Surfaces that bound a space must create a complete polyhedron.	…the translation tool can detect and cap incomplete polyhedra.
	Surfaces (or groups of surfaces) must be assigned to a layer corresponding to a thermal zone. Surfaces representing terrain or shading elements must be assigned to adiabatic layers.	…the translation tool offers automated zoning.
	A surface may serve as part of an envelope for no more than one space on each face.	…the translation tool can subdivide surfaces at detected space boundaries.
	Surfaces representing opposite sides of a wall must be coplanar with opposing normal directions.	…the translation tool can correct normal directions, add missing polygons for walls represented by single surfaces, and accommodate thick walls.

Table 1: Modeling protocol for architects.

3. COMMUNICATION PROTOCOL

Since the dominant trend in BES modeling is to construct the thermal model manually using late-stage architectural drawings as a guide, examples of a working communication protocol between CAD and BES software are hard to come across. The term communication protocol *does not* refer to an exchange file format, but rather to a process through which the software (in this implementation, a CAD plug-in) determines what geometry and object properties to send to the translation protocol. Additionally, because the CAD plug-in offers access to more than just geometric information within the CAD tool, it is uniquely positioned to assist in bidirectional communication between the CAD interface and the BES tool.

3.1. Geometry Transfer

The geometric information that must be transferred to the translation tool consists of two parts, a list of vertices and a list of surfaces. Vertices, expressed as Cartesian coordinates, may belong to multiple surfaces but need only be communicated once each. Each surface is then communicated to the translation tool by passing its name, material, layer, number of vertices, and the indices of the vertices from the vertex list. The name may be obtained from the CAD tool, but more likely will be generated by the plug-in since it is uncommon for CAD software to generate names for all drawn objects.

The process of retrieving surfaces will differ for each CAD package depending on its internal representation of geometry. In SketchUp, all surfaces belong to a single object class, the Face, and Faces may be stored at the model's root level or nested within Groups and Components. The list of model entities is traversed as a tree until all Faces are discovered and communicated (Figure 5).

In Rhinoceros, the basic geometric building block is the NURBS Surface. Through Grasshopper, geometry may be added as Polysurfaces, which may contain multiple faces. Each face is analyzed for planarity and topology. If a face is non-planar, contains holes, or has curved edges in its boundary, then the entire Polysurface is converted to a mesh of planar quadrilaterals and triangles. Meshing the entire Polysurface rather than the individual face ensures that no

seams open between faces. In the current implementation, this process relies on Rhinoceros' built-in meshing algorithms, but custom meshing algorithms may speed the process and result in fewer output surfaces in the future.

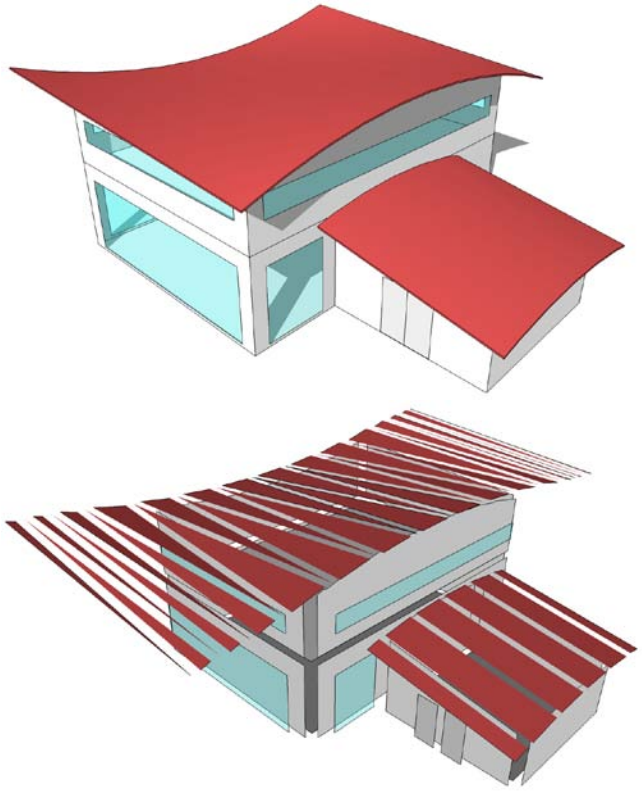

Figure 5. The communication protocol is responsible for traversing the CAD model (top) and identifying individual surfaces (bottom) that must be passed on to the translation tool.

In 3ds Max, the surfaces to be communicated must be stored within Editable Polys. Since groups must be exploded, and transformation stacks must be collapsed, the implementation of the protocol is surrounded with undo clauses so that the user's settings are not lost. The surfaces and vertices of each Editable Poly are then communicated to the translation tool. Care must be taken because 3ds Max allows Editable Polys to contain "dead" vertices which are no longer part of a surface but are still retained in memory with non-numeric coordinate values.

Recognizing that not all geometry created by the architect is intended to be part of a BES model, some common methods exist to exclude certain objects across implementations. Surfaces that have been hidden or made invisible are ignored, since these may belong to previous design versions. Similarly, surfaces with no assigned material are assumed to be construction guides and are ignored.

3.2. Bidirectional Link

A lightweight plug-in for the modeling environment can be used not only to send information, but to receive it as well. For instance, if the translation tool references the surface material name with a database of construction types, then the CAD plug-in can read from the same database to ensure that valid materials are available to the architect with appearances based on their physical properties. In SketchUp, time and geographic location are stored as part of a model in order to correctly display shadows. Since the translation tool implemented by the authors includes a graphic display of the thermal model along with controls for weather file selection and result display time during the simulated year, either program may be used to set the time and location, which are then reflected in both. Additionally, the current view of the model may be shared between the CAD and translation tools, allowing the user to visually identify each thermal surface with its corresponding object in the architectural model.

3.3. Parametric Optimization

The ultimate utility of the bidirectional link established through a socket connection would be the ability to perform automatic parametric design changes based on simulation results. Though not yet implemented, the final step will enable the architect to specify a large number of building geometry parameters and perform iterative optimization using hill climbing, genetic algorithms, or simulated annealing, for example. This will allow simulations across a wide design space, providing both quantitative and visual feedback on the effect of modifying specific building parameters (Pratt and Bosworth 2011).

4. TRANSLATION PROTOCOL

Up to this point, the data input by the user and communicated through the plug-in lacks information necessary for energy simulation. The translation protocol defines a set of heuristic algorithms that can reliably produce a BES model given geometric and material input. This protocol integrates three types of processes that act on the geometry and other data sent from the plug-in. At the conclusion of the automated translation, the authors' prototype implementation displays the thermal building model graphically and allows the user to check and alter its assumptions through a graphic interface. While the

implementation discussed here is designed to prepare data required by EnergyPlus (LBNL 2011), the same steps could be built around other BES software.

4.1. Geometry Correction

Because the CAD plug-ins are lightweight and purposefully do very little data processing, their output often includes extraneous or duplicated information that was stored by the CAD program. Clean-up reduces memory consumption and can reduce the time required for simulation, but does not alter the source CAD model. In this first translation step, degenerate polygons are deleted, and polygon vertices are removed if they form straight angles or are too close to neighboring vertices to be differentiated at the geometric resolution of EnergyPlus. Surfaces with unrecognized materials are removed. To meet the built-in geometric assumptions of EnergyPlus, polygon vertices may be reordered to start from the upper left corner, and concave shading polygons may be broken into smaller convex polygons (Figure 6).

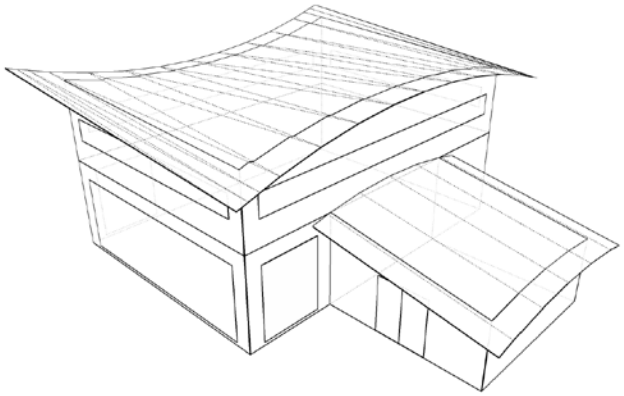

Figure 6. The translation protocol's first step is to clean up the modeled geometry. This includes subdivision of certain surfaces, welding adjacent surface edges, and culling degenerate polygons.

4.2. Surface Heuristics

The second step in translation uses a set of heuristics to determine thermal properties of surfaces based solely on information obtained about each surface from the CAD program. This information is either deduced from naming conventions or from surface normal vectors. The material name assigned in the CAD program is matched to a construction from a database. Certain types of surfaces, such as windows, doors, and below-grade exterior walls, may be identified at this point because their unique construction types can only serve certain purposes. However, construction information is not sufficient to differentiate most walls, floors, and ceilings since some constructions might be used for all three interchangeably. The surface normal vector makes this differentiation possible. Additionally, surfaces may be assigned to thermal zones by CAD layer.

4.3. Neighborhood Heuristics

The third step makes use of heuristics that examine a surface in the context of its surroundings. For instance, a surface may be defined as a floor given its normal vector, reversed to become a ceiling based on its relation to the space it bounds, and finally upgraded to a roof with knowledge of its relation to the building as a whole. These heuristics define spatial adjacencies and associate windows and doors with their parent wall surfaces.

The term "zone" is alternately used to refer to programmatic zones, actual rooms, areas of control for a mechanical system, and thermally similar building areas. For the purpose of simulation during early design, the translation protocol identifies each fully enclosed space with a thermal zone (Figure 7). Multiple spaces may belong to the same thermal zone if all of their surfaces reside on the same CAD layer. The surfaces themselves are understood as the boundaries between the space's air volume and the adjacent walls, floor, ceiling, windows, or doors, across which heat can flow to a neighboring space, the outside, or the ground. Using the method of pyramid volumes, the algorithm can quickly check that spaces are fully enclosed.

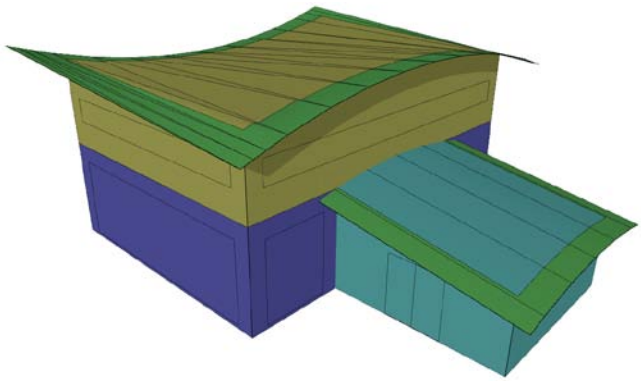

Figure 7. Using neighborhood relationships, the translation tool is able to identify enclosed spaces within the building and assign them to thermal zones, which are identified graphically by surface coloration.

Adjacent spaces and interfacing surface pairs are discovered by treating a first surface as invisible and looking beyond it (Figure 8). A user-defined allowable wall thickness determines the maximum distance to look. The

same technique can discover parent-child relationships between windows and walls. In keeping with the EnergyPlus requirement that adjacent surface from neighboring spaces have equal area, non-similar surface pairs are partitioned using polygon clipping (Vatti 1992).

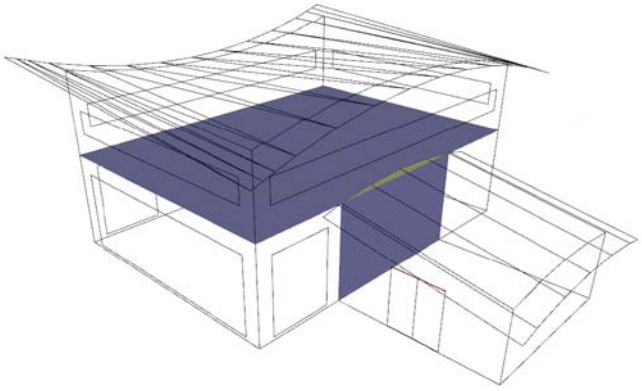

Figure 8. Neighborhood relations allow the translation tool to identify spatial adjacencies and to subdivide surfaces that are adjacent to multiple spaces. Boundaries with adjacent spaces are identified to the user by color for error checking.

Because the translation tool is designed to require little attention from the user, it provides default settings including occupancy schedules and thermostat settings for thermal zones. The architect is expected to be more interested in the building performance improvement achieved by altering the building's form and materials than by changing occupancy settings. Likewise, a simple purchased air HVAC system is automatically applied to each thermal zone since the architect is not expected to select mechanical systems during preliminary design.

The translation tool includes a graphic user interface so that the architect can visually inspect the translated model for errors. Within this interface, the translation tool can point out problem areas in the model where the user did not follow the modeling protocol. The interface also provides limited, self-explanatory controls for altering properties of individual surfaces, zones, or the building as a whole. These settings are persistent through multiple translations of the same CAD model, so the user need only set them once.

5. CONCLUSION

The development of user and software protocols for BES translation of an architectural model represents an important step toward automated real-time performative feedback for the design process. The authors' prototype implementation (Figure 9) demonstrates that by shifting focus from data exchange file formats to modeling process, building energy simulation can be performed on architectural CAD models starting at a very early design stage. Architectural models created without thermal data can be translated into energy models with little user effort beyond what is normally required to create a three-dimensional CAD model. Furthermore, this translation can occur in BES software, making it compatible with virtually any architectural design tool. As multi-processor, multi-screen workstations become ubiquitous in architectural firms, simultaneous design, simulation, and result display no longer poses a technical hurdle. When architectural and thermal models are created

Figure 9. The prototype implementation allows a single user to simultaneously model, simulate, and view BES results. The workstation's left screen shows the CAD input, while the center shows the translated model and the right contains BES output.

by the same user, at the same workstation, at the same time, performative feedback can be obtained almost immediately and can influence early design decisions.

While model translation can now be instantaneous, BES software must still improve before real-time feedback becomes a reality. In particular, many of the algorithms currently used by tools such as EnergyPlus were developed for older machines with severe memory limitations. In many cases, newer algorithms exists that could lead to much faster simulations; this is particularly true of radiant heat exchange (Jones et al. 2011). Also, further research is required in areas such as convective heat exchange to validate energy simulation for the increasing variety of building shapes that can be produced with today's CAD tools (Zuo and Chen 2009). Nonetheless, these improvements together with the implementation of appropriate modeling and translation protocols will allow BES analysis of early design models to enter the architectural mainstream.

Acknowledgements

This material is based upon work supported by the Department of Energy under Award Number DE-EE0003921.

Disclaimer

This report was prepared as an account of work sponsored by an agency of the United States Government. Neither the United States Government nor any agency thereof, nor any of their employees, makes any warranty, express or implied, or assumes any legal liability or responsibility for the accuracy, completeness, or usefulness of any information, apparatus, product, or process disclosed, or represents that its use would not infringe privately owned rights. Reference herein to any specific commercial product, process, or service by trade name, trademark, manufacturer, or otherwise does not necessarily constitute or imply its endorsement, recommendation, or favoring by the United States Government or any agency thereof. The views and opinions of authors expressed herein do not necessarily state or reflect those of the United States Government or any agency thereof.

References

AUTODESK, INC., 2011. Autodesk Revit 2011. Autodesk, San Rafael, CA.

AUTODESK, INC., 2011. Autodesk 3ds Max 2011. Autodesk, San Rafael, CA.

BAZJANAC, V. 2009. Implementation of semi-automated energy performance simulation: building geometry. In Dikbas, A., Ergen, E. and Giritli, H. (eds.), *CIB W78, Proc. 26th conf., Managing IT in Construction*. Istanbul, TK, 595-602. CRC Press.

BAZJANAC, V. AND CRAWLEY, D.B., 1997. The implementation of industry foundation classes in simulation tools for the building industry. Lawrence Berkeley National Laboratory. LBNL Paper LBNL-40681.

CRAWLEY, D.B. ET AL., 2001. EnergyPlus: creating a new-generation building energy simulation program. *Energy and Buildings*, 33, 319-331.

GOOGLE, 2011. Google SketchUp, Version 8. Google Inc., Mountain View, CA.

GREEN BUILDING STUDIO. 2010. gbXML schema. http://www.gbxml.org/. Accessed 6 November 2011.

LBNL, 2011. EnergyPlus, Version 7.0. Lawrence Berkeley National Laboratory, Berkely, CA.

JONES, N.L., GREENBERG, D.P. AND PRATT, K.B., 2011. Fast computer graphics techniques for calculating direct solar radiation on complex building surfaces. *Journal of Building Performance Simulation*. DOI: 10.1080/19401493.2011.582154.

NREL, 2011. OpenStudio, Version 0.5. National Renewable Energy Laboratory, Golden, CO.

PRATT, K.B. AND BOSWORTH, D.E., 2011. A method for the design and analysis of parametric building energy models. International Building Performance Simulation Association Conference – Building Simulation 2011, November 14-16 2011, Sydney, Australia.

ROBERT MCNEEL & ASSOCIATES, 2010. Rhinoceros 3D, Version 4.0. Robert McNeel & Associates, Seattle, WA.

ROBERT MCNEEL & ASSOCIATES, 2011. Grasshopper, Version 0.8. Robert McNeel & Associates, Seattle, WA.

SMITH, L., BERNHARDT, K. AND JEZYK, M. 2011. Automated energy model creation for conceptual design. 2011 Proceedings of the Symposium on Simulation for Architecture and Urban Design. 53-60.

VATTI, B.R., 1992. A generic solution to polygon clipping. *Communications of the ACM*, 35 (7), 56-63.

ZUO, W. AND CHEN, Q., 2009. Real-time or faster-than-real-time simulation of airflow in buildings. *Indoor Air*, 19, 33-44.

Dynamic Annual Metrics for Contrast in Daylit Architecture

Siobhan Rockcastle[1,2], Marilyne Andersen[1,3]

[1]MIT, Building Technology Lab
77 Massachusetts Avenue
Room 5-418
Cambridge, MA USA 02139

[2]Present Address
Northeastern University
360 Huntington Ave, 151Ryder Hall
Boston, MA USA 02115
s.rockcastle@neu.edu

[3]Present Address
EPFL, LIPID Laboratory
Building BP, Station 16
1015 Lausanne, Switzerland
marilyne.andersen@epfl.ch

Keywords: Contrast, Dynamic Daylight, Spatial Contrast, Luminance Variability

Abstract

Daylight is a dynamic source of illumination in architectural space, creating diverse and ephemeral configurations of light and shadow within the built environment. It can generate contrasting levels of brightness between distinct geometries or it can highlight smooth gradients of texture and color within the visual field. Although there are a growing number of studies that seek to define the relationship between brightness, contrast, and lighting quality, the *dynamic* role of daylight within the visual field is underrepresented by existing metrics. This study proposes a new family of metrics that quantify the magnitude of contrast-based visual effects and time-based variation within daylit space through the use of time-segmented daylight renderings. This paper will introduce two new annual metrics; Annual Spatial Contrast and Annual Luminance Variability. These metrics will be applied to a series of abstract case studies to evaluate their effectiveness in comparing annual contrast-based visual effects.

1. INTRODUCTION

Perceptual qualities of daylight, such as contrast and temporal variability, are essential to our appreciation of architectural space. Natural illumination adds depth to complex geometries and infuses otherwise static interior spaces with shifting compositions of light and shadow. Architectural space is greatly altered by the ephemeral qualities of daylight, yet there is a lack of metrics that address these perceptual factors on a dynamic scale.

Over the past several decades, there have been significant improvements in our understanding of daylight as a dynamic source of interior illumination. Illuminance-based methods of daylight analysis have developed from static metrics such as Daylight Factor (Moon and Spencer 1942) to annual climate-based metrics such as Daylight Autonomy (Reinhart et al. 2006) and Useful Daylight Illuminance (Nabil & Mardaljevic 2006) to account for a more statistically accurate method of quantifying internal illuminance levels (Mardaljevic et al. 2009). While these annual illuminance-based metrics represent a significant improvement in our understanding of climate-based lighting levels across the year, they still experience many of the same limitations as daylight factor in their static representation of performance through a single surface. (Reinhart et al. 2006). As occupants perceive space from a three-dimensional vantage point, illuminance-based metrics such DA and UDI cannot express the dynamic nature of sunlight from a human perspective.

Luminance-based methods of daylight analysis are more appropriate for determining the compositional impacts of contrast as they can evaluate renderings and/or photographs taken from an occupant's point-of-view (Newsham et al. 2005). Existing luminance-based metrics can be organized into two main categories: those that predict glare-based discomfort due to high ratios of contrast within the visual field, and those that evaluate luminance ratios or ranges to infer human preferences to brightness and composition.

Those metrics that quantify luminance-based sources of glare are fragmented among no less than seven established metrics (Kleindienst and Andersen 2009). The most ubiquitous of these metrics, Daylight Glare Probability DGP (Weinhold and Christofferson 2006), establishes that high levels of contrast within our field of view negatively impact visual comfort. Although glare-based metrics are capable of quantifying contrast ratios and anticipating sources of luminance-based *discomfort* within a perspectival view, they do not provide a method for quantifying the *positive* aspects of brightness, contrast, or daylight variability.

The second category of luminance-based analysis methods relies on existing scenes and/or digital images to identify the relationship between brightness, contrast, and occupant preferences toward the luminous environment. Two dimensions that are widely accepted to impact the field of view are average luminance and luminance variation (Veitch and Newsham 2000). The former has been directly associated with perceived lightness and the latter with visual interest (Loe et al. 1994). As brightness is subjectively evaluated by the human brain, contrast is often regarded as a qualitative indicator of performance, making it difficult to quantify in universal terms. Occupant surveys of existing interior spaces were once the primary method of data collection, but digital photographs have become a useful alternative for practical purposes (Cetegen et al. 2008). One such study engages subject surveys to establish a direct correlation between the average luminance across an HDR image and its perceived 'pleasantness' or relative 'excitement' (Cetegen et al. 2008). Another example is Claude Demer's daylight classification system which categorizes images of interior architecture by plotting the mean brightness of each composition against the standard deviation of its luminance values (Demers 2007). Although this method is useful in creating an early schematic design tool for comparing contrast-driven architectural types, and survey-based methods provide us with comparative data on the luminous composition of a single space under varied lighting conditions, neither can account for the complexity of variations that occur over time. Furthermore, these methods that assess average luminance values or overall luminance range cannot distinguish between compositions that vary in the density and location of local contrast values.

This paper will propose a compositionally-dependent method of analyzing contrast through the use of matrices so that local pixel values may be quantified within their spatial framework. Using this method, we will introduce two new annual metrics; Annual Spatial Contrast and Annual Luminance Variability. These metrics will analyze a set of annual images so that dynamic conditions of contrast and luminosity may be represented across the year.

2. SPATIAL CONTRAST

In order to introduce the concept of spatial contrast, we must first consider the distinction between two images that contain a similar distribution in overall brightness, yet varied densities in the composition of dark and light values. Figure 1a shows a dense pattern of light and shadow, with each small cluster of light pixels surrounded by a tight perimeter of darker ones, whereas Figure 1b, though similar in overall brightness, shows fewer distinct boundaries between light and dark pixels. If we look at the RGB histograms, we see that each composition contains roughly the same distribution of pixels, with a peak between RGB 50-100. Figure 1a has a mean brightness of 120 with a standard deviation of 18 while Figure 1b has a mean brightness of 132 with a standard deviation of 22. Despite the obvious differences in compositional density between the two images, they are similar in contrast typology according to Claude Demers' system of classification (Demers 2007).

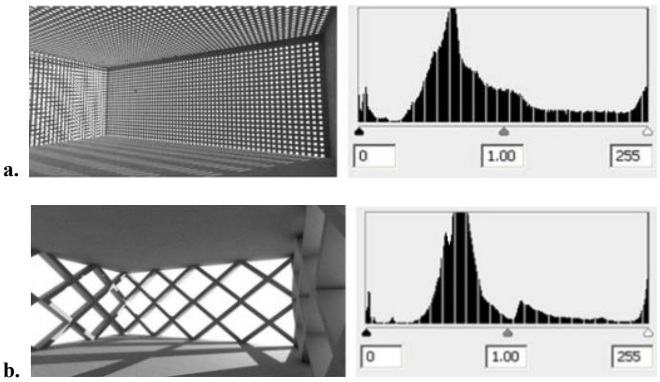

Figure 1. Mean brightness: a) 120, b) 132; Standard deviation: a) 18, b) 22.

2.1. Quantitative Approach

Rather than compute the standard deviation between luminance values, spatial contrast describes the difference between each pixel and that of its neighbor, computing the sum of all local boundaries within a given image. Figures 2a and 2b reiterate this concept through a diagrammatic representation of circles. The thickness of each circle represents the brightness of its underlying pixel, with the thickest circles representing RGB 255 (white) and the thinnest circles representing RGB 0 (black). Figure 2a shows a composition with several distinct boundaries between dark and light pixels. The abstraction of this image shows a topography of *hard peaks* between light and dark pixels. Figure 2b, on the other hand, shows a composition with few distinct tonal variations. This smooth *gradient* of tones shows pixels fading gradually in strength, whereas the density and magnitude of *peaks* represented in Figure 1b show a strong difference between light and dark pixels, increasing its spatial contrast across the image.

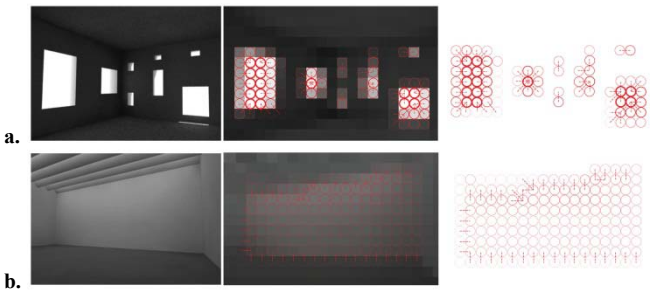

Figure 2. Rendering and representation of a) contrast 'peaks' (shown in red circles whose thickness corresponds to the brightness of underlying pixels), b) tonal 'gradient'.

In order to compute spatial contrast across an image of higher resolution, we use matrices to find the local difference between each pixel and that of its neighbors. We then take the sum of all local differences across the resulting matrix to find the total cumulative contrast. As this number is dependent on the pixel density of the image, we must convert the cumulative sum of spatial contrast into a relative quantity or ratio. To do this, we divide the total spatial contrast by the hypothetical 'maximum contrast' that could be achieved by a corresponding image of the same dimension. Figure 3a shows a sample image (5 x 6) with local contrast values shown in red, while Figure 3b shows a corresponding checkerboard of maximum spatial contrast for an image of the same dimension. The spatial contrast is found by dividing the sum of all local values in Figure 3a by the sum of all local values in 3b.

Figure 3. a) Sample image (5 x 6 pixels) with a cumulative spatial contrast of 1,212 (the sum of all values shown in red) b) Hypothetical maximum (5 x 6) with a cumulative spatial contrast of 12,495 (the sum of all values shown in red).

2.2. Annual Spatial Contrast

In order to understand the dynamic impacts of sunlight on our perception of spatial contrast over time, we must apply the method described in Section 2.1 to a series of images that capture the same view of space at several key moments across the year. Using a method of time segmentation that was originally developed for Lightsolve, a simulation platform for climate-based analysis and time-based visualization of daylight performance (Andersen et al. 2008, Andersen et al. 2011), we divide the year into a series of 56 symmetrical moments with 8 monthly and 7 daily intervals to generate a set of renderings for analysis. Figure 4 shows a sample set of images for a top-lit space in Boston, MA. The application of spatial contrast to this set of annual renderings allows us to calculate the cumulative *Annual Spatial Contrast* for a given view as well as plot individual instances across a temporal map to visualize daily and seasonal variations.

Spatio-Temporal Irradiation Maps (STIMAPS) were developed to represent annual data across a single graph, showing days of the year across a horizontal scale, and hours of the day across the vertical (Glaser 1999). Figure 5 shows how each of the 56 moments generated through the time segmentation method can be simultaneously represented in a temporal map. In lightsolve, these maps are used with a goal-based color scale to represent the degree to which the designer's objectives are fulfilled across the year.

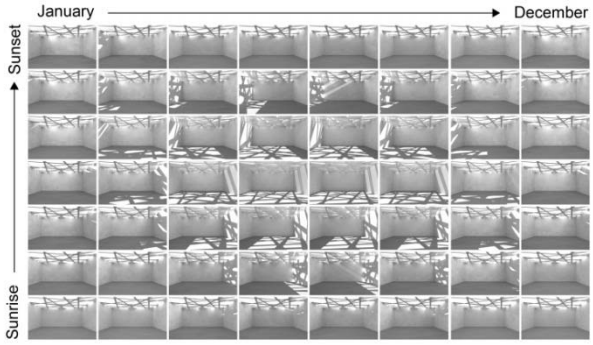

Figure 4. Sample set of 56 annual images produced using the time segmentation method developed for Lightsolve.

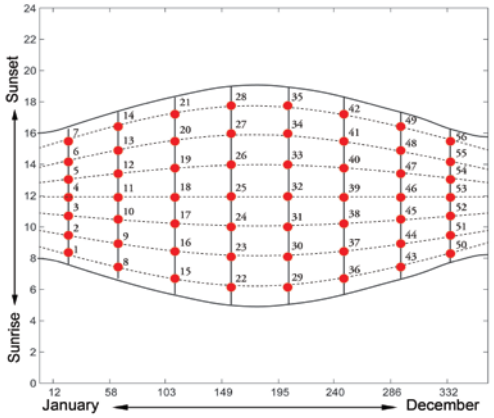

Figure 5. Temporal map showing the location of plotted values for each of the 56 renderings pictured in figure 4. Hours of the day are represented on the vertical scale, while days of the year are on the horizontal.

Annual Spatial Contrast adopts the 56 moments supported by the lightsolve method, but uses a CIE sunny sky model for all 56 renderings. This simplification allows for a consistent set of luminance maps that can be analyzed for relative changes in luminosity while creating an upper boundary for contrast and luminance variability.

2.3. Analysis and Graphical Representation

To calculate and visualize Annual Spatial Contrast, each of the 56 renderings shown in Figure 4 is processed to produce a matrix of local spatial contrast as well as a cumulative sum that represents the total spatial contrast across each image. Two sample matrices of local spatial contrast can be seen beneath their corresponding rendering in Figures 6a & 6b.

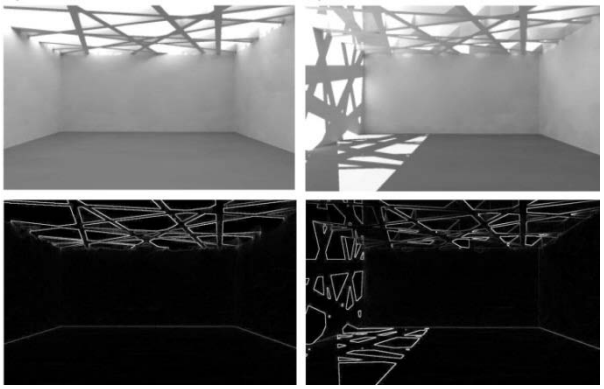

a. 1/13, 7:52 **b.** 5/30, 6:59

Figure 6. Renderings and corresponding spatial contrast maps for a selection of dates and times.

Annual Spatial Contrast takes the sum of all 56 instances to compare the magnitude and composition of spatial contrast over time. To visualize *where* this contrast occurs throughout the space, each of the 56 instances are combined to produce a cumulative matrix or image map. Figure 7a shows an example of this cumulative image map for a dramatic top-lit space in Boston, MA. The spatial contrast for each individual moment is then plotted on a temporal map to visualize *when* the space experiences the most dramatic contrast-based effects, and how abruptly it changes across the course of a day or season (shown in Figure 7b).

Annual Spatial Contrast provides the designer with a more holistic understanding of *when* and *where* sunlight impacts the composition of light and shadow within our field of view. The cumulative image map displays a dynamic range of information, highlighting both redundant and residual zones of contrast while the temporal map allows us to compare its strength and variation over time. This method of visualization challenges the static representation of contrast in daylit architecture, allowing us to represent its inherently dynamic characteristics.

The scale associated with Figure 7b has been adjusted to accommodate appropriate minimum and maximum spatial contrast values as determined by a series of case studies introduced in Section 4. As a result, Spatial contrast values between 0 and 0.33 should be considered low, values between 0.34 and 0.66 moderate, and between 0.67 and 1 are considered high. Those values exceeding 1 would represent very high spatial contrast in the context of the spaces studied. In order to create a truly universal scale for this metric, a large sample of existing architectural spaces would need to be modeled and analyzed to produce appropriate upper and lower thresholds for spatial contrast.

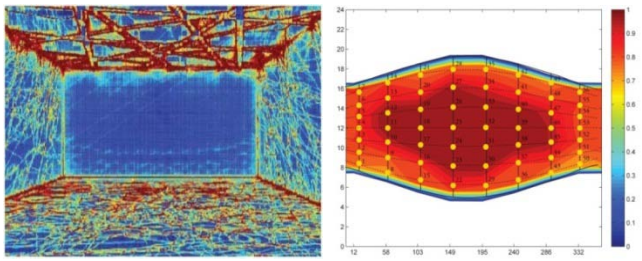

a. **b.**

Figure 7. a) Cumulative image map of annual spatial contrast b) Temporal map showing spatial contrast values across each of the 56 annual moments. The vertical scale represents sunrise to sunset while the horizontal scale represents January to December.

3. LUMINANCE VARIABILITY

The second metric presented by this paper describes the annual variation in luminance values across a rendered view, highlighting areas of temporal instability. Whereas Spatial Contrast identifies compositional contrast boundaries between pixel values within an image, and Annual Spatial Contrast maps the accumulation of those contrast boundaries over time, *Annual Luminance Variability* accounts for the cumulative difference in pixel values as they vary *between* images across the year. This metric is useful in describing the intensity of variation that occurs across a perspectival view of space as a product of time and dynamic natural lighting conditions. Many spaces that measure low in Annual Spatial Contrast may still measure high in Annual Luminance Variability as dramatic variations in luminosity may occur in smooth gradients or fractured patterns of contrasting light and shadow.

3.1. Quantitative Approach

The quantitative approach for this metric relies on the same 56 annual renderings introduced in Section 2.2, however it quantifies the difference between each rendering rather than treating each moment as an autonomous matrix of information. Annual Luminance Variability converts each of the 56 images into a matrix of RGB values and then computes the cumulative difference that each pixel experiences as it changes from one moment to the next. The resulting image matrix represents the cumulative sum of difference across all 56 annual moments, highlighting areas of high temporal variation.

When we use this method to quantify the variation in luminance values across a year, we must account for both daily and seasonal changes in the strength and orientation of sunlight. We must account for the difference between two renderings that occur sequentially throughout the day as well as those that occur across the seasons. In Figure 8 we see 42 data points that represent the absolute difference between neighboring moments, shown in green. This reduction of data points from 56 down to 42 occurs because we do not calculate the difference between sunrise and sunset of any given day, nor do we account for the difference between December and January of the same year.

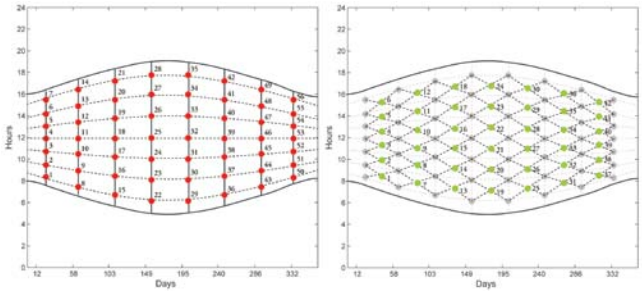

Figure 8. Reduction in data points from 56 down to 42.

Annual Luminance Variability is numerically defined by the sum of all 42 annual instances and represents the total cumulative variation in luminance across a rendered view. Similar to Annual Spatial Contrast, the resulting cumulative variation cannot be compared to images that vary in pixel density until it is converted into a relative value. In order to achieve this, the total sum of luminance variation across all 42 intervals is divided by the total pixel density of the input images. The current method relies on 8-bit images to accommodate a wide range of image production techniques, yet future versions would also accommodate a more dynamic range of pixel data through the integration of HDR images.

3.2. Representing Annual Luminance Variability

The following images illustrate a full set of results for Annual Luminance Variability; Figure 9a shows a cumulative image of all 42 frames of variation which graphically represent the spatial location of luminance variability across the space and Figure 9b shows a temporal map that interpolates the 42 annual data points. The temporal map shows us *when* dynamic variations in natural light occur throughout the year and how abruptly they vary while the associated cumulative image map shows us *where* these variations occur throughout the rendered view. The maximum value for luminance variability at any one instance was found to be 8,000,000 or 8 x 10^6, established from a range of case studies in Section 4. This value represents an upper threshold in context of this study and was used to scale all subsequent data.

The temporal map shows that variations in luminance are most extreme in the summer, when the sun is moving directly overhead. The cumulative image shows the most dramatic variation occurring on the floor, as direct light moves across the roof, casting dynamic patterns of light and shadow down into the space. Some variation can also be seen on the walls, with minimal variation occurring across the roof, where uniform levels of brightness create spatial contrast, but not high levels of luminance variability. This method of visualization engages our understanding of daylit space as a dynamic composition of light and shadow, showing us where and when it transforms. Both annual spatial contrast and annual luminance variability account for distinct, yet related attributes of visual performance and help contribute to a more holistic understanding of architectural space as it is transformed by dynamic shifts in sunlight across the day and year.

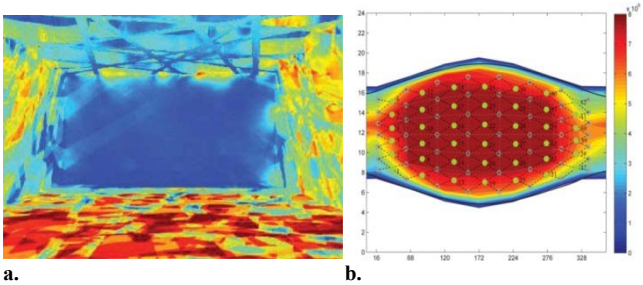

a. **b.**

Figure 9. a) Cumulative image of annual luminance variability. b) Temporal map showing luminance variability values across each of the 42 data points.

4. PRODUCTION OF CASE STUDY IMAGES

In order to evaluate these new annual metrics across a series of architectural conditions, 10 case study spaces were generated to represent a gradient of natural lighting conditions, from low to high contrast and temporal variability.

4.1. Development of Case Study Spaces

The evolution of these case studies, their typological ordering, and the development of a new contrast taxonomy will be presented elsewhere. These 10 case studies represent a compact version of a larger matrix, which was composed of 74 architectural spaces across 15 categories. Figure 10 shows the compact matrix which represents the authors' hypothesized gradient of visual effects (before the application of each metric) from high spatial contrast and luminance variability on the left to low spatial contrast and luminance variability on the right. Although these abstract spaces cannot possibly cover the full spectrum of daylit architectural typologies, this linear gradient is meant to present a range of examples against which alternate spaces can be compared and contextualized.

4.2. Production of Annual Renderings

Radiance, an industry standard rendering software based on backwards ray-tracing (Ward 1994) that embeds tone mapping algorithms, was used to generate images consistent with a human's perceptual view of space, in combination with the DIVA plugin for Rhinoceros (Lagios et al. 2010) to export geometry directly to Radiance.

Each of the 10 case studies was modeled in Rhinoceros with the same floor area, ceiling height, and camera location so that results could be accurately compared. Cameras were positioned to face South, centered in the East-West direction, and offset ten feet from the back wall to ensure an even distribution of wall, floor, and ceiling surfaces within each rendering. The Diva-for-Rhino toolbar was then used to export the camera view to Radiance, where materials were set to default reflectance values for floor, wall, and ceiling surfaces (0.3, 0.7, 0.9 respectively). The resolution of each images was rendered at 'high quality' (a present in DIVA) to accommodate adequate detail with a 640 x 480 pixel aspect ratio and a rendering was generated for each of the 56 dates and times determined by the time-segmentation method (described in Section 2.2) for clear sky conditions. Boston, Massachusetts was set as the location for all case-study renderings (latitude 42 N, Longitude 72 W). When the spaces were rendered under overcast sky conditions, the contrast and temporal diversity was minimized, making it difficult to compare relative changes between each space. In order to compare the impacts of contrast over time, it is necessary to use a sky condition that allows for maximized visual effects. Once a set of renderings has been produced from this method, it is imported into Matlab and analyzed for annual spatial contrast and luminance variability.

5. CASE STUDY RESULTS

Figure 11a and 11b show a linear gradient of results across each of the two annual metrics for the 10 case studies presented in Figure 10. Annual Spatial Contrast results are shown in Figure 11a and Annual Luminance Variability results are shown in Figure 11b. Each row of images has been re-ordered from left to right to display a relative gradient of cumulative annual results, with those case studies located on the left side of each figure representing the high end of the spatial contrast or variability spectrum and those on the right representing the low end. The value beneath each image in Figure 11a represents a cumulative sum of spatial contrast for each of the 56 time-segmented instances. The value beneath each image in Figure 11b represents the sum of all 42 instances of luminance variability described in Section 3.2. These values are ordered in a linear gradient to show the relative presence of cumulative spatial contrast and luminance variability within each case study.

When compared to the hypothesized gradient in Figure 10, the results for each annual metric maintain the overall pattern of anticipated results, with most case study spaces shifting no more than one position to the left or right. Because the hypothesized gradient did not differentiate between the two metrics, the results across each individual metric produce a distinct relative order. For example, case study 1 produced a maximum relative value for annual luminance variability but placed third in annual spatial contrast. Likewise, case study 10 produced a minimum relative value for annual luminance variability, but place 6th in annual spatial contrast. These results support the need for a multitude of quantitative indicators when we discuss the relative perceptual impacts of natural light on factors of visual interest.

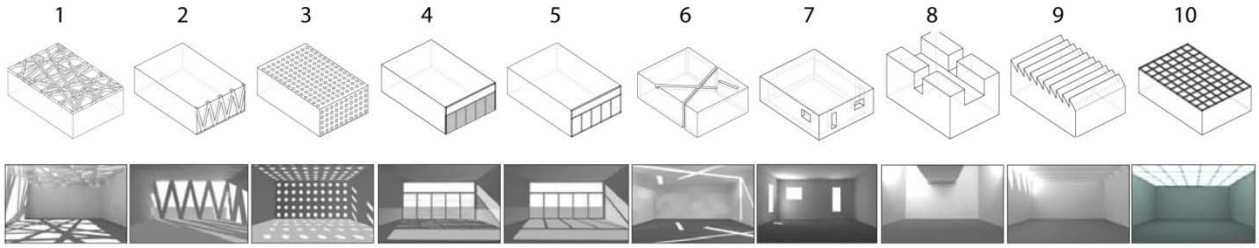

Figure 10. 10 case study models in a hypothesized linear gradient from high contrast & variability on the left

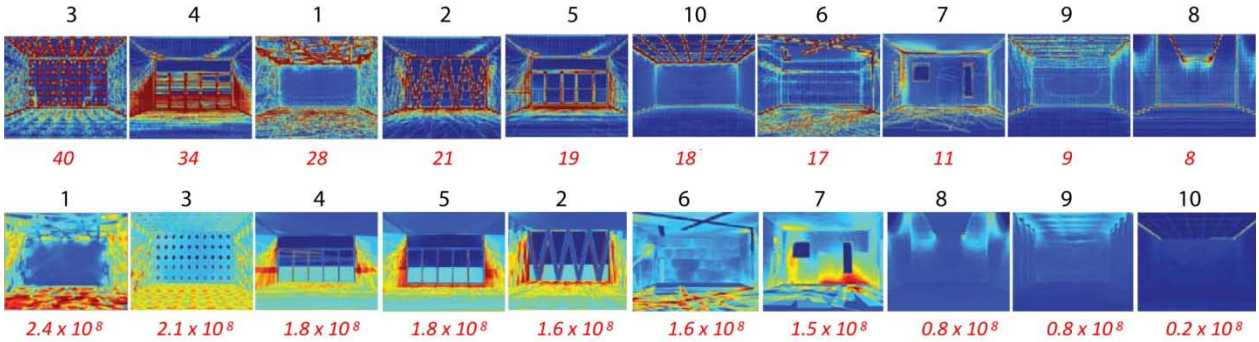

Figure 11. Analysis of all case studies re-ordered in terms of a) Annual Spatial Contrast and b) Annual Luminance Variability.

A more detailed look at the temporal maps for case studies 4 and 9 (the full spectrum be presented elsewhere) show the annual variation in each metric as a product of time. The cumulative images in Figure 12 and 13 provide a spatial snapshot of results for each metric, highlighting areas of contrast or variability within each renderings, but the temporal maps represent a dynamic view of *when* those values change across the year. The temporal map for annual spatial contrast in Figure 12 shows peaks of spatial contrast in the winter months as low sun angles penetrate the louvered façade of case study 4, driving sharp shadows onto the walls and floor. This pattern can also be seen in the temporal map for annual luminance variability as dynamic patterns move across the space in the winter, while remaining relatively static in the summer months. Figure 13 shows an indirect top-lit space with low annual spatial contrast. The temporal map for luminance variability, however, shows peaks of variation in the early morning and late afternoon as low sun angles penetrate the north-facing roof monitors. This map is particularly intriguing as it illustrates an atypical condition that dramatically impacts our perception of interior space at key moments. Future avenues of research would address a climate model to compare the effects of cloud cover and weather on these patterns of contrast.

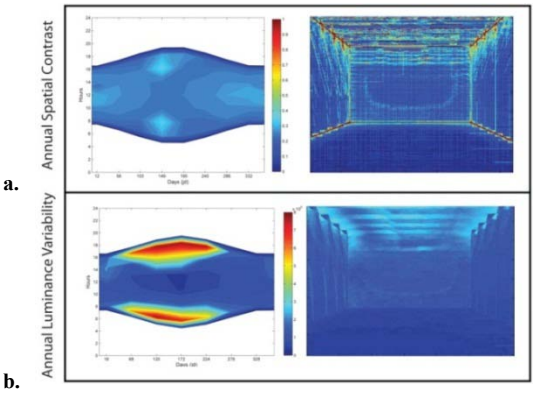

Figure 12. Cumulative image and temporal maps for case study 4: a) annual spatial contrast, b) annual luminance variability.

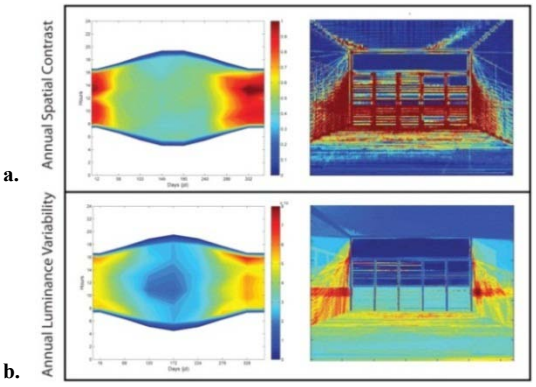

Figure 13. Cumulative image and temporal maps for case study 9: a) annual spatial contrast, b) annual luminance variability.

DISCUSSION & CONCLUSION

The metrics proposed by this paper present a new and novel approach to the dynamic analysis and visualization of contrast within architecture. Due to the spatial impacts of light and shadow on our perception of contrast and the inherent variability of daylit as a source of illumination, Annual Spatial Contrast and Luminance Variability evaluate the compositional and temporal impacts of daylight on our perception of interior space. While Annual Spatial Contrast quantifies the sum of all local contrast boundaries across a given view, Annual Luminance Variability accounts for the total change in luminance levels over time. The method of visualization for these metrics combines a cumulative image with a complimentary temporal map to identify *when* and *where* these dynamic variations occur. This approach moves beyond static representations of contrast and seeks a more specific method of quantifying compositional variations in brightness.

Each of these metrics is currently limited by the compression of annual data into a set of interpolated values. Future research will need to address a broader range of annual instances to fully validate the time-segmentation method used in this approach. Additional limitations include the time-intensive method of automated image production. A rigorous study and application of these metrics to existing architectural models will help to define a more appropriate numerical scale for resulting data. Future research must also investigate the relationship between compositional patterns of light and their impacts on our perception of contrast. An important vein of research would relate the proposed metrics to recommendations for contrast and temporal variation in programmed space.

A method of quantifying daily spatial contrast and luminance variability is currently underway using HDR time-lapse photography. This method (to be presented elsewhere) quantifies the dynamic changes in light across a much smaller interval of time. This increase in time-based resolution does raise new challenges, as moving subjects and objects within the scene provide sources of error, but it also allows designers to analyze existing buildings.

In conclusion, annual spatial contrast and luminance variability represent a shift toward dynamic luminance-based metrics that evaluate the relative impacts of contrast on our perception of architectural space over time. These metrics, although still preliminary in their development, seeks to understand the relationship between the composition and variability of daylit space. This research will help designers to contextualize positive aspects of daylit variability and compare contrast typologies on a dynamic scale.

REFERENCES

ANDERSEN, M., KLEINDIENST, S., YI, L., LEE, J., CUTLER, B., 2008. An Intuitive Daylighting Performance Analysis and Optimization Approach. *Building Research and Information*, vol. 36 (6), pp. 593–607.

ANDERSEN, M., GAGNE, J., KLEINDIENST, S., 2011. Informing Well-Balanced Daylight Design using Lightsolve. *In Proceedings of CISBAT 11: CleanTech for Sustainable Buildings - From Nano to Urban Scale*, September 14-15, Lausanne, CH

CETEGEN, D., VEITCH, J.A., NEWSHAM, G.R., 2008. View Size and Office Illuminance Effects on Employee Satisfaction. *Proceedings of Balkan Light*, October 7-10, Ljubljana, Slovenia, pp. 243-252.

DEMERS, C. 2007. A Classification of Daylighting Qualities Based on Contrast and Brightness Analysis. *Conference Proceedings of the American Solar Energy Society* (ASES), July 7-12, Cleveland, Ohio.

GLASER, D. AND HEARST, M. 1999. Space Series: Simultaneous Display of Spatial and Temporal Data. *Conference Proceedings of the IEEE Symposium on Information Visualization*, October 24-26, San Francisco, CA.

KLEINDIENST, S., AND ANDERSEN, M., 2009. Th e Adaptation of Daylight Glare Probability to Dynamic Metrics in a Computational Setting. *Proceedings of Lux Europa, 11th European Lighting Conference*, September 9-11, Istanbul, Turkey.

LAGIOS, K., NIEMASZ, J., AND REINHART, C., 2010. Animated Building Performance Simulation (ABPS) – Linking Rhinoceros/Grasshopper with Radiance/Daysim. *Proceedings of SimBuild 2010*, August, New York City, NY.

LOE, D.L., MANSFIELD, K.P., AND ROWLANDS, E. 1994. Appearance of Lit Environment and its Relevance in Lighting Design: Experimental Study. *Lighting Res. Rechnol*. Vol 26 pp 119-133

MARDALJEVIC, J., HESCHONG, L., AND LEE, E., 2009. Daylight Metrics and Energy Savings. *Lighting Research and Technology,* Vol 41 (3) pp 261-283.

MOON, P., AND SPENCER, D. 1942. Illumination from a Nonuniform Sky." *Illuminating Engineering*, Vol 37 (10), pp 707-726.

NABIL, A., AND MARDALJEVIC, J., 2006. The Useful Daylight Illuminance Paradigm: A Replacement for Daylight Factors. *Energy and Buildings*, Vol 38 (7), pp 905-913.

NEWSHAM, G.R., RICHARDSON, C., BLANCHET, C., AND VEITCH, J.A., 2005. Lighting Quality Research Using Rendered Images of Offices. *Lighting Research and Technology* vol 37 (2) pp 93-115

REINHART, C., AND MARDALJEVIC, J., AND ROGERS, Z., 2006. Dynamic Daylight Performance Metrics for Sustainable Building Design. Leukos, Vol 3 (1), pp 1-25.

VEITCH J.A., AND NEWSHAM, G.R., 2000. Preferred Luminous Conditions in Open-Plan Offices: Research and Practice Recommendations. *Lighting Res. Technol*. Vol 32, pp 199- 212.

WARD, G., 1994. The RADIANCE Lighting Simulation and Rendering System. *Proceedings of '94 SIGGRAPH Conference*, July, pp. 459-72.

WIENHOLD, J., AND CHRISTOFFERSEN, J., 2006. Evaluation Methods and Development of a New Glare Prediction Model for 152 Daylight Environments with the Use of CCD Cameras. *Energy and Buildings*, Vol 38, pp 743-757.

Performance Driven Design and Simulation Interfaces: A Multi-Objective Parametric Optimization Process

Angelos Chronis[1], Martha Tsigkari[1], Evangelos Giouvanos[1], Francis Aish[1], Anis Abou Zaki[1]

[1]Foster + Partners
Riverside, 22, Hester Road,
London, SW11 4AN, United Kingdom
achronis@fosterandpartners.com, mtsigkar@fosterandpartners.com, vgiouvan@fosterandpartners.com,
faish@fosterandpartners.com, azaki@fosterandpartners.com

Keywords: Multi-Objective Optimization, Environmentally Driven Façade, Parametric Modeling, Integrated Design Strategy, Simulation Interfacing Tool, Performance Driven Design.

Abstract

Despite the continuous development and integration of simulation interfacing tools in current architectural research, the availability and operability of off-the-shelf tools has still not met the timeframes and performance requirements of current architectural practice. The complexity and demanding performance goals of contemporary large-scale projects often require innovative approaches, as well as the development of novel simulation interfacing tools to meet these requirements.

This paper reports on a multi-objective optimization process, aiming at reducing incident solar radiations whilst optimizing daylight penetration, for the façade of a large-scale office building. This was achieved through the combined use of a parametric model and a genetic algorithm, along with an integrated data set of pre-computed results. To minimize the resources demand of analyzing the plethora of potential configurations of the façade, a number of strategically defined modular cases were modeled and simulated using bespoke interfacing tools to produce a database of results. This database was then linked to a parametric model, providing real time feedback and allowing for an exhaustive search of design configurations. To further explore potential optimal solutions, a multi-objective optimization process using a genetic algorithm, also linked to the results database, was implemented. The overall optimization process provided invaluable insight to the design problem at hand.

1. INTRODUCTION

1.1. Context

Architectural research has long been witnessing a continuous shift towards the development and integration of simulation tools, which aim to facilitate the feedback loop between design intentions and performance (Malkawi 2004). Recent developments range from whole-building energy simulation platforms (Rysanek and Choudhary 2012) and energy simulation tools for double-skin façades (Kim and Park 2011), to integration methods of daylight simulations in the architectural design process (Kim & Chung 2011) and fluid dynamics simulations for open joint natural ventilated façades (Sanjuan 2011) amongst many others. Apart from the continuous development of more effective and robust simulation models, current architectural research has also been engaged with the development of new interfacing tools, which aim to integrate the available simulation tools seamlessly into the architectural design process, as well as facilitate their utilization by non technical users. Recent examples include the linking of CAD packages to simulation engines, such as the DIVA plug-in that links the Rhinoceros software to the Radiance advanced raytracing software (Lagios et al 2010) or the development of design tools that integrate solar radiation, energy and windflow analysis modules, such as project Vasari by Autodesk Labs.

Despite this continuous effort towards the integration of simulation tools -which provide valuable performance feedback to the designer at all stages- the need to tackle the challenges of interoperability, ease of use, and resource requirements (all of which have been pointed out numerous times in the past e.g. Huang et al 2008, Lam et al 2004, Malkawi 2004), still remain. Moreover, with the advent of optimization computing paradigms in architecture, the need

for integrated and efficient performance feedback tools has become even more evident. Optimization techniques have become common ground in architectural research (Malkawi 2004) and are also widely applied in current practice. This trend for performance-driven solutions to architectural problems often dictates the emergence of ad-hoc development of demand-oriented tools (e.g. Mark 2010) or, possibly, the use of novel and less resource demanding simulation approaches (e.g. Chronis et al 2010). However in many cases the complexity of current architectural projects has been proven to be beyond the capacity of even the most capable systems (Hanna et al 2010). The amount of different – and often conflicting – parameters one needs to take into account requires not only novel and more efficient tools, but also innovative approaches towards performative solutions. These should combine the current computing capabilities with the ingenuity that lies in the designer's overview of an architectural problem.

In this paper we report on an innovative approach towards a multi-objective optimization process, aiming at reducing façade incident solar radiation whilst optimizing daylight levels, for a large-scale office building. The scope of this process was twofold, aiming on one hand to provide valuable real time feedback to the design team through the use of a parametric model, and on the other to generate optimized solutions through the use of a genetic algorithm. Both of these procedures were linked to a data set of pre-computed results for a number of specifically designed modular cases.

1.2. Diverse Problem Definition

The project to which the above process was applied was developed in the Middle East, and was an ideal candidate for deploying the aforementioned optimization techniques. This new development incorporates the urban planning and architectural design of three office parks, and its office accommodation was perceived as directly reflecting the needs imposed by its surrounding environment. The project was developed as a pioneering example of sustainable, energy-efficient design, responding to the culture and climate of Middle East. Under this spectrum, sustainability has been a central theme and driver for developing the scheme. The goal was to establish flexible, efficient, humane and sustaining environments: buildings with low energy consumption, high-performance cladding, solar shading and efficient insulation to achieve maximum comfort for those that use them.

Defining an exterior and interior (courtyard) envelope that responds to the sustainability goals set by the programme demanded a multilayered approach. Initially the basic shape of the individual buildings needed to be defined so, as to minimize the solar gains and maximize the self overshadowing capacity. Secondly a façade system had to be developed in such a way as to respect the structural grid of each building and allow for modularity and architectural variety. Thirdly an integrated process had to be set in place, by which multiple analysis iterations for the various configurations of the façade could be produced, analyzed and graded in terms of effectiveness, feasibility and sustainability. All of these within very frequent design cycles. Additionally, all of the above needed to be seamlessly integrated within a parametric model that allowed for quick design iterations, analysis and evaluation. The model form produced had also to be driven by specified parameters and constraints -representing the environmental, structural and buildability inputs- as well as promoting user interaction with the general form, in order to reflect interventions shaped by architectural and aesthetical criteria.

2. BACKGROUND

2.1. Initial Form Configuration

As a preliminary response to both the required spatial and environmental considerations, the initial form-finding was defined in conjunction to the input provided by the assigned environmental consultants. Therefore, the general shape started as an extruded box, on which different façade inclinations were tested against their total annual radiation score and self-shading capacity. This investigation resulted in a generic shape resembling an upside-down, four sided cone – a form that ensured lower radiation scores on the façade due to the ability of the higher floors to provide overshadowing to the lower ones. The addition of a considerably overhang roof also assured protection for the higher levels of each building. The optimal inclination for this configuration was set to 23 degrees.

In parallel, each floor was defined based on the base structural grid, measured from the centre of the building outwards. This grid was perceived as a sequence of bays that could be set back or protrude from the main form, in pursuit to the optimal environmentally driven response.

2.2. Environmental Parameters and Multiple Configurations

In addition to the development of the generic building form based on the above considerations, there was also a second set of defined sustainability criteria, which were namely the incident annual direct and diffuse solar radiation as well as each façade's potential daylight capacity. Under that spectrum, for each bay, a number of flexible parameters were defined to permit for an optimal solution. These were namely the glazing to wall ratio as well as the Solar Heat Gain Coefficient (G value) for the glazing itself.

This, consequently, added an extra degree of complexity due to the numerous parameters and potential differentiated forms that had to be iteratively designed, analyzed and evaluated. Each of the four façades of every building had hundreds of bays that could have thousands of different configurations of inward/outward offsets relative to each other, with each bay having 10 different glaze-to-solid ratios (from 10% to 100%) as well as various potential glass G-values. This resulted in tenths of millions of different configurations to process, an impossible feat for the given timeframe if using traditional design techniques.

2.3. Shaping a Parametric Environmental Response

An answer to the above requirements was the development of a) an integral parametric model and b) the specification of individual "test cases". The former incorporated an array of bespoke scripts and permitted the management of the model both based on specified constraints as well as direct form manipulations from the designers. The latter minimized the millions of potential configurations into a smaller selection pool, by specifying smart assumptions about the offset and glazing ratio as different test cases.

Based on these different cases, a set of models were developed and simulated and their solar radiation, daylight and vertical sky component results, were pre-computed and registered in tailored Excel spreadsheets. This method ensured direct feedback for any single manipulation of the parametric model as well as facilitation of the optimization process of the façade.

A very important aspect of this integral model was the possibility it gave to the designer to individually manipulate the model and get a direct feedback in relation to how well the drawn configuration performed. Every change in the offsets of singular bays, their glass ratio and G value could directly inform the designer of how good or poorly the new model performed relatively to any other given solution and allowed for educated decisions to be made during the form finding process.

2.4. Optimization Strategy

The final stage of this environmentally driven façade investigation included a multi objective optimization process, using a genetic algorithm, which generated a series of optimized façade configurations. Through several iterations of optimization runs and the manipulation of the weighting of conflicting parameters, that were made possible in the timeframe by feeding into the optimization process the pre-computed data set of results, a range of solutions to the given problem were produced.

The generated configurations were not considered as mere optimal solutions to the given problem, but rather formed part of the guidance of an overall informed architectural solution. The designer intervention was again a key aspect in shaping a solution that satisfies not only these specific performance criteria, but also a range of other architectural parameters, including but not limited to structural, aesthetic and other sustainability parameters of the problem.

3. METHODOLOGY

As already mentioned, for the optimization of the buildings' façade several steps had to be made. These were:

- The design and specification of key 'test cases' for analysis
- Precomputing of incident solar radiation and daylight results for the specified cases
- Development of a results database which allows interpolation lookup in between the specified cases.
- Development of a parametric model that links the precomputed results database and provides real-time feedback to the designer
- A multi-objective optimization process through the use of a genetic algorithm.

A detailed description of these steps follows.

3.1. Design of test cases

One of the most significant steps towards the minimization of the option pool, and therefore the complexity of the searchable solution space was the definition of key points in the movement range of the façade bays and the design of appropriate 'test cases'. The test cases were designed with the aim to minimize the required analysis runs but also cover all possible options.

For this reason, the effect of the protrusion or setback of the neighboring and top bays on the incident solar radiation and daylight performance of each bay was studied, and a set of test cases with a combination of neighboring and top protrusions and set backs were modeled. To cover all possible configurations of the façade the cases were designed in such a way that their combinations could be used to predict the performance of any possible bay option. For example, instead of allowing every bay to have innumerable potential offsets, a set of four points in the movement range was defined. This resulted in a total of 27 bay cases that needed to be simulated, produced by the combination of the effect of the three movement steps, for each neighboring bay (excluding one inward step which has no effect). For convenience, these were modeled as 9 different three-storey models, each of which represented three different cases per each orientation (Figure 1). By combining the effect of the protrusion of each neighbor the result for every possible configuration along those predefined steps is easily achievable. Furthermore, the interpolation of results between those steps, again for every neighboring bay, allows for every possible configuration to be assessed (Figure 2).

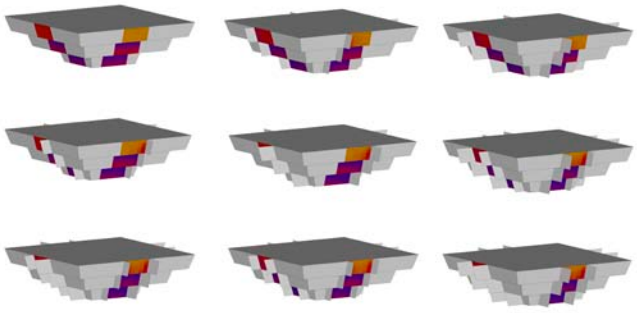

Figure 1. Solar radiation results for a number of test cases.

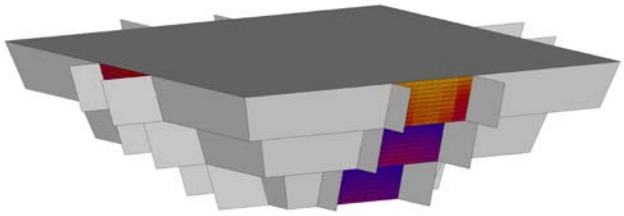

Figure 2. Solar radiation results for one test case.

3.2. Results database

For this defined set of test cases a series of simulations were run to precompute the incident solar radiation and daylight performance of each case. The incident solar radiation was calculated using a bespoke script that links the Radiance simulation engine to a standard CAD package. The results were given as annual solar radiation per panel, on a pre-defined grid of panels and for each test case. For the daylight performance the simulation was run using the Autodesk Ecotect software and the results were calculated on a grid of panels on the floor plane. For each test case, daylight results were computed for a series of different glazing ratios and for two specific time sessions, at 09:00 in the morning and 15:00 in the afternoon.

The combined set of results were then imported in a spreadsheet which was structured as a look-up table to facilitate both the quick look up of different façade configurations as well as the interpolation of results for non calculated options. A representation of the façade panels and their solar radiation results was also incorporated in the spreadsheet along with a number of changeable parameters, such as the solar heat gain coefficient and light transmissivity, providing the ability to explore the performance of different glass configurations (Figure 3). An indication of the percentage of performance improvement over the ASHRAE base case was also included both for the solar gains on the glazing as well as the solar gains passing through it. Finally a representation of the daylight results was incorporated as well providing visual and textual feedback on the daylight performance of each option (Figure 4).

The development of this pre-computed results database was a quite significant step not only because it provided the means to the real time feedback of the developed parametric model and allowed for a set of optimization iterations of the

GA, but most importantly because it provided a first level of understanding of the complexity of the problem.

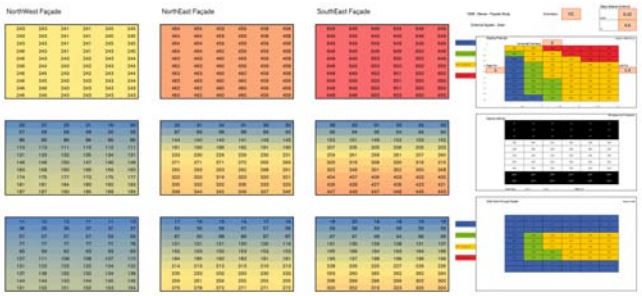

Figure 3. Solar radiation results database.

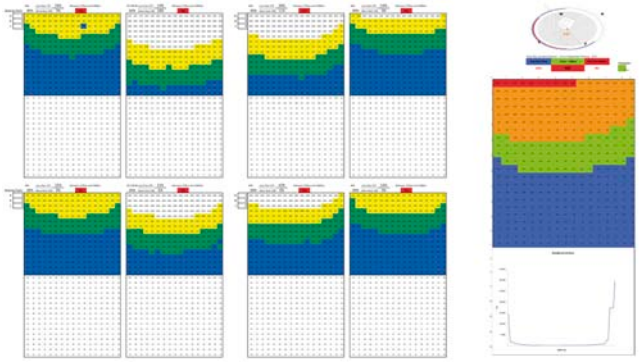

Figure 4. Daylight results database.

3.3. Parametric model

As already discussed, the development of a parametric model, which would be linked to the data set of results, aimed to provide valuable feedback to the design team for the assessment of performance of a given façade configuration and allowed for the exploration of many different design options. The parametric model, which was created using Bentley Generative Components (GC) was linked both to the pre-computed results database, as well as a color-coded set out spreadsheet, which allowed the user to have an overview of the complex set of parameters that define a configuration. The geometry of each building was generated using a series of GC scripts, according to the set out file which defined both the offset from the structural grid as well the glazing ratio of each bay. The resulting configuration was then used to query the database for solar radiation and daylight results for each bay and according to the offsets of its neighbors but also its specific glazing ratio. These results were then applied back to the parametric model giving both visual feedback as well as indicators of performance improvements of the specific configuration (Figure 5).

Through the manipulation of this informed parametric model the design team managed to explore a vast amount of different configurations without the intensive resource requirements of iterative simulation runs. Moreover the emergence of performative patterns on the façade highlighted the important aspects of the design parameters on the performance impact of the buildings and provided a deeper understanding of the problem at hand. Nevertheless a further investigation on optimal solutions, with the aid of computational methods was considered an important further step.

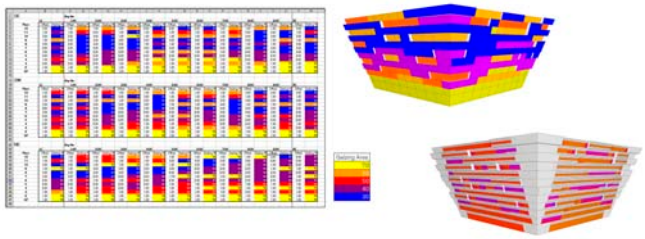

Figure 5. Set out file, generated geometry and results on the parametric model.

3.4. GA optimization

For the GA optimization process a bespoke application was developed in the Processing programming language which was also linked to the pre-computed results database. The choice of a custom written application was not only dictated by the specific needs of this problem but it was also proven invaluable in manipulating the optimization framework to accommodate the architectural constraints of the problem. The optimization framework was developed in accordance to the problem's needs, allowing the configuration of offsets and glazing ratios for each bay of the façade. These parameters were encoded in the genes of the GA enabling it to search through all of their possible configurations. A configuration of all the offsets and glazing ratios for every side of the façade was set out for each of the studied buildings. Also a look up table for the pre-computed results was developed, allowing the quick evaluation of each generation. In detail the algorithm was set out as follows:

- A random generation of configurations is initially generated
- For each member of the population the solar radiation and daylight performance is evaluated as follows:

- For each bay of the façade the relevant pre - computed cases are looked upon and the interpolated result is registered to the fitness function
- The member is evaluated and ranked, according to the different fitness functions used
- The algorithm continues to run until it converges

The optimization process was integrated seamlessly within the design process, including data exchange. The generated optimal solutions were properly exported as set out files for the developed parametric model facilitating the generation of 3d models and visualizations of the optimal solutions. The timeframe of an optimization run using the pre-computed results is not comparable with an equivalent optimization process that would require iterative simulation runs to assess the fitness of every member of the GA population. The time needed to calculate the performance of a building configuration was only a fraction of a second, making feasible the offspring of more than 150.000 generations in one optimization run (Figure 6).

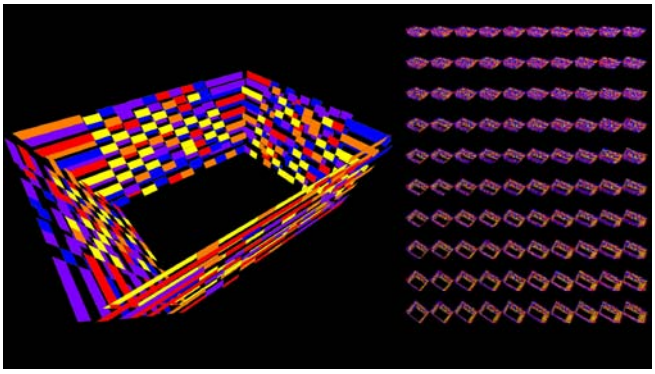

Figure 6. Optimization framework screenshot.

The first results of the optimization process showed clear trends towards offset and glazing patterns, however the conflicting objectives did not initially allow the scheme to converge to a single optimum solution. This led to a further experimentation with various different fitness functions which weighed the importance of the conflicting parameters. The fitness of each member of the GA population was assessed according to its performance in terms of minimizing solar gains and maximizing daylight, as well as its overall improvement ratio over the ASHRAE base case. These were calculated either per bay or per façade or as a combination of both, yielding different results in each case (Figure 7). To rule out solutions that would not be viable, such as minimal glazing ratios on the whole of the façade the optimization process was steered according to architectural constraints. Finally a two step optimization process was also implemented, allowing in a first step the optimization of the offsets of the bays and in a further one the optimization of the glazing ratios for the optimized massing. The final result clearly indicated a trend towards an egg-crate massing with minimal glazing ratio on protrusions and maximum ratio on the set-backs while also converging towards specific glazing ratios per orientation (Figure 8).

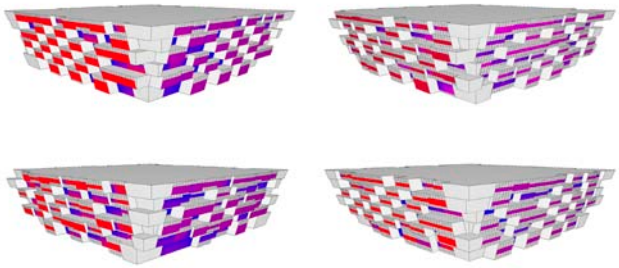

Figure 7. Trade-off between daylight and solar gain

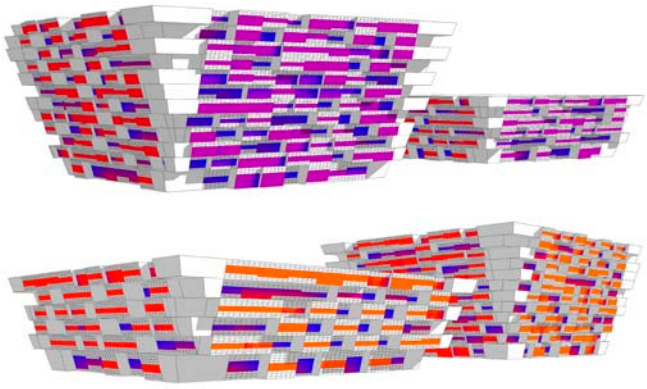

Figure 8. GA Optimization result – Incident solar radiation on the façade.

4. PERFORMANCE DRIVEN DESIGN

The above analytical approach was developed in such a way as to facilitate the development of a design that is shaped based on its performance. To achieve a seamless

process two factors needed to be taken into consideration: a) the complex nature of the problem definition and b) how to translate this multi-objective task into an easy to use interface/decision making tool.

4.1. Harnessing Complexity – Integration in Design

Design is, by default, a multidisciplinary affair. Therefore any given consideration has to span through various fields in order for any sort of optimization to be achieved in the scheme as a total. This complexity is actually in the heart of any design development and the way one harnesses it - in order to from design processes and procedures - can define the success or not of the outcome. In this aspect, integrated design as a practice allows for the designer to fully understand the underlying complexity of any given task and the various disciplines through which an optimal outcome should span. That has as a result an underlying weaving of a plethora of factors, which could even contradict each other, but are essential for the project's successful adaptation to the multidisciplinary fitness criteria set.

The parametric approach, thus, is the first step of visually defining the above rules and considerations. This is achieved via a defined compilation of variables and constraints that can reconfigure the model relatively to the various environmental, structural and managerial considerations. In addition to that, the definition of "key cases" for the environmental analysis investigation is essential, as it helps translate innumerable multiple configurations into a more manageable set of options to test against, thus taking upon the task of understanding the complex nature of the problem and then simplifying it as to make it controllable.

4.2. Simulation Interfacing Tool

After defining the above process the subsequent step is developing a tool that can, in real-time, provide the user with the simulation results and the score of each configuration. That is essential in assisting the designer to form the design intentions at an early stage of the process, based on direct feedback provided by the various analyses. Therefore the performance of quick simulations and their ensuing results instantaneously feeding back in the model are of paramount importance. This cycle provides an easy and straightforward way of shaping the design, not based on assumptions, but on synchronized analytical processes that can evaluate the success or failure of each iteration. Therefore the seamless interface between the analyses and its application to the model, where the user is not concerned with interoperability issues but rather directly witnesses the results of his manipulations to the model, provides a very powerful tool for decision making with performance driven design intent.

5. CONCLUSION

The techniques explored for the façade optimization of this project represent an integrated approach to design, achieved through a set of parametric simulation interfacing tools. In order for the form of the building to provide a direct response to the needs imposed by its environment, a bespoke design system was developed which allowed not only the direct manipulation of the model (based on specific constraints and parameters) but also a real-time feedback in terms of it achieving the sustainability goals set.

Based on the multilayered diversity of the problem, the workflow was distributed in different stages. Initially the basic form was analyzed and chosen relative to each self-shading capabilities. Then a parametric model was introduced in order to facilitate quick model changes to match the design cycles. Subsequently "key cases" were defined, so that to minimize the pool of configuration that were to be pre-computed and analyzed relative to environmental fitness criteria. This defined a mechanism of direct feedback in terms of the trade-off achievement between optimum daylight and minimal solar gains: every time the model was changed the designer could directly see how much better or worse the new solution worked relatively to the specified environmental goals. Finally a custom multi-objective Genetic Algorithm was developed so that a global optimal solution could be specified. This optimal candidate was not the "answer" but rather the guide towards a set of potential manipulations that could be taken into consideration in addition to all the architectural, structural, aesthetical and space planning criteria.

Throughout the development of the project it was made evident that an integrated approach to design is greatly facilitated via a set simulation tools that can interface in a parametric manner throughout the design process and allow for direct feedback in every stage of the model manipulation. Thus the user is no longer "guessing" of the configurations that may provide optimal results, but rather makes educated choices based on the instantaneous response of the various diagnostic analyses performed (either those

are environmental, structural, pedestrian or similar simulations). Although this approach was developed according to the needs of this specific project, it is expected to serve as a precedent for future relevant multi-objective optimization problems, as its efficiency, both in terms of resources, as well as in terms of integration in the design process, was considered significant. Such a strategy though requires a computational design approach that incorporates considerable custom programming in various languages of CAD or analysis packages, as well as the ability to interoperate between them. But in the same time those custom mechanisms empower the designer in meeting his goals and promoting innovative approaches to an integrated design processes driven by multidisciplinary concerns.

References

CHRONIS, A., TURNER, A. AND TSIGKARI, M. 2011. Generative Fluid Dynamics: Integration of Fast Fluid Dynamics and Genetic Algorithms for wind loading optimization of a free form surface. Proceedings of the Symposium on Simulation for Architecture and Urban Design at the 2011 Spring Simulation Multiconference, Boston, USA.

HANNA, S., HESSELGREN, L., GONZALEZ, V. AND VARGAS, I. 2010. Beyond Simulation: Designing for Uncertainty and Robust Solutions. Proceedings of the Symposium on Simulation for Architecture and Urban Design at the 2010 Spring Simulation Multiconference, Orlando, USA.

HUANG, Y.C., LAM, K.P. AND DOBBS, G. 2008. A Scalable Lighting Simulation Tool for Integrated Building Design. SimBuild 2008, San Francisco.

KIM, C.S. AND CHUNG, S.J. 2011. Daylighting simulation as an architectural design process in museums installed with toplights. Building and Environment, Volume 46, Issue 1. Pages 210-222.

KIM, D.W. AND PARK, C.S. 2011. Difficulties and limitations in performance simulation of a double skin façade with EnergyPlus. Energy and Buildings, Volume 43, Issue 12. Pages 3635-3645.

LAGIOS, K., NIEMASZ, J. AND REINHART, C.F. 2010. Animated Building Performance Simulation (ABPS) - Linking Rhinoceros/Grasshopper with Radiance/Daysim. Proceedings of SimBuild 2010. New York.

LAM, K.P., HUANG, Y.C. AND ZHAI, C. 2004. Energy Modeling Tools Assessment for Early Conceptual Design. Final Report to Northwest Energy Efficiency Alliance (Contract 10026). Pittsburgh, Carnegie Mellon University.

MALKAWI, A.M. 2004. Developments in environmental performance simulation. Automation in Construction 13(4). Pages 437-445.

MARK, E. 2010. Optimizing Solar Insolation in Transformable Fabric Architecture. Proceedings of the 28th eCAADe Conference, Zurich 2010, Germany. Pages 219-226.

RYSANEK, A.M. AND CHOUDHARY, R. 2012. A decoupled whole-building simulation engine for rapid exhaustive search of low-carbon and low-energy building refurbishment options. Building and Environment Volume 50. Pages 21-33.

SANJUAN, C., SUAREZ, M.J., BLANCO, E. AND HERAS, M.R. 2011. Development and experimental validation of a simulation model for open joint ventilated façades. Energy and Buildings, Volume 43, Issue 12. December 2011. Pages 3446-3456

Climatic Based Consideration of Double Skin Façade System: Comparative Analysis of Energy Performance of a Double Skin Facade Building in Boston

Mona Azarbayjani[1], Jigisha Mehta[1]

[1] Center for Integrated Building Design Research
Energy Performance Laboratory
School of Architecture, UNC Charlotte
mazarbay@uncc.edu

Keywords: Double skin façade, Energy performance, Climate-based design, Heating and Cooling loads.

Abstract

This study compares the energy performance of different configuration of double skin facades vs. single skin facade during prevailing summer, winter and shoulder season. While a great deal of interest exists in learning how to integrate DSFs into our current architecture, there is a little knowledge or demonstration of how the concept might work in the US climatic contexts. The primary goal of this research is to clarify the state-of-the-art performance of DSFs, so that designers can assess the value of these building concepts in meeting design goals for energy efficiency, ventilation, productivity, and sustainability. This investigation adopts an analytical approach using dynamic simulation software (Energy Plus/Designbuilder), to understand the performance of a double skin façade based on research rather than intuition. In this paper, a comparative analysis of cooling and heating loads on a single skin base case is compared against three possible changes to the physical properties of the external and internal layer of the double skin facade. Simulation results indicate that a reflective double skin facade can achieve better energy savings than a single skin with reflective glazing.

1. INTRODUCTION

With the emergence of energy-consumption reduction as a major national concern, the search for better approaches in improving both thermal comfort conditions and the energy efficiency of buildings is intensifying.

The concept of DSF is not new and dates back to many years ago where in central Europe; many houses utilized box-type windows to increase thermal insulation (Oesterle, 2000). Many authors claim that the double skin façade system can improve energy performance of the building due to the greater insulation provided by the outer skin. Design strategies need to consider the climatic conditions and local characteristics such as temperature, solar radiation, wind velocity and temperature in order to results in energy consumption reduction. The potential of using a double façade of the building in climates other than Europe has not been fully studied though. A number of interesting investigations and findings are reported in the literature pertaining to passive ventilation in buildings with double-skin facades. Even though most of the research has been done in temperate climate conditions, studies have revealed a close link between natural ventilation design and the DSF function. Grabe et al. (2002) developed a simulation algorithm to investigate the temperature behavior and flow characteristics of natural-convection DSFs through solar radiation. It was found that the air temperature increased near heat sources that are close to window panes and shading device. Gratia and Herde (2007a, 2007b, 2007c) attempted to look at natural ventilation strategies, greenhouse effects, and the optimum position of sun-shading devices for DSFs facing south in a northern hemisphere temperate climatic. They found that a sufficient day or night ventilation rate can be reached by a window opening, even if wind characteristics are unfavorable. The aim of this study is to reflect on strategies for double skin facades that are responsive to particular climate type of

Boston. The following questions will be answered satisfactorily in this study:

a) If buildings perform well in one climate such as central Europe, can we take the same design solution to a new location and climate, such as Boston?

b) How well does DSF technology perform in buildings in hot summer continental climates (Boston)?

To that end this study focused on comparative analysis between double skin façade and a single skin façade for an information center building in Boston. Annual heating and cooling loads were calculated and compared as a result of the study.

2. METHODOLOGY

As suggested by Ternoey et al. (1985), the easiest way to evaluate energy improvements in building design is to appraise energy use patterns with a base case. For this purpose, the building has been simulated with single skin as a base case.

Then a parametric study was carried out focusing on energy use. The base-case scenario with double low-E pane windows was simulated to calculate the energy demand during the occupation stage. Then the same building with the DSF was simulated. Moreover, parameters such as different types of glazing, and cavity depth were varied to study the impact of energy use. This study is divided into three main parts:

- Development and simulation of the reference single-skin building
- Simulations of the DSF in terms of energy performance
- Simulation and analysis of the alternatives.

2.1. Base Case- model description

The Cambridge Public Library it is 104,000 SF which 76,800 SF are for the new building and 27,200 SF for the historic building (Van Brunt & Howe, 1889). The new building is a project which incorporates a double face system; it's a pioneer of double skin curtain wall technology in the US.

Figure 1. Double skin façade building.

The specifications of the project are:

• 3'-0" Deep Airspace: provides added insulating depth and enables maintenance access

• Multi-story thermal flux: the greater height improves natural convection and makes the heat capture and exhaust more efficient.

• Movable 1'-0" Deep Sunshades: locating the blinds in the protected cavity allows them to collect the sun's heat energy before it enters the conditioned building. The lightweight aluminum louvers can be motorized to provide glare protection at all sun angles (important on a southwest exposure).

Some of the building features are as follows:

– A Unique High-Performance Facade:

• The double-skin facade (two surfaces of glass, creating an insulated airspace) is a multi-story (full height), full depth (3'), thermal flue. The facade allows for complete transparency while ensuring protection from excessive heat gain, heat loss, and glare:

– Energy Savings and Comfort:

• The facade achieves 50 % reduction compared with a conventional curtain wall and maximizes comfort at the reading spaces. The 3'airspace can be open in summer to keep heat from entering the building and closed in the winter to create an insulating "thermal blanket;"

– Natural Light:

• The facade brings a significant amount of balanced natural light into the library, carefully controlled by fixed and movable sunshades.

– Natural Ventilation:

• Operable windows in the facade allow for fresh air throughout the year (even in winter) without insect screens blocking and without concern for stolen books. In the winter, spring and fall, the windows allow heat from the cavity to be brought into the building.

Figure 2. New addition to the historic Cambridge library.

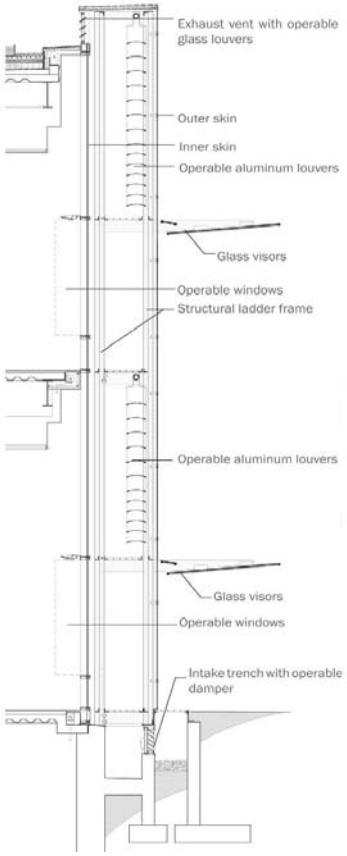

Figure 3. Double skin façade section and components, curtsey of the architect William Rawn Associate.

Figure 4. View towards double skin façade on the first floor.

After obtaining basic building and weather data, a simulation of the building's energy performance was undertaken. This was the base case simulation for a single skin facade system. The simulation software used for this research was Design Builder with EnergyPlus as an engine.

Since the behavior of double skin facades is highly dependent on the type of climate, following sections outline a process for selecting the type, analyzing characteristics and properties and selecting strategies preferable for a specific context.

Components of the studied double skin included internal layer, composed of 6 mm clear glass pane, 20 mm argon filled gap and 6 mm internal low-e glass and aluminum frame with thermal breaks. External layer consisted of 6 mm clear glass. Components of the single skin were similar, with double glazing composed of 6 mm external clear glass, 20 mm argon filled gap, internal 6 mm low-e glass and aluminum thermal brake frame. Both cases included shading blinds, where in the case of double skin they were placed in the cavity, and for double glazing on the interior of the building.

Nestled in the historic heart of Boston, the new additional Cambridge library is an architectural bridge that links the traditional past to a visionary future. The building will not only conserve significant amounts of energy, but it will also create a highly conducive environment for study and research while ushering in a new era of campus architecture focused on resource conservation.

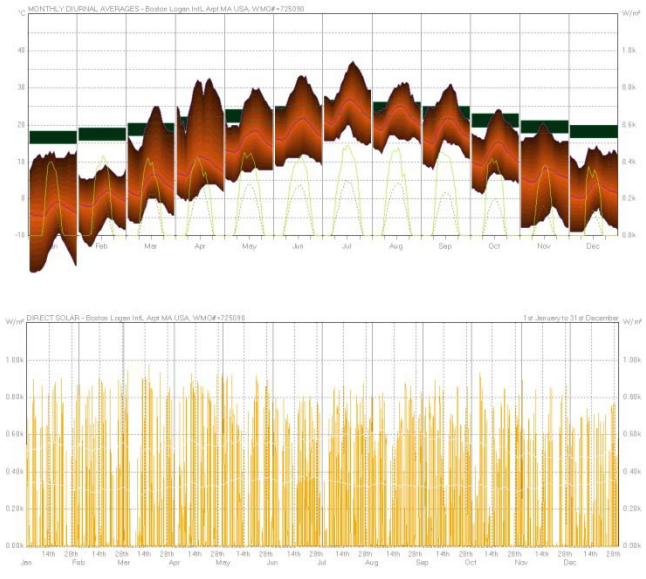

Figure 5. Climate analysis, average temperature and solar insolation.

The Boston climate is classified as a humid continental climate (Koppen Dfb with areas of Dfa). Summers are typically warm, rainy, and humid, while winters are cold, windy, and snowy. Spring and fall are usually mild, but conditions are widely varied, depending on wind direction and jet stream positioning. The hottest month is July, with a mean temperature of 73.9 °F (23.3 °C). The coldest month is January, with a mean of 29.3 °F (-1.5 °C). The city averages 42.5 inches (1,080 mm) of precipitation a year, with 41.8 inches (106 cm) of snowfall a year. Most snowfall occurs from December through March. There is usually little or no snow in April and November, and snow is rare in May and October. Prevailing wind directions throughout the year are South-West and North-West.

The building has 3 floors and a basement, and the zones are divided by the use of each one. We have 8 different zones, hall/lecture/assembly area, circulation area, display and public area, generic office area, reception, toilet, workshop-small scale, light plant room, cupboard.

2.2. Zoning

The plan was divided into multiple zones according to geometry, proximity, and use. Each zone was then assigned an activity template (indicated by color in images) which associate that zone with different energy profiles and schedules. These schedules are often repeated floor to floor. The atrium is treated as one single zone inside DesignBuilder, with openings in the floor and ceiling of the corresponding floors connecting them.

2.3. Model parameters and inputs for DSF

Many building system perimeters were left as their default setting when alternative information was not available significant modifications were:

ROOF: Type Concrete/insulated Overall R-value 40
Reflectivity 0.4

WALLS: Type Insulated precast concrete panels with additional insulation
Overall R-value 13.7
Glazing percentage 48
Basement/Foundation
Slab edge insulation R-value 10
Under slab insulation R-value 10

WINDOWS:

1. U-value
Double façade 0.23
Other 0.46
2. Solar Heat Gain Coefficient (SHGC)
Double façade 0.49
East open area 0.35
Other 0.27
3. Visual Transmittance
Double façade 0.64
East open area 0.63
Other 0.45

LOCATION: Latitude 42, Longitude -87.656

Orientation West (double) façade 252° off north

The default schedules for the library activity templates were based on a 9 hr/day, 6 days/week operational schedule. Outside this time plug, lighting, heating, cooling and DHW loads would shut off.

However, being a collegiate facility, the Center maintains significantly longer hours. For this model the schedule was simplified to 14hr/day (8 am – 10 p.m.) 7 days/weeks. While this schedule does not reflect daily variation in library hours, it averages to the same number of operational hours per week. Modified schedules were

implemented for public spaces, office spaces, and assembly spaces.

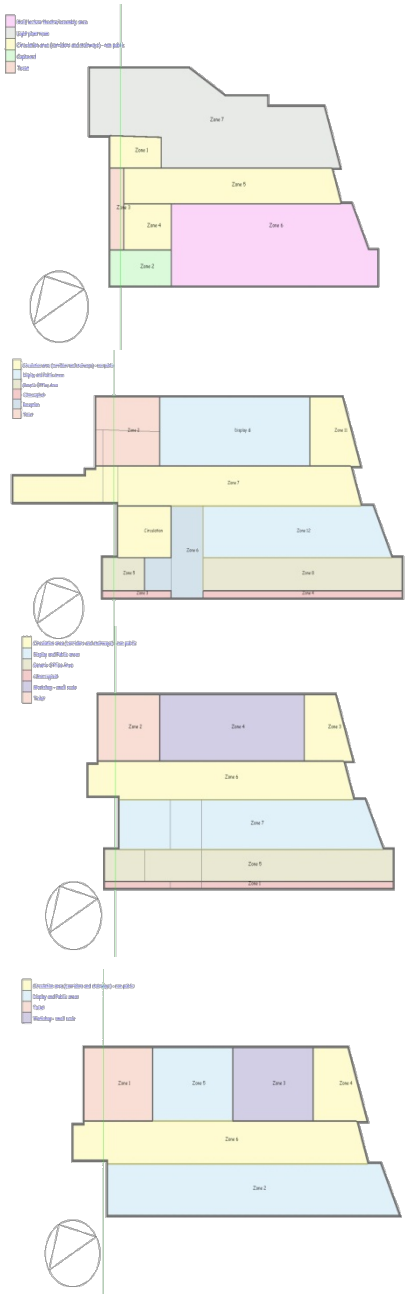

Figure 6. Zoning.

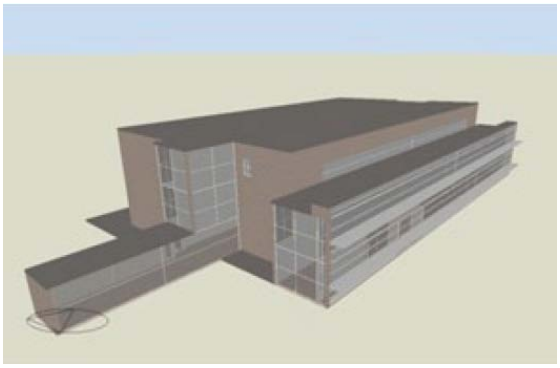

Figure 7. Model created in DesignBuilder.

3. RESULTS

The hourly energy simulation shows the daily variation in system loads since insolation, air temperature and internal gains vary throughout the day. The whole building results are somewhat difficult to meaningfully interpret as the occupied spaces are averaged with the façade cavity spaces. However if the data is separated it can be seen that the building systems are performing reasonably. The cavity, which is not heated or cooled, shows large temperature swings, high solar gains (up to ~1,500Kbtu/ hr) and high natural ventilation rates (up to 70 ac/hr) when the temperature rises above the set point. The interior zones, which are heated and cooled, have more stable temperature profiles, lower solar gains (~300 Kbtu/hr) and moderate ventilation rates (~ 2ac/hr). It can also be seen that internal gains follow the 8:00am – 10:00pm occupation schedule.

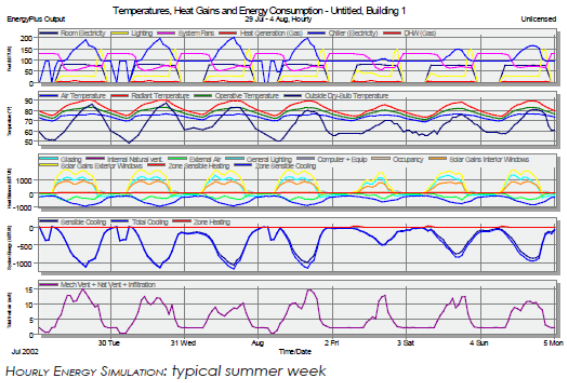

Figure 8. Hourly data on a typical summer week

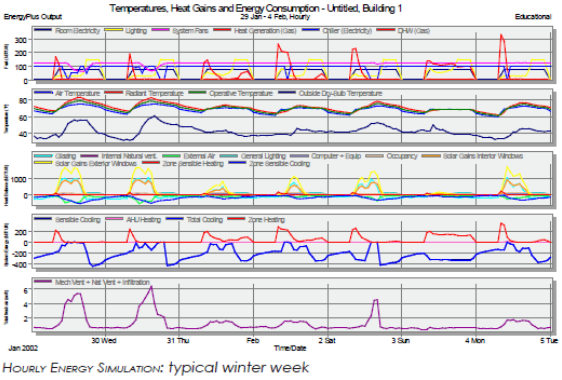

Figure 9. Hourly simulate data on a typical winter week.

3.1. Building performance and its consumption.

Monthly energy results average the daily variation and shows how energy loads respond to season variations. It can be seen that lighting loads are reduced during the summer, as the days are longer and day lighting can meet a larger portion of the lighting need. There is also a reduced fan load during the summer month. However these savings are offset by a roughly 40% increase in cooling loads during the summer months and total electric load remain fairly constant throughout the year.

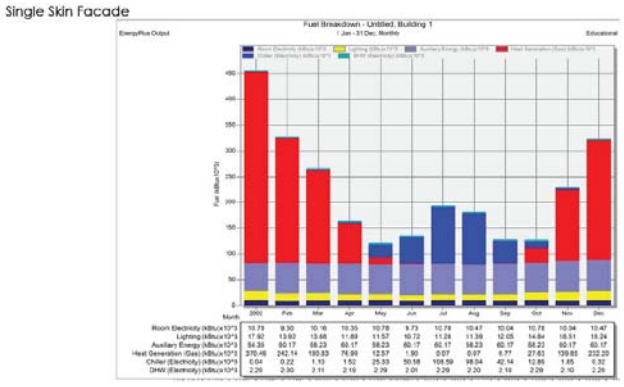

Figure 10. Single skin façade energy simulation results.

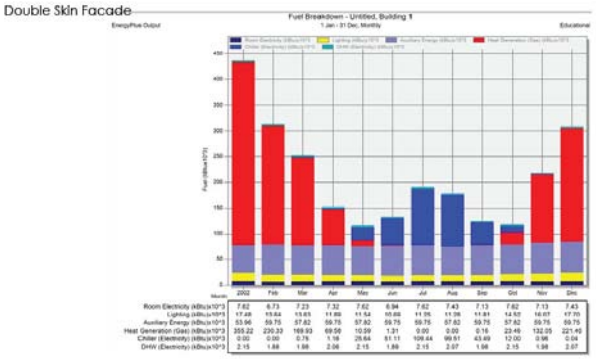

Figure 11. Double skin façade energy simulation results.

The benefit of the double façade becomes apparent comparing heating loads.

The annual energy consumption of the double skin has been compared with single skin as illustrated below. It was discovered that in total double skin façade consumes 5 percent less energy than single skin façade.

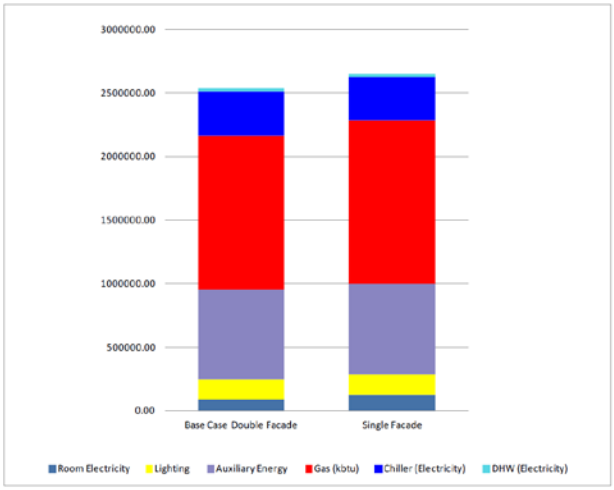

Figure 12. Total energy consumption comparison.

3.2. Modifications to the base case

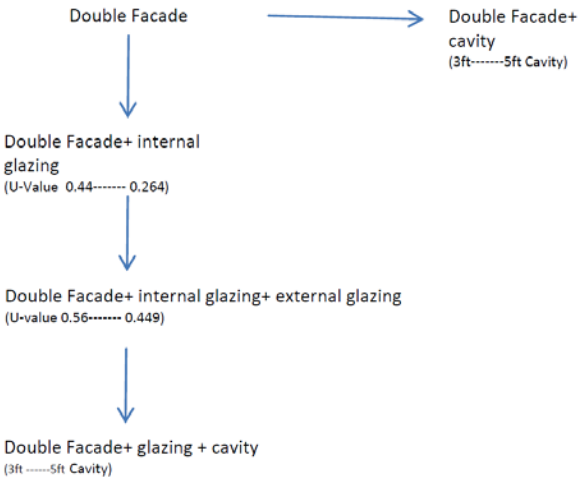

Figure 13. Alternatives.

In the second part of the analysis, the double skin façade system has been compared with four different alternatives illustrated in figure 13. The cavity size has been changed from 3 ft. to 5 ft. U-value of the internal glazing and

external glazing has been improved from .44 to 0.246 for internal and from 0.56 to 0.449 for external glazing respectively. The results of these alternatives has been tabulated and illustrated in figure 14 and 15.

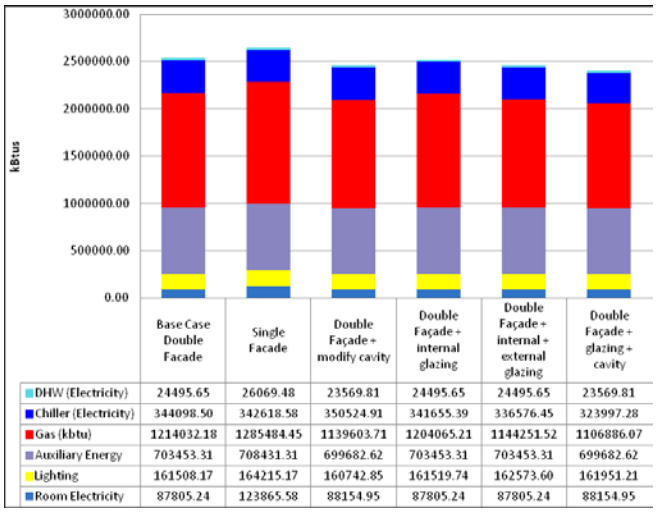

	Base Case Double Facade	Single Facade	Double Façade + modify cavity	Double Façade + internal glazing	Double Façade + internal + external glazing	Double Façade + glazing + cavity
DHW (Electricity)	24495.65	26069.48	23569.81	24495.65	24495.65	23569.81
Chiller (Electricity)	344098.50	342618.58	350524.91	341655.39	336576.45	323997.28
Gas (kbtu)	1214032.18	1285484.45	1139603.71	1204065.21	1144251.52	1106886.07
Auxiliary Energy	703453.31	708431.31	699682.62	703453.31	703453.31	699682.62
Lighting	161508.17	164215.17	160742.85	161519.74	162573.60	161951.21
Room Electricity	87805.24	123865.58	88154.95	87805.24	87805.24	88154.95

Figure 14. Alternatives annual energy breakdown comparisons [KBtus].

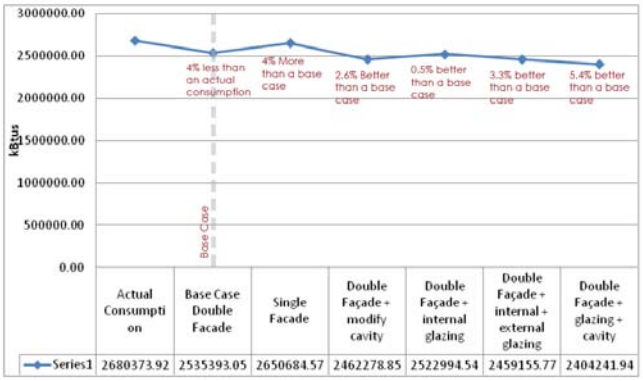

	Actual Consumption	Base Case Double Facade	Single Facade	Double Façade + modify cavity	Double Façade + internal glazing	Double Façade + internal + external glazing	Double Façade + glazing + cavity
Series1	2680373.92	2535393.05	2650684.57	2462278.85	2522994.54	2459155.77	2404241.94

Figure 15. Annual energy breakdown comparisons percentages [KBtus].

With the modifications in the cavity dimension and change in the glass property makes the base case perform 5.4 percent better.

4. FINDINGS AND ANALYSIS

In general, energy consumption in buildings is determined by function, climate, building components, construction, control, and settings. The climate and the ambiance are considered as-boundary conditions in energy simulation. Building function also has an important impact on energy use. Building components and construction both provide great potential for improvement of energy demand in such areas as adequate thermal insulation, a key component of energy consumption. A careful choice of windows and shading devices should help to avoid additional solar gains. Incorporating efficient HVAC equipment and heat recovery techniques may also reduce the energy use. Designing a high-performance facade system will make a tremendous impact in minimizing energy consumption and optimizing the thermal condition. The energy intensity use of this library is 96 KBT/ ft^2 yr.

One major goal of this study is to do a Building Performance Verification to compare the simulation result with the actual building energy consumption data. Second, is to change building operation schedule in the simulation tool with keeping all the other input parameters as it is and check the effect of building operation schedule on the traditional techniques for control of microclimates within this type of environment. These strategies include preferential glazing to admit or block insulation, appropriate location and orientation of spaces to introduce air currents within inhabited spaces, employment of passive strategies (ducts, wind towers and shafts) to promote circulation as well as heat extraction.

For Boston climate, the main advantage is improved thermal insulation. During the winter months, exterior skin increases external heat transfer resistance, therefore utilizing interior air for preheating air cavity is advantageous. During the summer, air must be extracted in order not to cause overheating, by natural, hybrid or mechanical modes. As illustrated in figure 16, heating consumption can be reduced by about 5.4 percent after implementing the modifications.

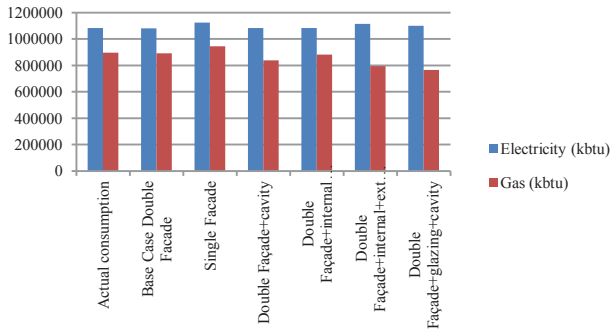

Figure 16. Simulation results for different alternatives.

5. CONCLUSION

Simulation Output data according to all the input data taken from the building's available information, is compared with the actual building energy consumption result. This performance verification result is only off by 4.5% from the actual consumption.

This proves the Simulation tool capabilities of DesignBuilder in predicting the building consumption after building is occupied and running. This study also concludes that for Boston climate types there is an increase on the performance of the double skin façade compared to single skin. Therefore, if this tool is used before hand at the design development stage then one can predict the building consumption, as well as, with some changes and by means of tests trials make the building perform better.

In addition, design strategies for double skin facades should reflect the climatic conditions. For Boston, reduction of heating loads is the primary concern, as well as balance with summer cooling load. Based on the results of this study, there are advantages in changing the air flow mode according to different seasons. In winter, there are advantages in utilizing trapped air to improve insulation and heat transfer between the exterior and interior. In summer, ventilation of air cavity is essential for reducing cooling loads. Location of double glazing on the exterior skin improves the overall energy consumption.

References

Afonso, C., and Oliveira, A. (2000). "A Solar chimneys: Simulation and experiment". Energy and Buildings, 32(1), 71-79.

Arons, D. (2000). Properties and Applications of Double-Skin Building Facades. MSc thesis in Building Technology, Massachusetts Institute of Technology (MIT), USA. Web address: http://libraries.mit.edu/docs

Azarbayjani, M. (2011). "Energy performance assessment of a naturally ventilated combined shaft-corridor DSF in an office building in Chicago". ARCC 2011, Detroit MI.

Azarbayjani, M. (2011). "Integration of natural ventilation in high-rise building with double skin façade". BESS 2011, Pamona, CA.

Champagne, C. (2002). Computational Fluid Dynamics and Double Skin Facades. Assignment for the Architectural Engineering Computer Labs, Pennsylvania State University, USA. Web address: http://www.arche.psu.edu/courses/ae597J/Champage-Hw1.pdf

Gratia, E., and De Herde, A. (2004). "Natural ventilation in a double-skin facade". Energy and Buildings, 36(2), 137-146

Hamza, N., and Underwood C, (2005). "CFD supported modeling of double skin facades in hot arid climates". 9th International IBPSA Conference Building Simulation 2005, Vol 1, Montreal (Canada). 365-372.

Hien, W. N., Liping, W., Chandra, A. N., Pandey, A. R., & Xiaolin, W. (2005). "Effects of double glazed facade on energy consumption, thermal comfort and condensation for a typical office building in Singapore". Energy & Buildings, 37(6), 563-572.

Macdonald, A. Melikov, Z. Popiolek, P. Stankov (2002), "Integrating CFD and building simulation". Building and Environment 37, pp. 865-871.

Mitchell, J.W., Beckman, W.A. (1995). Instructions for IBPSA Manuscripts, SEL, University of Wisconsin, Madison, WI.

Navvab, M., (2005). "Full scale testing and computer simulation of a double skin façade building". 9th International IBPSA Conference Building Simulation 2005, Vol 2, Montreal (Canada). 831-838.

Oesterle, E., Leib, R.D., Lutz, G., Heusler, B. (2001). "Double skin facades: integrated planning: building physics, construction, aerophysics, air-conditioning, economic viability, Prestel, Munich.

Safer, N., Woloszyn M., Roux J.J., Kuznik F. (2005). "Modeling of the double skin facades for building energy simulation: radiative and convective heat transfers". 9th International IBPSA Conference Building Simulation 2005, Vol 2, Montreal (Canada). 1067-1074.

Stec, W., and Passen D., 2003. "Defining the performance of the double skin façade with the use of the simulation model". 8th International IBPSA Conference Building Simulation 2003, Vol 2, Eindhoven (Netherlands). 1243-1250.

Torres, M., Alavedra P., Guzman A., 2007, "Double skin facades-Cavity and Exterior openings Dimensions for Saving energy on Mediterranean climate". IBPSA Proceedings of Building Simulation 2007, 198-205.

Wong, P.C., Prasad, D., Behnia, M. (2008). "A new type of double-skin facade configuration for the hot and humid climate". Energy and Buildings, 40(10), pp. 1941-1945.

Zöllnera, A. Wintera, E. R. F. and Viskanta, R. (2002). "Experimental studies of combined heat transfer "in turbulent mixed convection fluid flows in double-skin-façades." International Journal of Heat and Mass Transfer, 45(22), 4401-4408.

A Visual-Performative Language of Façade Patterns for the Connected Sustainable Home

Sotirios D. Kotsopoulos[1], Federico Casalegno[1], Guglielmo Carra[2], Wesley Graybil[3], Bob Hsiung[1]

[1]MIT, Comparative Media Studies
Mobile Experience Laboratory
77 Massachusetts Avenue,
Cambridge, Ma, USA, 02139
skots@mit.edu, casalegno@mit.edu,
bobh@media.mit.edu

[2]Politecnico di Milano
Building Environment Science & Technology
Via Bonardi 9
Milano, Italy, 20133
guglielmo.carra@mail.polimi.it

[3]MIT, Computer Science Department
Computer Science & Artificial Intelligence Laboratory
77 Massachusetts Avenue
Cambridge, Ma, USA, 02139
wgray496@mit.edu

Keywords: Shape Grammars, Performance, Aesthetics.

Abstract

The association between a building façade involving a matrix of programmable windows, for a prototype house, and the adjustment of the natural light at the house interior is treated algorithmically. The façade operates as a dynamic filter between exterior and interior: it filters solar radiation and heat by allowing the modification of the chromatism and light transmittance of each individual window. Varying the number and the distribution of the active windows on the façade permits the regulation of the incoming sun light and affects the visual presence of the house. A generative grammar producing the language of the optimum façade patterns, is presented. The novelty is that the grammar instead of encoding stylistic conventions, captures performative constraints and encodes them visually, to produce efficient and elegant patterns on the facade.

1. INTRODUCTION

The increasing cost of energy calls for the embrace of sustainable principles in the design and operation of buildings. Since artificial light and heat are energy-intensive, the efficient management of sunlight is crucial.

This paper addresses the designing of a programmable facade for a prototype house. The façade regulates solar radiation and heat at the house interior by enabling the modification of the chromatism and light transmittance of its electrochromic window panes. The variation in the number and the distribution of tinted windows on the facade is approached as a performative/visual language, as it affects both the energy performance and the visual presence of the house from the public street. A shape grammar encodes the constraints underpinning the production of optimum facade patterns, and links them to the visual properties of pattern generation on the two-diamensional plane. The grammatical rules are applied by the control system of the house to reprogram the electrochromic window panes real time, without storing patterns in the system's memory.

The prototype connected sustainable home, emerges at the intersection of 5 diverse systems: i) a passive high thermal mass envelope, ii) the dynamic façade, iii) a high thermal mass base with heating and cooling capability, iv) a cogeneration plant, and v) an intelligent control system, mitigating the relationship of all of the above. The high thermal mass envelope is a passive system securing high thermal resistance and low conductivity at the house interior. The programmable façade, oriented towards the south, is a reconfigurable component involving a matrix of 5 × 20 independently addressable windows (Figure 1). Each windowpane is an overlay of two digitally controlled materials: the first, polymer dispersed liquid crystal (PDLC) layer, provides the desirable degree of visibility to secure privacy; the second, electrochromic layer, provides the desirable degree of sunlight penetration to secure performance. A solar-powered cogeneration plant provides electricity, hot water and heated /cooled air.

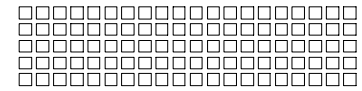

Figure 1. The 5 x 20 matrix covering the south elevetion of the connected sustainable home

Here is how it all works: Electrochromic technology permits the regulation of natural light and heat by enabling

the programming of the chromatism and transmittance value of each individual windowpane. Window transistions are optimally managed by the intelligent control system. The control system compiles feedback from sensors to activate the electrochromic material of the windows as needed, in order to exploit the high passive thermal capacity of the building envelope. During the hot summer days, keeping the interior temperature lower than the exterior becomes a high priority. To protect the interior from direct sun exposure, the control sets the electrochromic material to its maximum opacity. During the cold winter days, taking advantage of the sun heat becomes a priority. To expose the interior to the winter sun, the control system sets the electrochromic material to its maximum transparency, and permits the storage of sunheat in the home's high thermal mass envelope. At any given moment, the control reprogramms the facade based on the weather conditions, and the desires of the inhabitants. Since there is no class of facade patterns securing optimum results at all times, the system needs to be dynamic. The rules of a grammar are applied to generate patterns that comply to prescribed visual and performative constraints. In this way, the sun is used to maintain comfortable conditions with minimum use of artificial resources, while elegant facade patterns are formed.

After a short overview of related background work, this presentation is divided into three sections *generation*, *enumeration*, and *verification*. *Generation* presents the productive scope of the system: the visual rules of the pattern language. *Enumeration* presents the combinatorial scope of the system: the count of the patterns in the language. *Verification* presents the performative scope of the system: simulations of simple and composite patterns are compared to determine how interior illuminance is affected. The sequencing *generation* – *enumeration* – *verification* is retrospective. The production of façade patterns and the verification of their performance were advanced in parallel. The enumeration was conducted last.

2. BACKGROUND

This research links sustainable architecture with autonomous computing, distributed sensing, feedback infrastructure design and shape computation theory. A brief overview of related work in these fields follows next.

2.1. Building Control

Natural conditions vary with great degree of uncertainty, and so does human preference. An intelligent control system can secure the desirable living conditions at a house interior, while keeping energy cost minimal. The application of AI methods in building control has been pursued by computational sustainability research. For example, (Mady et al. 2011) employs the stochastic model-predictive control (SMPC) approach to significantly reduce energy consumption of a building with stochastic occupancy model. Further, (Kolter and Ferreira 2011) models end user energy consumption in residential and commercial buildings. Another relevant work (Li and Williams 2011), uses a robust plan executive for autonomous underwater vehicles.

The proposed plan executive for the connected sustainable home, p-Sulu OL, is built upon the Iterative Risk Allocation (IRA) algorithm (Ono and Williams 2008) and a deterministic plan executive, p-Sulu. This controler must allow the residents to specify desired ranges of room conditions, must minimize the use of non-renewable energy consumption, and must limit uncertainty risk to user specified levels. Previous research (Ono 2012) presents a risk-sensitive planner called p-Sulu, which has the above three capabilities. However, p-Sulu is an off-line planner: it pre-plans the control sequence for the entire plan duration. A planner of this type cannot execute effectively for the connected sustainable home, because: a) the home must be operated constantly, and b) the house control requires frequent re-planning every few seconds. To overcome the first challenge, the newly developed p-Sulu OL plan executive, uses a receding horizon control approach: at each planning cycle, a planning problem is solved with a finite duration, which is called a horizon. In the next planning cycle, the planning problem is solved again over a planning horizon with the same duration starting from the current time, by considering the latest observation of uncertain parameters. This re-planning process is repeated with a fixed time interval. The second challenge is overcome by building upon an anytime algorithm for chance-constrained programming (IRA).

2.2. Simulation

Electrochromic glass reduces the solar radiation flow by adapting its chromatism and transmittance value. The values of transmittance (τ) vary in electrochromic glass from 60-75%, for idle glass, to 3-8% for active obscured glass (Hausler et all, 2003). Given that electrochromic technology is not broadly known, a number of papers describing the state of the art in this particular domain are referenced here: Lee et al 2000, 2006 describes a study in which the effects

of electrochromic technology are monitored in a cube 3.0 m x 3.0 m x 3.0 m; Hausler et al 2006 presents a technical comparison of data determining the physical features of electrochromic glass; Selkowitz et al 2003 offers an overview on automated lighting and energy control systems; finally, Mardaljevic et al 2009 reviews the historical basis of building compliance methods determining minimum energy efficiency and comfort standards, and proposes a novel basis for more efficient metrics.

The analysis and evaluation of simulation data permits to identify how the activation of the electrochromic glass affects the thermal comfort and illuminance, on the specific house, at the specified site, throughout the four seasons. A software package providing reliable results was selected to analyze and evaluate the daylight conditions at the house interior. The software, *Relux Professional* by *Relux Informatik AG*, integrates the lighting standards determined by Italian law (UNI EN 12464-1/-2 and UNI EN 13201). In ray-tracing simulation *Relux Vision* (a plug-in of *Relux Professional* also by *Relux Informatik AG*) was used. Two models – established by the *Commission Internationale de l'Eclairage* (*CIE*) – were used. The first, *Standard Overcast Sky* model, provides an account of the natural light emitted through cloudy sky. The second, *Standard Clear Sky* model, computes natural light assuming that the sun is the single lighting source. Both models are static and fail to capture the natural phenomenon of sunlight variation, because they exclude transitory conditions, such as the passage of clouds across the sun (Wienold, 2007). To overcome these limitations and be able to determine the optimum settings for the management of the façade, simulations were performed for each day of the year and the data was integrated in the optimization algorithm of the control system. This database offers a basis for optimizing the facade. In combination with real time input from sensors, the effective management becomes attainable even in conditions that cannot be simulated by the static models.

2.3. Shape Grammars

A shape grammar encodes the performative constraints underpinning the production of optimum electrochromic patterns for the facade of the prototype home, while acknowledging the visual aspect of patern generation on the two dimensional plane. Shape grammars extend production systems and phrase structure grammars, to capture the interactions of visual elements in space (Stiny 2006). A shape grammar consists of a calculating and a syntactic-interpretive part. The calculating part engages an algebraic framework in which elements of 0, 1, 2 and 3 dimensions (points, lines, planes, solids, or combinations of these) are used in calculations that may take place in a space of 0, 1, 2 or 3 dimensions. The syntactic-interpretive part consists of production rules confining the syntactic and semantic attributes of sets of products, which are conventionally called *languages*.

A discussion of the dual character (generative-expressive) of spatial rule systems exists in Knight 2005. Stiny and Mitchell 1978; 1980 provide examples of grammars encoding stylistic principles pertaining to the generation, enumeration and classification of Palladian villa plans and Mughul garden designs. Two relevant articles on building optimization methods and performance-driven design tools are Luebkeman and Shea 2005, and Shea, Aish and Gourtovaia, 2005. Luebkeman and Shea 2005 shows how navigating the performance space of a design solution promotes design thinking and presents the relation between variations and performance. In Shea, Aish and Gourtovaia, 2005 performance-driven generative methods are used to produce design concepts and solutions based on modeling of conditions and performance criteria.

This paper extents the above contributions in the following way: a shape grammar is used to control the generation of performance driven facade patterns, real time. The grammar does not capture stylistic conventions, or principles of form generation. It captures performative constraints, which are encoded by visual rules. The rules aim to exaust the expressive/visual potential of the performative constraints and to secure the generation of efficient and elegant patterns on the facade.

3. GENERATION

Simulation testing dettermined two performative provisions:

Provision I: In an average luminous day, out of 100 electrochromic cells, 50 – 75 cells need to be active ("*on*"), to secure satisfactory luminosity levels in the house interior.

Provision II: No 4 consecutive cells can be simultaneously active on the same row. If n is the number of consecutive active cells in any row, $n \leq 3$, to secure fine distribution of active cells in the horizontal direction. Dense

accumulation of consecutive active cells horizontally casts linear shadows, disrupting smooth light distribution.

Based on *provision I*, three basic façade settings are determined: a) 0 % active (a single rule is required, *do nothing*), b) 50 % - 75 % active (12 rules organized into a grammar produce patterns), c) 100 % active (a single rule is required, *activate all*). Intuitively, the façade can remain clear, can be activated in a ratio equal to 2/4 – 3/4 of its area, or can be fully activated. The present grammar determines the generation of patterns for the setting (b) when 2/4 – 3/4 of the electrochromic area is active.

3.1. Modes of generation

Modes of rule application enforce the generation of diverse patterns. For this purpose, auxiliary markings are introduced: boundaries and axes, depicted in dashed grey line, in the algebra W_{12} divide the matrix into four partitions of 2½ × 10 glass cells each; a pair of labels (V, V) in the algebra V_{02} distinguishes the vertical and horizontal direction. Neighboring partitions are bilaterally symmetrical along the vertical or horizontal central axes. This description is formed in the product $< U_{12} \times W_{12} \times V_{02}>$.

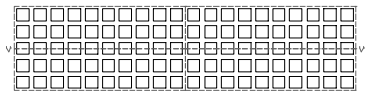

Seven modes of rule application are outlined, based on this partitioning. All shapes are parametric arrangements of lines, vertical and horizontal grey-line axes and labels, in the product algebra $< U_{12} \times W_{12} \times V_{02}>$. A rule r_i can apply along the horizontal axis: i) just once, on the left (*or* on the right) side of the vertical axis, or ii) twice, simultaneously on the left *and* on the right side of the vertical axis (note: the rule may apply under transformation).

(i) 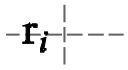

(ii) 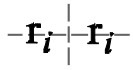

A rule r_i can be applied on the remaining four 2 × 10 partitions of the matrix: iii) just once, on any of the four partitions, iv) twice, in parallel, on the top (*or* bottom) horizontal partitions, v) twice, in parallel, on the left (*or* right) vertical partitions vi) twice, in parallel on the upper *and* lower partitions that are positioned diagonally, and vii) four times, simultaneously on all four partitions (note: if the same rule r_i applies more than once, this may happen under different transformations).

(iii) 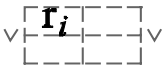

(iv) 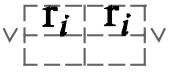

(v) 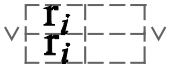

(vi) 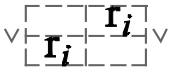

(vii) 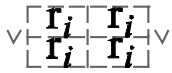

3.2. Shape algebras

The initial shape is the 5×20 matrix partitioned with the auxiliary grey lines in 4 partitions. The labels (A, A) along the horizontal axis indicate the derivation stage. The outmost columns of cells are marked with labels (X).

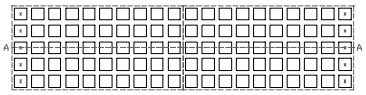

Three possible cell states are determined: a) *on* (active), b) *off* (inactive), or c) *excluded*. The excluded state serves strictly the generation process. All excluded cells turn necessarily into inactive (due to *provision II*) at the termination stage. During the course of the generation these cells are marked *excluded*, in order to be distinguished from the matrix cells that remain accessible to activation. The three states are depicted below: *on* (active-left), *off* (inactive-center), *excluded* (right).

A pattern description appears next at the second, intermediate, generative stage (B, B).

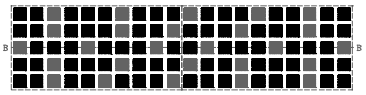

In the calculations to follow the elements are manipulated on the plane (j =2): the inactive square cells are depicted with black lines, in the algebra U_{12}; the auxiliary axes are depicted with grey lines, in the algebra W_{12}; tinted (active) cells are depicted as black squares, in the algebra U_{22}; excluded cells, due to *provision II*, are depicted as grey squares in the algebra W_{22}; letters X, A, B, C are used as labels, depicted in the algebra V_{02}. The overall description is formed in the product algebra: $< U_{12} \times W_{12} \times U_{22} \times W_{22} \times V_{02} >$.

3.3. Stages of derivation

The generation phase involves 12 rules satisfying the *provisions I* and *II*. The derivation is organized in 3 stages A, B, C. Stage A – the initiating stage – includes 4 rules that apply on the outmost 4 columns of the matrix. Stage A ends when the labels X marking the outmost cells are erased. The cells that can be affected at stage A are depicted next.

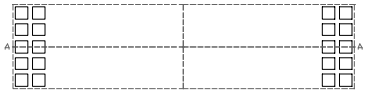

Stage B – the main productive stage – includes 5 rules. The cells that can be affected in stage B are depicted below.

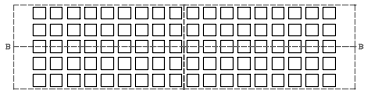

Stage C – the terminating stage – includes 3 rules. The cells that can be affected include the entire matrix.

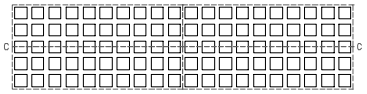

3.4. Rules

Based on Stiny (1992, 1991) a rule x → y, may apply in a product algebra including lines, planes and weights. For example, in a product $<U_{12} \times U_{22}>$ including lines and planes, a rule x → y

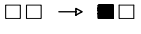

applies on C (left), to produce C' (right),

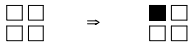

in two steps: first, a transformation *t* recognizes some part of C geometrically similar to x – the shape that appears on the left hand side of the rule; second, the same transformation *t* is used to *modify* C. It substitutes *t*(x) with *t*(y) – where y is the shape that appears on the right hand side of the rule – to produce C'. Concisely: C'= [C – *t*(x)] + *t*(y). Note that the rule may apply on C to produce C' under a transformation *t* in four ways. These correspond to the ways the shape on the left side of the rule can be "matched" on C.

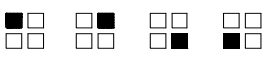

The rules of this grammar are noted with the letter r_i (with i = 1, 2,…12). Within the semantic context of façade pattern generation each productive rule: a) checks a number of neighboring cells, by matching the shape depicted on the left side of a rule, and b) activates a number of cells by modifying the state from *off* to *on* as depicted on the right side of a rule, or *excludes* cells.

3.4.1. Stage A

The productive rules 1-3 initiate the process. Rule 4 terminates stage A and introduces stage B.

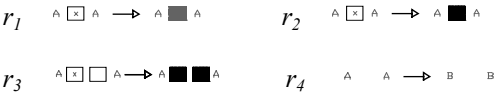

3.4.2. Stage B

The rules 5-8 are productive. Rule 9 terminates stage B and introduces stage C.

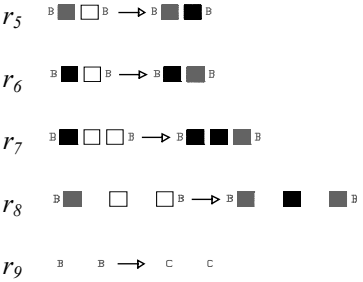

3.4.3. Stage C

There are no productive rules at this stage. Rule 10 erases the grey markers from the excluded cells and returns them as inactive cells. Rule 11 eliminates the auxiliary grey axes. Rule 12 terminates the process.

3.5. Derivation

A derivation of a pattern is presented in the Appendix I. The reading sequence is from left to right, top to bottom. Derivation arrows are not shown. The number of the rule r_i applied at each step appears on the upper center of the matrix. Productive rules apply twice at each step following the modes (ii) and (vi). The derivation starts from the initial shape, the inactive matrix (stage A). The derived pattern with activation percentage is 74 %, is:

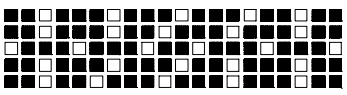

4. ENUMERATION

The enumeration of patterns was computed assuming the *Provisions I, II* of the grammar. Let n denote the number of active windows. Since we are primarily interested in the values for n between 50 and 75 (due to *Provision I*) we performed the calculation for this range only. The facade was decomposed into rows. Let r_i denote the number of active windows in row *i*. We distribute the n active windows across the rows with the requirement: $\sum r_i = n$ and $0 \leq r_i \leq 20$. Consider a single given row *i*. For a fixed number of active windows r_i we must calculate in how many ways we can arrange the active windows across the row *i*. Define the function $P(r, k)$ to be the number of arrangements of r active windows across a row of length k subject to the constraint that no three in a row may be active. The goal is to calculate $P(r_i, 20)$. To compute $P(r, k)$ we distinguish the following cases.

Case 1: The leftmost window is inactive. There are $P(r, k-1)$ ways to distribute the r active windows across the remaining $k-1$ windows.

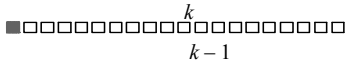

Case 2: The leftmost *window* is active. First, if the next window is inactive, the leftmost portion of the row will certainly not violate *provision I*, and we may choose the state of the 3rd window from the left with no restriction. This leaves $r-1$windows to activate across a total of $k-2$ remaining windows in the row. There are $P(r-1, k-2)$ possibilities.

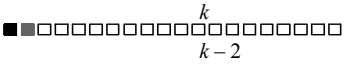

Second, if the next window is *active*, the two leftmost windows are active and the 3rd window from the left is inactive. This leaves $r-2$ windows to activate across a total of $k-3$ remaining windows in the row. Thus, there are $P(r-2, k-3)$ possibilities.

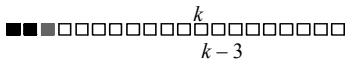

Third, if the next window is active, the three leftmost windows are active, so the 4th window from the left is necessarily inactive. This leaves $r-3$ windows to activate across a total of $k-4$ remaining windows in the row. There are $P(r-3, k-4)$ possibilities.

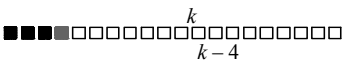

In total, this gives the recursive equation:

$$P(r, k) = P(r, k-1) + P(r-1, k-2) + P(r-2, k-3) + P(r-3, k-4)$$

To find the number of arrangements for a given n we sum over all possible values $r_1, \ldots r_5$. This yields an equation for the total number of arrangements E as a function of the number of active windows n.

$$E(n) = \sum_{\substack{r_1,\ldots r_5 \\ \sum r_i = n \\ 0 \leq r_i \leq 20}} \prod_{i=1}^{5} P(r_i, 20)$$

The results of the computation for E, for any n between 50 and 75 are provided in the Table 1, of Appendix II. Restricting the production of patterns to any n in the range 50 -75 yields 1.285×10^{24} possible configurations.

5. VERIFICATION

Managing daylight is a decisive parameter in energy efficiency. Next is described the process of simulation, determining the performative aim of the grammar. Although the physical prototype is also tracking temperature and humidity, these extensions for brevity are ommited here. After establishing an illuminance threshold based on Italian law, a number of simulations was conducted. The evaluation of the data shows how pattern generation affects illuminance on the specific building, at the specified site, throughout the year. We provide the daylight factor (D_{av}), the average illuminance value (E_{av}), calculated for a specific plane parallel to the floor, and the uniformity index (G_1). Based on UNI EN 12464 the absolute minimum value of illuminance for residential buildings is 300 lux. Given the experimental character of the prototype, we raised this threshold from 300 lux to 500 lux.

5.1. Determining the desired coverage ratio

A predictive model associating coverage ratio and illuminance, in a specified time interval dayly, is obtainable.

5.1.1. CIE Overcast sky conditions

The association of the number of active windows and the subsequent value in lux was determined for *Overcast Sky Conditions*. Eleven *base configurations* were tested, including the all clear and all tinted configurations. The number of active windows was mapped into a value of lux and a diagram associating average illuminance E_{ave} and

coverage ratio α was formed. The values and the diagram appear in Table 2, of Appentix II.

The interpolation of the table of values and the diagram permits the definition of a formula that calculates the value in lux corresponding to a coverage ratio α associated to it. This expression is a linear equation of the form $y = a*x+b$, where y represents the number of lux corresponding to the number of active windows x (where $x = \alpha*100$). Four explicit expressions calculate the values for a specific hour during the day (1:00 p.m. for both solstice and equinox).

December 21:	$y = -411{,}86x + 500{,}69$
March 21:	$y = -839{,}84x + 1020{,}4$
June 21:	$y = -1113{,}1x + 1365{,}4$
September 21:	$y = -848{,}63x + 1033{,}1$

Expressions yielding the y value for every hour and day of the year can be formed and the number of active windows can be calculated for any condition. Hence, we can: a) determine the number of active windows for reaching the illuminance threshold, and b) confine any patterns to this threshold. The values and the corresponding diagrams associating the number of active windows and the illuminance value for March 21, June 21 and September 21 at 1:00 p.m. in Overcast Sky, appear resoectively in Table 3, Table 4 and Table 5, of Appentix II.

After setting a desired value in lux we computed the number of active windows to reach this value. The model is confined within the geometric/generative conventions of the *base configurations* we used to determine its mathematical expression. The error between the model prediction and the simulation in *Overcast Sky Conditions* is 3-4% but for patterns with coverage ratio beyond 50-75 % it raises up to 5-6 %. The model gives the maximum number of active windows yielding the threshold value during the whole year. The maximum numbers of active windows for coverage ratio 50-75 %, at 1 p.m. in Overcast Sky, appear in Table 5, of Appendix II.

If the maximum number of active windows ensuring the illuminance threshold, is known, then it becomes possible to vary the distribution of active windows without affecting the interior daylight illuminance. The calculation was extended – for hourly intervals – over the entire year, and a database determining the number of active windows required to reach the illuminance threshold was obtained. The generation of façade patterns stops when the value of the active windows reaches 75%. This condition was encoded by *provision II*.

5.2. Verification of the derived pattern

The performance of the derived pattern in Appendix I, was simulated and a comparison between the values of average illuminance obtained using the predictive equations and the software simulation was made. The comparison confirmed the accuracy of the predictive model. The results appear in the Table 6 of Appendix II, where we predict and simulate the conditions of December 21, March 21, June 21 and September 21 at 1 p.m. in Overcast Sky and Clear Sky distribution.

The coverage ratio is 74% and the error margin remains within acceptable limits (5 %). In *Overcast Sky Conditions*, the 74% ratio yields acceptable interior illuminance only on June 21 at 1 p.m. The other three days the illuminance remains below the threshold, but it can be regulated by lowering the coverage ratio. In *Clear Sky Conditions*, the 74% coverage ratio yields illuminance above the threshold, but acceptable. Accordingly, the daylight simulation of the pattern proved our predictive model successful.

6. DISCUSSION

This paper addressed the designing of a programmable façade for a prototype house that is currently under construction in Rovereto, N. Italy. The paper linked some well-known principles of sustainable architecture with shape computation, autonomous computing, distributed sensing, and feedback infrastructure design. The novelty of the research is that it captures the performative constraints of interior daylight illuminance and encodes them visually, in the form of a shape grammar.

The dynamic façade is a responsive architectural element that it was introduced in the prototype house as an alternative to a traditional screening system. The adjustment of the electrochromic patterns on the façade allows to control solar radiation and heat at the house interior by enabling the modification of the chromatism and light transmittance of the electrochromic window panes. Hence, it affects the interior conditions of heat, daylight and privacy, and it transforms the way the house is perceived from the public street. The active electrochromic façade and the passive high thermal mass building envelope function as two complementary systems. The modification of the façade patterns affects the percentage of the incoming sunheat and enables the exploitation of the high thermal capacity of the passive building envelope. During the summer, keeping the interior temperature lower than the exterior becomes a high

priority. To protect the interior from direct sun exposure, the electrochromic material is set to allow minimum thermal transmitance. During the winter, taking advantage of the sun heat becomes a priority. To expose the interior to the winter sun, the electrochromic material is set to allow maximum thermal transmitance. At any given condition, the active electrochromic façade and the passive high thermal mass building envelope are managed to contribute to the global energy performance of the house.

The variation in the number and distribution of active electrochromic windows on the façade was approached as a visual/performative formal language. The proposed formal grammar links visual principles of 2-d pattern generation to interior daylight illuminance on the specific house, at the specified site, throughout the four seasons. In this way, comfortable conditions are maintained, while elegant façade patterns are formed. In clouded sky the grammar exhibits excellent flexibility and drives the production of façade patterns while securing optimal interior daylight. In clear sky, full activation of specific façade sub-areas, leaving others entirely inactive, could offer satisfactory results.

By storing behavioral and weather patterns the control system of the house projects the course of events to proactively save energy. Ultimate goal is to be able to predict user behavior and cater to the needs of the occupants. Until this vision can be realized, we permit users to command continuous, stochastic systems, in an intuitive and safe way. We are thus implementing a tablet-based interface that permits the users to set commands. Finally, we are implementing an application, which in conjunction with sensory feedback, will be tracking the residents to infer schedule and behavior patterns. This will make the prediction of user activity, and the adaptation to unexpected change without explicit user input, possible.

Acknowledgement

This research was made within the *Green Connected Home Alliance* between the Mobile Experience Laboratory of MIT, and the Fondazione Bruno Kessler of Trento, Italy.

References

Hausler T, Fischer U, Rottmann M and Heckner K H, 2003, “Solar optical properties and daylight potential of electrochromic windows, *International Lighting and Colour Conference*, Capetown.

Knight T, 2005, “Creativity. Rules”, *Proceedings of HI’ 05 Sixth International Roundtable Conference on Computational and Cognitive Models of Creative Design*, Heron Island, Australia.

Kolter J Z, and Ferreira J, 2011, "A large-scale study on predicting and contextualizing building energy usage", *Proceedings of Twenty-Fifth AAAI Conference on Artificial Intelligence* (AAAI-12)

Lee E S, Di Bartolomeo D L, Klems J H, Yazdanian M. and Selkowitz S. E., 2006, “Monitored energy performance or electrochromic windows for daylighting and visual comfort”, *ASHRAE Summer Meeting*, Canada.

Li H, and Williams C B, 2011, "Hybrid planning with temporally extended goals for sustainable ocean observing", *Proceedings of Twenty-Fifth AAAI Conference on Artificial Intelligence* (AAAI-11).

Luebkeman C, Shea K, 2005, “CDO: Computational design + optimization in building practice”, *The Arup Journal*, 3.

Mady A E D, Provan G M, Ryan C, Brown K N, 2011. "Stochastic model predictive controller for the integration of building use", *Proceedings of Twenty-Fifth AAAI Conference on Artificial Intelligence*

Ono M, 2012, *Robust, Goal-directed Plan Execution with Bounded Risk*. Ph.D. Dissertation, Massachusetts Institute of Technology.

Ono M, Graybill W, and Williams C B, 2012, "Risk-sensitive plan execution for Sustainable Connected Home", *Proceedings of AAAI Conference on Artificial Intelligence* (AAAI-12). (*in review*)

Ono M, Williams C B, 2008, "Iterative risk allocation: A new approach to robust model predictive control with a joint chance constraint." In *Proceedings of 47th IEEE Conference on Decision and Control*

Selkowitz S, Lee E and Aschehoug O, 2003, “Perspectives on advanced facades with dynamic glazings and integrated lightings controls”, presented at *CISBAT*, Lusanne, Switzarland.

Shea K, Aish R, Gourtovaia M, 2005, “Towards integrated performance-driven generative design tools”, *Automation in Construction*, 14, 253-264

Stiny G, 2006, *Shape: Talking about seeing and doing*, The MIT Press.

Stiny G, 1992, “Weights” Environment *and planning B: Planning and design* **19** 413-430.

Stiny G, 1991, “The algebras of design” *Research in Engineering Design* **2** 171-181.

Stiny G, Mitchell W J, 1978 “The Palladian grammar” Environment *and planning B: Planning and design* **5** 209-226

Stiny G, Mitchell W J, 1978 “Counting Palladian plans” *Environment and planning B: Planning and design* **5** 189-198

Stiny G, Mitchell W J, 1980, “The grammar of paradise: on the generation of Mughul gardens” *Environment and planning B: Planning and design* **7** 209-226

Wienold J, 2007, “Dynamic simulation of blind control strategies for visual comfort an energy balance analysis”, *International Building* Performance *Simulation Association*, Beijing, China, 1197-1204.

APPENDIX I

Stage A

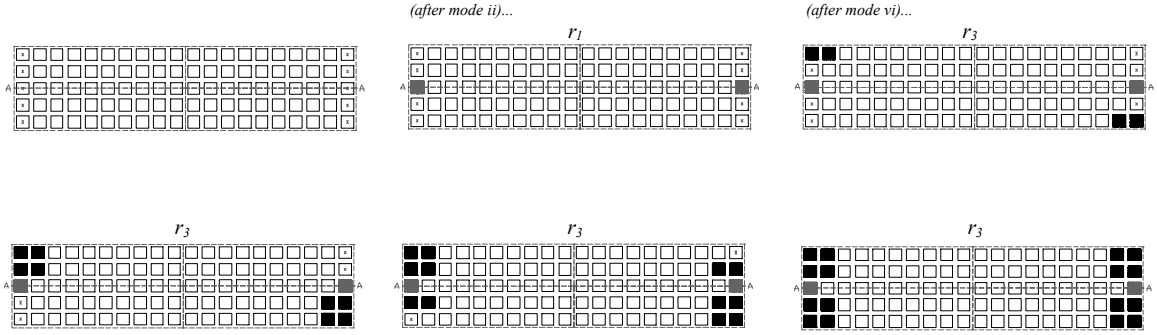

Stage B

(after mode ii)...

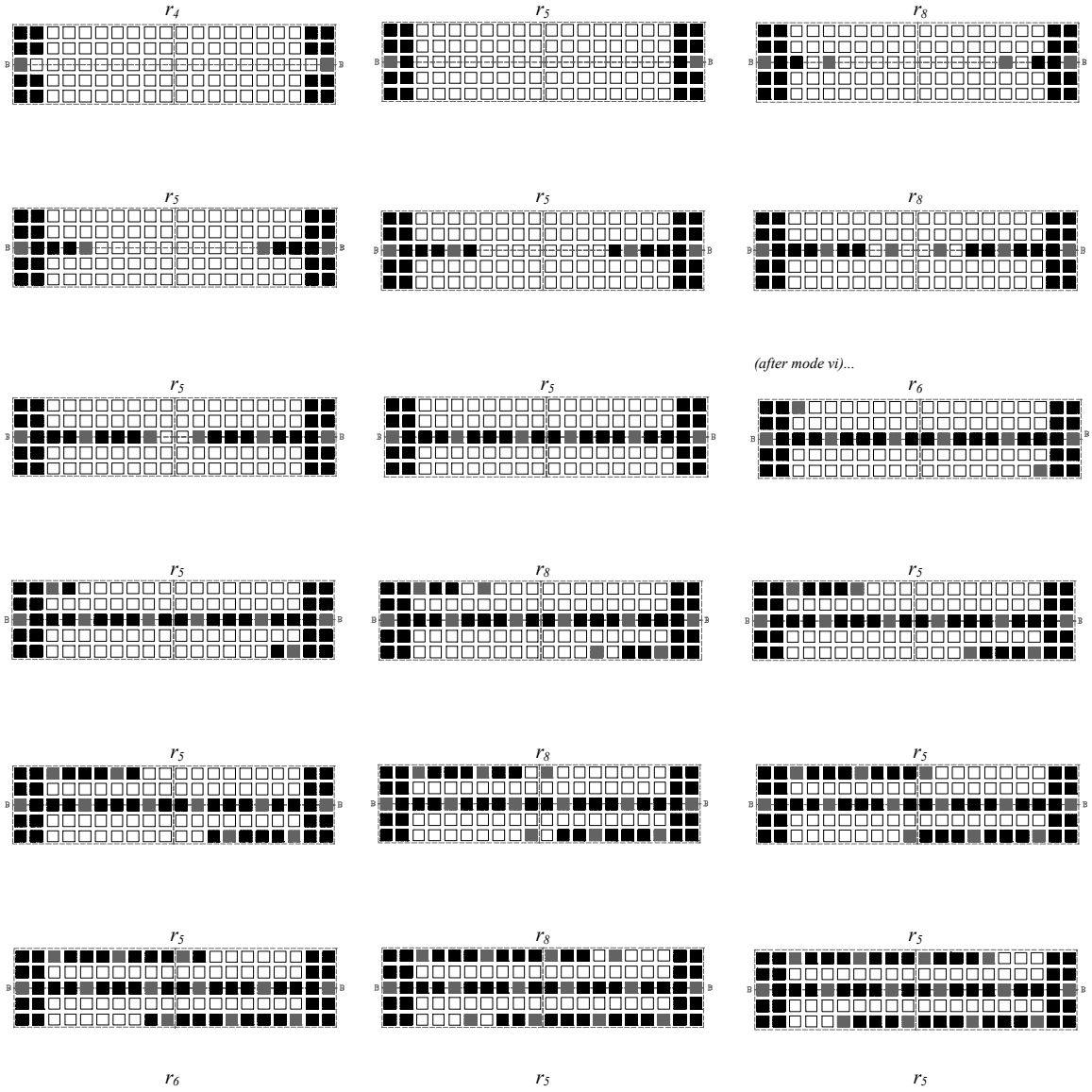

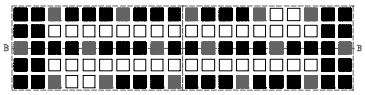

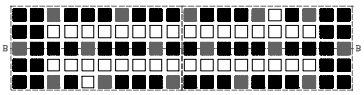

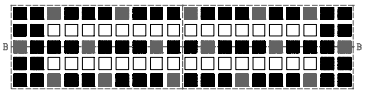

r_6

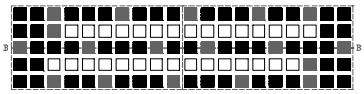

r_8

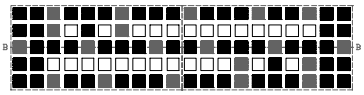

r_5

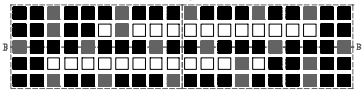

r_5

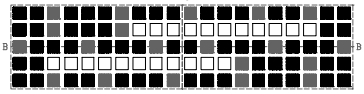

r_5

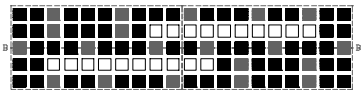

r_7

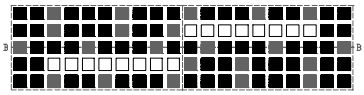

r_8

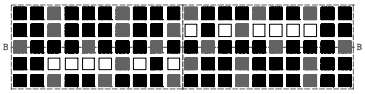

r_5

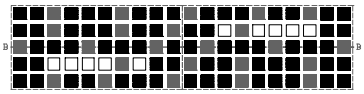

r_5

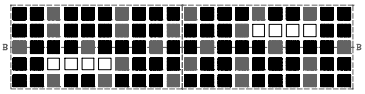

r_8

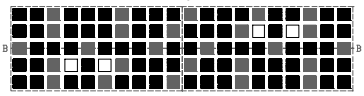

r_5

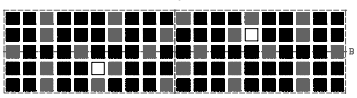

r_5

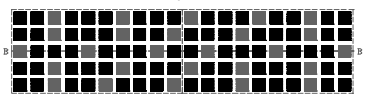

Stage C

(after modes ii & vi)...

r_9

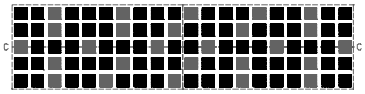

r_{10}

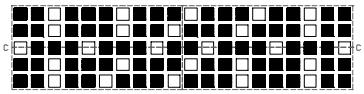

r_{11}

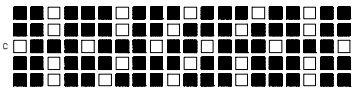

r_{12}

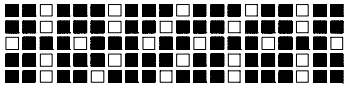

APPENDIX II

n	*E(n)*	*n*	*E(n)*	*n*	*E(n)*
50	1.751×10^{27}	60	1.285×10^{24}	70	1.285×10^{16}
51	1.191×10^{27}	61	3.891×10^{23}	71	1.285×10^{15}
52	7.566×10^{26}	62	1.061×10^{23}	72	1.285×10^{13}
53	4.484×10^{26}	63	2.590×10^{22}	73	1.285×10^{12}
54	2.470×10^{26}	64	5.611×10^{21}	74	1.285×10^{10}
55	1.265×10^{26}	65	1.069×10^{21}	75	550,731,776
56	5.986×10^{25}	66	1.774×10^{20}		
57	2.610×10^{25}	67	2.529×10^{19}		
58	1.048×10^{25}	68	1.285×10^{18}		
59	3.844×10^{24}	69	1.285×10^{17}		

Table 1: Enumeration of distinct patterns with activation 50%-75%

	Base configuration	x	α	E_{ave}
0	Extreme	0	0,00	497
1	Mixed	40	0,4	335
2	7th vertical	45	0,45	308
3	3rd vertical	50	0,50	305
4	8th vertical	50	0,50	303
5	1st vertical	50	0,50	293
6	6th vertical	55	0,55	286
7	5th vertical	60	0,60	241
8	2nd vertical	70	0,70	221
9	4th vertical	75	0,75	188
10	Extreme	100	1,00	82

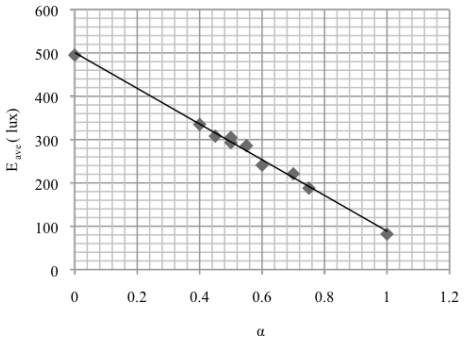

Table 2: Number of active windows and illuminance value, for December 21, at 1 p.m. for Overcast Sky distribution

	Base configuration	x	α	Lux
0	Extreme	0	0,00	1010
1	Mixed	40	0,4	682
2	7th vertical	45	0,45	625
3	3rd vertical	50	0,50	621
4	8th vertical	50	0,50	617
5	1st vertical	50	0,50	597
6	6th vertical	55	0,55	583
7	5th vertical	60	0,60	491
8	2nd vertical	70	0,70	452
9	4th vertical	75	0,75	382
10	Extreme	100	1,00	167

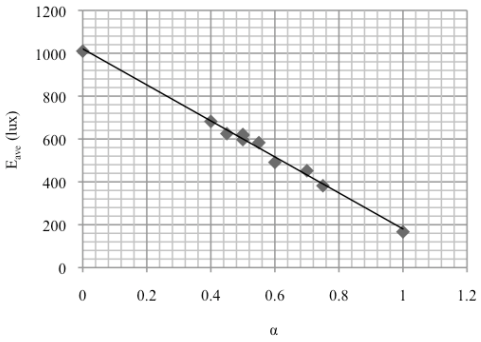

Table 3: Number of active windows and illuminance value, for March 21, at 1 p.m. for Overcast Sky distribution

	Base configuration	x	α	Lux
0	Extreme	0	0,00	1340
1	Mixed	40	0,4	923
2	7th vertical	45	0,45	846
3	3rd vertical	50	0,50	840
4	8th vertical	50	0,50	833
5	1st vertical	50	0,50	808
6	6th vertical	55	0,55	788
7	5th vertical	60	0,60	665
8	2nd vertical	70	0,70	611
9	4th vertical	75	0,75	516
10	Extreme	100	1,00	226

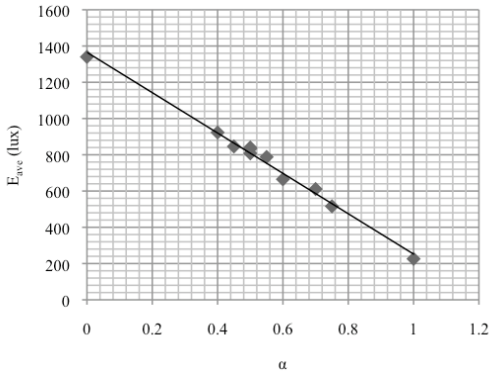

Table 4: Number of active windows and illuminance value, for June 21, at 1 p.m. for Overcast Sky distribution

	Base configuration	x	α	Lux
0	Extreme	0	0,00	1020
1	Mixed	40	0,4	693
2	7th vertical	45	0,45	635
3	3rd vertical	50	0,50	631
4	8th vertical	50	0,50	624
5	1st vertical	50	0,50	607
6	6th vertical	55	0,55	591
7	5th vertical	60	0,60	499
8	2nd vertical	70	0,70	459
9	4th vertical	75	0,75	387
10	Extreme	100	1,00	169

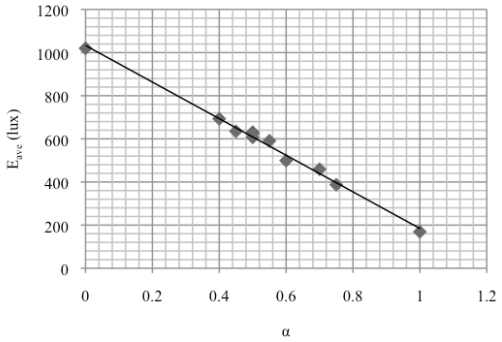

Table 5: Number of active windows and illuminance value, for September 21, at 1 p.m. for Overcast Sky distribution

	1p.m. -21st	x	α
1	December	0	0,00
2	January	18	0,18
3	February	45	0,45
4	March	62	0,62
5	April	72	0,72
6	May	75	0,75
7	June	75	0,75
8	July	75	0,75
9	August	72	0,72
10	September	63	0,63
11	October	45	0,45
12	November	16	0,16
13	December	0	0,00

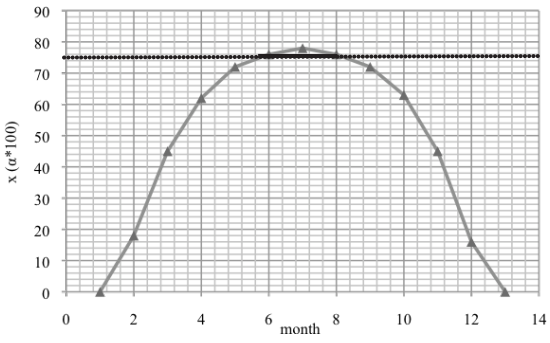

Table 6: Maximum number of active windows throughout the year at 1 p.m. in *Standard Overcast Sky*. In doted line is the 75 % limit.

	Prediction with the model E_{ave} *(lx)*	Verification with Relux Pro E_{ave} *(lx)*	Error
December 21st	195	186	5 %
March 21st	398	379	5 %
June 21st	541	513	5 %
September 21st	404	385	5 %

	Prediction with the model E_{ave} *(lx)*	Verification with Relux Pro E_{ave} *(lx)*	Error
December 21st	2586	2630	2 %
March 21st	3826	4030	5 %
June 21st	2505	2490	0 %
September 21st	3816	3840	0 %

Table 7: Left: Comparison of E_{ave} between simulation and prediction in *Overcast Sky Conditions*. Right: Comparison of E_{ave} between simulation and prediction in *Clear Sky Conditions*.

Session 4: Urban Planning

Urban Network Analysis: A New Toolbox for Measuring City Form in ArcGIS **111**
Andres Sevtsuk, Michael Mekonnen
Singapore University of Technology and Design (SUTD), Massahusetts Institute of Technology (MIT)

The Parametric Exploration of Spatial Properties – Coupling Parametric Geometry Modeling and the Graph-Based Spatial Analysis of Urban Street Networks **123**
Sven Schneider, Martin Bielik, Reinhard König
Bauhaus University

Urban Network Analysis: A New Toolbox for Measuring City Form in ArcGIS

Andres Sevtsuk[1], Michael Mekonnen[2].

[1]City Form Lab
Singapore University of Technology & Design
20 Dover Drive, Singapore 138682, Singapore
asevtsuk@mit.edu

[2]Massahusetts Institute of Technology
Department of Computer Science & Electrical Engineering
Room 38-401, Cambridge, MA 02139
mikemeko@mit.edu

Keywords: City form, spatial networks, centrality, accessibility, urban design, GIS.

Abstract

We introduce an open-source Urban Network Analysis (UNA) toolbox for ArcGIS, which can be used to compute five types of centrality measures on spatial networks – *Reach*; *Gravity Index*; *Betweenness*; *Closeness*; and *Straightness*. Though primarily developed for the analysis of urban street- and building-networks, the toolbox is equally suited for other spatial networks, such as building layout-, highway-, or utility networks. Unlike previous network analysis tools that operate with two network elements (nodes and edges), the UNA tools include a third network element – buildings – that are used as spatial units of analysis for all measures. Neighboring buildings on the same street segment can therefore obtain different accessibility results. UNA tools allow buildings to be weighted according to their characteristics – more voluminous, more populated, or otherwise more important buildings can be specified to have a proportionately stronger effect on the analysis outcomes. The paper demonstrates its application in Cambridge and Somerville, MA.

1. INTRODUCTION

Network analysis is widely used in the study of social networks, but so far fairly little in the spatial analysis of cities. While the study of spatial networks goes back to Euler and his famous puzzle of Königsberg's seven bridges in the 18th century, there were until recently few freely accessible tools available for city designers and planners to calculate computation-intensive spatial accessibility measures on dense networks of city streets and buildings (Jing, Claramunt et al. 1999; Turner 2001; Okabe 2001). A few software tools that have been developed, have been proprietary and difficult to obtain, and primarily focused on the two-dimensional characteristics of the street networks, ignoring the three-dimensional distribution of building stock and land uses (Hillier, 1996; Jing, Claramunt et al. 1999; Turner 2001; Porta, Crucitti et al. 2005; TransCAD[i]). Research has shown, however, that network centrality measures can be useful predictors for a number of interesting urban phenomena. They have been helpful in explaining the importance of particular junctions in transportation networks (Garrison 1960; Garrison and Marble 1962; Kansky 1963; Haggett and Chorley 1969), the spatial relationships between rooms inside buildings (Levin 1964; Casalania and Rittel 1967; Rittel 1970; March and Steadman 1971), the flow of pedestrian traffic on city streets (Hillier, Burdett et al., 1987; Ozbil, Peponis et al. 2011), and the distribution of retail and service establishments in urban environments (Okabe 2001; Porta, Crucitti et al., 2005; Sevtsuk, 2010). As increasing amounts of geographic data are becoming available, readily accessible tools are needed to make network analysis available to spatial analysts across disciplines. This paper introduces a new open-source toolbox for spatial network analysis in ArcGIS. The toolbox includes a number of features that make it flexible and suitable for different types of spatial networks and research questions.

The paper will first describe the network representation framework used in the toolbox, and introduce some of its analytic features. We then describe the five available centrality indices and explain the computational process behind the calculations. Examples of applications of the toolbox are shown using data from Cambridge and Somerville, MA.

2. NETWORK REPRESENTATION OF THE BUILT ENVIRONMENT

Most spatial network studies to date have represented networks using two types of network elements – nodes and edges. In the case of urban street networks, edges typically represent street segments, and nodes the junctions where two or more edges intersect (Porta, Crucitti et al. 2005). This is known as the primal representation of spatial graphs. Some analysts invert this representation for analytical purposes, illustrating street segments as nodes and junctions as edges, known as the dual representation, exemplified by the Space Syntax methodology (Hillier 1996). The outcomes in both cases illustrate the degree to which an edge or node is spatially connected to the surrounding path network. This approach economizes computation power and allows the analysis to be run on large networks, but the exclusive focus on nodes and edges also complicates the theoretical interpretation and practical applicability of the results. First, buildings, which accommodate activities where most urban trips begin and end, are missing from the picture. What does the connectivity of a street tell us if buildings are not accounted for? Whether the objective of the analysis is traffic flow, business-location choice, or land values, buildings accommodate most urban activities and act as the crucial origins and destinations of urban movement. Edges and nodes of the street network are spaces that accommodate traffic, which flows between buildings.

Second, since a great deal of urban decision making happens at the building level, the node or edge level results can also be difficult to use in practice. With edges as units of analysis, all activities or buildings located along a given street segment obtain identical values of accessibility. A building located at the corner of a major intersection is attributed the same level of accessibility as a building in the middle of a block, effectively ignoring local differences that could play an important role in actual built environments.

Third, most urban graph representations to date have been used in unweighted form, treating each element of the network (e.g. edge) as equal. Unweighted representation of network elements may simplify the analysis, but it also conceals important hazards. An unweighted urban network implies that a street that has no buildings on it is weighted equally with a street that accommodates a number of skyscrapers. Likewise, an area covered with industrial land uses, for instance, is weighted equally with an area that accommodates commercial land uses. Unweighted node-edge representations of urban street networks strictly limit the analyses to the geometric properties of the street network itself, ignoring all information about the buildings and activities located on these streets.

To address these shortcomings, the UNA toolbox introduces two important modifications to the network representation of the built environment. First, we add buildings (or other event locations, such as land parcels, transit stations etc.) to the representation, adopting a tripartite representation that consists of three basic elements: edges, representing paths along which travelers can navigate; nodes, representing the intersections where two or more edges intersect; and buildings, representing the locations where traffic from streets enters into indoor environments or vice versa. Our unit of analysis thus becomes a building, enabling the different graph indexes to be computed separately for each building. This allows us to account for both uneven building densities and land use patterns throughout the network, neither of which are addressed in most current urban network analysis methods. We assume that each building connects to a street (edge) that lies closest to it along the shortest perpendicular connection [ii]. This representation is well suited for ArcGIS Network Analyst extension, where origins and destinations of travel paths are represented with geographically positioned points [iii]. Should the analyst wish to compute the graph centrality measures for nodes of the network instead of buildings, then nodes illustrating street intersections can also be used as inputs.

Second, the UNA toolbox introduces a weighted representation of spatial network elements. Each building obtains a set of attributes that connect the building in the graph with the true characteristics of the corresponding structure in the city. The attributes can capture any measurable properties of the structures around them: their size, establishment mix, number of residents or jobs, height, etc. The weighted representation of buildings thus opens up a range of options for studying spatial relationships between buildings, economic establishments, and people, in a network of city streets.

This network representation framework is illustrated in Figure 1. The left side of the figure presents a fragment of Harvard Square in Cambridge MA in plan drawing. The same plan drawing is shown in graph form on the right. If the spatial configuration of the environment under study can

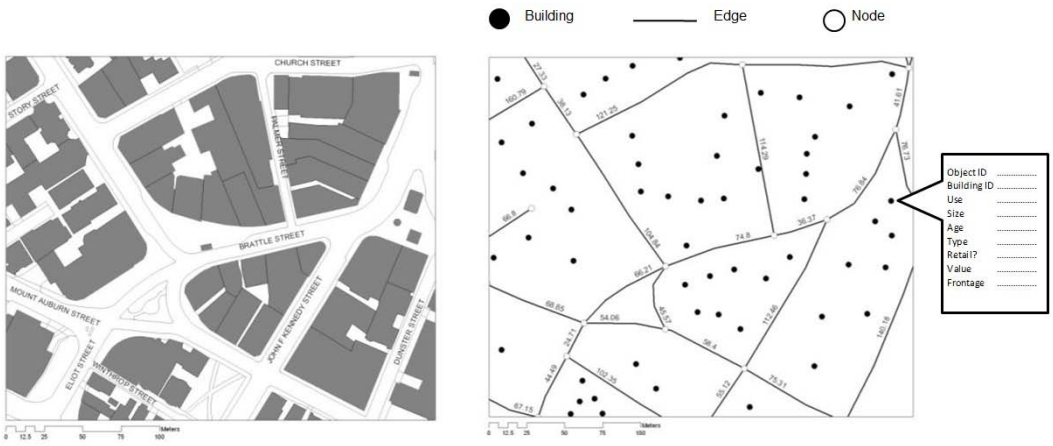

Figure 1. *Left*: Plan drawing of Harvard Square in Cambridge, MA. *Right*: a graph representation of the same plan drawing.

not be represented in a two-dimensional graph – as may be the case if the network contains underpasses, overpasses, or three-dimensional circulation routes inside buildings – then a similar graph can also be represented three dimensionally. Network Analyst in ArcGIS10 supports three-dimensional spatial networks using vertical z-axis values on each of the network elements.

3. NETWORK CENTRALITY MEASURES

Network centrality measures are mathematical methods of quantifying the importance each node in a graph. As the name implies, centrality metrics focus primarily on how centrally each graph element is located with respect to its surrounding elements. The Urban Network Analysis toolbox can be used to compute five different types of centrality metrics on spatial networks of buildings – *Reach, Gravity Index, Betweenness, Closeness,* and *Straightness* – as shown in the graphic user interface of the toolbox in Figure 3. We describe each of these five metrics in detail below.

The Search Radius input specified in the user interface defines the network radius at which the metrics are computed. For each input building, only those other buildings whose geodesic distance from the given building is less or equal to the specified Search Radius, are considered in the analysis. If no Search Radius is defined, then the default infinite radius is used to reach all other buildings in the graph.

3.1. Reach

The reach centrality $Reach^r[i]$ of a node i in a graph G at a search radius r, describes the number of other nodes in G that are reachable from i at a shortest path distance of at most r. It is defined as follows:

$$Reach^r[i] = \sum_{j \in G-\{i\}; d[i,j] \leq r} W[j] \qquad (1)$$

Where $d[i,j]$ is the shortest path distance between nodes i and j in G, and $W[j]$ is the weight of a destination node j (Sevtsuk 2010) [iv]. The weights can represent any numetric attribute of the destination buildings – their size, the number of employees they contain, the number of residents they accommodate etc. Using weights allows the analyst to compute how many of such attributes (e.g. residents, jobs) can be reached from each building within a given network radius.

Figure 2 illustrates how the Reach index works visually. An accessibility buffer is traced from the building of interest i in every direction on the street network until the limiting radius r is reached. The Reach index is then computed as the number of destinations j that are found within the radius. In Figure 2, location i reaches twenty surrounding locations in radius r.

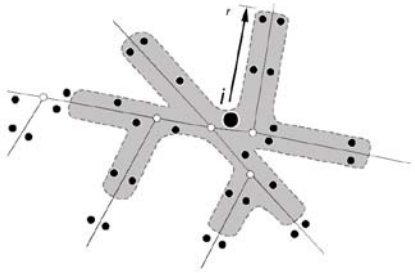

Figure 2. Visual illustration of the Reach index.

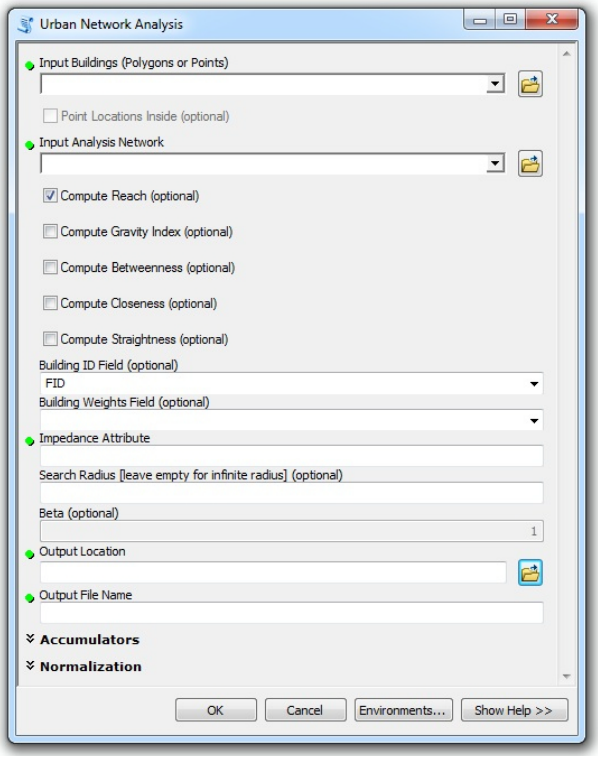

Figure 3. The graphic user interface of the UNA toolbox.

Appendix 1 illustrates the Reach measure with a radius of 600 meters applied to individual buildings in Cambridge and Somerville, MA, weighted by building volume. The output shows how much surrounding built volume can be reached from each building in a 600-meter walking radius. We see that higher Reach values result in areas, where buildings are larger, more densely spaced, or where the street network is denser. Along Massachusetts Avenue near MIT, a typical building reaches roughly 50 million cubic feet of built space in a 600-meter walking radius, whereas in a residential area around Fresh Pond, ten times less volume can be reached during the same walk. The distinction between the two areas originates from their differences in sizes and spacings of buildings on the network, as well as the geometry and topology of the street network itself.

3.2. Gravity Index

Whereas the Reach measure simply counts the number of destinations around each building within a given Search Radius (optionally weighted by building attributes), the Gravity measure additionally factors in the spatial impedance required to reach each of the destinations. First introduced by Hansen (1959), the Gravity index remains one of the most popular spatial accessibility measures in transportation research. So far it has been mainly applied in Euclidian space rather than on spatial networks.

The gravity index, $Gravity^r[i]$ of a node i in graph G at a radius r is based on the intuition that centrality is inversely proportional to the shortest path distance between i and each of the other nodes in G that are reachable from i within a geodesic distance r. It is defined as follows:

$$Gravity^r[i] = \sum_{j \in G-\{i\}; d[i,j] \le r} \frac{W[j]}{e^{\beta \cdot d[i,j]}} \qquad (2)$$

where β is the exponent that controls the effect of distance decay on each shortest path between i and j and $W[j]$ is the weight of a particular destination j that is reachable from i within the radius threshold r. If beta is set to zero, then no distance effect is applied and the Gravity Index becomes equivalent to Reach. If the buildings in G are weighted, then the Gravity Index is directly proportional to the weight of each of the other buildings that can be reached within the given search radius. Appendix 2 illustrates how the Gravity Index is applied to the same dataset in Cambridge and Somerville MA, using building volumes as weights, and a 600-meter limiting radius.

3.3. Betweenness

The betweenness centrality, $Betweenness^r[i]$, of a building i in graph G estimates the number of times i lies on shortest paths between pairs of other reachable buildings in G that lie within the network radius r (Freeman 1977). If more than one shortest path is found between two buildings, as is frequently the case in a rectangular grid of streets, then each of the equidistant paths is given equal weight such that the weights sum to unity. It is defined as follows:

$$Betweennessy^r[i] = \sum_{\substack{j,k \in G-\{i\}; \\ d[i,j] \le r; \\ d[i,k] \le r}} \frac{n_{jk}[i]}{n_{jk}} \cdot W[j] \qquad (3)$$

where n_{jk} is the number of shortest paths from building j to building k in G, and $n_{jk}[i]$ is the subset of these paths that pass through i, with j and k lying within the network radius r from i, and and $W[j]$ is the weight of a particular destination j.

As the name suggests, the Betweenness measure may be used to estimate the potential of passersby at different locations of the network. If the analysis is weighted by demographics of a certain type in the surrounding buildings for instance, then Betweenness centrality can capture the potential of passersby of that particular demographic at building i. Adjusting the Search Radius from a ten-minute walking range to a ten-minute driving range, for instance, allows the user to measure Betweenness for different traffic modes.

Appendix 3 illustrates the Betweenness centrality of individual buildings in Cambridge and Somerville, MA in a 600-meter Search Radius using building volumes as weights. Buildings that are located along the main thoroughfares of the two towns intuitively obtain higher betweenness results, since such routes offer geodesic paths between numerous surrounding destinations. Empirical research has shown that the Betweenees of a location can be an important consideration for retail and service establishemtns (Porta, Strano et al. 2009; Sevtsuk 2010).

3.4. Closeness

The closeness centrality $Closeness^r[i]$ of a building i in a graph G is the inverse of the total distance from i to all other buildings that are reachable in G within radius r along shortest paths (Sabidussi 1966). It is defined as follows:

$$Closeness^r[i] = \frac{1}{\sum_{j \in G-\{i\}, d[i,j] \leq r} (d[i,j] \cdot W[j])} \quad (4)$$

Whereas Betweenness centrality estimates the potential traffic passing by each location in the graph, the Closeness measure indicates how close each of these locations is to all other surrounding locations within a given distance threshold. Unlike the Gravity Index, the Closeness measure does not use the weights of destination buildings in the enumerator, effectively making the measure purely illustrative of how far a building is from its surrounding neighbors.

Appendix 4 illustrates the application of Closeness in Cambridge and Somerville, MA. As no limiting radius is imposed in this example, then we can see how buildings located closer to the center of the graph obtain higher Closeness values. In order to avoid this edge effect, a Search Radius limit should be used to constrain the analysis to a consistently bounded area.

3.5. Straightness

The straightness centrality, $S^r[i]$, of a building i in a graph G illustrates how closely the shortest network distances between i and other buildings in G that are reachable within radius r, resemble Euclidean distances (Vragovic, Louis et al. 2005; Porta, Crucitti et al. 2005). It is defined as follows:

$$Straightness[i]^r = \sum_{j \in G-\{i\}; d[i,j] \leq r} \frac{\delta[i,j]}{d[i,j]} \cdot W[j] \quad (5)$$

where $\delta[i,j]$ is the as-a-crow-flies distance between buildings i and j, $d[i,j]$ the shortest network distance between the same buildings, and $W[j]$ the weight of destination j. As a ratio between the Euclidian distance and the geodesic distance from each location i to the surrounding locations j, Straightness can only be estimated if the units of impedance are in linear distance (e.g. miles), not time (e.g. minutes). It is clear from Appendix 5 that Straightness increases as the mean distance to surrounding destinations increases. The highest values in the buildings along the periphery of Cambridge and Somerville suggest that longer network paths tend to resemble straight lines more closely than shorter network paths. It is this important to use a search radius to limit the analysis to a similar number of neighbors, or to normalize the results, which the toolbox also allows. However, the example also reveals that buildings along some of the straight thoroughfares, which provide numerous direct connections to surrounding destinations, intuitively obtain higher Straightness values than those on side streets.

4. TRANSPORTATION COSTS

The UNA toolbox is designed to handle a variety of different impedance attributes to model transportation costs. These can include metric distance (e.g. kilometers); topological distance (e.g. turns); and time distance (e.g. minutes). The impedance attributes that are available as inputs to the toolbox are automatically obtained from the input network, they therefore need to be pre-coded into the input network that is used [v]. In case of kilometers, for instance, the different centrality measures are computed

with a limiting radius in kilometers. The Reach centrality will thus be limited to only neighboring buildings that can be reached within the specified number of kilometers (e.g. 2 km). In case of a topological impedance attribute, such as turns, a limiting radius of two turns would instead limit the analysis to all neighboring buildings that are less or equal to two turns away from each origin building [vi]. The different attributes for transportation costs and Search Radii allow the toolbox to compute centrality measures for a variety of different transportation modes.

5. CALCULATION STEPS

When using the toolbox to compute any of the five centrality metrics, six calculation steps are typically traversed in order to yield the results (Figure 4). First, an adjacency matrix is computed between all input buildings in the graph. The adjacency matrix represents neighbor relationships and distances between a building i and every one of its immediately closest neighboring buildings j along all available circulation routes that originate from i. Since this step can be computationally rather expensive, if the same network dataset, input points, and building identifiers are used for more than once, then the adjacency matrix is automatically reused from the previous run. Second, a graph is constructed from the adjacency matrix. Third, if weights are specified, then building-weight attributes are retrieved from the input points file so that they can be used as part of the centrality computations. Fourth, the centrality computation is run to calculate all the specified metrics. The UNA toolbox uses a highly efficient algorithm for computing the centrality measures, originally developed by Brandes (2001) for computing Betweenness centrality. In step five, the results of the centrality computation are registered in a table and written to an output layer. Finally, in step six, the analysis results are visualized in the ArcMap environment.

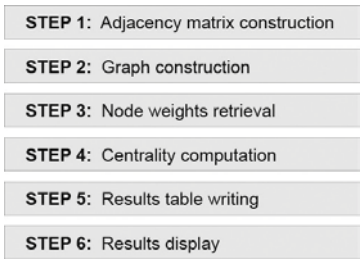

Figure 4. Computation steps of the UNA toolbox.

6. DISCUSSION

The immediate value of the Urban Network Analysis toolbox is that it provides architects, planners, geographers and other scholars of the built environment an opportunity to measure accessibility and centrality metrics on spatial networks, which remain prohibitively labor intensive without computers and accessible software. Applications for these measures are rapidly growing with the increasing availability of geospatial data and improvements in computational power.

Unlike traditional areal density measures that describe events per unit area of land (e.g. floor area ratio; people per acre), which are widely used by architects and planners, the network-based accessibility indices offer a more nuanced view of event densities, where the resulting measures are unique for each building. Network based accessibility indices also produce more intuitive and accurate outcomes than Euclidian accessibility measures since their specification is close to a person's actual perception of urban fabric around a particular building, as experienced when walking or driving along the available streets.

Such measures allow one to investigate how urban form and activity patterns accommodated therein interact with each other. By focusing on the effects of urban form, land use patterns, or a combination thereof, each attribute of a city can be measured independently and intuitively under the constraints of urban geometry. Weighing the centrality metrics by built volume, as shown in the applied examples in the paper, focuses the analysis exclusively on the two- and three-dimensional geometry of urban form. The outcomes of centrality metrics are in this case entirely determined by the spatial configuration of the built environment and can only be altered if the buildings, streets, or intersections of the environment are altered. Setting the weights on jobs, on the other hand, centers the outcomes on the spatial accessibility to jobs that are hosted within the built fabric. Using urban geometry measures side by side with land use accessibility measures allows one to estimate the importance of each factor on an outcome of interest, while controlling for covariates (Sevtsuk 2010). The toolbox thus combines the historically separate approaches of graph analysis and land-use accessibility analysis into a combined framework (Bhat, Handy et al. 2000), and thereby opens up new empirical ground for both fields of study (Batty 2009).

For architects and planners, the toolbox offers a practical solution for quantifying the effects that spatial development proposals might have on existing urban areas. 'Before and after' measurents can illustrate how a particular proposal changes the adjacencies and proximities of a particular urban place with respect to access qualities of interest. A comparison of such scenarios can also be readily juxtaposed with prior measurements of other well-known reference areas elsewhere. Even though the representation of the built environment via three simple elements – nodes, edges and buildings – may appear limiting at times, a thoughtful use of building attributes, travel costs and analysis radii seems to offer a rather powerful representation framework for analyzing various research questions. Perhaps most importantly, the toolbox allows the different professionals engaged in the process of urban development to share a common language for talking about the spatial relationships embedded in the built environment.

The toolbox is distributed in open-source form. Each download comes along with the latest source code and we invite all interested researchers to contribute to the further development of these tools. [vii]

Endnotes

[i] TransCAD is a GIS-based transportation analysis software package produced by Caliper. For more reference, see: http://www.caliper.com/tcovu.htm (accessed September 20, 2011).

[ii] This assumption can be erroneous in building polygons whose centroids lie closest to side streets, rather than the streets of their true entrances. To overcome this bias, a user can input points to represent building locations instead, making sure that the points points reflect the locations of the true entrances.

[iii] In order to accurately model buildings that have multiple entrances on different streets, a user can provide a different input point for each entrance and divide the total attribute weights of the corresponding building by the number of entrances used. The end result of multiple entrance points belonging to the same building should eventually be summed.

[iv] The Reach metric is equivalent to the cumulative opportunities type accessibility measure discussed in Bhat, Handy et al. (2002), but applied on a network rather than Euclidian space.

[v] GIS Network Analyst offers a variety of options for adding different transportation cost attributes to network datasets.

[vi] Note that turns can be defined in a number of ways. One approach for coding turns to network datasets in ArcGIS is shown in Sevtsuk (2010), Appendix One.

[vii] Instructions for open-source development can be found on the City Form Lab webiste: http://cityform.mit.edu/projects/urban-network-analysis.html

References

Batty, M. (2009). Accessibility: in search of a unified theory. Environment and Planning B, 36(2), pp. 191-194.

Bhat, C., Handy, S., Kockelman, K., Mahmassani, H., Chen, Q., & Weston, L.(2000). Development of an Urban Accessibility Index: Literature Review. (B. of E. R. Center for Transportation Research The University of Texas at Austin, Ed.). Austin, TX: The University of Texas at Austin.

Brandes, U. (2001). A faster algorithm for betweenness centrality. *Journal of Mathematical Sociology*, *25*(2), 163-177.

Casalania, V., & Rittel, H. (1967). Generating Floor Plans from Adjacency Matrices. MIT, Cambridge, MA.

Freeman, L. C. (1977). A set of measures of centrality based on betweenness. Sociometry, 40, pp. 35-41.

Garrison, W. L., & Marble, D. F. (1962). The Structure of Transportation Networks. (U. S. A. T. Command, Ed.). U.S. Army Transportation Command Technical Report.

Garrison, W. L. (1960). Connectivity of the Interstate Highway System. Regional Science Associations, Papers and Proceedings, 6, 121-137.

Haggett, P., & Chorley, J. C. (1969). Network Analysis in Geography. London: Butler & Tanner Ltd.

Hansen, W. G. (1959). How Accessibility Shapes Land Use. Journal of the American Planning Association, 25(2), 73-76.

Hillier, B. (1996). Space is the machine : a configurational theory of architecture (p. xii, 463 p., [8] p. of plates). Cambridge ; New York, NY, USA: Cambridge University Press.

Hillier, B., Burdett, R., Peponis, J., & Penn, A. (1987). Creating Life: Or, Does Architecture Determine Anything? Architecture et Comportement / Architecture and Behavior, Vol. 3(No. 3), pp. 233-250.

Jiang, B., Claramunt, C., & Batty, M., (1999), Geometric accessibility and geographic information: extending desktop GIS to space syntax, Computers, Environment and Urban Systems, 23(2), 1999, pp.127-146.

Kansky, K. J. (1963). Structure of transportation networks: relationships between network geometry and regional characteristics (155 p.). University of Chicago, Chicago, IL.

Levin, P. H. (1964). The Use of Graphs to Decide the Optimum Layout of Buildings. Architects' Journal, 7 October.

March, L., & Steadman, P. (1971). The geometry of environment: an introduction to spatial organization in design (p. 360 p.). London, RIBA Publications.

Okabe, A. (2001). A Computational Method for Estimating the Demand of Retail Stores on a Street Network and its Implementation in GIS. Transactions in GIS, 5(3), 209-220.

Okabe, A., & Shiode, S. (2001). SANET: A toolbox for spatial analysis on a network. Journal of Geographical Analysis, Vol.38(No. 1), pp.57-66.

Ozbil, A., Peponis, J., & Stone, B. (2011). Understanding the link between street connectivity, land use and pedestrian flows. Urban Design International, 16, pp. 125-141.

Porta, S., Crucitti, P., & Latora, V. (2005). The network analysis of urban streets: a primal approach. Environment and Planning B, 35(5), 705-725.

Porta, S., Strano, E., Iacoviello, V., Messora, R., Latora, V., Cardillo, A., Wang, F., et al. (2009). Street centrality and densities of retail and services in Bologna,Italy. Environment and Planning B: Planning and Design, 36, 450-465.

Rittel, H. (1970). Theories of Cell Configuration. In G. T. Moore (Ed.), . Cambridge, MA: MIT Press.

Sabidussi, G. (1966). The centrality index of a graph. Psychmetrika, 31, 581-603.

Sevtsuk, A. (2010). Path and Place: A Study of Urban Geometry and Retail Activity in Cambridge and Somerville, MA. PhD Dissertation, MIT, Cambridge.

Turner, A. (2001). Depthmap: A Program to Perform Visibility Graph Analysis. 3rd International Symposium on Space Syntax. Georgia Institute of Technology, 7-11 May 2001.

Vragovic, I., Louis, E., & Diaz-Guilera, A. (2005). Efficiency of information transfer in regular and complex networks. Physics Review E., 71(026122).

APPENDIX

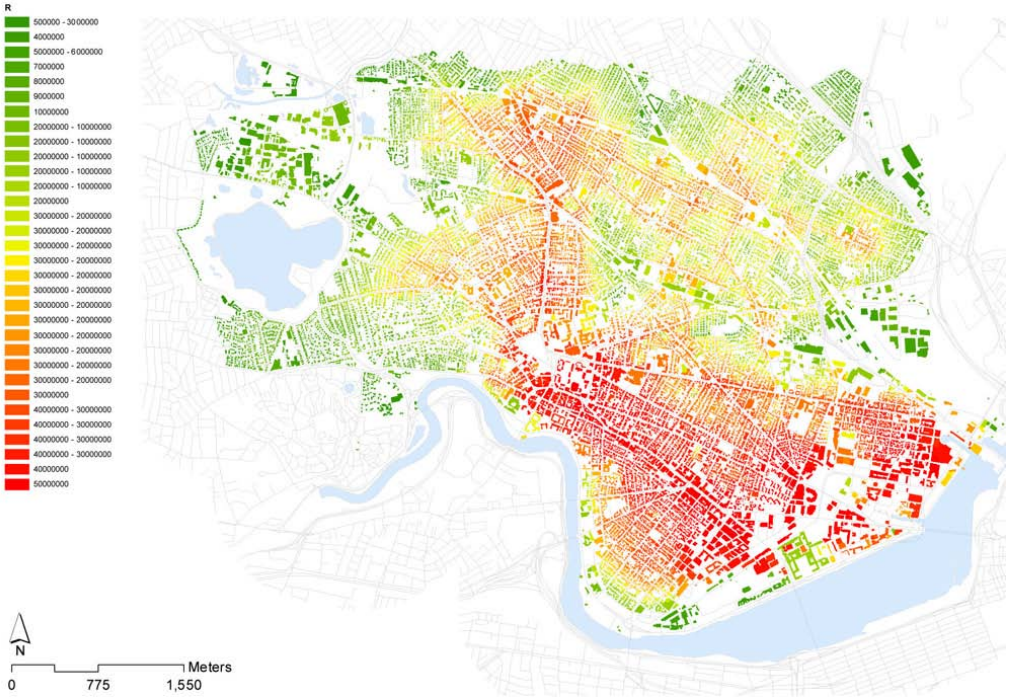

Appendix 1. Reach to built volume within a 600-meter network radius from each building in Cambridge & Somerville. (Building volume data source: MassGIS 2002).

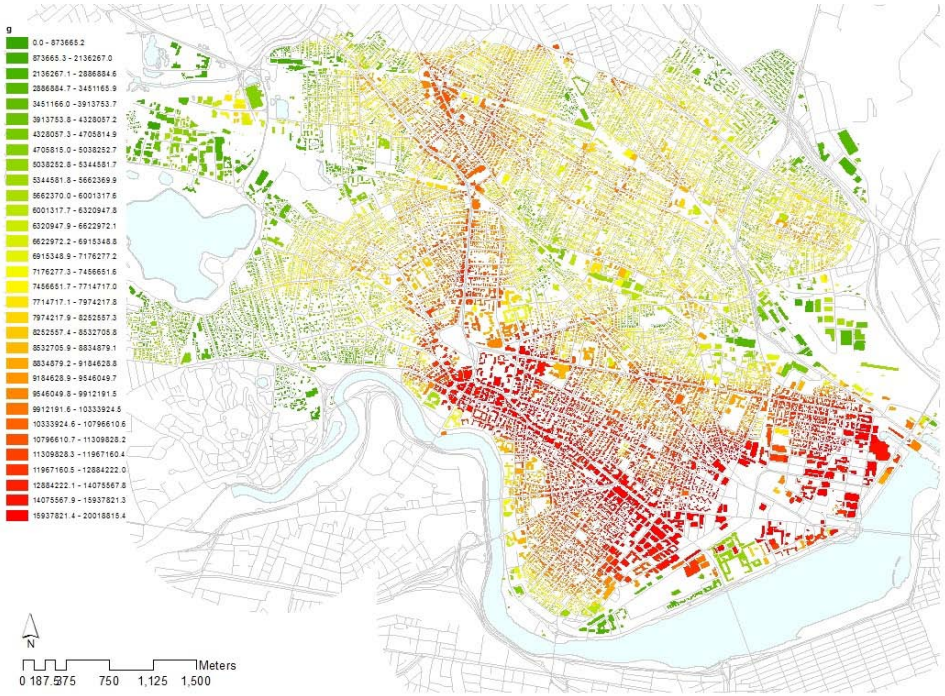

Appendix 2. Gravity Index measured to built volume within a 600-meter network radius (Beta=0.00217) from each building to every other building in Cambridge & Somerville.

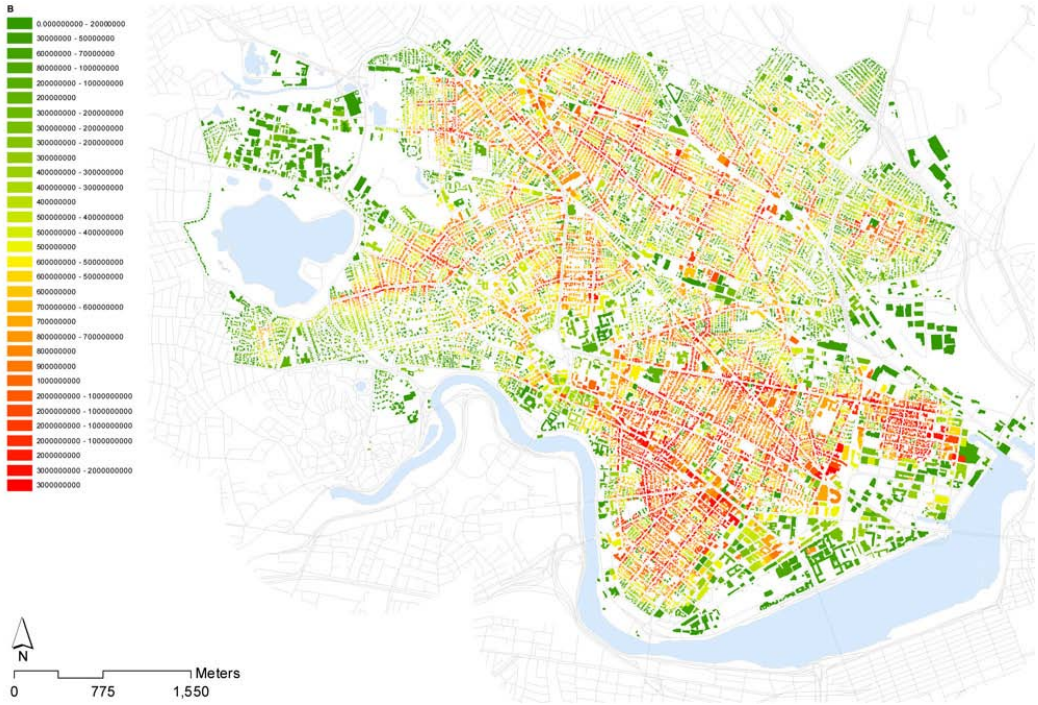

Appendix 3. Betweenness centrality in a 600-meter network radius, weighted by building volume in Cambridge & Somerville.

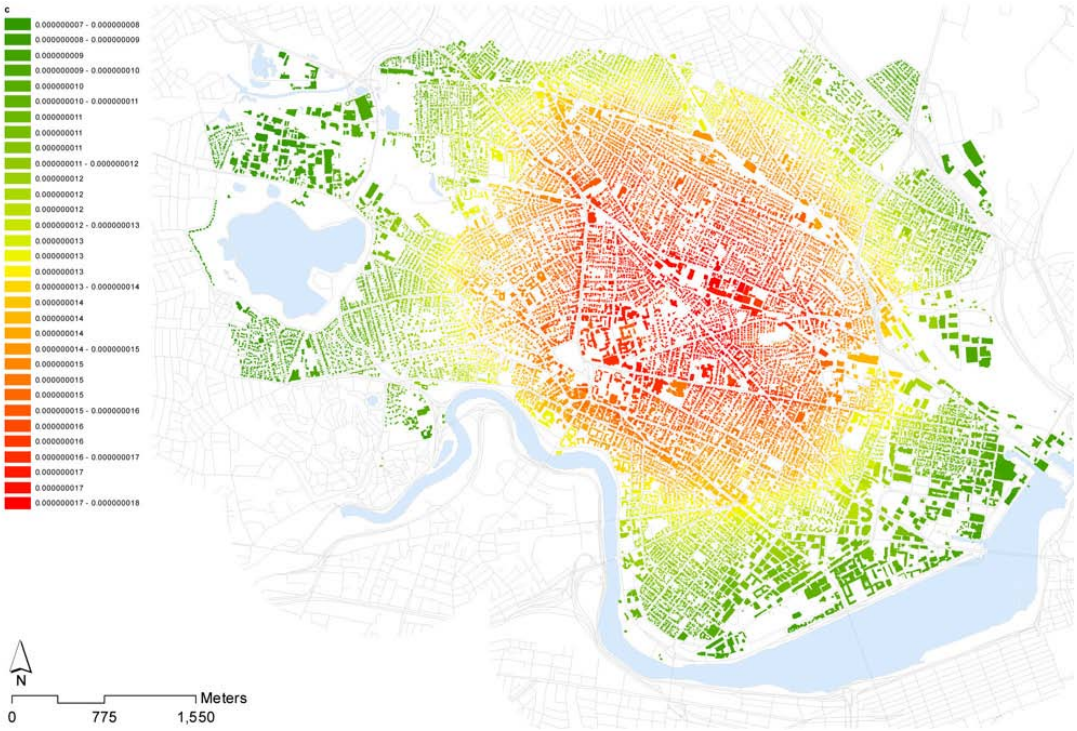

Appendix 4. Closeness centrality to surrounding buildings with no limiting radius nor weights in Cambridge & Somerville.

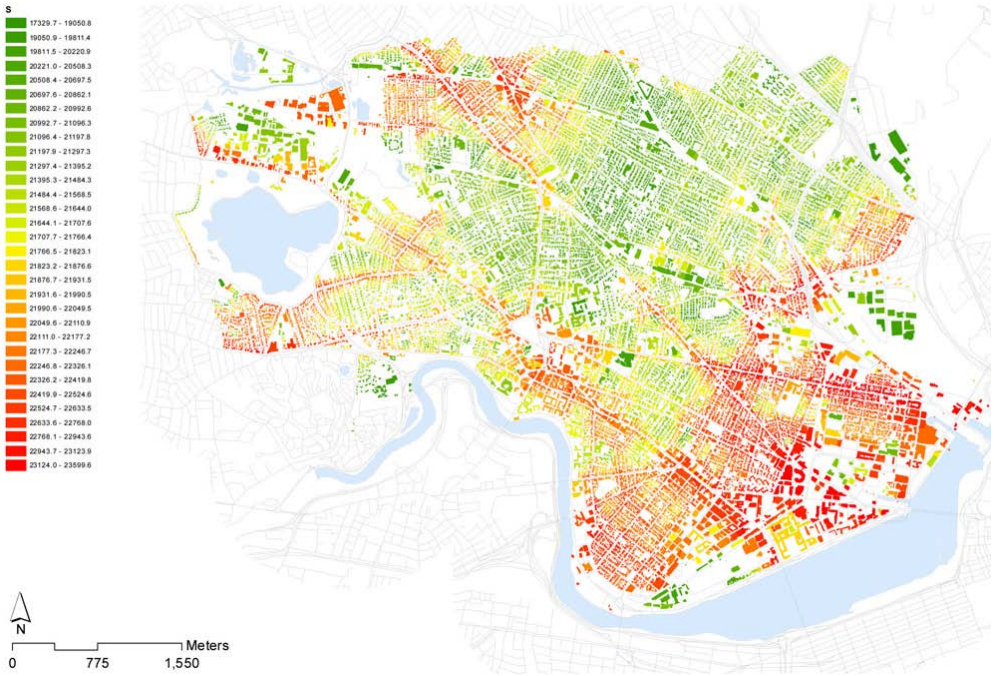

Appendix 5. Straightness centrality with no limiting radius, weighted by building volume in Cambridge & Somerville.

The Parametric Exploration of Spatial Properties – Coupling Parametric Geometry Modeling and the Graph-Based Spatial Analysis of Urban Street Networks

Sven Schneider, Martin Bielik, Reinhard König

InfAR - Chair for Computer Science in Architecture
Bauhaus-University Weimar, Faculty of Architecture
Belvederer Allee 1, 99423 Weimar, Germany
sven.schneider@uni-weimar.de, martin.bielik@uni-weimar.de, reinhard.koenig@uni-weimar.de

Keywords: parametric modeling, spatial analysis, space syntax, design process, tool development.

Abstract

Parametric modeling is a powerful tool that allows designers to explore a wide range of variants of their design concept. However, when evaluating the spatial properties of such variants, the tools for parametric modeling offer little support. While on the other hand a wide range of methods exists for analyzing geometry in terms of its spatial properties via graph-based-measures, the available software for analyzing these properties offers limited capabilities for changing the geometry. After analyzing the geometry, design changes then have to be made in another program, which hinders the design workflow and with it the desinger's willingness to explore a wide range of variants. This paper describes an approach that attempts to bridge the gap between parametric geometry modeling and methods for measuring the spatial properties of this geometry. To this end we developed a component for a well-known parametric modeling software package for graph-based analysis. This component is able to interpret segment maps from parametric line drawings (e.g. urban networks) and calculates centrality (integration) and betweenness (choice) for different radii. We demonstrate the applicability of the method in a test scenario.

1. INTRODUCTION

The aim of the article is to present a method for combining parametric modeling and the analysis of geometric structures in terms of their spatial properties. As this concerns two different areas of computer-aided design we start by briefly explaining the two methods and their terminology.

1.1. Parametric Modeling

Parametric modeling denotes the creation of geometric models by defining relationships between the properties of geometric objects (such as points, lines or surfaces). These relationships are defined by numerical parameters (e.g. the number of repetitive elements) or by linking the geometric elements themselves (e.g. a line defined by two points). If changes are made to either the values of the parameters or the properties of the associated geometric objects (such as moving a point) this has a direct impact on the overall geometry. Geometric models whose elements relate to one another in the manner described above are referred to as parametric models. They allow one to construct complex geometric structures by relatively simple means, and they enable one to quickly generate a large amount of variants by changing the parameters. The range of these variations depends on the structure of the parametric model and can vary from slight variations to structurally different solutions. A comprehensive introduction to the principles of parametric modeling can be found in Woodbury (2010).

It is worth mentioning that this type of geometry modeling has become a standard tool in both architectural education as well as architectural practice, which is reflected not least in the increasingly complex forms of contemporary architecture. Parametric modeling is used in particular in the design of structures, facades and unusual building shapes. Complex design concepts can be controlled by relating geometry to few parameters, as in the case of the Mercedes Benz Museum in Stuttgart (Hemmerling & Tiggemann, 2010). At the same time, tools for analyzing the structure and energy performance of buildings can be integrated to assit in the optimization of the building geometry (Luebkeman & Shea, 2005).

Besides the examples mentioned, another application of parametric modeling is the creation of urban structures. One example is the formal experiments by Schumacher (2009), which have become known under the term "Parametric Urbanism". One problem here lies in the fact that the parameters that were used for the generation of the structures are not related to spatial and functional conditions (e.g. movement patterns), serving only as regulators for individual gestalt-principles (e.g. density, contrast, gradients). While aesthetically appealing structures can emerge, the evaluation of their suitability as real urban structures must be judged by the designer. Certainly, this work represents an extreme case of the application of parametric models in an urban scale but it does clearly illustrate the potential as well as the problems associated with this methodology. On the one hand, it enables the creation of highly complex structures. On the other hand, this complexity also complicates the evaluation of the structures, since the number and variety of elements produced is difficult for humans to comprehend. Analyses, which assist in the assessment of spatial relationships are therefore of great benefit. How such spatial relationships can be evaluated, is described in the following section.

1.2. Graph-based methods for spatial analysis

The geometric characteristics of the public space of a city (the network of public roads and squares) have a significant influence on the life of its inhabitants. It structures the movement patterns of residents, which determine to a large degree how vibrant certain parts of a town or an urban district are.

Using graph-based methods certain properties of spatial structures can be measured. In the context of architecture and urban planning, these methods have become known through the work of the Space Syntax group (Hillier & Hanson, 1984; Hillier, 1996). Here, space is understood as a 'configuration' which can be represented and analyzed through a representation based on geometric elements. The conversion of a spatial situation into a 'configuration' can be done through various forms of representation, such as the subdivision into convex spaces (convex map), into a set of sight / motion axes (axial map) or into a grid of vantage points and their relations to each other (visibility graph) (see figure 1). For the purposes of analysis, these representations need to be converted into a graph: the elements (e.g. lines of sight) are interpreted as nodes and their relationship to each other (e.g. intersections) as edges of the graph. The edges are usually non-directed, since the mutual visibility of the elements plays a central role in creating the representations. The resulting graph can be analyzed according to certain measures. An example of this is "integration" and "choice", which in graph theory are better known under the names "Centrality" and "Betweenness".

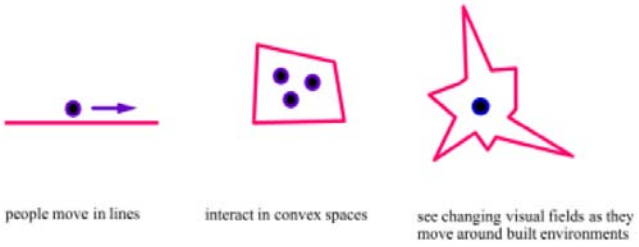

Figure 1. Representations of space in Space Syntax (Hiller, 2005).

Centrality (or Integration) measures the average distance from one element to all other elements (global integration) or to elements within a certain radius (local integration). Based on the analysis results one can see where the global and where the local centres of a structure are located. These centres are the places that have the least distance to other elements in the structure. At these points one can usually find the highest concentration of pedestrians and shops in a city (Hillier, 1993).

Betweenness (or Choice) measures how often an element is passed if all shortest paths in the graph (of each element to all the other elements) are traversed. The higher the value of betweenness of an element is, the more often this element is part of the shortest paths in a structure. Hillier and Iida (2005) have shown that this value strongly correlates with movement frequencies. Depending on the radius of the calculation, movement patterns can be evaluated on a local scale (for pedestrians) and on a global scale (for motorized traffic).

Since the analysis methods mentioned above focus on the pure geometrical arrangement of spatial elements and require no additional data on land use or traffic for their calculations, they are particularly suitable for examining design alternatives in terms of their spatial characteristics. Suitable software includes GIS programs that support graph analysis. A software package that was specially made for Space Syntax analysis is Depthmap (Turner, 2001). However, the problem with many such analysis programs is that they offer no method for the generation of shapes or structures (modeling). If changes need to be made on the

basis of the analysis, a separate modeling program is required, which hinders the design workflow.

The next section briefly discusses one typical characteristic of the design process that shows why it is useful to seamlessly combine the creation of geometry and graph-based spatial analysis.

2. DESIGN WORKFLOW

Architectural and urban design is an activity in which, starting from a given task (design brief), a solution needs to be worked out. The process by which this is achieved is very complex and hard to formalize because, as Lawson (2006) explains, analysis, synthesis and evaluation often take place simultaneously in complex mental processes. However, despite the obvious difficulty of formalizing design, one characteristic that applies to all design processes can be identified, namely, their iterativity. In a first stage solutions are proposed (so-called prototypes in the form of sketches, models, drawings), which then need to be evaluated according to different criteria and finally, where necessary, modified or completely revised on the basis of the evaluations. This process is repeated several times over until a satisfactory solution is found. Simon (1969) describes this process as a Generate-Test Cycle. The same pattern appears in a slightly modified form in numerous publications on the design process: Rittel (1992) names the "elementary activities" of design the generation and reduction of variety. Zeisel (1984) described it as a cycle consisting of imaging, presenting and testing and Schön (1992) speaks of a See-Move-See dialogue.

Within this iterative process, the tools used to create prototypes play a central role. They are required to externalize the ideas and thoughts that are in the head of the designer (Gänshirt, 2007). As such, manageable artifacts are produced which can in turn be evaluated by the designer. For the design process to be effective, it is critical that the cycle of ideas, design tools and artifacts (see Figure 2) is not interrupted unnecessarily. This is one reason for the success of traditional design tools such as pencil and paper, because these tools can be used without any special knowledge and their usage facilitates a continuous flow of thoughts (Petruschat, 2001).

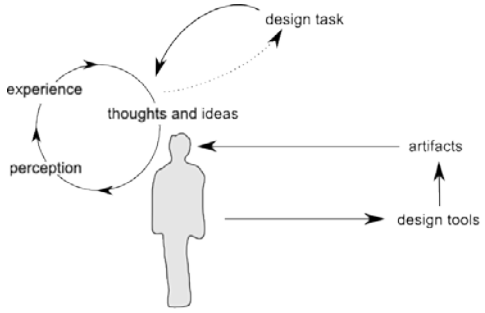

Figure 2. Designing is a cyclical process where artifacts are created with the help of design tools (see Gänshirt, 2007).

If we consider the use of digital methods when designing, it is not unusual for different programs to be required for different tasks – for example, a modeling program to create geometry and analysis software for the spatial analysis of that geometry. In order to use the output from one program in another, it is necessary to import and export data via an exchange format. This break in the workflow causes two major problems that adversely affect the design process. Firstly, the complicated exchange of data inhibits the willingness of designers to analyze their design-options. The interruption in workflow costs time, which results in the designer undertaking fewer iterations, and by implication the possible omission of potentially better solutions. In a sense it potentially limits the exploration of solution space. Secondly, the results obtained in the analysis cannot be used directly for the modeling process. This contradicts the principles of parametric modeling, which are intended to generate smart forms or structures through the skillful combination of parameters.

The aim of achieving an effective design process that uses parametric modeling and spatial analysis could, therefore, be realized through the direct coupling of the two methods (generation and evaluation). This would make it possible to effectively analyse variants on the one hand and to incorporate the analysis results in the modeling process on the other.

3. COUPLING GRAPH ANALYSIS AND PARAMETRIC MODELING

To demonstrate the desired direct coupling of the two methods, we developed an extension for a well-known parametric modeling system: Rhino modeling software in combination with the plugin Grasshopper (see Figure 3). Grasshopper allows you to create parametric models by interconnecting so-called components with their data input

and output (in the realm of software programming this method is known as visual dataflow programming). These components include, for example, geometric elements (lines, points, surfaces, etc.), calculation methods for the analysis of geometric objects (distance calculation, curve and surface analyis, etc.) and algorithms for creating com plex geometric structures (Voronoi, Delaunay, etc.). As described in 1.1, by linking these components, complex geometric models can be created and controlled by parameters (numerical as well as graphical). A useful aspect of Grasshopper is that it can be extended by programming additional components. Therefore an SDK is available for the development of Grasshopper components that provides mechanisms for the exchange of data (input and output of the component). The development of the components described in Section 3.1 was done with C # based on the .NET Framework 3.5.

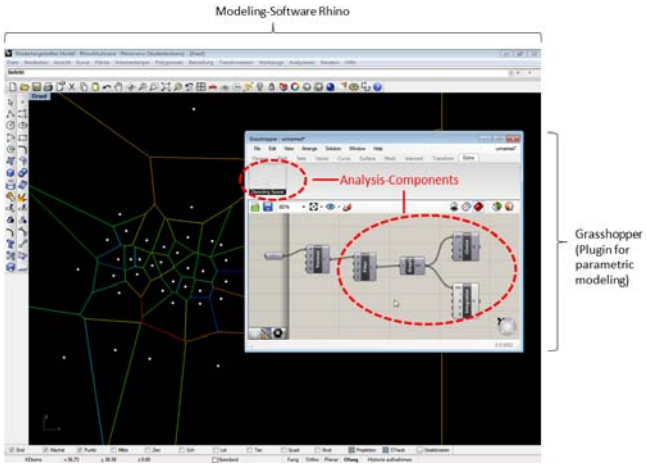

Figure 3. Screenshot of Rhino, Grasshopper and the new Spatial Analysis Components.

For the spatial analysis, we decided to use segment-map analysis (Hillier & Iida, 2005). On the one hand, this form of representing spatial structures can be easily mapped in a parametric model because it relates directly to the road network and does not, as is the case for example with an axial map, require an urban plan for the prior generation of lines of sight. On the other hand, it has been shown that this method of analysis strongly correlates with pedestrian movement and distribution, and is therefore of direct practical benefit for the design of cities and neighbourhoods.

3.1. Description of the analysis framework

For the design of the analysis tool we have chosen a modular structure (see Figure 4). There are several reasons for this. Firstly, it is easier for the user, because one does not have to configure one complicated component but can connect several simple components as needed. Secondly, breaking the whole down into individual components proved to be efficient, since steps that are needed for different analyses do not need to be repeated. For example once a structure is converted into a graph, different measures can be derived after this step. Finally, the modular design facilitates future expansion as it can be built on top of existing components. For example, if the framework is extended by different forms of spatial representation, such as Convex Spaces, Axial Lines or Isovists the analysis of those representations can be done using the pre-existing graph-components analysis.

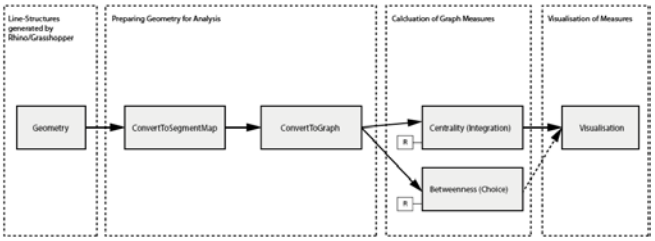

Figure 4. Modular concept of the spatial analysis framework for Grasshopper.

In the following we describe the functionality of the different components we developed.

3.1.1. ConvertToSegmentMap component

Since the segment analysis only works with line segments, but designers often create models in which axes, curves and splines occur, these drawings must first be converted into segments. This step is important to ensure that designers retain formal freedom as, for example, splines are easier to control than single lines made up of composite curves. The component reads the geometry (any set of lines, polylines, curves and splines) and converts it into a segment map. The curves and splines are first subdivided into a finite number of segments and then segments are created between the intersections of all lines (Figure 5).

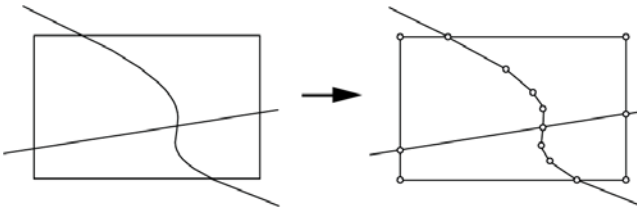

Figure 5. The ConvertToSegmentMap Component converts geometric structures into segment maps.

Since Rhino, the modeling program, makes it possible to model a 3-dimensional structure it is not necessary to specially treat line segments that do not intersect (such as bridges and underpasses). These elements just need to be given different Z-coordinates.

3.1.2. ConvertToGraph component

The ConvertToGraph component converts the geometry resulting from the ConvertToSegmentMap component (a segment map) into a graph. The graph is formed by interpreting each segment as a node and the connection to other segments (in the case of equal endpoints) as edges (see Figure 6).

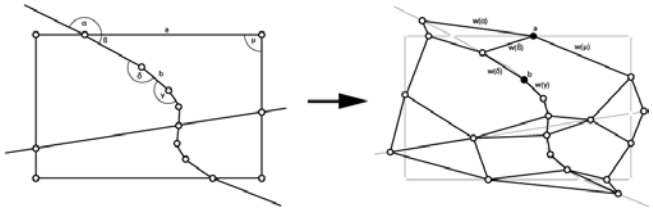

Figure 6. Converting a segment map into a graph (for details see Hillier & Iida, 2005).

The weighting of the edges of the graph is based on the angle between intersection points of the segments. This is due to the assumption that humans prefer to take routes through a city that deviate as little as possible from the intended direction (i.e. minimal angular deviation). An angle of 90° is therefore weighted high, while an angle of 0° between two segments has no weight.

3.1.3. GraphAnalysis components

After a graph has been created from the segment map using the ConvertToGraph component, various analysis-components can be applied to calculate different graph-measures. Components have been developed for two major measures: centrality (integration) and betweenness (choice). As described in 1.2, the measures can be calculated for different radii. By default radius N is chosen, corresponding to a global analysis. To evaluate movement patterns on a smaller scale level, a certain radius can be set (a typical measure for pedestrian movement is a radius of 800m, equivalent to a walk of about 10 minutes).

3.1.4. Visualisation component

The visualisation component takes over the visual representation of the results of the analysis. The segments are coloured according to the values derived from the graph analysis component. The colouring is carried out by means of false colours from red to blue. Segments with high values are displayed in red, segments with low values are displayed in blue.

3.2. Verification

In the following the applicability of the previously described components is demonstrated using a simple scenario. The scenario consists of the generation of a road network for a fictitious urban district. It shows two ways in which the coupling of the two methods described above can be productively used in the design process. It should be noted that the applied parametric structure is not yet useful for real urban structures; it only demonstrates the applicability of the coupling described.

3.2.1. Comparison of different variants of a simple parametric model

For the generation of the road network a simple subdivision algorithm is used which is implemented by default in Grasshopper (substrate-component). This algorithm recursively divides a given rectangle into sub-areas. The parameters with which the algorithm can be controlled are the number of subdivisions, the angle of the subdivisions, and the degree of randomness with which the angles are changed. The resulting structure has been linked to the analysis components. Several design variants were evaluated with regard to centrality and betweenness (see Figure 7).

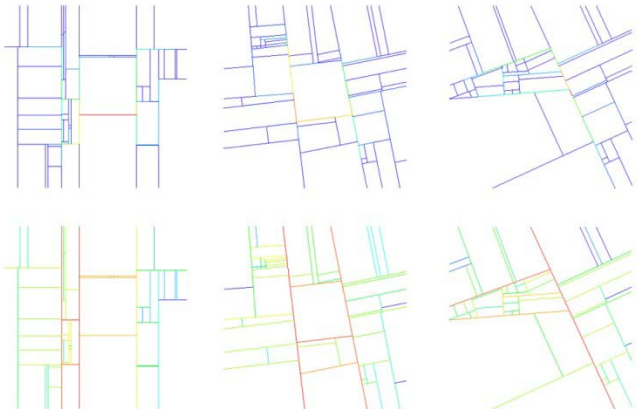

Figure 7. Three design variants deriving from a simple parametric model, analysed in terms of betweenness (first row) and centrality (second row).

The time required for the calculation of parameters determines the degree of interactivity of the software, i.e. the faster the analysis results respond to changes in the geometric structure the better the designer can understand the impact of his or her actions on the spatial properties. The aim is to achieve a very quick response time (~1/10 second). However, this is virtually impossible to achieve because the number of comparisons in the graph analysis increases exponentially with an increasing number of segments. On a computer with average performance (2.4 GHz), an betweenness analysis of 100 segments requires approximately 0.4 seconds. The computing times rises for 200 elements to 1.4 s, and to 4.6 s for 400 elements.

3.2.2. Application of the analysis results for the definition of a parametric model

The second advantage of the integration of spatial analysis in a parametric modeling system is that the results of the analysis can be used directly as parameters for controlling other geometric elements. How these values are used as parameters of the model, of course, depends on the intentions of the designer. To demonstrate the technical feasibility, two morphological characteristics of the urban quarter were associated with the analysis results: the width of streets and the height of the building. The width of the roads was associated with the betweenness value according to the principle that the more frequented a road segment, the more space it should provide for pedestrians / cars (see Figure 8).

Figure 8. Relating betweenness to the width of streets.

The height of the building was linked to the centrality value. Here the idea is that in the centre of cities there is greater demand for housing and office space than in the peripheral areas, resulting in increasing building heights in these areas (Figure 9).

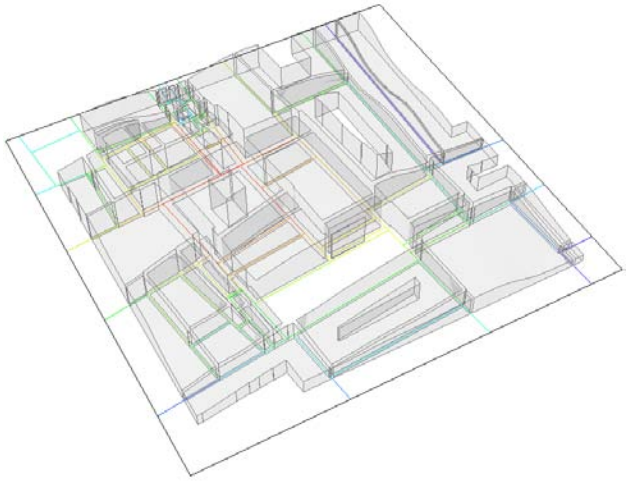

Figure 9. Relating centrality to the height of buildings.

4. CONCLUSION & OUTLOOK

In this article software components have been presented that allow one to easily couple parametrical models with the analysis of their spatial properties (centrality, betweenness). This offers two main advantages: Firstly, the analysis can be

run directly in a CAD environment (using Rhino as a geometric modeller) which makes the workflow more effective when creating and evaluating variants. Secondly, the analysis results can be related directly to the parametric model, which opens up new ways of thinking of how we can incorporate analysis in the creation of forms.

Future developments of the analysis software presented here will incorporate further analysis types. These include the creation and analysis of convex maps, axial maps and visibility graphs. Furthermore, the visualisation component will be extended by displaying J-graphs and scatter diagrams. Another interesting point we want to examine is the extent to which spatial structures can be optimised with the developed framework. A promising concept, therefore, is offered by evolutionary strategies, which search the solution space for optima by systematically varying the parameters.

The components described in section 3 can be downloaded from www.decodingspaces.de (videos and a tutorial can be found there as well).

References

GÄNSHIRT, C. 2007. Tools for Ideas: An Introduction to Architectural Design. Birkhäuser. Basel.

HEMMERLING, M. & TIGGEMANN, A. 2010. Digitales Entwerfen, UTB. Paderborn.

HILLIER, B. AND HANSON, J. 1984. The Social Logic of space. University Press. Cambridge.

HILLIER, B. 1993. Natural Movement. Environment and Planning B, 1993 (20), pp. 29 – 66.

HILLIER, B..1996. Space is the Machine. Electronic re-issue 2007.

HILLIER, B., 2005. The art of place and the science of space, World Architecture 11/2005 185, Beijing, Special Issue on Space Syntax, pp. 96-102.

HILLIER, B. AND IIDA, S. 2005. Network effects and psychological effects: a theory of urban movement. Proceedings of Spatial Information Theory: International Conference, N.Y., U.S.A. pp. 475-490.

LAWSON, B. 2006. How Designers Think. (4th Edition) Architectural Press Oxford.

LUEBKEMAN, C AND SHEA, K. 2005. Computational design and optimization in building practice. In: The Arup Journal 2005 (3) pp. 17-21.

PETRUSCHAT, J. 2001 Bemerkungen zum Zeichnen. In: form+zweck, Heft 18, pp. 70 – 77.

RITTEL, H. 1992. Planen - Entwerfen - Design. Reuter, W. (ed.), Stuttgart.

SCHÖN, D.A. 1992. Designing as a refelective Conversation with the materials of a design situation. In: Reseach in Engineering Design 1992 (3) pp. 131-147.

SCHUMACHER, P. 2009 Parametricism - A New Global Style for Architecture and Urban Design. AD Architectural Design - Digital Cities, Vol 79, No 4.

SIMON, H. 1995. Die Wissenschaft vom Künstlichen. 2nd edition. Springer. Wien

TURNER, A. 2001. Depthmap: A Program to Perform Visibility Graph Analysis. Proceedings of the 3rd International Symposium on Space Syntax. Atlanta.

WOODBURY, R. 2010. Elements of Parametric Design. Routledge. London.

ZEISEL, J. 1984, Inquiry by design. University Press. Cambridge.

Session 5: Work in Progress

Spatial Simulation Model of Urban Retail System 133
Sanna Iltanen
Tampere University of Technology (TUT)

Automatic Building Design with Genetic Algorithms and Artificial Neural Networks 137
Negin Behboudi, Fouad Butt, Abdolreza Abhari
Ryerson University

Visualization Framework of Thermal Comfort for Architects 141
Pascal Goffin, Arno Schlueter
Swiss Federal Institute of Technology Zurich (ETH Zürich)

Experimental Validation of Simulation Software for Daylight Evaluation in Street Canyons 145
Manolis Patriarche, Dominique Dumortier
KiloWattsol, Université de Lyon

A Morpho-Energetic Tool to Model Energy and Density Reasoned City Areas: Methodology (Part I) 149
Laetitia Arantes, Olivier Baverel, Daniel Quenard, Nicolas Dubus
Ecole Nationale Supérieure d'Architecture de Grenoble, Centre Scientifique et Technique du Bâtiment (CSTB), École des Ponts Paris-Tech

Spatial Simulation Model of Urban Retail System

Sanna Iltanen
Tampere University of Technology, School of Architecture
BOX 600, FIN-33101 Tampere,
sanna.iltanen@tut.fi

Keywords: retail system, agent based modelling, network city, accessibility, spatial organisation

Abstract

The paper introduces a dynamic spatial model of urban retail systems in which the 'retail units' of different sizes and types compete with each other and the households continuously re-evaluate their shopping orientation. The model is currently at "work-in-progress" stage and needs still more work on calibration methodology. The goal of the model is to show the serial evolution of spatial distribution of retail units. The simulation model has been built within Gabriel Dupuy's (1991) three level model of urban networks. In the model, the spatial approach is emphasised through morphological types of retail units and the transportation network which defines the spatial framework for the whole model. The model enables observation how different boundary conditions - set by the typology and transportation networks - affect the spatial organisation of retail units in urban environments. The simulation model utilises both modern agent based modelling techniques and methodologies of traditional spatial interaction models (e.g. Wilson-Bennett 1985). The interest lies in the process in which the competing retail units form generations of spatial distributions. The case study has been executed in the Helsinki city region in Finland.

1. INTRODUCTION

This study aims to develop a spatial simulation model of an urban retail system. The aim of the model is to show the evolution of the retail units based on the interaction of households, retail units and infrastructure. The purpose is to observe the changes and behaviour on system level rather than predict a location of a single retail unit. Trading has always been one of the core activities of cities and today this economic activity is highly competitive and dynamic. The dynamic nature of this activity makes it challenging for planning practice. The actors in the retail sector continuously search for new locations and modes of production and consumption in order to gain comparative advantage. This continuous interaction and development has been interpreted as complex phenomena in several contexts (e.g. Jacobs 1961, Schelling 1978, Allen 1981, Batty 2005).

Widely used traditional planning methods are not fully able to answer the challenges of this new operational environment where the understanding and conceptions of dynamic urban development have shifted towards the conceptions of complexity theory. This paradigm change and processual approach has created a new demand for planning tools that increase knowledge of the development process and the cumulative influence of individual interactions. New planning instruments should be able to reveal causal relations and boundary conditions that can lead to system phase transitions. The boundary conditions in simulations are defined through the retail unit typology, which specifies the retail unit sizes that are allowed in the model; distribution of households, including income data; and transportation network which defines the generalised travel cost between all spatial entities, for example road segments between crossroads. Modelling tools can work as useful instruments in discussions between the private and public sectors in planning processes and particularly in situations where tensions exist between different interest groups.

2. THEORETICAL FRAMEWORK

The focus in this study is on the spatial organisation of retail units and how this process can be simulated in agent based models. The objective is to find out how the selected boundary conditions affect retail unit lifecycles on the regional scale. The model exploits the detailed data of the environment and the focus is in particular on the effects of the structural properties of urban transportation networks.

This study observes a city as a complex system: the approach emphasises the self-organising phenomena of urban dynamics. The overall structure of the simulation model follows Gabriel Dupuy's theoretical model of urban networks conceptualised as a three-level structure (Dupuy 1999).

The simulation model comprises all the three level elements: (1) infrastructural networks, (2) networks of production and consumption, and (3) networks of individuals. As the focus of the model is on the dynamics among the three elements, it also gains from the tradition of spatial interaction modelling (e.g. Batty 1976, Wilson 1985). This study aims to combine these approaches from different theoretical backgrounds with agent based modelling techniques.

The boundary conditions in the model are defined through the typology of retail units that form the most dynamic part of the model. The intention is to test several different sets of retail types. Households in the model are fixed on certain locations, but they continuously re-evaluate their shopping destinations and thus also produce dynamics in the model. One of the objectives is to study how the different aspects of accessibility influence consumer behaviour and the spatial self-organisation of retail units. In particular, the focus is on the relationship between accessibility measures and spatial structures.

3. METHODOLOGY AND RESEARCH OPERATIONS

The model consists of two major modules: (1) an initialisation module and (2) a simulation module. The initialisation module includes functions that read all the input data for the model. The input data includes information concerning households, retail services and transportation systems. The actual processing of the data then happens in the simulation module, which runs the given number of simulation cycles. As an end result, the series of simulation cycles produce a development path for the retail system as an output.

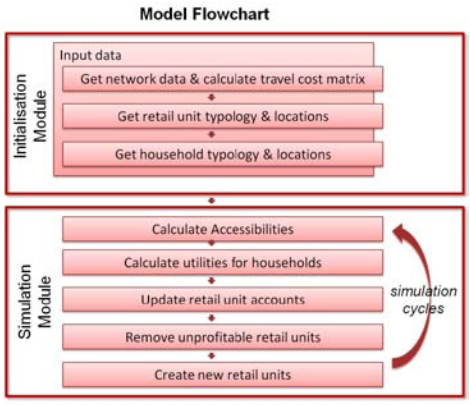

Figure 1. Model flowchart.

A more accurate description of the model can be seen in the model flow chart represented in Figure 1. The initialisation module reads and combines the gis-network data (Mapinfo tab-fileformat) with the parameter data included in txt-files. The network data includes all location data: the number of households of each type and the number of retail units of each type within each road segment (or other spatial entity defined by the network file). The network data also includes the travel cost data for each road segment. The parameters which are related to the retail unit type (size, revenue limit, catchment radius) and household type (incomes) are defined in separate txt-files. The travel cost matrix calculation is based on the road network graph structure and on the travel cost data which is included in the network file individually for each network link (i.e. road segment). The generalised travel costs, which can be defined as metric distance, time, currency or combination of these, are calculated between all the possible locations and are stored in this 2-dimensional table. Thus the travel cost matrix defines the spatial framework and boundary conditions for the simulation.

In the simulation phase the model utilises accessibility measures in multiple ways as the simulation progresses (Figure 2). At first it calculates an accessibility measure (Acc R-R) from every retail unit to every other retail unit, which indicates the degree of clustering of each retail unit. Thus, if the accessibility from one retail unit to all other retail units is high, the retail unit benefits more from the clustering, compared to the units that have low accessibility to other retail units.

In the second step, the model calculates utilities (to retail units) for every household, and their shopping orientation is based on this ranking of retail units (ordinal utility). After every household has selected the most beneficial retail units for them, the purchasing power of every household is allocated to retail units and retail units' accounts are updated. Every retail unit type has a certain revenue limit that they have to reach in order to survive to the next simulation cycle. If a retail unit does not achieve the revenue limit, it goes bankrupt and is removed. An accessibility factor (for the household to the retail unit, Acc Hh-R) is also included in the utility function. At the end of each simulation cycle, new retail units are created to replace any units that went bankrupt. The location of the new retail units is based on the accessibility of the network (Acc Network). Each retail unit type has a catchment radius

parameter and the location of each new unit is selected randomly from among those network sections which are highly accessible within the movement scale (defined by the catchment radius). The simplified process that generates new retail units is based on the accessibility of the units from the customer point of view. Other factors affecting store location choice are ignored so far. The new generation of retail units created at the end of each simulation cycle initialises the next cycle, and the series of these generations form the development path of the system.

The formulas for calculating the accessibility and the utility measures are as follows:

Accessibility from a retail unit to every other retail unit is defined as

$$Acc_{R-R} = A_u = \frac{1}{n}\sum_{u=1}^{n} T_{uv},$$

where T_{uv} is travel cost from retail unit *u* to retail unit *v*. The clustering indicator of the retail unit *u* is then defined as

$$C_u = c_t A_u,$$

where c_t is the coefficient which controls the magnitude of clustering for each retail type. The effect of the size of each retail unit is defined as

$$R_u = s_t S_u,$$

where s_t is the coefficient depending on the unit type and S_u is size of the retail unit. Similarly the accessibility for a household in segment *i* to retail unit in segment *j* can be formulated as follows:

$$Acc_{Hh-R} = A_{ij} = t_t T_{ij},$$

where t_t is the coefficient depending on unit type and T_{ij} is travel cost from segment *i* to segment *j*. Finally, these can be combined into the utility function. The utility of a household in segment *i* for retail unit *u* in segment *j* is defined as

$$U_u = \frac{C_u R_u}{A_{ij}},$$

New retail units generated at the end of every simulation cycle are located on the basis of network level accessibility within a given radius *R*. The network accessibility measure for each segment *i* is defined as

$$Acc_{Network} = A_i = \frac{1}{n}\sum_{i=0}^{n} T_{ij} \quad (i,j \in R),$$

where T_{ij} is the travel cost from segment *i* to segment *j*.

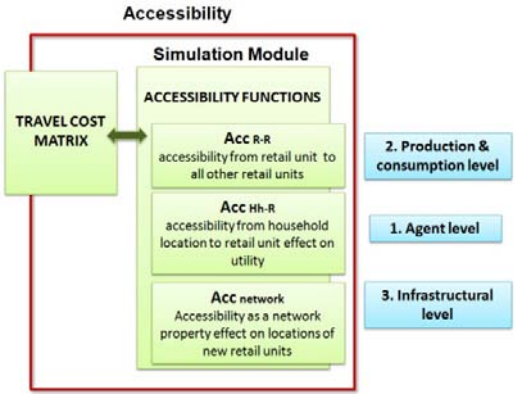

Figure 2. Accessibility in the simulation module.

3.1. Case study and data

The case study has been executed on the Helsinki City region in Finland. The model currently uses the Census database of households. The original database includes the number of households (three income brackets) in grid format. The model also utilises a company register database which includes the classification of companies in the area according to company size and branches. The retail typology is derived from a classification based on the national version of the Statistical Classification of Economic Activities in the European Community, NASE Rev.2. Both of these data sets are combined with the topologically intact network data set (Mapinfo tab file format).

At the more general level, the urban environment is represented in this study as a set of discrete spaces including information relating one discrete space to every other discrete space. This representation can also be defined as a generalised travel cost matrix. The simulation presented here has been undertaken by using the travel cost matrix, which is based on a topological road network structure where one road segment corresponds to one discrete space, but the model structure also allows the travel cost matrix to be based on any other relevant transportation means or spatial entities, e.g. public transportation or lots.

4. EXPECTED RESULTS

The research increases knowledge about the relationship of retail dynamics and the structural properties of urban physical environment, e.g. the configuration of road

networks. The simulation model will produce a series of different development paths of the spatial self-organisation of retail units. The model will eventually succeed in showing how the typological combinations develop with certain given conditions, but so far the variation of parameter combinations that has been tested is incomplete. Future work for the model (until the end of 2012) concentrates on a more extensive coverage of parameter combinations and on the development of the calibration process. The model enables the observation of factors behind location choice in the retail sector that take into account consumers' shopping strategies as dependent on urban structure. Thus, it enables observation of how the distribution of retail units emerges from individual agents' decisions.

The following series of maps and attached animation (34.gif) represent examples of a 40 step simulation cycle from the test phase of the model development (Figure 3). The simulation has been undertaken with a simplified retail unit typology which includes three daily and specialty units of different sizes. From these simulation cycles can be extracted the spatial distribution of each type separately and also the total number of each type of unit, as shown in the figure. One of the next development steps for the simulation software is the module that calculates the total amount of shopping trips. This information has a close relationship to energy consumption and thus it is an important topic in the evaluation of sustainability issues.

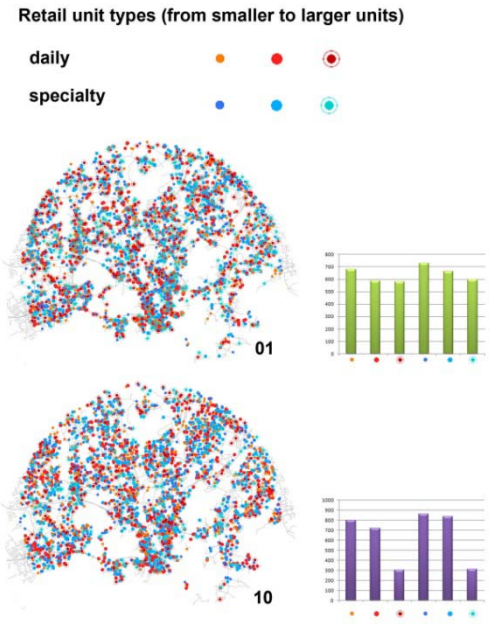

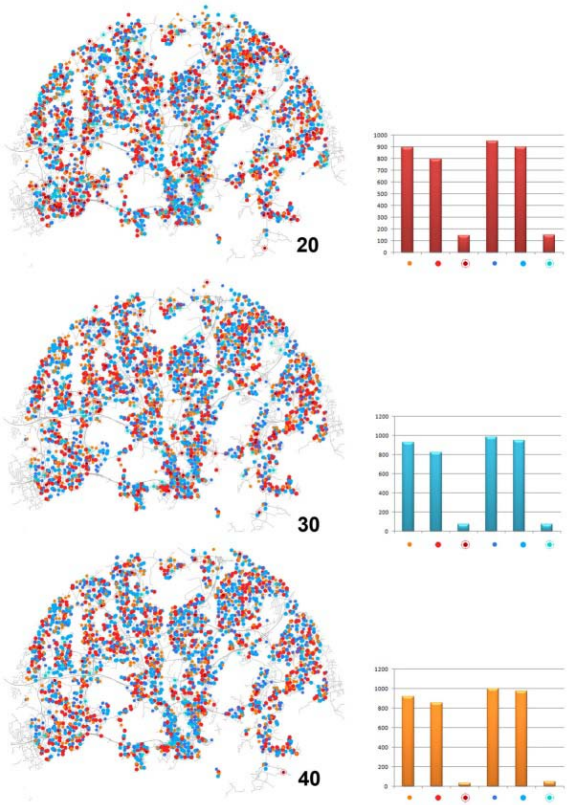

Figure 3. Example of simulation cycles from the test phase of the model development.

References

ALLEN, P.M., SANGLIER, M. 1981. Urban Evolution, Self-Organization, and Decision Making. Environment and Planning A vol. 13. no 2, pp167-183.

BATTY, M. 1976. Urban Modelling: Algorithms, Calibrations, Predictions. Cambridge: Cambridge University Press.

BATTY, M. 2005. Cities and Complexity. Understanding Cities with Cellular Automata, Agent-Based Models, and Fractals. Cambridge, MA.: The MIT Press.

DUPUY, G. 1991. L'Urbanisme des Réseaux – Théories et Méthodes. Paris: Armand Colin Editeur,.

JACOBS, J. 1969. The Economies of Cities. New York: Vintage.

SHELLING, T.C. 1978. Micromotives and Macrobehavior. Toronto, Canada: George J. McLeod Ltd.

WILSON, A.G., BENNETT, R.J. 1985. Mathematical Methods in Human Geography and Planning. London: John Wiley & Sons.

Automatic Building Design with Genetic Algorithms and Artificial Neural Networks

Negin Behboudi[1], Fouad Butt[2], Abdolreza Abhari[3]

[1]Ryerson University
350 Victoria Street,
Toronto, Ontario, Canada, M5B 2G9
negin.behboudi@ryerson.ca

[2]Ryerson University
350 Victoria Street,
Toronto, Ontario, Canada, M5B 2G9
f2butt@ryerson.ca

[3]Ryerson University
350 Victoria Street,
Toronto, Ontario, Canada, M5B 2G9
aabhari@scs.ryerson.ca

Keywords: thermal comfort, wireless sensor networks, genetic algorithms, neural networks, building design

Abstract

It is our goal to develop an automatic system that employs soft computing techniques to automate the design process of a building. Neural networks replace simulation processes. Structural characteristics, occupant behavior and also external factors influence the thermal comfort level perceived by the occupants of a building. Conflicting design objectives of thermal comfort, structural properties and cost form a complex search space of design solutions highlighting the utility of multi-objective genetic algorithms as an attractive technique for searching the solution space.

1. INTRODUCTION

Thermal comfort in buildings is an important factor since human beings spend most of their time inside buildings. A survey with more than 10,000 participants in USA and Canada reveals that people spend 90% of their time indoors even during the summer and only 2-4% of their time outdoors during the winter (J.A. Leech et al. 2000).

The design process of a building involves, to a degree, some trial and error and an artistic license. Numerous visual arrangements may be formed for structural objects with several material characteristics. In addition, the structural nature of a building is also limited by conflicting objectives. Thermal comfort forms one objective of designing a building. Material cost and time constraints and the type of materials that are available also limit the types of structures that may be developed.

Increasing automation in the design process while accounting for thermal comfort levels and cost constraints would prove especially useful in the industry and this is the main objective of our work. As a result of our work, the end product will be a tool that will receive structural, thermal comfort and cost data from the user and present design solutions that fit within their requirements.

The primary stage in achieving our objective involves data collection related to the thermal comfort of a building. This data will form the knowledge required by artificial neural networks (ANNs) to learn the relationship between thermal comfort and structural properties of a building. Software development of the automatic building design system will follow the data collection process. The process of automatic building design is explained in more detail in Section 5.

2. RELATED WORK

2.1. Thermal comfort

There is a large body of work related to thermal comfort and how to determine thermal comfort temperature in various settings. Studies have been carried out in different countries. A survey conducted in naturally ventilated buildings in five cities in Pakistan shows the relationship between indoor comfort and outdoor conditions that are in line with an adaptive approach to thermal comfort (J.F. Nicol et al. 1999).

Predicted Mean Vote (PMV) is an index ranging from +3 to -3 (Fanger 1970). In their work, PMV has been used as the comfort index and indicates the satisfaction of the thermal comfort which is identified by six thermal variables: human activity level, clothing insulation, mean radiant temperature, humidity, air temperature and velocity of indoor air (Atthajariyaku and Leephakpreeda 2004).

2.2. Genetic algorithms for building design

The conceptual design process of buildings is optimized through the use of genetic algorithms (GAs) by (Rafiq et al. 2003). The system developed by Rafiq et al. permits the exploration of multiple designs with various configurations in terms of construction methods and materials. However, the error function considers only capital expenditure and expected revenue income (2003). Beam-slab layout design is a largely heuristic task with a complex search space and is automated by Nimtawat and Nanakorn by utilizing GAs (2009). Though the optimization by (Rafiq et al. 2003) is unconstrained, wall and slab constraints are applied to the optimization process by (Nimtawat and Nanakorn 2009). The authors solve 5 layout problems, the results of which provide an indication of the utility of GAs for beam-slab layout design.

Wang et al. apply multi-objective genetic algorithms (MOGAs) to develop building designs that are optimized to be environmentally friendly (2006). The authors are able to draw several conclusions related to the types of materials and the shape of floor plans in efficient green building design. Magnier and Haghighat follow a multi-stage approach that combines the utility of ANNs and MOGAs (2010). While Wang et al. explore the trade-off between life-cycle cost and environmental impacts in building design (2006), Magnier and Haghighat instead study the trade-off between thermal comfort and energy consumption (2010).

ANN and GAs for design automation has been studied previously (Magnier and Haghighat 2010; Sedano et al. 2010). In contrast, it is our goal to analyze the relationships between thermal comfort, the structural properties of a building and cost metrics as part of the design process. However, similar to the work by (Magnier and Haghighat 2010), we plan to employ ANNs to reduce the time required to simulate the performance of unit structures. The unit structures are then manipulated by GAs to explore design possibilities of larger structures that match the requirements for thermal comfort as well as any cost metrics.

To validate the simulation results produced by the ANNs in our work, the primary stage of the research process involves data collection. Thus, data is collected using a Wireless Sensor Network (WSN) with 9 sensors.

3. WSN NODE CONFIGURATIONS

Data collection was performed on the 4th floor of an educational building. Construction of the building was completed in the mid-1970s.

The WSN consists of multiple node locations as indicated in Figure 1. Node locations and nodes will be used interchangeably. Each node location consists of one or more physically separate sensors. Three types of sensors were utilized: air velocity, humidity and temperature. The process of data collection was divided into two distinct time periods: Phase 1 and Phase 2. Two phases are used as it was noted in the first phase that the measured quantities do not vary greatly within small areas and sensors may be dispersed further apart. Thus, each phase is further distinguished by the number of sensors at node locations in that phase.

In the first data collection phase (Phase 1), WSN nodes, each consisting of one or more sensors, are placed in different regions of the southern and eastern hallways. In this phase, 3 sensors are placed at node location E; 3 sensors are placed at node location G; and, 2 sensors are placed at node location H.

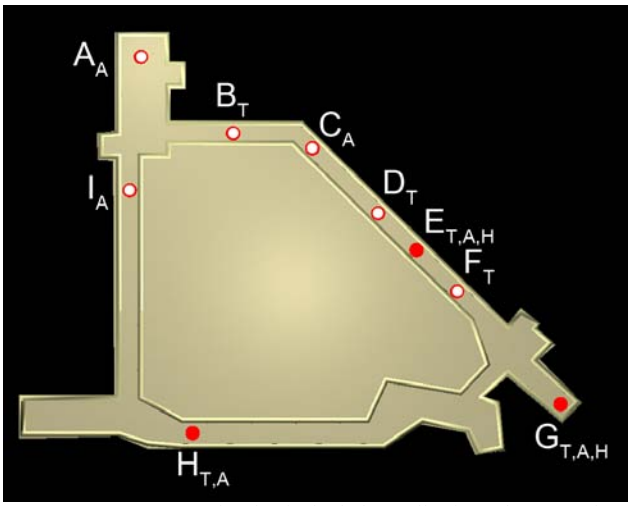

Figure 1. Arrangement of nodes for both data collections phases. Nodes from Phase 1 are shown as filled circles and nodes from Phase 2 are shown as hollow circles. Subscripts beneath each node location indicate the type of sensors at that node location. *A*-air velocity; *H*-humidity; *T*-temperature.

In the second data collection phase (Phase 2), the WSN nodes are dispersed across the northern and western hallways. In this phase, each node location consists of only 1 sensor. The type of sensor at each node location in both Phase 1 and Phase 2 is depicted in Figure 1.

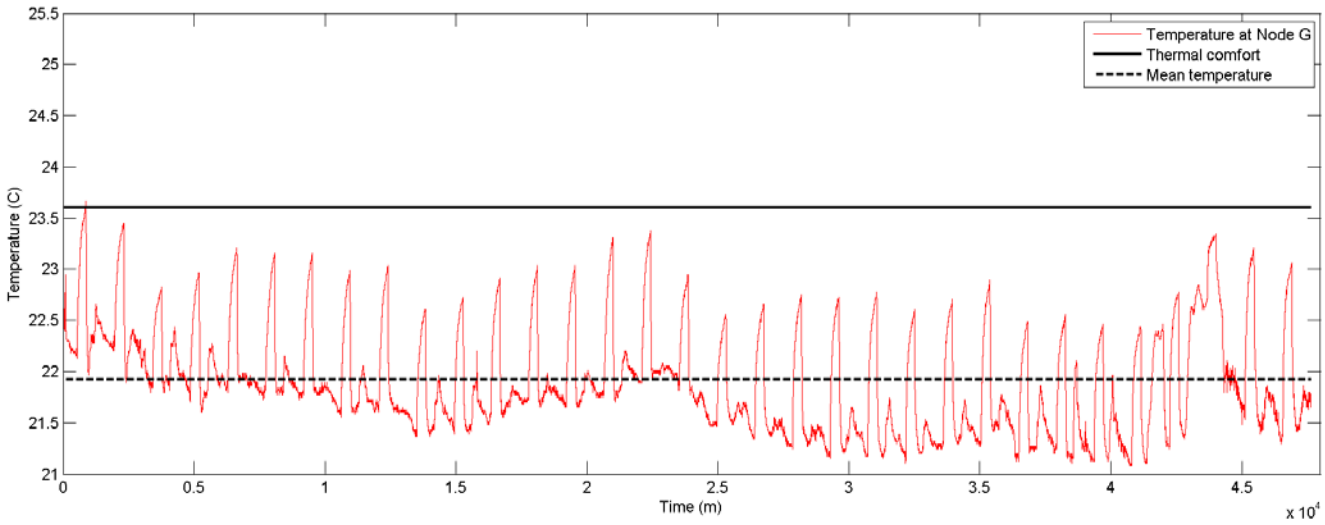

Figure 2. Temperature (red), thermal comfort (black) and mean temperature (black dotted) data collected over approximately 32 days or 1 month at node G.

Data from both data collection phases encompasses the fourth floor of the educational building. The total area covered is approximately 3144 m^2 or 33846 ft^2. For simplicity in modeling in the future, only corridors are used for quantitative measurements. A 3D visualization of the floor and quantities is available (http://www.scs.ryerson.ca/~aabhari/).

4 TEMPERATURE AND THERMAL COMFORT

We evaluate whether the floor is comfortable based on the model by Humphreys and Nicol (1998), which requires only mean indoor and outdoor temperature. Figure 2 presents the temperature, thermal comfort and mean temperature for node location G.

We evaluate the thermal comfort level of the floor to ensure that it matches the expected value. Table 1 presents the mean and standard deviation of the collected data at node locations E, G and H.

Table 1: Descriptive statistics for data collected from nodes in Phase 1.

Air Velocity (m/s)			
	E	*G*	*H*
Mean	0.226	0.15	0.196
Stdev	0.29	0	0.014
Temperature (°C)			
	E	*G*	*H*
Mean	22.738	21.93	23.467
Stdev	0.292	0.61	0.58
Humidity (%)			
	E	*G*	*H*
Mean	58.39	63.779	N/A
Stdev	6.284	7.849	N/A

We focus only on air temperature and how it relates to thermal comfort. The average indoor temperatures are compared to the model by Humphreys and Nicol, which accounts for the outdoor air temperature to define the thermal comfort level for the indoor environment of a building with heating and cooling. The authors define the following equation (1998):

$$T_{chn} = 23.9 + 0.295(T_{ave} - 22)e^{([-\frac{T_{ave}-22}{33.941}]^2)} \quad (1)$$

T_{chn} is the thermal comfort level, T_{ave} is the average outdoor mean temperature for one month. The mean outdoor temperature for August, 2011 was 21.3 °C (Climate Data Online, 2012). The thermal comfort level defined by Equation (1) for the month of August, 2011 is thus 23.6°C. The difference between the mean indoor temperature and the thermal comfort level indicated by Equation (1) is 23.6°C - 22.7°C = 0.9°C. It may thus be concluded that the thermal comfort level of the floor is within the expected range according to the metric by Humphreys and Nicol (1998).

5 AUTOMATIC BUILDING DESIGN

The data collected in this work is a preliminary examination of the thermal dynamics of an educational building. The variables of air velocity, humidity and temperature are only partially responsible for the level of thermal comfort experienced by the occupants. Mean radiant temperature, the behaviour and the number of occupants inside the building also contribute to the thermal comfort level of a building (Fanger 1970). We are currently

exploring possibilities for collecting data related to these other variables that affect thermal comfort. In the future, we also plan to include the effects of humidity and air velocity on thermal comfort.

An abstracted view of the automatic building design system is presented in Figure 3. The automatic building design system is initially provided with actual physical data that was collected in the form of structural properties and thermal dynamics of a building. The structural properties form the inputs to an ANN, while the outputs are the thermal dynamics. With a varied dataset, the ANN learns the relationship between the structural properties and the thermal dynamics of small structural units. In this manner, the ANN replaces Computational Fluid Dynamics (CFD) simulations as it is noted that such simulations can be time-consuming (Magnier and Haghighat 2010; Sedano et al. 2010).

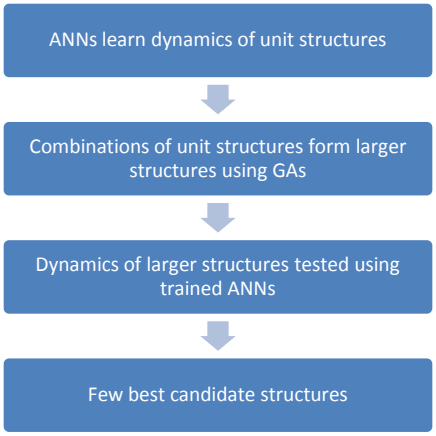

Figure 3. General view of the automatic building design system computation process.

The smaller structural units or compartments may be arranged in numerous ways to form the design of a building. To search this complex solution space of combinations of structural units, GAs are utilized. Every combination of smaller structural units must be evaluated for its fitness. The fitness evaluation is performed using ANNs, which have learned the relationship between the structural characteristics and thermal dynamics of smaller units. In the end, the user is presented with a few best candidate solutions for building designs.

A key question we aim to address with our research is: given the thermal dynamics and structural characteristics of several buildings, can an automatic system propose usable structural designs that also meet design requirements? This raises several other questions, which will form the body of work for our future research efforts.

Acknowledgements

The authors would like to express their gratitude to the Natural Sciences and Engineering Research Council of Canada for the financial support. We also would like to thank the industrial partner of this work, AutoDesk Canada Inc., for providing technical support.

References

Humphreys, M., Nicol, J.: 1998, Understanding the Adaptive Approach to Thermal Comfort, ASHRAE Trans.

J.A. Leech, R. Burnett, W. Nelson, S.D. Aaron, A. Raizenne: 2000, Outdoor air pollution epidemiologic studies, American journal of Respiration and Critical Care Medicine 161 (3) (2000) A308.

J.F. Nicol, A.R. Iftikhar, A. Arif, J. Gul Najam: 1999, Climatic variations in comfortable temperatures: the Pakistan projects, Energy and Buildings 30 (1999) 261–279.

Magnier, L. and Haghighat, F. Multiobjective optimization of building design using trnsys simulations, genetic algorithm, and artificial neural network. Building and Environment, 45(3):739-746, 2010.

Mayer, E.: 1993, Objective criteria for thermal comfort, building and Environment 28 (4) 399-403.

Nimtawat, A. and Nanakorn, P. Automated layout design of beam-slab floors using a genetic algorithm. Computers and Structures, 87(21-22):1308-1330, 2009.

P.O. Fanger: 1970, Thermal Comfort: Analysis and Applications in Environmental Engineering, McGraw-Hill, New York.

Rafiq, M. Y.; Mathews, J. D., and Bullock, G. N. Conceptual building design evolutionary approach. Journal of Computing in Civil Engineering, 17(3):150-158, 2003.

Sedano, Javier; Curiel, Leticia; Corchado, Emilio; de la Cal, Enrique, and Villar, José R. A soft computing method for detecting lifetime building thermal insulation failures. Integr. Comput.-Aided Eng., 17:103-115, April 2010. ISSN 1069-2509.

Wang, W.; Rivard, H., and Zmeureanu, R. Floor shape optimization for green building design. Advanced Engineering Informatics, 20(4):363-378, 2006.

Wang Z. A: 2006, Field study of the thermal comfort in residential buildings in Harbin.Building and Environment ;41:1034–9.

Climate Data Online. http://climate.weatheroffice.gc.ca/climateData/canada_e.html, 2012. [Online; accessed 19-January-2012].

Visualization Framework of Thermal Comfort for Architects

Pascal Goffin, Arno Schlueter

Architecture and Sustainable Building Technologies
ETH Zürich
Schafmattstrasse 32,
Zurich, Switzerland, 8093
pascal.goffin@arch.ethz.ch, schlueter@arch.ethz.ch

Keywords: Visualization, Thermal comfort, Building energy simulation, Architecture, Information visualization.

Abstract

For a successful integration of building energy simulation tools into the architectural workflow there is a need for better communication of the information obtained through simulation. One appropriate way of communicating that information to the technically experienced architect is by using appropriate visualization techniques. A problem-driven approach is employed to create visualizations to support sustainable building design. Currently, there is a lack of appropriate visualization in the field of thermal comfort and is therefore investigated herein. By using methods from information visualization, a better understanding of thermal comfort in buildings can be provided allowing a more user-friendly decision making process at an early design stage. The proposed approach follows the guidelines of the information visualization mantra. It proposes starting with an overview and then through interaction techniques like zooming and filtering more levels of information are presented.

1. INTRODUCTION

In recent years there have been many papers describing algorithms and models to create faster and more accurate building energy simulations. These simulations produce a wealth of information. However, not much research has been done to provide an understanding of the resulting data for people that would benefit the most from that information such as technically experienced architects.

Thus, our research focuses on the visualization of simulation data at an early stage in the design process. At this point, the most significant impact on the design at a low cost is still possible (DGNB 2009). The better the decision support and the more available information the easier it will be to make the most appropriate decision (Clarke 2001). In addition to design support, visualizations are beneficial to communicate design ideas as well as building performance information.

Currently thermal comfort visualizations, like Autodesk Ecotect Analysis, consist of graphs (bar charts, line graphs) depicting different quantities like the zone temperature. Additionally, basic coloring of the floor with the zone temperature is proposed. Unfortunately, there is no visual or interactive linking between the various factors, which leads to context switches for the user. One potential solution is to combine all this information into one view and augment it with interaction techniques like *brushing* to navigate the data in an easy way (Roberts 2007). An improvement is Autodesk Simulation CFD, which computes thermal comfort measures: Mean Radiation Temperature, Predicted Mean Vote, and Predicted Percentage of Dissatisfaction (Figure 1). The 3D visualizations from these products are compelling, but they do not inherently communicate cause-and-effect. In contrast, 2D visualizations have the advantage of potentially showing all data in a static state and to easily compare multiple data sets for design iteration.

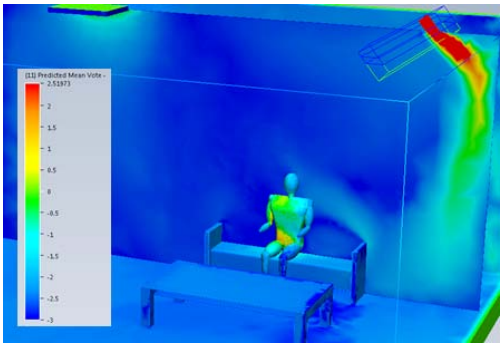

Figure 1. Autodesk Simulation CFD visualization of thermal comfort.

Our interest lies in sustainable building design by means of investigating novel visualization methods with an emphasis on the visualization of comfort. The definition of comfort comprises different factors such as air quality, acoustics or noise level, optical factors e.g. availability of day lighting, glare, and thermal comfort (Fanger 1970). Within this range, the visualization system focuses on thermal comfort, which is defined by the building envelope and by building systems that maintain the indoor climate of the building (Bauer et al. 2007). The link between thermal comfort and building systems is particularly interesting as improvements to the systems can have a significant impact on the sustainability of the building design.

A spectrum of approaches is available to the researcher to tackle the challenge of data visualization. Within this scope, a problem-driven approach has been employed, which focuses on investigating a domain together with domain experts and hence, developing visualization systems regarding their demand of complex and exploratory data analysis tasks (Meyer 2011). Problem-driven approaches have already been used successfully for visualization in other fields of research, especially in biology (Meyer et al. 2010). This approach can be divided into four nested levels, in which each level has distinct evaluation methodologies: (1) characterizing the task and data in the vocabulary of the problem domain, (2) abstracting it into operations and data types, (3) designing visual encoding and interaction techniques, and (4) creating algorithms to execute these techniques efficiently (Munzner 2009; Meyer 2011).

For architects, thermal comfort is defined by standards and regulations. Humans depending on age, gender, cultural background, clothes etc. sense thermal comfort differently. This means the guidelines cannot be defined by simply specifying a specific temperature as comfortable which has to be maintained to satisfy thermal comfort in a given space. Fanger introduced the Predicted Percentage of Dissatisfied (PPD) (Fanger 1970) which defined thermal comfort through statistics. With the PPD, we can define that a room for example is considered comfortable if the PPD < 20%. This introduces a range of temperatures where around 80% of the inhabitants will be satisfied with the thermal comfort (ASHRAE Standard 55 2004). In this context we investigate radiation asymmetry as one factor of thermal comfort for which the PPD < 20% provides the range of comfortable temperatures. As range limits we took 17°C for the lower limit and 31°C for the upper limit (Peeters et al. 2009).

2. VISUALIZATION FRAMEWORK

The proposed visualization system aims for an at-a-glance visualization of thermal comfort in a building. It is supposed to facilitate the identification of zones and surfaces perceived as comfortable or uncomfortable. In addition, it should provide a better understanding of the factors that influence thermal comfort in a specific building. The designer should be able to identify cause-and-effect using interactive visualization, which is not only presenting the data but also means being able to interact with the data (Card et al. 1999). Our work is based on the well-known design principle called the *information visualization mantra*: first, an overview is provided, then by means of zooming and filtering, the tools to navigate through the data are provided. Finally, the details are shown on demand (Shneiderman 1996).

The data to be visualized comprises different time and spatial scales. The information embedded at each of these scales is critical for the process of understanding what is happening in the building in terms of thermal comfort and has to be communicated to the user in an appropriate way. High-resolution data of building elements, systems and spatial conditions originates from a building energy simulation. To investigate thermal comfort related to radiation asymmetry, only temperature values of exterior surfaces over time (at hourly intervals) are considered.

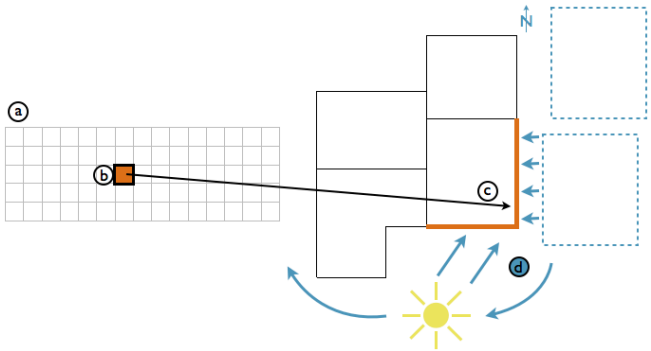

Figure 2. a) Overview **b)** When does it feel uncomfortable? **c)** Where does it feel uncomfortable? **d)** Why does it feel uncomfortable?

We first identify the types of tasks the system needs to support (Munzner 2009). These tasks can be summarized as:

1) identifying zones of discomfort (a),
2) identifying time points/periods of discomfort (b),
3) identifying the spatial location of discomfort (c),
4) identifying the causes of discomfort (d).

The first task (Figure 2a) is to provide an overview of the data with an at-a-glance view of thermal comfort in the building. The identified zones of thermal discomfort also show where improvements to the building concept are necessary. An appropriate visual encoding for this task is a heatmap (Wilkinson and Friendly 2009). The benefit of a heatmap is to be able to visually encode quantitative data with color using an area mark (Bertin 1976; Mackinlay 1986). It provides a high information density in an easy to understand compact overview. Basically it is a matrix (Figure 3) where each row describes the temporal change of a thermal comfort metric for a building element e.g. wall, floor or roof. Each column describes a specific time point/period. This means a cell describes a thermal comfort metric for a specific point/range in time for a specific building element. Each area mark is color coded with green, red or blue. Green encodes comfortable temperatures while an uncomfortable state is shown in red (temperature too high) and blue (temperature too low).

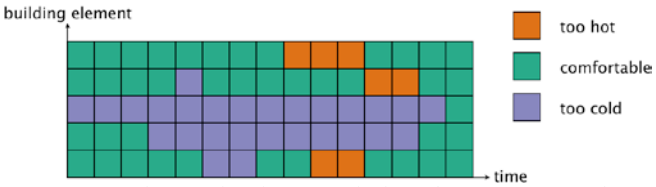

Figure 3. Overview matrix using a quantitative colormap (Brewer and Harrower 2010).

To support the identification of time points/periods of discomfort (Figure 2b), there is a need to switch from an overview to a more detailed information view. The aim is to navigate through different time scales in an easy and intuitive manner. For this purpose abstraction methods have to be employed to provide a summary of the information at this specific spatial and temporal location and from which a zoom into more information is possible. Hence, a metric is required. This metric will describe comfort in time and space. Currently we are investigating two directions for this metric: visualization methods and statistical methods. The visualization method tries to represent the information for a higher level (e.g. day) by using the visualization of the lower level (e.g. hours) at a higher density. The statistical methods deal with the analysis of attributes in association with spatial location (Slocum et al. 2010).

After identifying a point/period in time when it is uncomfortable, the next task (Figure 2c) is to find out where in the building the discomfort arises. For this purpose a link from the overview/time filtering view to a spatial localization view is required. This link provides possible indications for the causes of the thermal discomfort. Currently, the visual encoding of the spatial localization of thermal comfort is investigated by using 2D and 3D views and their combination. The decision to use 2D or 3D visualizations is based on the task we want to fulfill. For example for spatial localization the most promising result seems to be a 2D only view as a variety of studies and formal user studies have demonstrated that 2D data encoding and representation are generally more effective than 3D ones for tasks involving spatial memory, spatial identification, and precision (Borkin 2011).

After localizing discomfort in time and space the last task (Figure 2d) is to find reason(s) for the discomfort. To understand the complete picture, the gathered information about spatial and temporal location is not comprehensive enough. Additional information is needed to make a sound decision, for example the topology of the neighborhood or information about the sun and the subsequent solar gains in the building, but also the employed building components and systems need to be known. This information will have to be provided through additional 2D or 3D visualizations and is a topic of ongoing research. As cause-and-effect becomes more complex, the supporting visualization will likely also become more complex.

3. CONCLUSION AND OUTLOOK

The four tasks presented in the previous section form the backbone of the concept for the visualization of thermal comfort of a building. The visualizations are currently being designed and implemented (Figure 4) using the Processing programming language. As part of future research, the addition of the remaining parts that constitute comfort to provide a consistent visualization framework is intended.

We strongly believe that providing better means of comfort visualization supports the creation of sustainable architecture. The use of such a visualization system can be envisioned for architects that integrate sustainable building systems into their design concepts. We also see a potential and practical use for such a system for building retrofitting. Older buildings often require large amounts of energy to provide thermal comfort for their inhabitants.

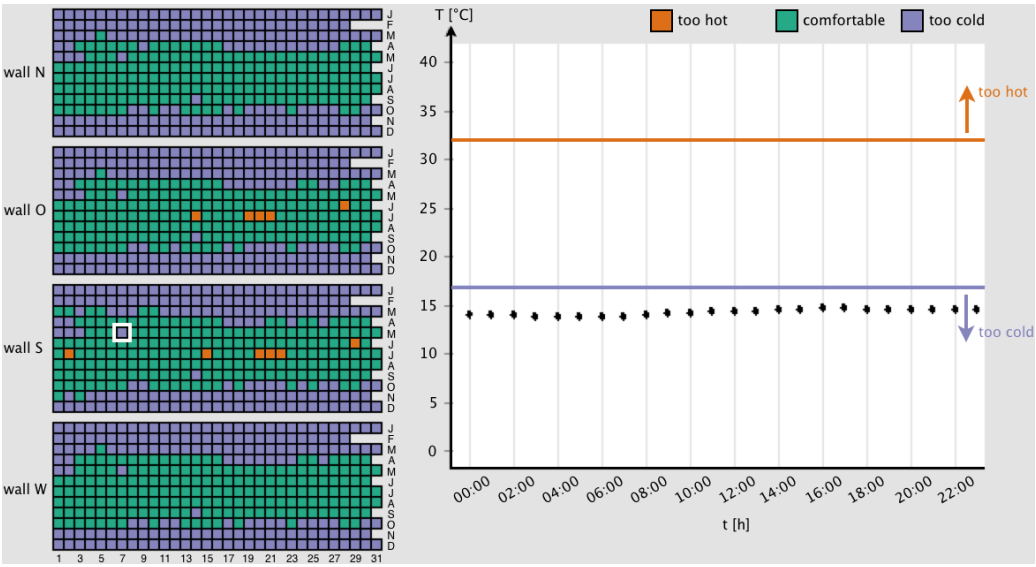

Figure 4. Mockup of current prototype with quantitative colormap (Brewer and Harrower 2010), white rectangle is the selected day for graph on the right.

References

ASHRAE Standard 55. 2004. Thermal Environmental Conditions for Human Occupancy. American Society of Heating, Refrigerating, and Air-Conditioning Engineers.

Bauer, M., Mösle, P., and Schwarz, M. 2007. Green Building: Konzepte für nachhaltige Architektur. Callwey.

Bertin, J. 1976. Sémiologie Graphique: Les diagrammes – Les réseaux – Les cartes. Reissued by Editions de L'Ecole des Hautes Etudes en Sciences 1999.

Borkin, M., Gajos, K., Peters, A., Mitsouras, D., Melchionna, S., Rybicki, F., Feldman, C., Pfister, H. 2011. Evaluation of Artery Visualization for Heart Disease Diagnosis. IEEE Transactions on Visualization and Computer Graphics. 17 (12). 2479-2488.

Brewer, C., and Harrower, M. 2010. ColorBrewer 2.0: color advice for cartography. http://colorbrewer2.org/.

Card, S., Mackinlay, J., and Shneiderman, B. 1999. Readings in Information Visualization: Using Vision to Think. Morgan Kaufmann Publishers Inc.

Clarke, J.A. 2001. Energy Simulation in Building Design. Butterworth-Heinemann.

Deutsche Gesellschaft für Nachhaltiges Bauen e.V. (Hrsg.). 2009. DGNB Handbuch: Neubau Büro- und Verwaltungsgebäude. Kohlhammer Druck.

Fanger, P.O. 1970. Thermal Comfort: Analysis and Applications in Environmental Engineering. Danish Technical Press.

Mackinlay, J. 1986. Automating the Design of Graphical Presentations of Relational Information. ACM Transcriptions on Graphics. 5 (2). 110-141.

Meyer, M., Wong, B., Styczynski, M., Munzner, T., Pfister, H. 2010. Pathline: A Tool for Comparative Functional Genomics. Computer Graphics Forum. 29 (3). 1043-1052.

Meyer, M. 2011. Workshop: Problem-Driven Visualization. Research Dagstuhl Seminar on Scientific Visualization.

Munzner, T. 2009. A Nested Model for Visualization Design and Validation. IEEE Transactions on Visualization and Computer Graphics. 15 (6). 921-928.

Peeters, L., de Dear, R., Hensen, J., D'haeseleer, W. 2009. Thermal comfort in residential buildings: comfort values and scales for building energy simulation. Applied Energy. 86. 772-780.

Roberts, J. 2007. State of the art: Coordinated & multiple views in exploratory visualization. In Proc. Coordinated & Multiple Views in Exploratory Visualization. 61-71.

Shneiderman, B. 1996. The Eyes Have It: A Task by Data Type Taxonomy of Information Visualization. Proceedings of the IEEE Symposium on Visual Languages. 336-343.

Slocum, T., McMaster, R., Kessler, F., and Howard, H. 2010. Thematic Cartography and Geovisualization. Pearson Education International.

Wilkinson, L., and Friendly, M. 2009. The History of the Cluster Heat Map. The American Statistician. 63. 179-184.

Experimental Validation of Simulation Software for Daylight Evaluation in Street Canyons

Manolis Patriarche[1], Dominique Dumortier[2]

[1]KiloWattsol
14 rue Rhin et Danube,
Lyon, France, 69009
mpatriarche@kilowattsol.com

[2]DGCB LASH-ENTPE
Université de Lyon, 3 rue Maurice Audin,
Vaulx-en-Velin, France, 69120
dominique.dumortier@entpe.fr

Keywords: street canyon, daylight, simulation, experimental validation.

Abstract

New tools for the evaluation of daylight availability at the urban scale have been recently developed. This paper describes a methodology to assess the accuracy of three of them: Citysim, Daysim and Heliodon. We designed a moveable scale model representing an idealized street canyon. The geometry of the canyon and the materials used for the facades can easily be changed. Illuminance sensors have been placed on the facades and on the ground in the middle section of the canyon. The model is located on the roof of our laboratory. Measured illuminances for various combinations of canyon geometry, orientation, façade reflection factors and sky types will be compared to illuminances computed by each simulation tool for the same combination of parameters using data collected from an onsite daylight measuring station as input weather file. At the end of the project, we will be able to provide recommendations regarding the accuracy of these three simulation tools.

1. INTRODUCTION

Half the world's population now lives in cities, urban areas are getting bigger and denser which implies reduced access to daylight and solar radiation (UN-DESA 2010). The impact of urban topology on daylight availability has to be evaluated.

The process of shortwave radiation exchange between surfaces is well known and has been applied to urban context (Verseghy and Munro 1989; Arnfield 1982). A canyon is the simplest representation of a street; mathematical calculation methods provide precise calculations for this configuration, however since they deal with idealized geometry, the results are not accurate. Indicators to quantify the obstruction to the sky from a given point of a street have been defined and compared allowing a better consideration of the geometry (Robinson 2006). The progress in computing power has contributed to the emergence of new tools like ray tracing programs that perform calculations for any given 3D geometry. For instance, RADIANCE has been widely used for radiation budget of indoor and outdoor use (Reinhart and Herkel 2000; Compagnon 2004). Studies have highlighted the impact of urban fabric on the solar potential of buildings and provided recommendations on city layout (Cheng et al. 2006; Littlefair 1998). However, little or no consideration was given to existing building surface materials regarding their impact on the overall street daylight availability.

The amount of daylight available in a street canyon has an impact on building energy consumption and human comfort. A darker street will induce an increased use of artificial lights in the adjacent building. A lighter façade exposed to the sun will induce an increased use of shading devices to protect building occupants against glare. The key parameters which should be taken into account are the street canyon geometry, its façades' reflection properties and the site sky conditions.

Citysim, Daysim and Heliodon are simulation tools that can calculate illuminances at given points for any 3D geometry with consideration of site parameters and climate using different degrees of complexity (Robinson 2009; Reinhart and Walkenhorst 2001; Beckers et al. 2007). With these tools, it is possible to evaluate the influence of the key parameters on the amount of daylight available in a street canyon.

The final objective of our study is to assess the accuracy of the results produced by these three simulation tools. We have chosen to do this by means of comparison between illuminances computed by each individual tool and illuminances measured on a moveable scale model placed under real sky conditions. In this paper, we present the methodology which will be used. We particularly focus on the experimental set-up since the measurement campaign will not be completed before June 2012.

2. METHODOLOGY

The chosen parameters correspond to typical street canyons of Lyons. In this study, a street canyon is defined as two fronts of aligned buildings facing each other between two crossroads. Buildings have the same height and the same coating.

2.1. Experimental set-up

The scale model has been designed to be moveable. The Height to Width ratio can be changed for any value between 0.25 and 10. For this study we used three H/W: 0.5, 1 and 1.5, because they are typical in French cities. The street canyon can be orientated along a north/south or east/west axis.

The façades of the street canyon are made of wooden boards fixed on an aluminium profile structure; every material is treated to be weather resistant. The model represents a 2 meter long idealized street canyon in 1:50 scale, each façade is 40cm height by 28cm width. The ground is painted in black with a measured albedo of 0.2. The aluminium parts of the grounds are also painted in mat black to avoid specular contribution of light coming from the structure (Figure 1).

There are 4 sets of façades: (1) black and (2) white façades leading respectively to the lowest and the highest contribution by diffuse reflections, (3) beige roughcast façades with reflection properties between black and white, (4) beige roughcast and glass façades similar to real façades with strips of rectangular windows. These are made of glass, glued on black paint and partially covered with the beige roughcast coating.

There are 7 façades on each building front. Most street canyons of Lyons have 6 buildings but an odd number was chosen to measure values at the center of the middle façade. Hence, 13 Licor LI210 illuminance sensors are placed in the middle section of the canyon: 6 on each façade and 1 on the ground. Each sensor stands for a storey. Thus for a 20m height building each storey is 3.3m height which correlates with the land-use planning of Lyons.

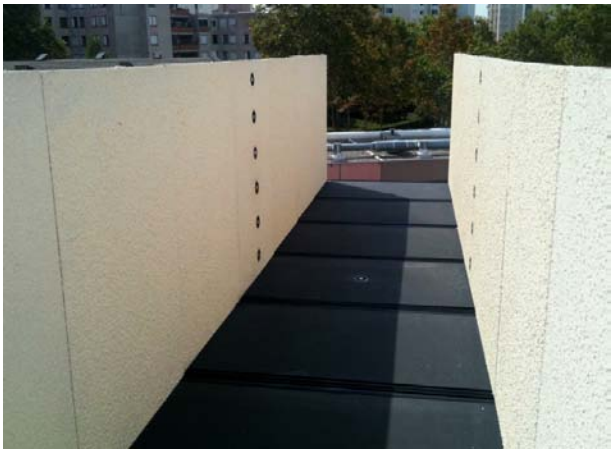

Figure 1. Scale model with roughcast façades.

The scale model has been placed on the roof of our laboratory. It is located in a city surrounded with hills. The buildings and the landscape may hide part of the sky vault and at times shade the sun. This has to be evaluated and taken into account when comparing site measurements with simulation results.

Obstructions are characterized using shading angles. These have been measured using a camera (Canon EOS 50D) with fisheye lens (Sigma, 4.5mm) and placed horizontally and pointing toward the zenith. The fish-eye lens produces an equidistant projection of a hemisphere. Therefore, there is a linear relationship between the view angle of a pixel and its distance to the center of the projection circle. On the image, the line separating the sky vault from buildings, trees, hills, was drawn manually through visual inspection. Then, a computer program was used to compute the shading angles from the line.

The resulting obstruction line has been improved using NASA-SRTM data because of the unreliability of the fisheye lens projection law for large field angles due to geometrical distortion. This database provides global altitudes with a resolution of approximately 90 meters. We created a computer program to represent the terrain seen from a given point. The maximum value of each curve has been taken to represent the sky vault obstruction (Figure 2).

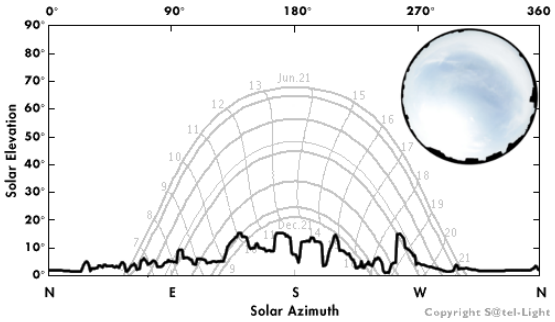

Figure 2. Altitude/Azimuth of the scale model obstructions.

For validation purposes, a calibration factor has been determined for each sensor. Before the installation of the model, sensors were placed on a horizontal plane and measurements were compared to illuminances from the CIE-IDMP station. Therefore a calibration factor has been determined for each sensor to convert measured current to illuminance considering the same reference.

Illuminances are measured every minute from 5am to 11pm using a Licor LI1400 datalogger. Then data are processed to look for any odd results by comparison with data produced by our CIE-IDMP daylight measuring station situated close to the model (IDMP 1991). This station uses a standardized quality control procedure (CIE 1994). Resulting data are displayed on charts and can be imported into spreadsheet applications.

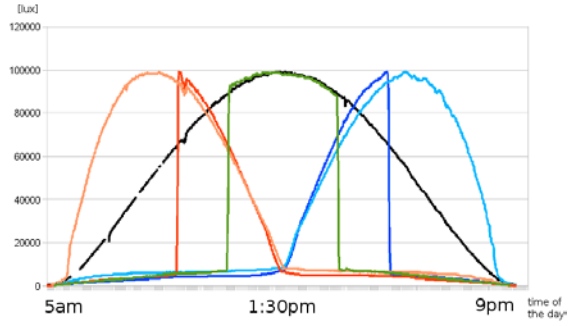

Figure 3. Illuminances in the street canyon under a clear sky.

The data collected by sensors for a specific day (2011, 4th may) is presented (Figure 3). During this day the street canyon had a Height to Width ratio of 1, mat black façades and North/South orientation. The black curve represents the CIE-IDMP global horizontal illuminance, the red and orange curves are illuminances from two sensors located on the western façade, respectively at the lowest and the highest position. The blue and cyan curves are illuminances from the corresponding sensors on the eastern façade. The green curve is shows the values of the sensor located on the ground on the middle of the canyon. A sharp rise occurs when a sensor is no longer shaded or when it becomes shaded by a façade. The diffuse radiation is only about 5000 lux when there is no direct sunlight. This is because black façades avoid multiple reflections that would contribute to higher amount of light. Hence we can see that direct radiation has much more impact than diffuse radiation in this configuration of the street canyon.

For a larger canyon, the time of the day the sharp rise occurs will be different, inducing a longer period of light availability for this geometry. In addition a brighter coating will increase the diffuse contribution inside the street canyon. The expected dataset will allow quantifications of the impacts of such parameter variations.

2.2. Simulation software

Three tools with different levels of complexity were selected for the comparison: Citysim, Daysim and Heliodon. They feature different computational methods, input parameters and interface capabilities (Table 1).

	Citysim	Daysim	Heliodon
CAD	yes	no	yes
Import geometry	kml, dxf, rad	3DS, rif	stl
Weather file	cli	epw	-
Sensor type	surface	point	surface
Results	text	text	text, graph

Table 1: Main features of the three tools used for the comparison.

Citysim and Daysim use the widely used Tregenza sky subdivision together with the Perez sky luminance model to determine direct and diffuse radiation components (Tregenza 1987; Perez et al. 1990). Hence, both take into account the part of sky that is visible from a surface of the scene. Heliodon assumes an isotropic sky and only considers air mass influence for the direct flux. It doesn't take into account any reflection that can occur in the scene. On the opposite, Citysim and Daysim consider diffuse and specular reflections, though the latter also deal with partially specular surfaces.

Since Citysim and Daysim deal with real weather data, we developed a conversion program to create a weather file for each, from the 1 minute measurements of our CIE-IDMP sation. These include direct, diffuse and global

horizontal irradiances as well as global and diffuse horizontal illuminances.

The three simulation tools are able to compute illuminances on any given surface or at any given point. The geometry of the scale model was used in each one. Virtual sensors were placed at the same position as the real ones on the scale model.

2.3. Future comparison

For any given one-minute time slot, illuminances within the canyon will be computed using each tool and compared to the illuminances measured within the scale model. We will use the Perez sky luminance model and the 15 CIE standard sky types to categorize the sky conditions for that given minute (CIE 2004).

Mean bias errors and root mean square errors between computed and measured illuminances will be presented for all sky conditions and specific ones. Differences between orientations, Height to Width ratios and façade coatings will be highlighted. Data collection began during summer 2011; it will last one year in order to cover many different sky conditions and sun altitudes for each of the 24 street canyon configurations (2 orientations, 4 façade coatings, 3 Height to Width ratios).

3. CONCLUSION

The described methodology allows qualitative comparison between the three simulation tools. Recommendations for the use of each one will be done. Depending on the outcomes, designers and researchers will have useful information to decide which software tool is the most relevant for their projects. In addition, the measured illuminances on the scale model will be organized as a dataset available to other researchers.

4. NEXT STEP

The methodology described in this paper considers a scale model of an idealized street canyon as a reference. In order to validate software for more realistic configurations, it is scheduled to measure illuminances in existing streets of Lyons and compare measured values with illuminances modeled by the three simulation tools using the 3D geometry of the same streets. The geometry has already been taken from an existing database generated using recent LIDAR measurements of the city. Measured values of reflection factors for real façades will be assigned to 3D models. We expect the same outcomes, though the complexity of the scene should increase the gap between modeled and measured values.

References

ARNFIELD, A. 1982. An approach to the estimation of the surface radiative properties and radiation budgets of cities. Physical Geography 3(2). 97-122.

BECKERS, B., MASSET, L., ET AL. 2007. Una proyeccion sintetica para el diseño arquitectonico con la luz del sol. Ibero-american Conference of Mechanical Engineering. Cusco.

CHENG, V., STEEMERS, K., ET AL. 2006. Urban form, density and solar potential. PLEA. Geneva.

CIE. 1994. Guide to Recommended Practice of Daylight Measurement. CIE 108-1994.

CIE. 2004. ISO 15469:2004(E)/CIE S 011/E:2003: Joint ISO/CIE Standard: Spatial Distribution of Daylight - CIE Standard General Sky

COMPAGNON, R. 2004. Solar and daylight availability in the urban fabric. Energy and Buildings 36(4). 321-328.

IDMP. 1991. http://idmp.entpe.fr/vaulx/stafr.htm

LITTLEFAIR, P. 1998. Passive solar urban design: ensuring the penetration of solar energy into the city. Renewable and Sustainable Energy Reviews 2(3). 303-326.

PEREZ, R., INEICHEN, P., SEALS, R., MICHALSKY, J., AND STEWART, R. 1990. Modeling daylight availability and irradiance components from direct and global irradiance. Solar Energy. Volume 44, Issue 5. 271-289.

REINHART, C. F., AND HERKEL, S. 2000. The simulation of annual daylight illuminance distributions, a state-of-the-art comparison of six RADIANCE-based methods. Energy and Buildings 32(2). 167-187.

REINHART, C. F., AND WALKENHORST, O. 2001. Validation of dynamic RADIANCE-based daylight simulations for a test office with external blinds. Energy and Buildings 33(7). 683-697.

ROBINSON, D. 2006. Urban morphology and indicators of radiation availability. Solar Energy 80(12). 1643-1648.

ROBINSON, D., HALDI, F., ET AL. 2009. CitySim: Comprehensive micro-simulation of resource flows for sustainable urban planning. IBPSA. Glasgow.

TREGENZA, P.R. 1987. Subdivision of the sky hemisphere for luminance measurements. Lighting Research and Technology. Volume 19, Issue1. 13–14.

UN-DESA, http://esa.un.org/unpd/wup/index.htm

VERSEGHY, D., AND MUNRO, D. 1989. Sensitivity studies on the calculation of the radiation balance of urban surfaces: I Shortwave radiation. Boundary-Layer Meteorology 46(4). 309-331.

A Morpho-Energetic Tool to Model Energy and Density Reasoned City Areas: Methodology (Part I)

L. Arantes[1,2], O. Baverel[1,3], D. Quenard[2], N. Dubus[1]

[1] UR AE&CC, Ecole Nationale Supérieure d'Architecture de Grenoble
60 avenue de Constantine, BP 2636
38036 Grenoble Cedex 2

[2] Centre Scientifique et Technique du Bâtiment (CSTB)
24 rue Joseph Fourier
38400 Saint Martin d'Hères

[3] UR Navier, École des Ponts Paris-Tech, 6-8 avenue Blaise Pascal, Cité Descartes, Champs-sur-Marne
F-77455 Marne-la-Vallée cedex 2

Keywords: Sustainable Cities, Urban Forms, Compactness, Density, Energy Saving, Sunshine, Genetic Algorithm.

Abstract

This paper presents an urban modeling tool that analyzes the morphology of low energy and dense city areas. Even if the link between building form and energy has been established, the correlation is less obvious at the urban scale. The density of grouped buildings introduces a significant new issue for consideration. Maximizing energy production in urban environments requires the minimization of sun shading. The tool we describe in the paper below relates three parameters: density, energy performance and sun penetration. By optimizing population density, the tool proposes to find the optimal building layout in a city area from sun shading and energy performance criteria. The optimization is accomplished with the genetic algorithm tool *Bianca*. Our ultimate goal in the development of the tool is to find the optimal form(s) of a low energy and dense city area.

1. INTRODUCTION

Today, many French urban planners recommend dense and compact cities to suit the imperatives of sustainable development. Typically, this urban morphology is believed to be low energy and land saving. In the last twenty years, many studies showed a link between buildings compactness and heating loads. The more compact a building is, the less its heating needs are. At the urban scale, this "morpho-energetic" relation is less obvious. City forms are complex. Are compact cities really sustainable and low energy? The study we present in this paper follows earlier research, which focused on a simple calculation method to quickly approximate the whole energy balance of residential buildings (Arantes 2010). The energy-balance approach takes into account the entire energy consumption and gain of the residential structure. Energy consumption includes everything from heating to electricity for appliances. In this model, the embodied energy of materials is also included as energy consumption. Active energy production made possible by photovoltaic and thermal panels is also included as an energy gain of the overall system. Here, this simplified energy calculation method is applied at an urban scale, to find the optimal form(s) of a low energy and dense city area. The density of grouped buildings in an urban environment requires that sun penetration must be addressed. Thus the new tool we are developing aims to find the optimal building layout in a city area by correlating the population density with respect to sun shading and energy performance criteria. The optimization is accomplished with the genetic algorithm tool *Bianca* (Vincenti *et al.* 2010). Through the development and application of this tool, we aim to assess the link between city form and energy efficiency.

2. CITY AND ENERGY: LITERATURE REVIEW

Research analyzing link between urban form and energy use has been the topic of many publications. There are three main approaches to investigate the link: through city and transportation energy use, through building energy and urban geometry, and through city and solar production capacity. With respect to city and transportation energy use, an analysis of 32 cities across North America, Asia, Australia and Europe, (Newman and Kenworthy 1988) showed that energy use for fuel is closely tied to urban density. The denser a city is, the higher its fuel consumption is. For instance, dense Asian cities have lower car use and thus lower energy consumption for transport than sprawled American cities. The correlation between density and transport energy has sustained research since 1988 (Gordon and Richardson 1989, Gomez-Ibanez 1991, Kirwan 1992,

Fouchier 1998, Bertaud and Malpezzi 2003). It continues to foster debate (Ménard 2010, O'Brien *et al.* 2010). The impact of urban geometry on building energy consumption is the focus of a second category of research into urban energy efficiency. In 2005, (Ratti *et al.* 2005) suggested that urban geometry creates a twofold variation of building energy consumption. In 2010, (Salat and Nowacki 2010) showed that for lighting and for thermal comfort energy, low-rise urban blocks of traditional European cities are more energy efficient by a factor of at least four than recent Chinese cities with isolated tower blocks. Gradually, research has turned to the development of more complex urban models to analyze correlations between form and energy use. Some researches deal with solar production capacity as it relates to urban forms. Designing cities for solar access is not a new approach. In the twelfth century CE, the Pueblo Indians built their Acoma settlement according to solar access laws. In the settlement terraced houses face south to capture the winter sunlight, and are protected from summer overheating by the roof terraces. In the nineteenth century, (Knowles 1981) referred to the Acoma Pueblo in the development of his *Solar Envelope* concept. In Knowles method a three dimensional volume constrains development within a site to ensure adjacent neighbors have a minimum direct solar access for a specified amount of time per day throughout the year. The *Solar Envelope* has been the topic of many studies (Littlefair 1998, Capeluto and Shaviv 2001, Knowles 2003, Niemasz *et al.* 2011). In 2004, (Robinson and Stone 2004) described three alternative methods to account for sky obstruction and to model solar radiation in the urban context utilizing the ray-tracing program *Radiance*. The analysis of the link between urban form, density and solar potential thus continues to be the subject of study (Cheng *et al.* 2006, Kämpf and Robinson 2010). In describing a tool that aims to model energy and density correlation in urban areas, our paper expands upon this earlier research.

3. OPTIMIZATION PROTOCOL

Our tool uses a genetic algorithm to optimize the layout of buildings within a city area according to energy, density and solar access criteria. Many factors affect city energy consumption including building form, size, and layout. Additionally, sun shading impacts the efficiency of photovoltaic solar panels (Hanitsch 2001). As a result, direct solar access is also a factor in determining overall city energy consumption.

3.1. Description of the problem

This study focuses on an isolated city area that is not part of a larger urban context. Figure 1 illustrates the urban layout problem: *nbat* buildings $B_{i,j}$ are laid out according to a rectangular weft, whose dimensions are mx_i (on the horizontal axis) and my_j (on the vertical axis). The buildings are different in height $n_{i,j}$ and length $L_{i,j}$. They all have the same orientation from the South axis $\alpha_{i,j}$. The data to be optimized is mx_i, my_j, $n_{i,j}$, $L_{i,j}$ and $\alpha_{i,j}$. The user chooses objectives and constraints among three criteria; density (*eg.* maximize the urban population density), energy use (only consumption items) or balance (with active solar gains), and solar shading (*eg.* number of shaded stories in a building during six hours per day throughout the year). When defining an objective, the user has to choose to *minimize* or *maximize* relative to the selected criteria. When defining a constraint, he or she has to define a limit threshold. Note that the tool only considers single-objective optimization problems. However single-objective and dual-objective constraints can be assigned. In addition, the tool can be used without constraints.

3.2. Optimization stages

The optimization problem is solved through the use of a genetic algorithm tool called *Bianca* developed by Paolo Vannucci *et al.* at the French Institute Jean Le Rond d'Alembert (Montemurro *et al.* 2011). Three other tools are used; *Fortran* (FORmula TRANslator) as programming language (Backus *et al.* 1957), *Microsoft Excel* as a user interface and *Rhinoceros*® (with the *Grasshopper* plugin) to visualize the optimized urban form. Figure 2 documents the workflow of the optimization process. (1) In the first step, the user enters the necessary data into an *Excel* spreadsheet. Data parameters are defined in the spreadsheet relative to the buildings characteristics (materials, equipment, envelope thermal efficiency, etc.) and to the optimization inputs (number of buildings *nbat*, objective function, constraints, etc.). *An Excel* macro registers the entered data into a series of .txt files that are read by our *Fortran* program. (2) In the second step, *Bianca* is run to optimize the input data according to the chosen objective and constraints. *Bianca* is a genetic algorithm based solver for combinatorial optimization problems in engineering. In particular it was developed for the design of composite laminates (Ahmadian *et al.* 2011). It runs within a *command-line interface* and uses *Fortran* as its formal language. A subroutine defines optimization fitness in the

Fortran environment and details the calculation stages. The optimization is then run according to a genetic algorithm. The genetic algorithm mimics Darwin's process of natural selection. It encodes candidate solutions to a search problem and evolves toward better solutions. This process results in the Pareto front of optimized solutions for the considered problem. (3) The results are registered in .txt files. The data includes every optimized parameter; the buildings characteristics (number of levels $n_{i,j}$, length $L_{i,j}$ and orientations $\alpha_{i,j}$) and the weft dimensions (*mx* and *my*). Data results also indicate the value of the objective function—*ie* the density, energy or shading efficiency of the "optimized" city area. (4) These data are then processed in an *Excel* sheet. (5) Finally, *Grasshopper* "reads" the data from the *Excel* sheet into a *Ghuser* object. From this data, a three-dimensional visualization of the results is rendered to the active *Rhinoceros*® window.

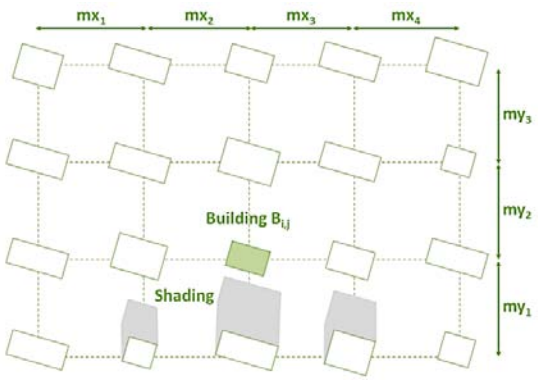

Figure 1. Scheme of the building layout within the city area**.**

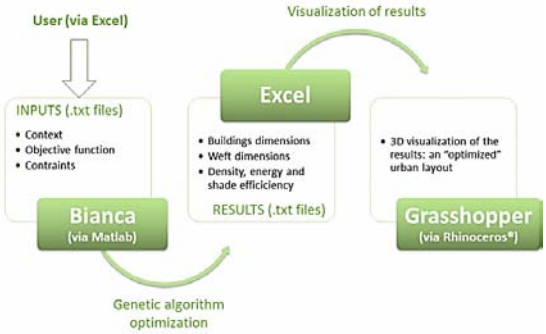

Figure 2. The optimization stages**.**

4. RESULTS AND DISCUSSION

At the time, development of our tool is in process. As a result, very few results are available at this time. In this section, we deal with some of our anticipated results.

4.1. The optimization criteria

The city area contains 20 buildings (*cf.* Figure 1). The weft size is not regular. mx_1, mx_2, mx_3 and mx_4 can be different. my_1, my_2 and my_3 are also able to vary. The optimization parameters are detailed in tables 1 and 2 below. In the case shown, maximizing the population density is the objective. The maximum building energy balance (120 $kWh_{primary_energy}/m^2_{SHON}$.year) is the first constraint. The second constraint is the maximum shade height (zero level) between 11 am and 1 pm in December; 10 am and 2 pm in January, February, October and November; and 9 am and 3 pm in the remaining months.

Number of populations	Number of individuals in a population	Number of generations
1	2000	500

Table 1: Genetic parameters.

Number of levels (-)	Length (m)	Orientation (°)	Weft width (m)	Weft height (m)
$n_{min} - n_{max}$	$L_{min} - L_{max}$	$\alpha_{min} - \alpha_{max}$	$mx_{min} - mx_{max}$	$my_{min} - my_{max}$
0 – 30	6 – 60	-165 – 180	6 – 120	20 – 80

Table 2: Bound values of the optimization parameters.

4.2. Preliminary results

The optimization process took seventeen hours. It resulted in a *.bio* file that synthesizes data about the best feasible solution for each generation. After data processing in an *Excel* sheet, the best feasible solution was read into *Rhinoceros*® utilizing *Grasshopper Read XL* units and visualized in the active *Rhinoceros*® window. Despite the high number of potential solutions (matching the number of individuals per generation), the optimization process did not reach a solution that observed all constraints. Indeed, solar access was not respected during the obliged time slots. This occurred because *Bianca* follows *Automatic Dynamic Penalization* rules. Through the use of penalizing coefficients, a total objective including constraints is created (Montemurro *et al.* 2011). In this way, a solution can be created that is efficient regarding the total objective while not observing all constraints. We are currently working to solve this problem. Figure 3 shows that the optimization tool results in high and long-spread buildings to reach high densities. 18 out of 20 are more than 10 levels in height (*ie* 30 meters) and their lengths are spread between 24 and 59 meters. However keep in mind that the displayed solution is not really optimized since there is shading within the city area. The study is currently in progress and we hope to give more successfully completed results in a further paper.

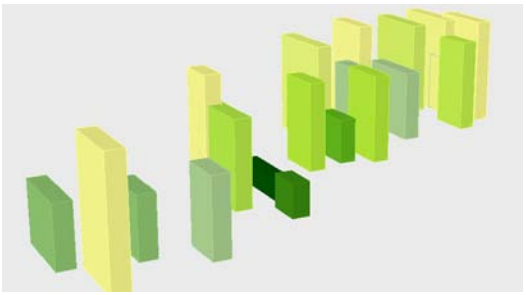

Figure 3. A city area solution visualized on *Rhinoceros*® screen**.**

5. CONCLUSION

This paper describes a methodological process to find the optimal layout of a city area to reach a maximal population density by respecting energy and solar access constraints. At present, we cannot give a ruling on the theory that density might be sustainable. However, by the end of our project, we expect to provide a better understanding of sustainable urban form. Specifically, we hope to be able to demonstrate the advantages and drawbacks of densification and sprawling and the relevance of sustainable urban towers.

Acknowledgements

We would like to thank Paolo Vannucci, Angela Vincenti and Marco Montemurro for the methodological, technical and scientific support they provided our research.

References

AHMADIAN, M. R., VINCENTI, A., VANNUCCI, P. 2011. A general strategy for the optimal design of composite laminates by the polar-genetic method, Materials & Design, vol.32, pages 2317-2327

ARANTES, L., BAVEREL, O., ROLLET P., QUENARD, D. 2011. A simple method to consider energy balance in the architectural design of residential buildings, in ATTAR R., SimAUD 2011 Proceedings, Boston, MA, USA, april 2011, pages 107-114

BACKUS, J.W. 1957. The Fortran automatic coding system for the IBM 704, the first programmer's reference manual for Fortran

BERTAUD, A., MALPEZZI, S. 2003. The Spatial Distribution of Population in 48 World Cities: Implications for Economies in Transition

CAPELUTO, I.G., SHAVIV, E. 2001. On the use of 'solar volume' for determining the urban fabric, Solar Energy, Vol.70, N°3, pages 275-280

CHENG, V., STEEMERS, K., MONTAVON, M., COMPAGNON, R. 2006. Urban form, density and solar potential, PLEA, The 23rd Conference, Geneva, Switzerland, 6 pages

FOUCHIER, V. 1998. La densité humaine nette: un indicateur d'intensité urbaine, in PUMAIN, D., MATTEI, M.-F., Données Urbaines (Vol. 2), Éditions Anthropos, Paris, pages 181-189

GOMEZ-IBANEZ, J.A. 1991. A Global View of Automobile Dependence, A review of Cities and Automobile Dependence: International Sourcebook, Journal of the American Planning Association, Vol.57, n°3, pages 376-379

GORDON, P., RICHARDSON, H.W. 1989. Gasoline consumption and cities - a reply, Journal of the American Planning Association, Vol.55, n°3, pages 342-345

HANITSCH, R.E., SCHULZ, D., SIEGFRIED, U. 2001. Shading effects on output power of grid connected photovoltaic generator systems, Revue des Energies Renouvelables, pages 93-99

KÄMPF, J.H., ROBINSON, D. 2010. Optimisation of building form for solar energy utilisation using constrained evolutionary algorithms, Energy and Buildings, n°42, pages 807-814

KIRWAN, R. 1992. Urban form, energy and transport: A note on the Newman-Kenworthy thesis, Urban Policy and Research, Vol.10, n°1, pages 6-22

KNOWLES, R. 1981. Sun Rhythm Form, Mit Press, Cambridge MA USA

LITTLEFAIR, P. 1998. Passive solar urban design ensuring the penetration of solar energy into the city, Renewable and Sustainable Energy Reviews, n°2, pages 303-326

MÉNARD, R. 2011. Dense cities in 2050: the energy option?, ECEEE 2011 Summer Study, Energy efficiency first: the foundation of a low-carbon society, pages 873-884

MONTEMURRO, M., VINCENTI, A., VANNUCCI, P. 2011. A two-step optimisation approach for the design of composite stiffened panels, Part I: global structural optimisation, 27 pages

NEWMAN, P.W.G., KENWORTHY, J.R. 1989. Cities and Automobile Dependence, Gower Technical, Sidney

NIEMASZ, J., SARGENT, J., REINHART, C.F. 2011. Solar zoning and energy in detached residential dwellings, in ATTAR R., SimAUD 2011 Proceedings, Boston, MA, USA, april 2011, pages 97-105

O'BRIEN, W.L., KENNEDY, C.A., ATHIENITIS, A.K., KESIK, T.J. 2010. The relationship between net energy use and the urban density of solar buildings, Environment and Planning B: Planning and Design, n°37, pages 1002-1021

ROBINSON, D., STONE, A. 2004. Solar radiation modelling in the urban context, Solar Energy, n°77, pages 295-309

SALAT, S., NOWACKI, C. 2010. De l'importance de la morphologie dans l'efficience énergétique des villes, in Liaison Énergie-Francophonie, n°86, ADEME, IEPF, Québec, pages 141-146

VINCENTI, A., AHMADIAN, M.R., VANNUCCI, P. 2010. BIANCA: a genetic algorithm to solve hard combinatorial optimisation problems in engineering, Journal of Global Optimisation, n°48, pages 399-421

Presenting Author Biographies

Abdolreza (Abdy) Abhari

Dr. Abdolreza Abhari is an Associate Professor in the Department of Computer Science at Ryerson University in Toronto, Canada. He obtained his Ph.D. in computer science from Carleton University in Ottawa, Canada (2003). Prior to that he received his M.Sc. in information systems and his B.Sc. in computer engineering from Sharif University of Technology in Tehran (1992 and 1989 respectively). He has worked as a system consultant for industrial and research institutions in Iran, the Netherlands, Germany and Canada. Dr. Abhari's research interests are in the areas of distributed systems focusing on sensor networks and their applications in building design, web mining and database systems, soft computing and modeling and simulation.

Andres Sevtsuk

Andres Sevtsuk is an Assistant Professor in Architecture and Sustainable Design at the Singapore University of Technology and Design (SUTD). Andres leads the City Form Lab at SUTD, which investigates the influence of urban form on the social, economic and environmental performance of cities using state of the art spatial analysis tools. He is also the founding principal of City Form Office, an architecture and planning practice currently based in Singapore.

Before joining SUTD in 2011, Andres taught as a lecturer in Architecture and Urban Studies & Planning at MIT. He studied at L'École d'Architecture de la Ville & des Territoires (BArch) and MIT (SMArchS, PhD) and has worked as an architect, urban designer, consultant and researcher in Estonia, France and the United States. He has published a number of articles and book chapters on urban design, urban technology, and spatial analysis.

Angelos Chronis

Angelos Chronis is a member of the Applied Research and Development team at Foster + Partners, UK. His academic background was initiated by a diploma in Architecture, which was awarded by the University of Patras, Greece. His dissertation, entitled "A Parametric Approach to the Bioclimatic Design of a Student Housing Building in Patras, Greece" was presented at the eCAADe 2010 conference and was selected among the 10 best papers for publication in a special issue of the Automation in Construction journal. He gained an MSc in Adaptive Architecture & Computation from the Bartlett School of Graduate Studies, UCL, with distinction, in the context of which he studied the integration of computational fluid dynamics and genetic algorithms as part of his dissertation.

At SimAUD 2011, his paper titled "Generative Fluid Dynamics: Integration of Rast Fluid Dynamics and Genertic Algorithms for Wind Loading Optimization of a Free From Surface" received the best paper award.

Ben Doherty

Ben has a background in Architecture and Design Computing. He's been a Smart geometry tutor, taught at lots of universities, and currently is a computational designer at BVN working on the complex bits projects and developing tools to make peoples lives better. He is also a design tutor at UTS and runs the compDesGrp arm in Sydney.

David Jason Gerber

In 2009 Dr. Gerber was appointed Assistant Professor of Architecture at the University of Southern California (USC). He has since been awarded a courtesy joint appointment at USC's Viterbi School of Engineering. Prior to joining the USC faculty Dr. Gerber was full time faculty at the Southern California Institute of Architecture from 2006-2009.

Professionally, Dr. Gerber has worked for Zaha Hadid Architects in London, Gehry Technologies in Los Angeles, Moshe Safdie Architects in Massachusetts and The Steinberg Group Architects in California.

David Gerber received his Bachelor of Arts in Architecture from the University of California Berkeley (1996). He completed his Master of Architecture at the Design Research Laboratory of the Architectural Association in London (2000). He earned both his Master of Design Studies and Doctor of Design from the Harvard University Graduate School of Design (2003 and 2007 respectively).

Julien Nembrini

Julien Nembrini is currently at the Universität der Künste (UdK) Berlin where he studies the interaction of form-finding scripting techniques with realistic building physics simulations such as Radiance and EnergyPlus. Before joining UdK, Julien performed as a post-doctoral assistant at the wood construction laboratory IBOIS at EPFL (CH) where he worked on energy-conserving integration techniques for beam and shell simulation.

In obtaining his Ph.D. from the Bristol Robotics Lab (UK), Julien explored self-organization of autonomous robots. Prior to that he earned a diploma in Mathematics from University of Geneva (CH).

Julien Nembrini together with Guillaume Labelle is also one of the developers of the ANAR+ library for architectural parametric scripting within the Processing.org IDE.

Laëtitia Arantes

Laëtitia Arantes is a French PhD candidate in civil engineering at the Architecture School of Grenoble and at the French Scientific Centre for Building Science (CSTB). She holds a Master's degree in urban engineering from the ENTPE (Ecole Nationale des Travaux Publics de l'Etat in Lyon, France) and a Master's degree in Architecture from the ENSAG (Ecole Nationale Supérieure d'Architecture de Grenoble, France). Her current research deals with architecture and energy, particularly energy and density reasoned urban forms.

Liam (William) O'Brien

Liam (William) O'Brien, Ph.D. is an Assistant Professor at Carleton University's new Architectural Conservation and Sustainability program. His research is focused on design processes and energy simulation for high-performance solar buildings. In his latest research initiative, he is working to build a highly-instrumented green roof with an integrated photovoltaic array at the University of Toronto to study the interactions between the two systems.

For his Ph.D., he developed a design tool for solar houses that will enable efficient and highly-visual exploratory design of both passive and active solar systems. The tool was directly inspired by some of his professional consulting experience. This work was a major task within the NSERC Solar Buildings Research Network, a $6-million nationwide strategic network.

Dr. O'Brien has twenty conference and journal publications and is an active researcher for International Energy Agency – Solar Heating and Cooling Task 40: "Towards Net-Zero Solar Buildings". He has organized multiple academic conferences and numerous workshops aimed at graduate students and professionals. He has given many presentations to local and international researchers, architects, and engineers and gave a talk at TEDxRideau Canal in January, 2012.

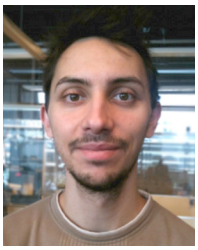

Manolis Patriarche

Manolis Patriarche is a Ph.D. student at the Housing Sciences LAboratory (LASH) of the National Engineering School of State Public Works (ENTPE) in Lyon, France. His Ph.D. research focuses on the influence of a street canyon morphology and building materials on daylight availability.

He holds a master's degree in computer engineering from the USTV (France). He has worked on the development of a yield assessment tool for solar photovoltaics power plant at KiloWattsol, a French engineering consulting firm located in Lyon.

Mansour Nasser Jadid

Mansour Nasser Jadid is an Associate Professor of Civil Engineering at the College of Architecture and Planning at the University of Dammam, Saudi Arabia. Currently, he is the General Supervisor of University projects where he manages projects exceeding 1.5 Billion US dollars. He obtained his Ph.D. in the Application of Artificial Intelligence in Civil Engineering from the University of Edinburgh (1994). He earned his Master of Science in Civil Engineering from Penn State (1987), and his Bachelor of Science in Civil Engineering from the University of Washington (1981). He was a Fulbright Scholar at the University of Maryland, College Park between 1999 and 2000.

Martin Tamke

Martin Tamke is an Associate Professor at the Center for Information Technology and Architecture (CITA) at the Royal Academy of Fine Arts, School of Architecture in Copenhagen. Martin Tamke joined the newly founded research center, CITA, in 2006 where he is pursues design led research on the interface and implications of computational design and its materialization.

Martin also shaped the center's design based research practice. Projects on new design and fabrication tools for wood production, curved creased surfaces or fractal systems led to a series of digitally fabricated speculative probes, prototypes and 1:1 demonstrators that explore an architectural practice engaged with bespoke behaviour.

He lectures extensively and has taught workshops at Vienna, Berlin, Barcelona, St. Petersburg, Hamburg, Istanbul, Aarhus, Trondheim, Innsbruck, Copenhagen and Moscow.

Mona Azarbayjani

Mona Azarbayjani is an Assistant Professor at the School of Architecture at the University of North Carolina at Charlotte (UNCC). At UNCC she teaches core building technology courses, sustainable design and the use of renewable energies in architecture. At the Center for Integrated Building Design Research (cIBDR) she explores energy performance, natural-ventilation, transparent skins and carbon neutral buildings.

Dr. Azarbayjani holds a Ph.D. from the University of Illinois Urbana Champaign.

Nathaniel Jones

Nathaniel Jones is a researcher at Cornell University's Program of Computer Graphics. His research focuses on creating fast, easy-to-use building energy simulation algorithms and tools that provide intelligible feedback. This work earned him a best research paper award at the Building Simulation 2011 conference in Sydney, Australia. This work was recognised for speeding direct solar radiation calculations in EnergyPlus by four orders of magnitude. He has also studied the use of genetic algorithms to optimize building form for temperature and lighting conditions in a variety of climates.

Nathaniel received his Master of Architecture degree from Cornell University (2009) and his B.Sc. in Civil Engineering from The Johns Hopkins University (2005).

Pascal Goffin

Pascal Goffin holds a degree in Computer Science from ETH Zurich (2010). After graduating he started work as a scientific researcher in the Architecture & Sustainable Building Technologies (SuAT) group at the Department of Architecture (ETH Zurich). In the summer of 2009 he studied Sustainable Urban Management and Nanoscience at the University of Tokyo in Japan. Pascal's personal interests include computer graphics, sports and languages.

Sanna Iltanen

Sanna Iltanen is an architect currently working as a researcher and Ph.D. student at the School of Architecture at Tampere University of Technology. Her research interests include urban modeling, parametric design, urban morphology and measuring urban form. She also teaches urban planning and design and GIS (geo information systems) to architects and planners. Previously, she worked as a designer at a private architecture practice.

Siobhan Rockcastle

Siobhan is currently serving as a Teaching Fellow in the School of Architecture at Northeastern University in Boston. She teaches courses in environmental systems, comprehensive design and performance simulation. In the spring of 2011, Siobhan graduated with her SMArchS degree from the Building Technology Lab at MIT. Her thesis research explores the relationship between architectural design and the ephemeral performance of daylight and was awarded a top thesis prize by faculty in the department of architecture. Siobhan graduated from Cornell University in 2008 with her Bachelors of Architecture. She was awarded the Alpha Rho Chi medal for professional merit and an Eidlitz travelling fellowship to study renewable energy trends in Iceland. After graduation, Siobhan was invited back to Cornell as a Teaching Associate for the 2008-2009 academic year where she taught first year design. Siobhan was born and raised in Minneapolis, Minnesota.

Sotirios D. Kotsopoulos

Sotirios D. Kotsopoulos studied at MIT where he earned a Ph.D. in Design & Computation (2005) and an S.M. Arch in Design Technology (2000). Under a fulbright scholarship, he earned an M. Arch from SCI-Arc (1994). Sotirios acquired his Diploma in Architectural Engineering from the National Technical University of Athens (1992).

He practiced design in Athens and Los Angeles receiving numerous awards in various international competitions.

Since 2009, he has been performing as a post-doctoral researcher at the Mobile Experience Laboratory at MIT. Sotirios' academic contributions focus on the impact of computation on the way we conceptualize and practice design. He is using shape grammars to study and formalize the intertwining of structure, appearance and performance in the production of architectural form. In addition, he has taught design courses and multidisciplinary workshops at MIT.

Sven Schneider

Sven Schneider is Computer Science professor in Architecture at the Faculty of Architecture at the Bauhaus University in Weimar. He has studied Media computer science at the Technical University of Chemnitz, architecture at the Technical University of Dresden and at the Bauhaus University Weimar. His research and projects focus on generative design, programming, design automation, design methodology and analysis of spatial configurations. Most recently, he has been developing a creative evolutionary design method for layout problems in architecture and urban planning.

Zheng Yang

Zheng Yang is currently pursuing his PhD degree at USC's Viterbi School of Engineering. Zheng Yang graduated from TianJin University, where he specialized on both Mechanical Engineering and Construction Engineering Management. During his studies, Zheng participated in several projects held by Ministry of Housing and Urban-Rural Development, Ministry of Railways, ENFI, YANG JIANG Nuclear Power etc., and completed academic exchange with other professionals from Berkeley, Purdue and Florida.

Organizers

General Chair

Lira Nikolovska
User Experience Architect, Autodesk

Co-Chair

Ramtin Attar
Senior Design Research Associate, Autodesk Research

Program Committee

Azam Khan
SimAUD founder and Head of the Environment & Ergonomics Research Group, Autodesk Research (SimAUD advisory board)

Robert Aish
Director of Software Development, Autodesk

Marilyne Andersen
Associate Professor of Sustainable Construction Technologies, École Polytechnique Fédérale de Lausanne

Michael Glueck
Research Scientist, Autodesk Research

Sean Hanna
Academic Fellow, UCL Bartlett School of Graduate Studies

Neil Katz
Associate, Skidmore, Owings & Merrill

Ian Keough
Solutions Architect, Vela Systems

Judit Kimpian
Head of Sustainability and Advanced Modeling, Aedas

Terry W. Knight
Professor of Computation, MIT School of Architecture and Planning

Branko Kolarevic
Faculty of Environmental Design, University of Calgary

Liam O'Brien
Assistant Professor, Faculty of Engineering, Carleton University

Christoph Reinhart
Associate Professor, Harvard Graduate School of Design(SimAUD advisory board)

Jenny Sabin
Assistant Professor, Cornell University, Smart Geometry

Gabriel Wainer
Associate Professor, Carleton University and
General Chair of the Symposium on Theory of Modeling and Simulation (DEVS'12) (SimAUD advisory board)

Technical Paper Reviewers

Marilyne Andersen

Ramtin Attar

Burcin Becerik-Gerber

David Benjamin

Jason Crow

Alan Fung

David Jason Gerber

Rhys Goldstein

Sean Hanna

Matt Jezyk

Mitch Joachim

Neil Katz

Ian Keough

Azam Khan

Judit Kimpian

Terry Knight

Yoshihiro Kobayashi

Branko Kolarevic

Zach Kron

Vidar Lerum

Jeff McGrew

Thomas Mical

Maria Mingallon

Ian Molloy

Erin Morrow

Philam Nguyen

Liam O'Brien

Mine Ozkar

Brady Peters

Jenny Sabin

Greg Schleusner

Andres Sevtsuk

Dennis Shelden

Patricio Simari

Meli Stylianou

Alex Tessier

Gabriel Wainer

Sponsors

Sponsored by

Autodesk®

In co-operation with

Cover Image Credits

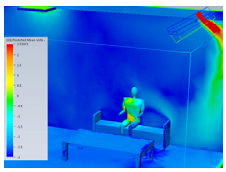

Visualization Framework of Thermal Comfort for Architects

Pascal Goffin, Arno Schlueter

The Swiss Federal Institute of Technology Zurich (ETH Zürich)

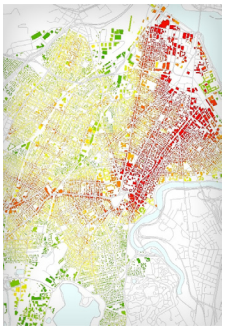

Urban Network Analysis: A New Toolbox for Measuring City Form in ArcGIS

Andres Sevtsuk, Michael Mekonnen

Singapore University of Technology and Design (SUTD), Massahusetts Institute of Technology (MIT)

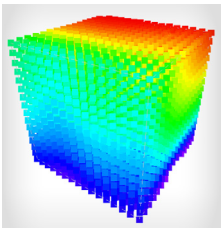

Combining Sensitivity Analysis with Parametric Modeling to Inform Early Design

Julien Nembrini, Steffen Samberger, André Sternitzke,Guillaume Labelle

Universität der Künste Berlin (UdK), École polytechnique fédérale de Lausanne (EPFL)

A New Material Practice - Integrating Design and Material Behavior

Martin Tamke, Elisa Lafuente Hernández, Anders Deleuran, Christoph Gengnagel, Mark Burry, Mette Ramsgard Thomsen

Centre for Information Technology and Architecture (CITA), The Royal Danish Academy of Fine Arts, Royal Melbourne Institute of Technology (RMIT), Universität der Künste Berlin (UdK)

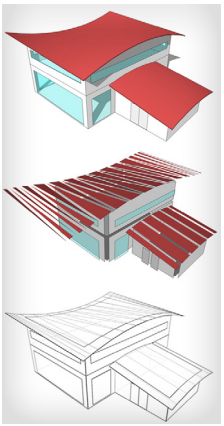

Automated Translation of Architectural Models for Energy Simulation

Kevin B. Pratt, Nathaniel L. Jones, Lars Schumann, David E. Bosworth, Andrew D. Heumann

Cornell University

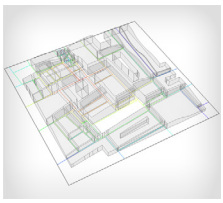

The Parametric Exploration of Spatial Properties – Coupling Parametric Geometry Modeling and the Graph-Based Spatial Analysis of Urban Street Networks

Sven Schneider, Martin Bielik, Reinhard König

Bauhaus University

Author Index

A
Abhari, Abdolreza 137
Aish, Francis 81
Andersen, Marilyne 73
Azarbayjani, Mona 89

B
Badrah, Mustafa K. 13
Barnes, Ben 31
Becerik-Gerber, Burcin 49
Behboudi, Negin 137
Bielik, Martin 123
Bosworth, David E. 65
Burry, Mark 5
Butt, Fouad 137

C
Carra, Guglielmo 97
Casalegno, Federico 97
Chronis, Angelos 81

D
Deleuran, Anders 5
Doherty, Ben 31
Dumortier, Dominique 145

G
Gengnagel, Christoph 5
Gerber, David Jason 23
Giouvanos, Evangelos 81
Goffin, Pascal 141
Graybil, Wesley 97

H
Hernández, Elisa Lafuente 5
Heumann, Andrew D. 65
Hsiung, Bob 97

I
Iltanen, Sanna 133

J
Jadid, Mansour N. 13
Jones, Nathaniel L. 65

K
König, Reinhard 123
Kotsopoulos, Sotirios D. 97

L
Labelle, Guillaume 39
Li, Nan 49
Lin, Shih-Hsin (Eve) 23

M
Mehta, Jigisha 89
Mekonnen, Michael 111

N
Nembrini, Julien 39

O
O'Brien, William (Liam) 57
Orosz, Michael 49

P
Pan, Bei (Penny) 23
Patriarche, Manolis 145
Pratt, Kevin B. 65

R
Rockcastle, Siobhan 73
Rumery, Dan 31

S
Samberger, Steffen 39
Schlueter, Arno 141
Schneider, Sven 123
Schumann, Lars 65
Sevtsuk, Andres 111
Solmaz, Aslihan Senel 23
Sternitzke, André 39

T
Tamke, Martin 5
Thomsen, Mette Ramsgard 5
Tsigkari, Martha 81

Y
Yang, Zheng 49

Z
Zaki, Anis Abou 81
Zhou, Bin 31

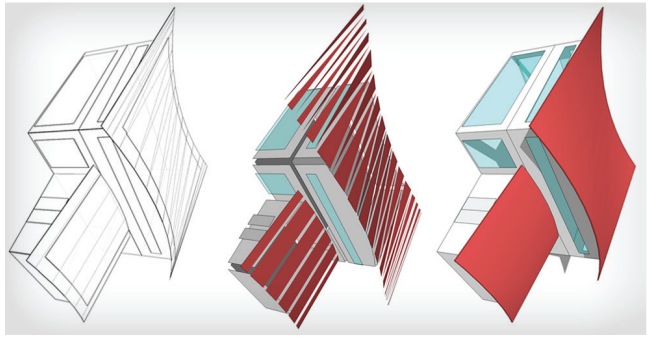

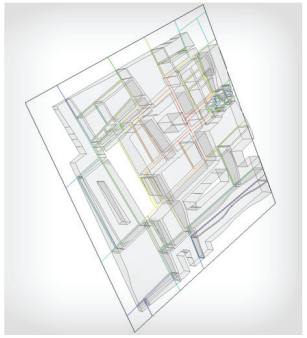
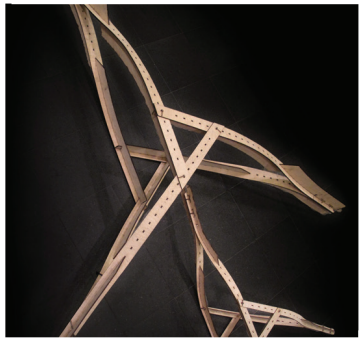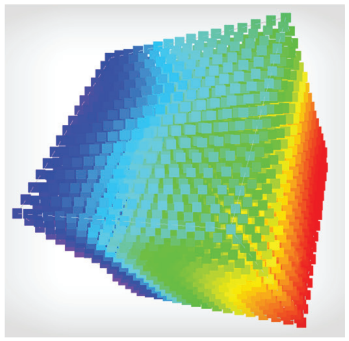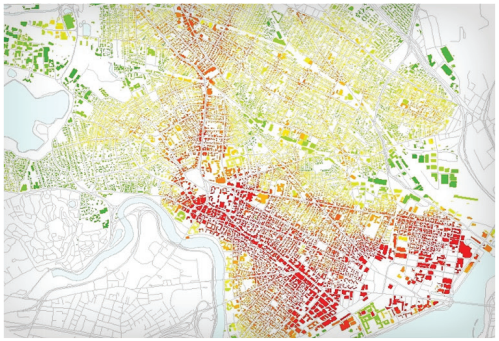
Symposium on Simulation for Architecture and Urban Design
2012